STATENS GEOTEKNISKA INSTITUT
SWEDISH GEOTECHNICAL INSTITUTE

Undrained shear strength in clay slopes – Influence of stress conditions

A model and field test study

HJÖRDIS LÖFROTH

Report 71

LINKÖPING 2008

Report | Swedish Geotechnical Institute
SE-581 93 Linköping

Order | Information service, SGI
Tel: +46 13 20 18 04
Fax: +46 13 20 19 09
E-mail: info@swedgeo.se
Internet: www.swedgeo.se

ISSN | 0348-0755
ISRN | SGI-R--08/71--SE

THESIS FOR THE DEGREE OF DOCTOR OF PHILOSOPHY

Undrained shear strength in clay slopes - Influence of stress conditions

A model and field test study

HJÖRDIS LÖFROTH

Department of Civil and Environmental Engineering
Division of Geo Engineering
Geotechnical Engineering
CHALMERS UNIVERSITY OF TECHNOLOGY
Göteborg, Sweden 2008

Undrained shear strength in clay slopes
- Influence of stress conditions
A model and field test study

HJÖRDIS LÖFROTH

ISBN 978-91-7385-165-7
Doktorsavhandlingar vid Chalmers tekniska högskola
Ny serie Nr 2846
ISSN 0346-718x

Department of Civil and Environmental Engineering
Division of Geo Engineering
Geotechnical Engineering
CHALMERS UNIVERSITY OF TECHNOLOGY
SE-412 96 Göteborg
Sweden
Telephone +46 (0)31-772 1000

Utges även av
Statens geotekniska institut
Serien “Rapport”
Rapport Nr 71
ISSN 0348-0755

Reproservice, Chalmers University of Technology
Göteborg, Sweden 2008

Undrained shear strength in clay slopes - Influence of stress conditions

A model and field test study

HJÖRDIS LÖFROTH
Department of Civil and Environmental Engineering
CHALMERS UNIVERSITY OF TECHNOLOGY

ABSTRACT

To counteract natural hazards such as landslides, current methods for evaluation of soil properties as a mean for determining the safety level of natural slopes need to be refined. The empirical relationships used for estimation of the undrained shear strength from piezocone and field vane test are based on the stress conditions valid for horizontal ground and normally consolidated or slightly overconsolidated soil. Limited studies indicate that the different relations between vertical and horizontal stresses that exist in a slope and for overconsolidated soil have a large influence on these results.

The aim of the present study is to document the influence of horizontal stresses on the undrained shear strength, evaluated using piezocone and field vane tests and, if necessary, modify the evaluation accordingly.

Model tests with a mini vane and mini piezocone in large triaxial cells were conducted in order to study the effects of the ratio between horizontal and vertical stresses on the undrained shear strength as determined using piezocone and vane tests under controlled conditions. The results were compared with results from direct simple shear tests. The aim was to simulate the stress conditions in the active and the passive zones of a slope as well as for horizontal ground surface.

The results from the analysis of the data from the vane model tests indicate that the horizontal preconsolidation pressure and the OCR in the horizontal direction have a major influence on the vane shear strength. Together with empirical data from earlier studies, also the results from the piezocone model tests indicate that the net cone resistance is primarily dependent on the horizontal preconsolidation pressure.

Field tests were carried out at two test sites consisting of homogeneous clay and with slopes eroded from originally horizontal ground. The undrained shear strength at the test sites were estimated from piezocone tests, field vane tests and direct simple shear tests. The undrained shear strength from the field vane tests and the piezocone tests at the toe of the test site slopes were also predicted based on the results of the model tests and the stress conditions in the slopes. The undrained shear strength evaluated from the adapted model test results for the field vane test corresponds quite well with the empirical relationship that includes a correction for OCR, for both test sites. This indicates that there is a need for an extra correction of the field vane test results for overconsolidation.

Keywords: clay, slope, undrained shear strength, horizontal stress, preconsolidation pressure, piezocone test, field vane test, direct simple shear test, consolidation, model test, field test.

Errata

Page	Printed	Corrected
iii	Karin Rankka	Karin Lundström
17	$\beta = 60°$	$\beta = -60°$
89	Terzaghi and Frölich, 1936	-
188	-	Chowdhury, RN. (1978). Slope analysis. Developments in geotechnical engineering, 22 (Elsevier), 423 s. Amsterdam.
191	-	Larsson, R. (1993). CPT-sondering, Utrustning – utförande – utvärdering. Cone penetration test, Equipment – testing – evaluation (In Swedish). Swedish Geotechnical Institute, SGI. Information 15. Linköping.
192	-	Pamukcu, S, Suhayda, J. (1988). Low-strain shear measurement using a triaxial vane device. ASTM. Special Technical Publication; STP 1014.
193	-	Schmidt, B. (1967). Lateral stresses in uniaxial strain. Danish Geotechnical Institute. Bulletin No 23.

PREFACE

The work presented in this thesis deals with the undrained shear strength in clay slopes and the influence of horizontal stresses on the field vane and piezocone shear strength. The study was carried out between 1999 and 2008 at the Division of Geo Engineering, Department of Civil and Environmental Engineering at Chalmers University of Technology in Gothenburg and at the Swedish Geotechnical Institute (SGI) in Linköping. It was supported financially by the Swedish Rescue Service Agency and the Swedish Geotechnical Institute.

The work was performed as an industrial study for a PhD degree and I am most grateful to my employer, the Swedish Geotechnical Institute, for giving me the opportunity to devote part of the last nine years to such in-depth research.

I wish to thank my supervisor at Chalmers, Professor Göran Sällfors, for valuable discussions, for guiding me throughout the work, for giving me inspiration when needed and helping me to get back on track when lost in interesting sidetracks. I wish to thank my co-supervisor at the SGI, Rolf Larsson for guidance and valuable discussions, especially with evaluation and interpretation of the model test data and critical in-depth examination of the manuscript. I also would like to thank my "sounding board" Per-Evert Bengtsson, SGI, for theoretical support and fruitful discussions about different aspects of my findings as well as numerical modelling and critical examination of the manuscript.

A number of other people have supported me during the course of this work and I would like to extend my special thanks to them: Sadek Baker, Skanska (formerly Chalmers) for initial numerical modelling as a guide on how to perform the model tests. Jacques Connant, WSP (formerly Chalmers), for help with the design and development of the model test equipment. Aaro Pirhonen, Chalmers, for manufacturing the equipment. Peter Hedborg, Chalmers, for help with the final modifications and improvements to the model test equipment, development of the data acquisition system and for carrying out most of the tests. Mats Olsson, SGI, for carrying out some of the model tests. Inga-Maj Kaller, SGI, for carrying out direct simple shear tests. Kjell Nätterdal (formerly Chalmers) and Ingemar Forsgren, Chalmers, for help with the field investigations. Veijo Puustinen, SGI, for help with figures. Karin Rankka, SGI, for critical examination of parts of the manuscript. Patrick O'Malley for language editing. My superiors at the SGI for their support throughout this work. My

colleagues at Chalmers and SGI for their friendship and valuable discussions.

Finally I would like to express my thanks to my husband Björn for his encouragement, patience and consideration during these years and to our daughters Kajsa and Sandra, who entered my life during this time and who help me continuously to see the important things in life.

Linköping, June 2008

Hjördis Löfroth

TABLE OF CONTENTS

SUMMARY

Introduction

For better assessment and more effective use of the economic resources of society to take preventive measures to counteract natural hazards such as landslides, current methods for evaluation of soil properties as a means of determining the safety level of natural slopes need to be refined. The undrained shear strength in clay evaluated using *in situ* methods (piezocone and field vane tests) is founded on empirical relationships, based mainly on the stress distribution valid for horizontal ground and normally consolidated or slightly overconsolidated soil. For these conditions the results from laboratory tests and field tests generally show a good level of agreement. However, limited studies imply that the different relationships between horizontal and vertical stresses in a slope and for overconsolidated soil have a significant influence on how the results from field vane and piezocone tests should be evaluated. Such an influence does not affect the interpretation of, for example, direct simple shear test results in the laboratory.

The aim of the present study is to document the influence of horizontal stresses on the undrained shear strength, evaluated using piezocone and field vane tests, and if necessary modify the evaluation accordingly.

Model tests

Model tests were conducted in order to study the effects of the ratio between horizontal and vertical stresses on the undrained shear strength as determined using piezocone and vane tests under controlled conditions. The aim was to simulate the stress conditions in the active and passive zones of a slope as well as for horizontal ground surface.

To carry out the model tests, two types of triaxial cells were designed and built. The first type was used to consolidate clay specimens for isotropic stress conditions and for conditions with greater horizontal stress than vertical stress ($K>1$). The second type was used to consolidate clay specimens for isotropic stress conditions or for stress conditions with larger vertical stresses than horizontal stresses ($K<1$). In the model tests a mini-piezocone from Fugro Engineers BV was used and mini-vane equipment was designed and built within the framework of the project.

For each chosen stress condition, model piezocone and vane shear tests were conducted and the cone resistance, penetration pore pressure and torque were measured. In order to check the stress history of the clay specimens, each specimen was consolidated for stresses above its natural vertical and horizontal preconsolidation pressures. All samples were taken from the upper part of the soil profile, under the dry crust, at one of the test sites.

The results were compared with results from direct simple shear tests using the equation that describes how the undrained shear strength varies with the preconsolidation pressure and the overconsolidation ratio (e.g. Ladd et. al., 1977).

Results of the vane model tests

One reason for analysing the model tests was to try to evaluate whether it is the horizontal stress, the vertical stress or a weighted stress that is the main influence on the vane shear test results. The results were therefore normalised against the horizontal preconsolidation pressure, the vertical preconsolidation pressure and a weighted preconsolidation pressure: 1/7 of the vertical preconsolidation pressure and 6/7 of the horizontal preconsolidation pressure. The weighted stress is generally believed to best reflect the influence of horizontal and vertical preconsolidation pressure on the undrained shear strength determined using the vane shear test (Bjerrum, 1973). Another purpose of the analysis was to study the possible effect of the overconsolidation ratio in various directions (and consequently also the influence of the consolidation stresses in these directions). The normalised shear strength was therefore plotted against the horizontal, vertical or weighted OCRs. The relationships were compared with the empirical equation that directly or indirectly describes how the undrained shear strength varies with the preconsolidation pressure and overconsolidation ratio (e.g. Ladd et. al., 1977 and Jamiolkowski et al., 1985):

$$\frac{c_u}{\sigma'_{cv}} = a \cdot OCR_v^{b-1} \qquad (1)$$

The empirical values of 0.22 for the *a*-factor for direct simple shear and 0.8 for the *b*-factor were applied. The choice of these values was supported by results from direct simple shear tests on specimens consolidated for effective stresses 2.5 times the natural preconsolidation pressure and then unloaded to various OCRs according to the SHANSEP procedure (Ladd & Foot 1974) and also by results of tests performed according to the modified SHANSEP procedure normally used in Sweden.

Independently of how normalisation of the model test results took place, a considerable scatter in the data was observed. The amount of data from the model tests was also limited. It was therefore not possible to obtain a high degree of significance for any of the relationships. However, the significance was enhanced considerably when the shear strength was normalised against the horizontal preconsolidation pressure or the weighted average preconsolidation pressure compared to normalisation against the vertical preconsolidation pressure.

The results from the analysis of the data indicate that the horizontal preconsolidation pressure and the OCR in the horizontal direction have a major influence on the vane shear strength. However, as the relationship for the vane shear test data cannot be considered quite significant, this conclusion is tentative. The vane shear strength normalised against the weighted preconsolidation pressure and plotted against a weighted OCR for the tests at a depth of 120 mm is shown in Figure 1.

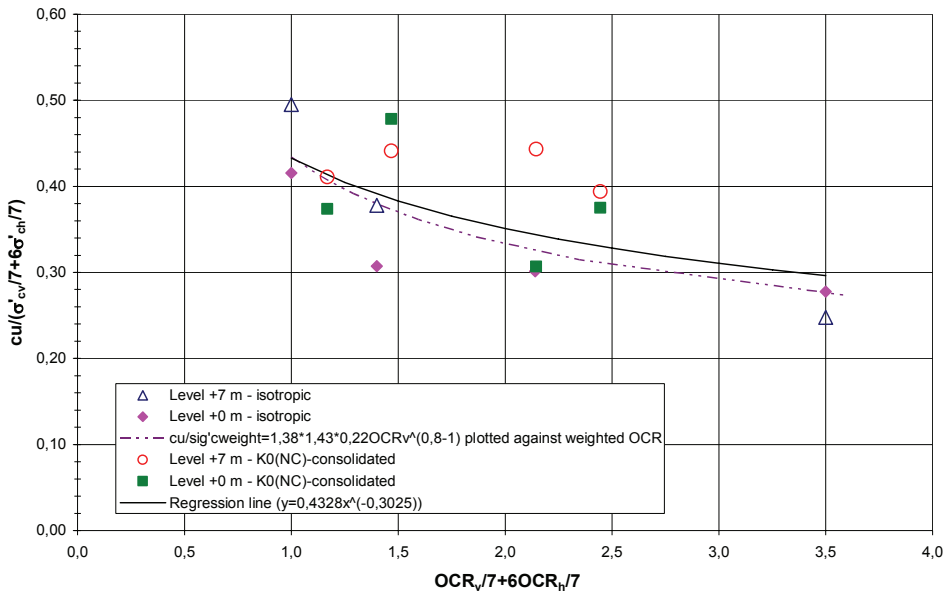

Figure 1 *The vane shear strength at 120 mm depth normalised against the weighted preconsolidation pressure and plotted against the weighted OCR.*

Results of the piezocone model tests

The focus in this study was to find out which stresses exerted the main influence on the net cone resistance (q_T-σ_{v0}). Consequently, (q_T-σ_{v0}) was normalised against the horizontal preconsolidation pressure, the vertical

preconsolidation pressure and the mean preconsolidation pressure. To study the effect of the overconsolidation ratio (OCR), the normalised net cone resistance was plotted against the horizontal, vertical and mean overconsolidation ratios. However, to compare these relationships with the empirical Equation 1 above, it was necessary to include the cone factor, N_{kt}. In the empirical curves in the diagrams, c_u in the equation has thus been multiplied by N_{kt}. The empirical relationship of N_{kt} corresponding to the shear strength at direct simple shear for normally and only slightly overconsolidated Swedish clays was then used.

The scatter of the data from the piezocone tests was greater than for the vane shear tests. As a result, the significance of the relationships was considerably lower than for the vane shear tests. The significance was actually very low for all the piezocone relationships. The net cone resistance normalised against the horizontal preconsolidation pressure and plotted against the horizontal OCR is shown in Figure 2.

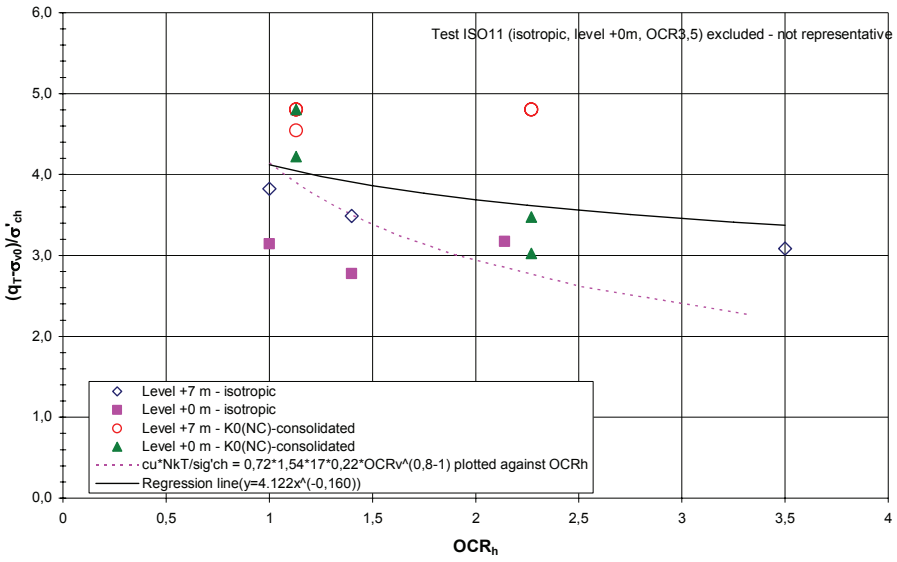

Figure 2 *The net cone resistance normalised against the horizontal preconsolidation pressure and plotted against the OCR in the horizontal direction.*

Based on the results alone, it has not been possible to confirm whether it is the horizontal, the vertical or the mean preconsolidation pressure that has the greatest influence on the net cone resistance. This is because of the low significance and the difficulty distinguishing the type of relationship that best correlates with the empirical equation.

It may be possible to estimate the influence of the vertical or the horizontal preconsolidation pressure using empirical data from earlier studies. Combining the relationship found by Larsson (1977),

$$K_{0NC} = 0.31 + 0.71(w_L - 0.2) \qquad (2)$$

with the relationship by Larsson & Mulabdic' (1991),

$$\frac{q_T - \sigma_{v0}}{\sigma'_{cv}} = 1.21 + 4.4 \cdot w_L \qquad (3)$$

gives an expression for the relationship between the net cone resistance and the horizontal preconsolidation pressure

$$\frac{q_T - \sigma_{v0}}{\sigma'_{ch}} = \frac{1.21 + 4.4 \cdot w_L}{0.31 + 0.71 \cdot (w_L - 0.2)} \qquad (4)$$

In Figure 3 the net cone resistance is normalised against the vertical preconsolidation pressure and the horizontal preconsolidation pressure respectively and plotted against the liquid limit using Equations 3 and 4. It can be clearly seen that there is hardly any change in the net cone resistance normalised against the horizontal preconsolidation pressure with the liquid limit, whereas the net cone resistance normalised against the vertical preconsolidation pressure is a clear function of the liquid limit. This indicates that the net cone resistance is mainly dependent on the horizontal preconsolidation pressure.

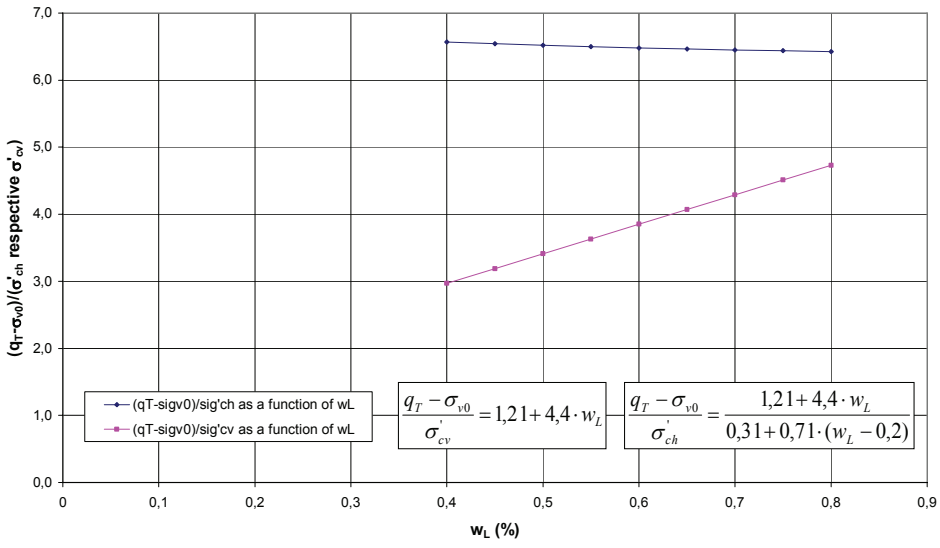

Figure 3 *The net cone resistance normalised against the horizontal preconsolidation pressure and the vertical preconsolidation pressure respectively and plotted against the liquid limit.*

Field tests

Field tests were carried out at two test sites in this project. Both test sites are located in the Göta River valley. The test sites were chosen because they are eroded from flat ground, consist of homogeneous clay up to the ground surface, they have a low factor of safety and it is possible to carry out field investigations also at the toe of the slope. At the test sites, piezocone tests, field vane tests, dilatometer tests and undisturbed sampling were carried out.

Undrained shear strength in the test site slopes

The undrained shear strength of the clay in the test site slopes has been evaluated from field vane tests and piezocone tests in the field and direct simple shear tests in the laboratory, at the toe of the slopes, at the crest and far behind the crest. Evaluation of the undrained shear strength from field vane and piezocone tests has been done both with the Swedish relationships without correction for overconsolidation, which are based on normally consolidated and slightly overconsolidated soils, and with the relationships that have an extra correction for overconsolidation. Comparisons were made at the toe of the slopes where the degree of overconsolidation is highest. Estimation of the undrained shear strength from all field and laboratory tests together with empirical experience and using the relationships for the piezocone and field vane test without correction for OCR gave an undrained shear strength that was marginally to slightly higher compared to that estimated using all data and using the relationships with a correction for OCR.

The undrained shear strength from the field vane tests and the piezocone tests at the toe of the test site slopes has also been predicted based on the results of the model tests and the stress conditions in the slopes. The field tests performed far behind the crest of the slope were used as references, corresponding to stress conditions at almost horizontal ground conditions.

The undrained shear strength evaluated from the adapted model test results for the field vane test corresponds quite well with the new relationship, which includes a correction for OCR, for both test sites. This indicates that there is a need for an extra correction of the field vane test results for overconsolidation.

For the piezocone test it can be seen that the undrained shear strength evaluated from the model tests is lower or in the lower range of the

undrained shear strength based on the relationship that includes a correction for OCR. This indicates that there is a need for an extra correction of the piezocone test results for overconsolidation. The fact that it is also lower than the undrained shear strength based on the relationship that has a correction for OCR indicates that this correction should possibly be even greater than that in the current relationship. Figure 4 shows the undrained shear strength from the field vane test from the Partille test site, evaluated with and without correction for OCR, compared with the undrained shear strength evaluated from the model test results.

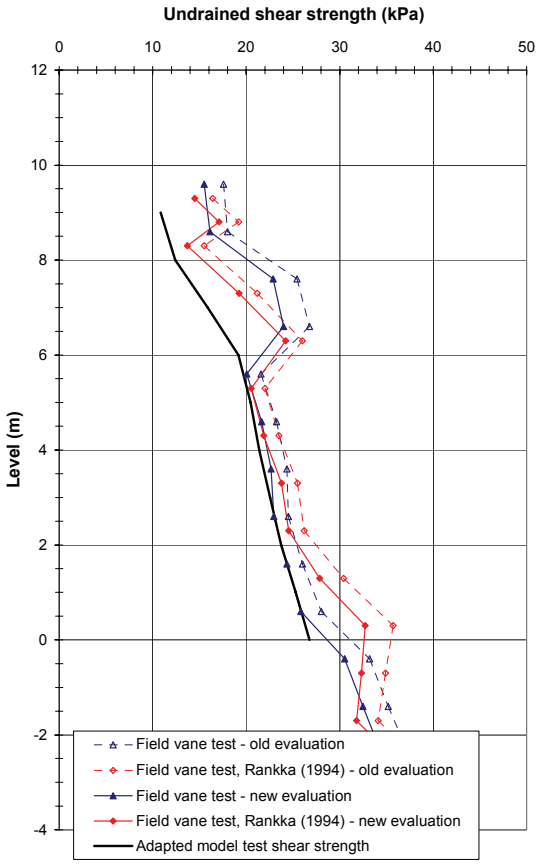

Figure 4 *Undrained shear strength evaluated from the model vane test results compared with evaluated field vane test results.*

LIST OF SYMBOLS AND ABBREVIATIONS

Roman letters

a_s	Swelling index
a	Factor, material parameter
b	Factor, material parameter
c'	Cohesion intercept
c_u	Undrained shear strength
c_v	Consolidation coefficient
c_{vv}	Consolidation coefficient, vertical compression, vertical flow
c_{vh}	Consolidation coefficient, vertical compression, horizontal flow
D	Diameter
E	Young's modulus
F_c	Factor of safety, undrained analysis
F_k	Factor of safety, combined analysis
g	Acceleration due to gravity
H	Height
k	Permeability
k_v	Permeability in the vertical direction
k_h	Permeability in the horizontal direction
K	Earth pressure coefficient in general
K_a	Active earth pressure coefficient
K_p	Passive earth pressure coefficient
K_0	Earth pressure coefficient for horizontal ground surface
$K_{0(NC)}$, K_{0NC}	Earth pressure coefficient for normally consolidated soil
K_{0rb}	Earth pressure coefficient for overconsolidated soil
M	Oedometer modulus
M_0	Oedometer modulus for stresses lower than the preconsolidation pressure
M'	Oedometer modulus number
M_L	Oedometer modulus for effective stresses in the normally consolidated range
M_{LV}	Oedometer modulus in the vertical direction for effective stresses in the normally consolidated range
M_{LH}	Oedometer modulus in the horizontal direction for effective stresses in the normally consolidated range
N_{kt}	Cone factor for evaluation of undrained shear

	strength
OCR	Degree of overconsolidation
q_c	Total cone resistance, piezocone test
q_t	Cone resistance corrected for pore pressure effects, piezocone test
R	Operator for calculation of autocorrelation
r	Radius
S_t	Sensitivity
t	Time
T	Time factor
T_v	Time factor in the vertical direction
T_h	Time factor in the horizontal direction
U	Degree of consolidation
w_N	Natural water content
w_L	Liquid limit

Greek letters

α_{smax} , $\beta_{\alpha s}$	Creep parameters
γ	Unit weight of the soil
Δ *(e.g.* $\Delta\sigma'_c$*)*	Difference in general (e.g. difference in preconsolidation pressure)
Δ	$\Delta = (\sigma_{v0} - \sigma_{h0})/2c_u$ see for example Teh (1987)
ε	Strain
ε_v	Vertical strain
ε_h	Horizontal strain
ϕ'	Angle of internal friction
μ	Correction factor for values of the undrained shear strength from the fall cone test and field vane test
μ_{OCR}	Correction factor for overconsolidation for values of the undrained shear strength from the field vane test
ν	Poisson's ratio
σ'_v	Effective vertical stress
σ'_{v0}	Initial effective vertical stress
σ'_h	Effective horizontal stress
σ'_{h0}	Initial effective horizontal stress
σ'_c	Preconsolidation pressure
σ'_{cv}	Vertical preconsolidation pressure
σ'_{ch}	Horizontal preconsolidation pressure
σ'_L	The effective stress where the modulus starts to increase again

Abbreviations

CRS	Constant rate of strain
OCR	Overconsolidation ratio
OCR_v	Vertical overconsolidation ratio
OCR_h	Horizontal overconsolidation ratio
SGI	Swedish Geotechnical Institute

1. INTRODUCTION

1.1 Background

A range of measures are currently being taken to protect against natural hazards such as landslides. For more effective use of the economic resources of society in the implementation of preventive measures and exploitation, present methods for remedial work and evaluation of soil properties as a means of determining the safety level of natural slopes need to be refined. This study focuses on the determination of soil properties of soft clay with respect to undrained shear strength.

Evaluation of the shear strength in clay using *in situ* methods (piezocone test and field vane test) is based on empirical relationships. For Swedish clays, these relationships are based mainly on the stress distribution valid for horizontal ground and normally consolidated or slightly overconsolidated soil. For these conditions, the results from laboratory tests and field tests generally show good agreement. However, the limited studies available on how the various principal stresses influence the test results imply that the different relationships between horizontal and vertical stresses that exist in a slope and overconsolidated soil have a large and fairly large influence respectively on the results from field vane and piezocone tests. This influence does not normally affect shear test results in the laboratory, as is the case with the results from direct simple shear tests.

1.2 Purpose and scope of the study

The purpose of this study is to document the influence of the horizontal stresses on the undrained shear strength evaluated using piezocone and field vane tests and, if necessary, modify the evaluation accordingly.

To accomplish this, a comparison is made between the undrained shear strength determined using field vane tests and piezocone tests *in situ* and direct simple shear tests in the laboratory, undertaken for selected slopes. Furthermore, the influence of the horizontal and vertical stresses on the piezocone and vane shear test results is studied using model tests, i.e. model piezocone and model vane tests are carried out in large triaxial cells. The results from the model tests are then used together with the field tests carried out far behind the crest of the slopes, which correspond to almost horizontal ground conditions, to predict the undrained shear strength at the toe of the slopes where the stress conditions are different.

2. LITERATURE SURVEY

2.1 Introduction

The literature survey in this study focuses mainly on three areas. The first area concerns model tests in clay in calibration chambers or triaxial cells. The second area concentrates on common methods for evaluation of soil properties in clay from the field and laboratory tests used in this study. The third and most extensive area concerns stress conditions and their influence on undrained shear strength.

The literature survey on model tests in calibration chambers and triaxial cells was carried out in order to gain an understanding of how to design the model tests. It involves different types of equipment, the dimensions of the equipment and the relationship between the sizes of the test equipment (vane, piezocone) to be inserted into the clay and the clay specimen in order to limit boundary effects.

The survey on evaluation of soil properties from field and laboratory tests is limited to the tests used in this study. It concentrates on the evaluation of undrained shear strength, preconsolidation pressure and horizontal stress. It also concentrates on the evaluation methods commonly used in Sweden, which have also been used in this project.

The final part of the literature survey focuses initially on stress conditions in clay slopes. This is followed by a description of different studies concerning the influence of the stress conditions on undrained shear strength evaluated using field vane and piezocone tests. There is an emphasis on the conclusions regarding which stresses have a major influence on the undrained shear strength.

In addition to the literature presented in this chapter, other references have for example been used related to the geology in the test areas, the permeability of clay, the consolidation of clay and temperature effects. The findings of these studies are presented in addition to the analyses made at a later stage in this work.

2.2 Model tests in clay

2.2.1 Tests in calibration chambers

Calibration chamber tests are conducted mainly to calibrate *in situ* testing devices or to carry out model tests on foundations, e.g. piles or anchors. Several authors have conducted tests using a piezocone, vane, pressure meter or dilatometer in clay specimens prepared from slurries. The research described below includes descriptions of tests involving *in situ* testing devices in calibration chambers with a focus on the size relationship between the test equipment and the tested specimen. In the case of tests using a piezocone or vane related to differences in stress conditions, the results of these tests are included mainly in Section 2.6.3 and 2.6.4 .

Rosenfarb and Krizek (1978) studied the anisotropic strength behaviour of kaolin clay subjected to different stress conditions by performing vertical and horizontal vane tests in a consolidometer. Clay slurries with flocculated and dispersed intrinsic fabrics were consolidated in large-diameter consolidometers under conditions of no lateral strain, to different values of the major principal stress. The prepared samples were 200 mm in diameter and 100 to 150 mm high and the height and diameter of the vane were both 12.7 mm (H/D = 1). To carry out vane tests in two directions in the consolidated clay blocks while they were still in the slurry consolidometer under their ambient state of stress, a vane shear test system capable of using vertically and horizontally oriented vanes was incorporated into the slurry consolidometer. During consolidation the vanes were fully retracted in their protective housings, and then introduced into the clay specimens when these were fully consolidated. The results of the tests showed higher shear strength for flocculated clay than for dispersed clay. Vanes with their axes oriented perpendicularly to the direction of the principal consolidation stress yielded higher strengths than those with axes parallel to that direction, see also section 2.6.3.

Almeida and Parry (1983 and 1985) used a small vane (18 mm diameter and 14 mm high), a 10 mm diameter cone penetrometer and a 12.7 mm diameter piezocone to carry out tests in reconstituted clay in a consolidometer. The equipment had been developed to measure soil properties in centrifuge model tests during flight. The purpose of the study was to provide correlations between point resistance, shear strength, overburden pressure and overconsolidation ratio. Kaolin clay slurry and Gault clay slurry were consolidated to 150 kPa and 126 kPa respectively in an 850 mm diameter consolidometer. For the kaolin clay at pressures

corresponding to OCR = 1, OCR = 3 and OCR = 10 and for Gault clay at OCR = 1, OCR = 1.9 and OCR = 7, tests were performed at a distance of 150 mm from the inner wall of the chamber. The ratio between the distance to the consolidometer wall and the radius of the largest cone was 24 in order to prevent any chamber size effects. The authors concluded, among other things, that the variation in the vane shear strength with OCR for kaolin agrees with the undrained shear strength measured in isotropically consolidated triaxial tests in another study and that the cone factors increased the higher the OCR, see also sections 2.6.3 and 2.6.4.

Huang et al. (1988) describe a calibration chamber system, procedures for preparing reproducible specimens K_0-consolidated from slurry and techniques for model pressure meter testing. The calibration chamber accommodated a specimen 200 mm in diameter with a maximum height of 360 mm. The central measurement section of the pressure meter had a diameter of 11.1 mm and a height of 111 mm. The diameter of the chamber specimen was 18 times that of the pressure meter, which was considered sufficient to minimise chamber size effects. The tests were performed under constant vertical and constant lateral stresses. Among other things, the authors conclude that the results indicated a clear "lift off" point, which was very close to the applied lateral boundary stress. This was considered a strong indication that, at least as far as the variation in lateral stress is concerned, specimens of cohesive soils with minimum disturbance can be prepared and tested in the chamber.

Anderson et al. (1991) describe the design of a calibration chamber suitable for preparation of uniform clay beds in which the performance of full-size field test devices may be studied. The chamber was designed so that uniform clay beds can be prepared from a slurry by means of one-dimensional (K_0) consolidation or triaxial consolidation. The prepared clay beds could be subjected to either isotropic stresses or different vertical and horizontal stresses. The calibration chamber had a diameter of 785 mm and the authors performed full-size pressure meter tests using a pressure meter with a diameter of 80 mm, which gives a ratio of chamber diameter to pressure meter diameter of 9.8 (d_{chamb}/d_{press}= 9.8).

To investigate the influence of factors such as soil type, stress history, penetration boundary conditions and filter location, eight cone penetration tests in a calibration chamber were carried out by Kurup (1993), Kurup et al. (1994). The tests were carried out either under boundary conditions of constant vertical and lateral stress or constant vertical stress and zero lateral strain. The chamber had an inner diameter of 525 mm and an inner height

of 815 mm. In the tests, a piezocone (PCPT) with a cross area of 100 mm^2 (d_{cone} = 11.3 mm) and a quasi-static cone (QCPT) with a cross area of 127 mm^2 (d_{cone} = 12.72 mm) were used. Tests were performed in three different locations: in the centre, 75 mm from the centre and 150 mm from the centre. The PCPTs were conducted at least 112 mm from the inner wall (wall distance/ cone radius = 19.8). The tip resistances from the PCPTs at the different locations did not show any noticeable difference and the authors therefore concluded that the influence of boundary effects and interference from adjacent tests could be ignored. The spatial pore pressure distribution in the specimens also indicated that the specimen size and boundary conditions had no significant influence on the cone penetration test results for diameter ratios ("d_{chamb}"/d_{cone}) greater than 15. However, this may not be the case for heavily overconsolidated specimens. The authors observed an influence of the initial stress conditions on the piezocone results, which is described in section 2.6.4.

To acquire a better understanding of the relationship between the Marchetti dilatometer readings and soil parameters, particularly the effect of the horizontal stress, Smith (1993) conducted nine tests in a calibration chamber. The calibration chamber allowed clay specimens one metre in diameter and one metre in height to be prepared. The relationship from an analysis of an undrained cylindrical cavity expansion proposed by Yu (1990) was used to determine the required width of the clay bed in order to prevent large distortions reaching the boundaries. A research dilatometer with a width of 95 mm and a thickness of 14 mm was used in the tests. The results from the study indicated, among other things, that the P_0 reading of the dilatometer is mainly controlled by the undrained strength and the level of the horizontal stress.

2.2.2 Tests in triaxial cells

A few researchers have conducted tests with miniature test devices in triaxial cells.

Kenney et al. (1965) give a description of a laboratory research apparatus, called the vane-triaxial apparatus, which enables vane tests to be performed on soil specimens mounted in a triaxial compression cell. The vane-triaxial apparatus was constructed in conjunction with a laboratory investigation of the vane test, which was initiated as part of a research programme dealing with the undrained shear strength of soils. The vane had blades made of 0.33 mm thick spring bronze and were fixed to a 2.0 mm diameter silver steel shaft. To eliminate friction between the shaft and the soil, the shaft

was enclosed in an oil-filled stainless steel tube with an inner diameter of 2.1 mm. Standard Geonor triaxial cells with a pedestal area of 2,000 mm^2 were used. Vanes of several shapes and sizes were used, but for the common vane shape (h = 2d) the height-diameter dimensions were 16 x 8 mm^2. The research work carried out with the vane-triaxial apparatus addressed three different aspects of the vane test i.e. failure surface, shear stress distribution and rate of strain.

To simulate conditions under a test embankment and to study the effect of various consolidation pressures on the vane strength, Law (1979) performed vane tests with a triaxial-vane apparatus, which was a combination of the triaxial cell and the laboratory vane test apparatus. The vane had blades made of 0.28 mm nichrome, was 20 mm high and had a diameter of 10 mm. A coupling between the rod and the vane made it possible to separate the rod friction torque from the total torque. The specimens in the triaxial cell were 80 mm high and had a diameter of 36.5 mm. The series of tests conducted with the vane-triaxial apparatus and the results is presented in section 2.6.3.

Pamukcu and Suhayda (1988) used a triaxial vane device equipped with a computer-aided data acquisition system to detect low strain shear deformations under quasi-static loading conditions. The results were compared with results from resonant column tests. The apparatus consisted of a large triaxial cell connected to a constant pressure unit and a laboratory vane machine. The vane would initially rest on recesses inside a housing. Four perpendicular slits situated around a circular hole at the bottom of the cap would allow insertion of the vane into the specimen. The diameter of the kaolinite specimens used in the triaxial vane device was 50 mm and the vane was 10 mm in diameter and 20 mm in height with a blade thickness of 0.25 mm. The authors found the same trend for the dynamic and static moduli reduction curves as other authors and that the ratio of maximum static shear modulus to maximum dynamic shear modulus was around 0.85.

2.3 Determination of the undrained shear strength of clay

2.3.1 Field tests

2.3.1.1 *Field vane test*

In 1947, Cadling invented the vane borer (later called the field vane test) for *in situ* measurements of the undrained shear strength. The vane borer, its method of application, the shape, failure and stress distribution across

the surface of rupture, the influence of various factors, as well as calculation of the shear strength and interpretation of test results, are described by Cadling and Odenstad (1950).

In this study the evaluation of the undrained shear strength from the field vane test was made done according to the proposal from Cadling and Odenstad (1950). This evaluation is also used in the recommended Swedish standard for the field vane test (SGF, 1993).

$$c_u = \frac{6M_{\max}}{7\pi D^3}$$

The calculation is based on the assumptions that the surface of the rupture is a circular cylinder surrounding the vane and that the height and diameter of this cylinder are equal to those of the vane. Furthermore, the stress distribution at the maximum torsion moment (M_{max}) is assumed to be uniform across the whole surface of the cylinder, which also includes its end surfaces.

In order to obtain the undrained shear strength of the soil, the strength value from the field vane test is today corrected in the light of empirical experience, based on the liquid limit. At a technical meeting in 1969, (Swedish Geotechnical Institute, 1970) the first correction factor, μ, based on the liquid limit was recommended. In 1984, a new correction factors in accordance with Figure 2-1; $c_u = \mu \cdot \tau_v$ were recommended (Larsson et al., 1984). This correction, which is also based on the liquid limit, is valid for normally consolidated and slightly overconsolidated clay.

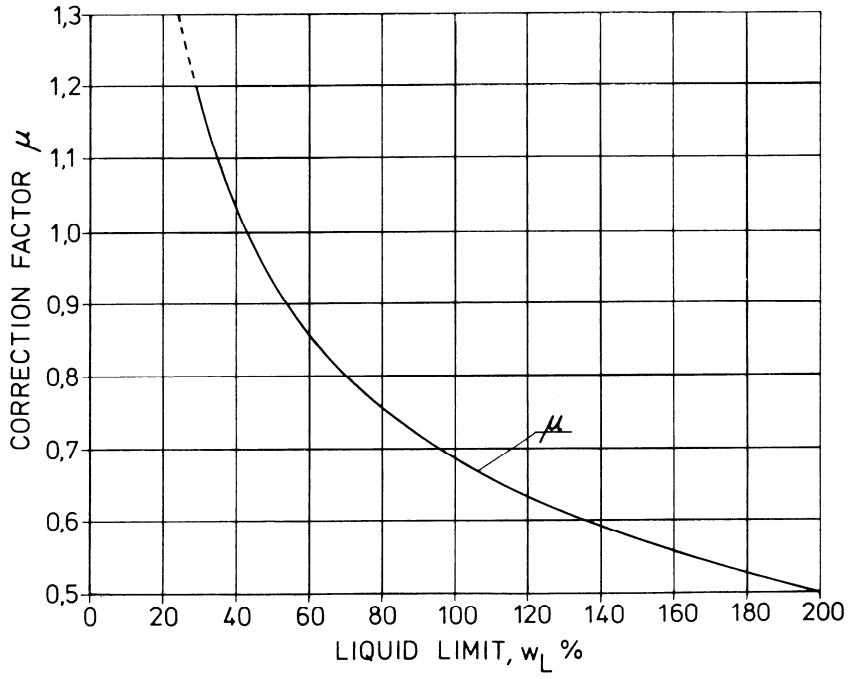

Figure 2-1 Correction factors for τ_v (Larsson et al. 1984).

Larsson and Åhnberg (2003), proposed that an extra correction, μ_{OCR}, should be applied in overconsolidated soils (OCR > 1.5). This correction should be approximately $\mu_{OCR} \approx OCR^{-0.15}$. However, as the ordinary correction with respect to the liquid limit is based on soils with an overconsolidation ratio of about 1.3, corrections for overconsolidation up to this value can be assumed to be included. The evaluation of the undrained shear strength from field vane tests thereby becomes:

$$c_u = \tau_v \cdot \mu_{w_L} \cdot \mu_{OCR} \qquad \text{where} \qquad \mu_{OCR} = \left[\frac{OCR}{1.3}\right]^{-0.15}$$

2.3.1.2 *Piezocone test*

Larsson and Mulabdic (1991) and Larsson (1993) proposed an evaluation of the undrained shear strength from piezocone tests, based on the net tip resistance. The formula below, which has also been used in this project, could be applied in non-fissured, normally consolidated and slightly overconsolidated clays.

$$c_u = \frac{q_T - \sigma_{v0}}{13.4 + 6.65 w_L}$$

The undrained shear strength evaluated in this way is intended to be equal to the undrained shear strength from corrected field vane tests, corrected fall cone tests and direct simple shear tests.

Larsson and Mulabdic (1991) also proposed an alternative method for evaluation of the undrained shear strength based on the generated excess pore water pressure measured at the standard filter location just above the conical tip:

$$c_u = \frac{\Delta u_{face}}{16}$$

These formulas could be used in normally consolidated and slightly overconsolidated clays.

Larsson and Åhnberg (2003) proposed that the evaluation method should be used with an extra correction for overconsolidation. The undrained shear strength evaluated from piezocone test results thereby becomes:

$$c_u = \frac{q_T - \sigma_{v0}}{13.4 + 6.65 w_L} \left[\frac{\sigma'_{cv}}{1.3 \sigma'_{v0}} \right]^{b-1}$$

The empirical value of $b = 0.8$ has been used in this study.

2.3.2 Laboratory tests

2.3.2.1 *Direct simple shear test*

The direct simple shear tests in this project have been carried out according to the proposal in the Swedish national rules for slope stability analysis (1995). The samples were first consolidated for stresses close to the preconsolidation pressure ($0.85 \cdot \sigma'_{cv}$), and thereafter unloaded to the *in situ* vertical stress. The specimen was then sheared with a constant rate of deformation. The shearing rate was about 0.6% of the sample height per hour.

Evaluation of the undrained shear strength from direct simple shear tests took place according to the recommendations of the Swedish Geotechnical Society: SGF Notat 2:2004. The shear stress is plotted versus the shear deformation and the undrained shear strength is evaluated at the maximum shear stress or at 15% strain.

2.4 Measurement of preconsolidation pressure and horizontal stress

2.4.1 CRS oedometer test

CRS oedometer tests have been carried out to determine the preconsolidation pressure, the oedometer modulus, the permeability and the coefficient of consolidation. The preconsolidation pressure has been estimated according to Swedish practice using the method proposed by Sällfors (1975). The tests were performed using the standard deformation rate of 0.0024 mm/min and the monitored strain was plotted on a graph with effective stress on the horizontal axis and strain on the vertical axis, both on linear scales. Evaluation of the consolidation parameters from a CRS oedometer test according to Swedish practice is shown in Figure 2-2 (Sällfors, 1975, Larsson, 1981, Larsson and Sällfors, 1985). The parameters thus obtained are the preconsolidation pressure σ'_c, the effective stress where the modulus starts to increase again, σ'_L, the oedometer modulus M_L and the modulus number M'. The permeability, k, and the parameter β_k are also obtained. The coefficient of consolidation, c_v, is a function of the modulus and the permeability:

$$c_v = \frac{k \cdot M}{g \cdot \rho_w}$$

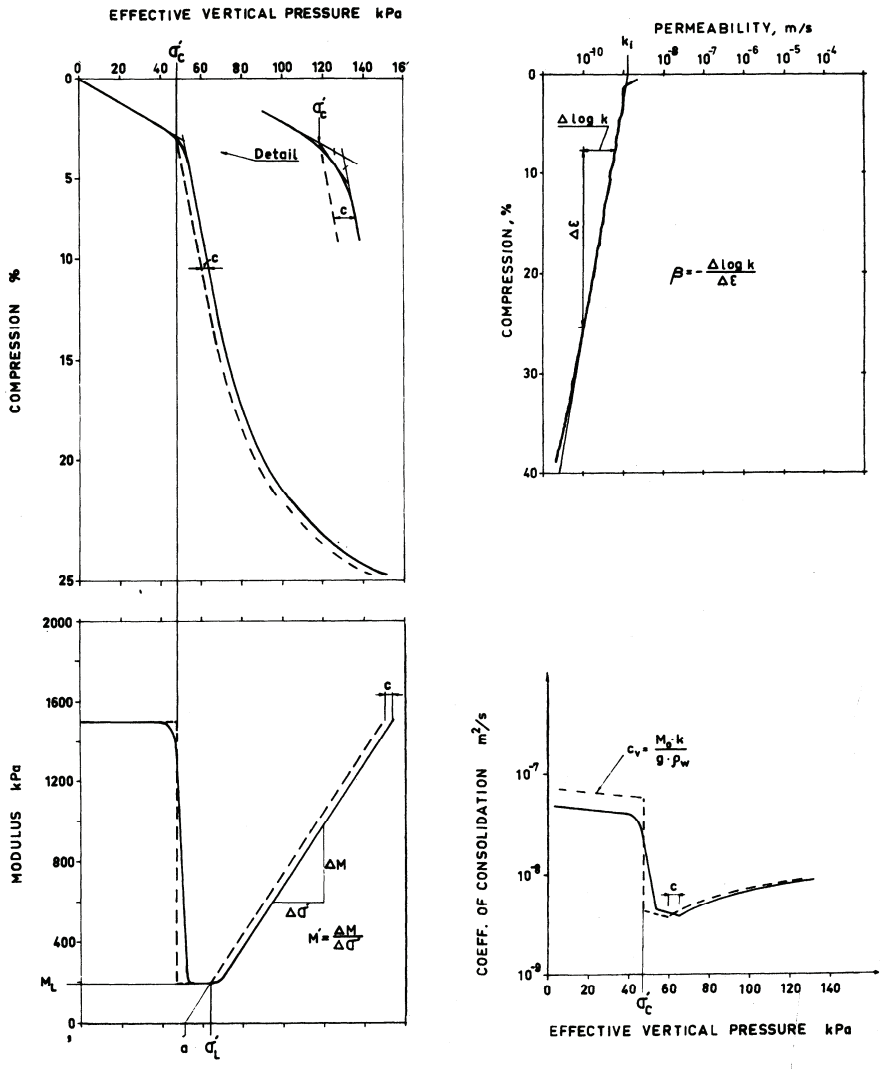

Figure 2-2 Interpretation of the CRS oedometer test (Larsson and Sällfors, 1985).

2.4.2 Dilatometer test

Dilatometer tests have been carried out to determine the earth pressure coefficient, K_0, of the soil. The earth pressure coefficient is estimated empirically from a horizontal stress index, K_D. According to the original relationship by Marchetti (1980), K_0 could be estimated from the relationship:

$$K_0 = \left[\frac{K_D}{1.5}\right]^{0.47} - 0.6$$

However, the basis of this relationship was limited and the reference values uncertain. Since then other relationships have been proposed by other authors (e.g. Lacasse and Lunne, 1988, Powell and Uglow, 1988). A relationship based on experience from Swedish clays was proposed by

Larsson and Eskilsson (1989). This relationship, which is normally used in Swedish practice, has been used in this project.

$$K_0 = 0.24 \cdot K_D^{\,0.84}$$

This relationship normally gives values within ± 25% of the reference values.

2.5 Stress conditions in clay slopes

Rankka (1994) investigated the *in situ* stress conditions in clay slopes and how they vary during changes, such as seasonal variations in pore pressures or excavation and filling of earth material. Seven test sites were studied: six sites in the Gothenburg area and one site situated 235 km north of Gothenburg. The test sites were used primarily for three types of study. One group included natural slopes, where studies of total stress changes, owing to seasonal variations in pore pressures and fluctuating water levels, were carried out. This group comprised the sites at Partille and Ugglum. In a second group, the stability was increased either by excavating in the active zone or filling in the passive zone. Studies of these conditions were carried out at Alafors, Ugglum and Vålberg. The third group contained slopes formed by excavation in an area that was originally horizontal ground. This was carried out at Hede.

As regards the horizontal stress distributions, Rankka (1994) concludes that higher total horizontal stresses were measured in the passive zone compared to the active zone. The differences varied between 2 and 30 kPa. The total stress increase with depth was smaller in the active zone than in the passive and middle zones. Moreover, by plotting the effective horizontal stress against the height above sea level, the author found that the stresses at a given height above sea level were almost the same irrespective of where on the slope the measurements were made. This means that the effective horizontal stresses have not been changed significantly by the erosion that formed the slope and the associated vertical unloading.

At the Partille test site, which is studied further in this project, the stresses measured at the deepest levels (13 m and 14.5 m depth) in the active zone were considered to be small compared to measurements at the other test sites. This was believed to be due to installation difficulties for deeply situated cells. Cells placed at shallow depths in the passive zone, i.e. less than 5 m (Ugglum and Partille), indicated stresses lower than the stress

situation during deposition. This was explained by a study of the stress paths, see Figure 2-3. A stress path for an erosion process involving unloading of the whole area is supposed to go from 1 to 2. Further erosion in the passive zone results in a further decrease in effective vertical stress and possibly in an increasing horizontal stress (stress path going from 2 to 3). At shallow depths, these changes may result in stress paths reaching the failure line and any further decrease in the effective vertical stress is accompanied by a relatively large decrease in effective horizontal stress (stress path from 3 to 4).

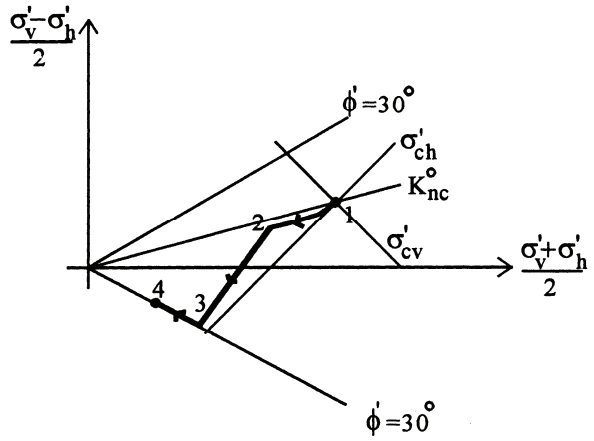

Figure 2-3 Stress path for clay at shallow depths in a passive zone due to an erosion process (Rankka, 1994).

On the basis of the measurements, Rankka suggested that the effective horizontal stress should be predicted first by estimating the original position of the ground surface and the corresponding pore pressure conditions at that time. The initial stresses should then be calculated with a careful estimate of the K_{0NC} value. The effective stress changes from the initial condition due to erosion or excavation are limited to vertical stresses, whereas the effective horizontal stresses are changed only if the stress conditions fall outside the yield envelope.

Rankka (1994) also studied changes in horizontal stresses due to seasonal variations in pore pressures. These studies show that the total horizontal stresses and the pore pressures generally follow each other well. Therefore, the K values and the pore pressures vary simultaneously. Two main conclusions were drawn from the studies of stress paths. One is that seasonal variations in the groundwater table result in stress paths, which mainly move inwards and outwards between the lines representing σ'_h = constant and $(\sigma'_v-\sigma'_h)/2$ = constant. Close to a stream with variations in water level, the stresses are mainly affected by the related changes in pore pressures. The horizontal stresses do not change as much as the pore

pressures when the latter change rapidly, which results in stress paths moving almost horizontally in the plot above.

At three test sites (the Hede, Lärje and Ugglum test sites) horizontal stresses were measured both directly using earth pressure cells and indirectly using dilatometer tests. According to the author, at the Hede test site the dilatometer test evaluation gave total horizontal stresses 6-15% higher (5-15 kPa) than those measured using the earth pressure cells. At the Lärje test site the dilatometer gave a lower stress than that measured with the cell at the toe of the slope (difference 25%) and higher than that measured with the cell at the crest (difference 36%). At the Ugglum test site the dilatometer gave both higher and lower values than those measured by cells (differences up to 13%).

Studies of changes in horizontal stresses due to man-made changes in the slope geometry were also carried out. These measurements indicated that man-made changes only have an effect on the horizontal stresses and the pore pressures in the area closest to the earthworks.

2.6 Influence of stress conditions on the shear strength

2.6.1 Effect of anisotropy

The shear strength anisotropy in clay deposits is a well-known factor, which has been described by several authors (e.g. Bjerrum, 1973, Ladd and Foot, 1974, Ladd et al. 1977, Jamiolkowski et al., 1985). It can be divided into two components. One component is the inherent anisotropy, which is the result of major differences in soil structure that arise during formation of the soil. Oblong and flaky particles tend to become oriented in a horizontal direction during one-dimensional deposition and subsequent loading. Varved clays that have alternate layers of "silt" and "clay" have a high degree of inherent anisotropy. The other component is a stress-induced anisotropy, occurring whenever the effective consolidation stresses are not equal in all directions, $K_{0NC} \neq 1$. This results from the fact that different increments of shear stresses are required to produce failure as the major principal stress at failure varies between the vertical and the horizontal direction (Ladd et al., 1977). In engineering practice, it is the combined anisotropy resulting from both the inherent and the stress system-induced components that is of main interest.

Larsson (1977) proposed a model for Scandinavian soft clays from which the undrained shear strength in planes with different orientation could be

calculated. The basis for the model is that a horizontal plane has been prestressed for the preconsolidation pressure σ'_c and a vertical plane for a stress of $K_{0NC} \cdot \sigma'_c$. A plane with an orientation where the angle between the plane and the horizontal plane is α will be prestressed for the normal stress:

$\sigma'_\alpha = \sigma'_c(\cos^2 \alpha + K_{0NC} \cdot \sin^2 \alpha)$ see Figure 2-4.

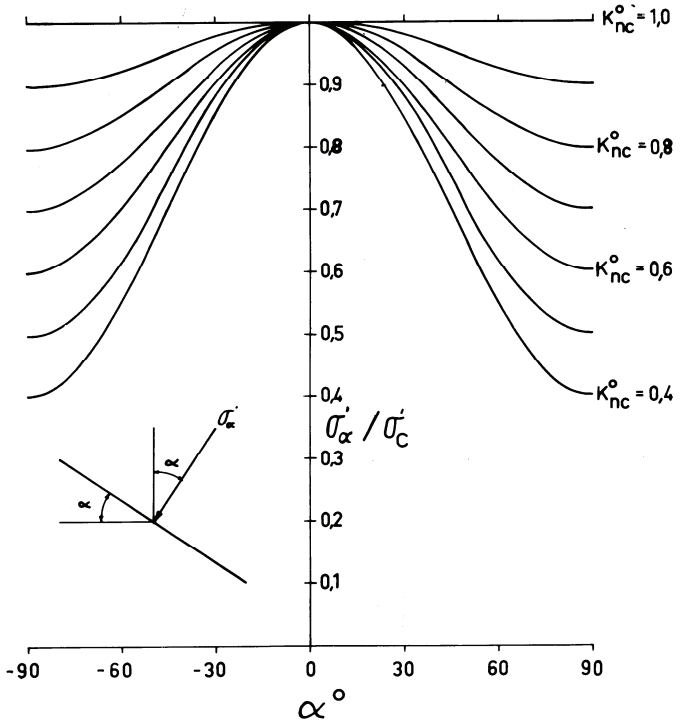

Figure 2-4 Effective prestress in planes with different orientation (Larsson, 1977).

This prestress is a yield stress and in undrained shear of soft clay the pore pressure development will be such that σ'_α can be reached but not exceeded. If σ'_α is the major stress in a shear test, failure will occur along a plane with the angle $(45 - \phi'/2)$ between the plane and the direction of σ'_α. Larsson (1977) used the empirical value $\phi' = 30°$, the result being that the maximum undrained shear stress in any plane can be calculated from $\frac{\sigma'_1 - \sigma'_3}{\sigma'_1 + \sigma'_3} = \sin\phi'$ which for $\phi' = 30°$ gives: $\tau_{fu} = \frac{\sigma_1 - \sigma_3}{2} = \sigma'_\alpha / 3$, see Figure 2-5.

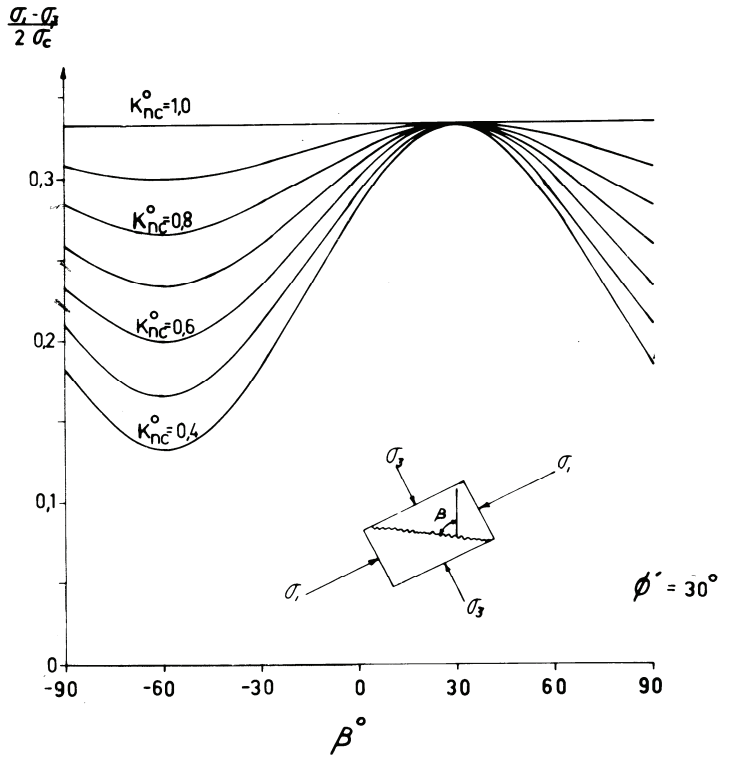

Figure 2-5 Undrained shear strength in planes with different orientation (Larsson, 1977).

In Figure 2-5, β is the angle between the failure plane and the vertical direction. The angle β = 30° corresponds to an active triaxial compression test, β = 60° corresponds to a passive triaxial extension test and β = ±90° corresponds to a direct simple shear test. The model applies to clay deposits with a fairly flat horizontal ground surface during consolidation where the clay has consolidated for its own weight and possibly an even widespread surcharge, and where the major and minor principal preconsolidation pressurees are thereby vertical and horizontal.

2.6.2 Effect of stress history

The fact that many cohesive soils exhibit a behaviour that can be normalised with regard to the preconsolidation pressure was observed as early as in the 1940s and was elaborated in the early 1960s in work at Imperial College using remoulded clays and at Massachusetts Institute of Technology (MIT) on a wide range of cohesive soils. It was found that the results of laboratory tests on clay specimens with the same overconsolidation ratio (OCR), but with different consolidation stresses and therefore different maximum past pressures, exhibit very similar strength and stress-strain characteristics when normalised with regard to the consolidation stress (Ladd & Foot 1974, Ladd et al. 1977). This is

illustrated in Figure 2-6 which shows idealised stress-strain curves for isotropically consolidated clay with two different consolidation stresses (σ'_c). When normalised using $(\sigma_1-\sigma_3)/\sigma'_c$, the two plotted curves coincide. The normalised plot thus obtained can be used to represent the behaviour of other normally consolidated specimens of the same clay with different σ'_c values when sheared in the same type of test. In practice, there is usually some divergence in the normalised plots obtained for different consolidation stresses due to other factors and also due to heterogeneity in the soil.

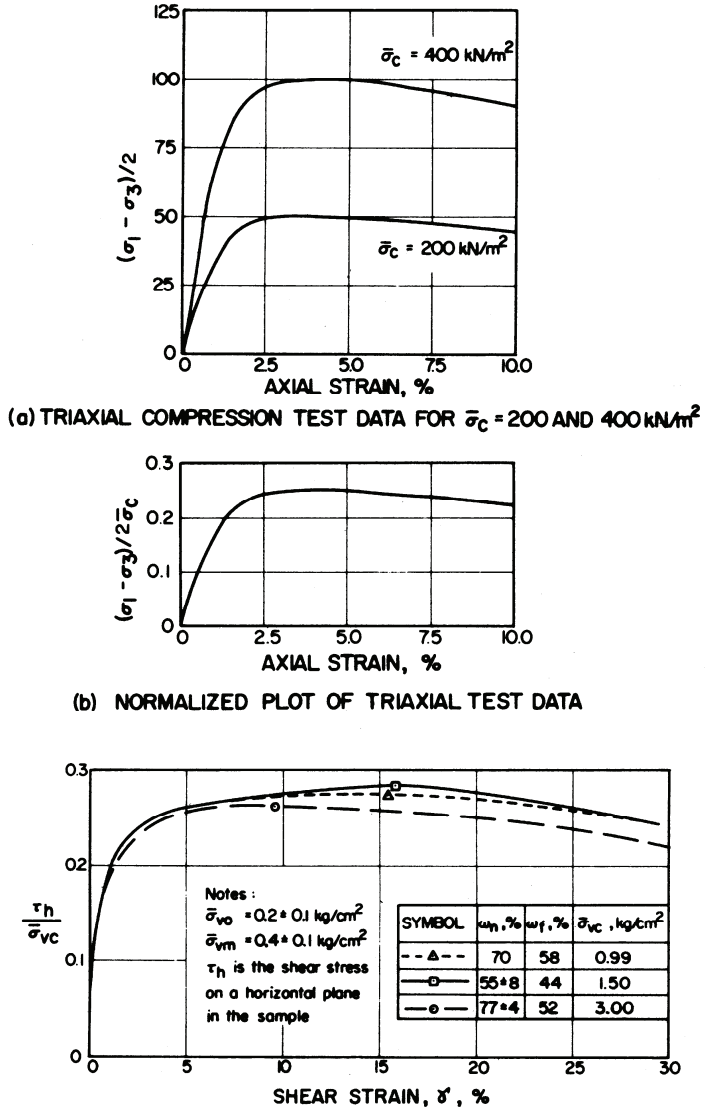

Figure 2-6 Normalised behaviour using idealised triaxial compression test data for homogeneous clay and direct simple shear test data for normally consolidated Maine organic clay (Ladd and Foot, 1974).

Nevertheless, the variations in the undrained shear strength with preconsolidation pressure and overconsolidation ratios are in most general models, directly or indirectly, reasonably well defined by the expression

$$c_u = a \cdot \sigma'_v \cdot OCR^b \text{ alt. } c_u = a \cdot \sigma'_c \cdot OCR^{b-1}$$

(e.g. Ladd et al. 1977, Jamiolkowski et al. 1985)

These relationships are obtained in both direct simple shear tests and triaxial tests in the laboratory. Results presented by, for example, Larsson (1980), Jamiolkowski et al (1985) and Mayne (1988), show that the factor *a* is about 0.33 for active triaxial tests on clay. For direct simple shear tests and passive triaxial tests, the factor *a* has been found to vary with the liquid limit. An average value of 0.22 is often used in the case of direct simple shear. The *b* factor is normally between 0.75 and 0.85 in both triaxial tests and direct simple shear tests (Jamiolkowski et al 1985 and Mayne 1988). It is normally set at 0.8 according to the empirical pattern.

Based on these relationships, the SHANSEP procedure – stress history and normalised soil engineering properties – (Ladd and Foot, 1974, Ladd et al. 1977, Jamiolkowski et al. 1985) was proposed as a design procedure for estimating the *in situ* undrained properties of a clay deposit. It consists of the following steps for any given uniform layer and required mode of failure:

1. Establish the stress history, i.e. the profiles of σ'_v and σ'_{cv}, which determines the range of OCR values for which data are required.
2. Perform a series of CK_0U direct simple shear tests on specimens consolidated beyond the *in situ* preconsolidation pressures, approximately to stresses 1.5 times, 2.5 times and 4 times the *in situ* σ'_{cv}. A clay exhibiting normalised behaviour will yield a constant value of c_u/σ'_v. If c_u/σ'_v varies consistently with stress the normalised soil parameter (NSP) concept does not apply to the clay.
3. For a clay exhibiting normalised behaviour use the minimum value of σ'_v as the laboratory σ'_{cv} and perform CK_0U direct simple shear tests at OCR values of 2±0.5, 4±1 and 6±2. Establish normalised soil parameter versus OCR relationships, e.g. c_u/σ'_v versus OCR.
4. Use these NSP relationships and the stress history information to determine profiles of the undrained shear strength.

According to experience, Swedish clays normally exhibit a behaviour that can be normalised in relation to the natural preconsolidation pressure and therefore step two in the SHANSEP procedure is seldom carried out in

Sweden. Furthermore, to avoid destroying the structure of the highly compressible soft clay, loading to such high pressures beyond the *in situ* preconsolidation pressures as stipulated in the SHANSEP procedure is normally not conducted in Sweden. In general, reconsolidation just below the *in situ* preconsolidation pressures is carried out and thereafter unloading to various OCR values [1]. CK_0U direct simple shear tests and/or triaxial tests are then carried out at these OCR values.

2.6.3 Effect of stress conditions on the vane shear strength

The influence of various factors such as vane shape, time to failure, etc. on the results from the field vane test have been studied by many researchers over the years (e.g. Aas, 1965, Torstensson, 1973). The research described below includes studies or descriptions concerning the influence of stress conditions on the shear strength determined by the vane test.

In his general report, Bjerrum (1973) states that if c_{uv} and c_{uh} are the values of the shear strength that can be mobilised on a vertical and a horizontal plane respectively, the shear strength measured by a standard vane with a height equal to twice the diameter will be:

$$c_u = 0.86 \cdot c_{uv} + 0.14 \cdot c_{uh}$$

In addition to a correction factor for the time effect (μ_R), Bjerrum proposes a factor (μ_A) correcting for the anisotropy of the clay and its variation depending on the inclination of the slip surface. The value will vary from point to point along a curved sliding surface depending on its inclination. The less plastic the clay the larger the value. Based on an analysis of a number of embankment failures in soft clay in different parts of the world, Bjerrum (1973) proposes the correction factor μ as a function of the plasticity index of the clay, Figure 2-7.

[1] In practice, the preconsolidation pressure is determined by means of oedometer tests and the specimens in the strength tests are consolidated for stresses safely lower than this value in order to avoid destroying the structure of the soil on reconsolidation, e.g. Commission on slope stability (1995) and Swedish Geotechnical Society (2004).

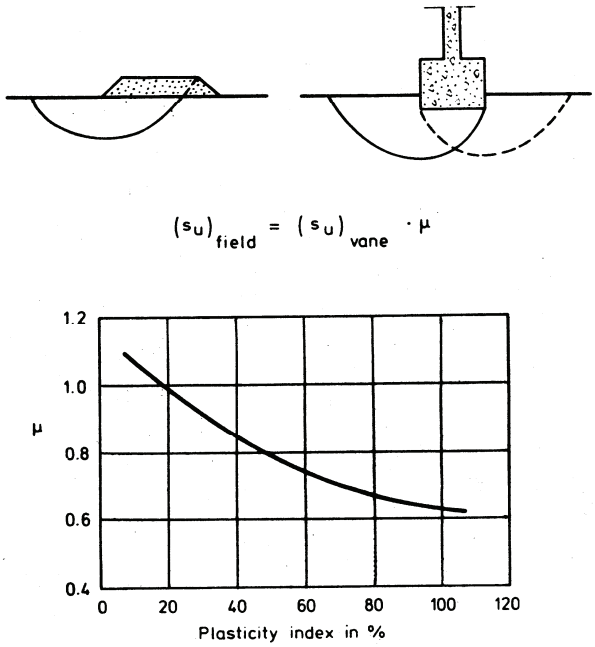

Figure 2-7 Principle of analysis of the stability of embankments and bearing capacity of footings on soft clay based on corrected vane shear strength (Bjerrum, 1973).

In 1969, in Sweden, the experience gained from the field vane test and comparisons between the undrained shear strength determined by fall cone tests and field vane tests had made it clear that the correction factors used for the fall cone test should also be applied to the vane test (Swedish Geotechnical Institute, 1970). Other correction factor proposals for the vane shear strength have been suggested (e.g. Pilot, 1972 and Helenelund, 1977). The currently used correction factors in Sweden for normally consolidated and slightly overconsolidated clays were proposed by Larsson et al. (1984), see Figure 2-1, section 2.3.1.1. The Swedish correction factor μ is a function of the liquid limit of the clay and should be applied to both fall cone tests and field vane tests. It can be calculated as

$$\mu = \left(\frac{0.43}{w_L}\right)^{0.45} \geq 0.5$$, see also Figure 2-1.

In a study of overconsolidated clay from three test sites, Larsson and Åhnberg (2003) found that there was a need for an extra correction of the undrained shear strength measured by means of a field vane test for overconsolidation. The authors propose the correction:

$$\mu_{OCR} = \left(\frac{OCR}{1.3}\right)^{-0.15}$$

Rosenfarb and Krizek (1978) studied the anisotropic strength behaviour of kaolin clay subjected to different stress conditions in vertical and horizontal vane tests in a consolidometer (see also section 2.2.1). Clay slurries with flocculated and dispersed intrinsic fabrics were consolidated under conditions of no lateral strain. A total of six tests were conducted on clay blocks consolidated to vertical effective stresses of 220, 440, and 700 kPa. Both the vertical and horizontal vane tests were performed with a rotation rate of approximately 20º per minute. After failure, the vane was rotated manually about five turns and a second strength determination was made on the "remoulded" clay. Average undisturbed strength values for each vane orientation are shown in Figure 2-8. Among other things, the authors concluded that independent of fabric or vane orientation, the development of the *in situ* vane shear strength was nonlinear with respect to the effective major principal consolidation stress. They also concluded that vanes oriented perpendicularly to the direction of the principal consolidation stress yielded higher strength than those positioned parallel to it.

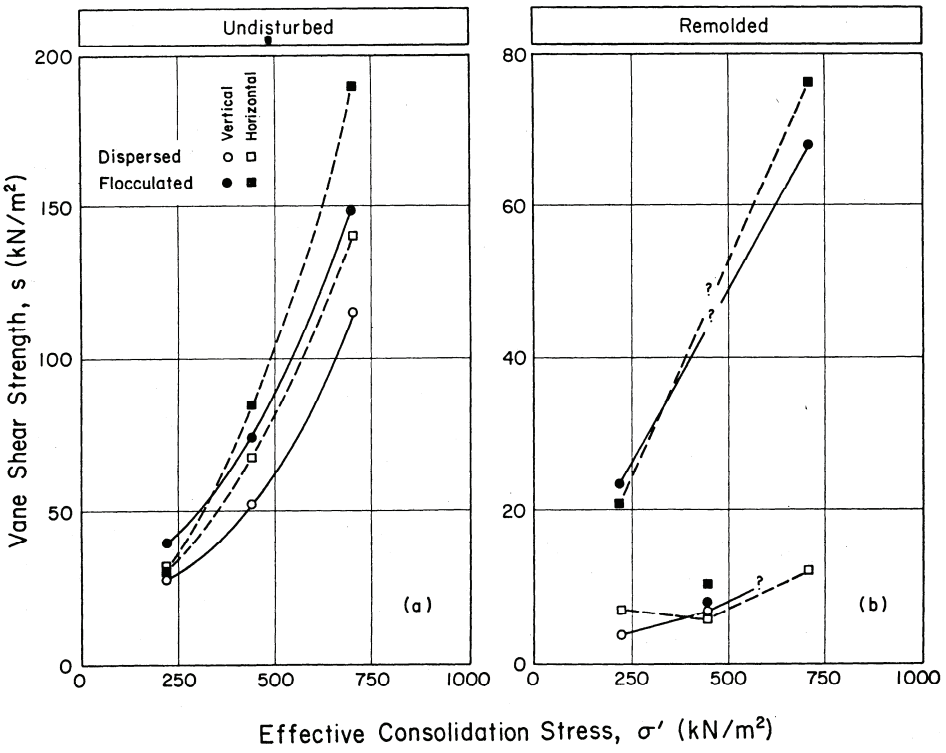

Figure 2-8 Effect of consolidation stress and intrinsic fabric on the vane shear strength (Rosenfarb and Krizek, 1978).

Law et al. (1977), conducted a series of field vane strength measurements in the subsoil beneath four fills of different geometry constructed on Champlain Sea clays near Ottawa, Canada. From these measurements the authors concluded that the field vane strength did not change for up to 16 years after placement of the fill, independent of loading geometry and load

intensities up to values moderately beyond the preconsolidation pressure. However, triaxial tests did show that there had been a strength increase beneath the fills. Field evidence and preliminary analyses also supported the view that there was a strength gain under the sustained loading.

To simulate conditions under a test embankment, Law (1979) studied the influence of the vertical and horizontal stresses on the vane shear strength. This was done using an apparatus that was a combination of the triaxial cell and the laboratory vane test machine (see also section 2.2.2). The specimens were 36.5 mm in diameter and 80 mm high and the tests were conducted on soft Leda clay, a soft, sensitive, silty marine deposit, lightly overconsolidated with a liquid limit of 48%.

Three series of tests were conducted. In the first series, the change in shear strength in conjunction with a change in all-around effective consolidation pressure was studied. In the second series, the influence of a change in horizontal effective consolidation pressure was studied and in the third the influence of a change in vertical effective consolidation pressure. The test results showing an increase in the all-around consolidation pressure showed a steady increase in torque with consolidation pressure throughout the studied pressure range. For example, with an increase in the all-around consolidation pressure from 40 to 80 kPa, the measured torque increased by 35-55%. A similar relationship was obtained at an increase in the horizontal consolidation pressure when the vertical pressure was kept constant, see Figure 2-9. Within the exemplified pressure range, the increase in the torque was then about the same. On the other hand, the tests using constant horizontal consolidation pressure and an increase in the vertical consolidation pressure showed only a small increase in the torque with the vertical pressure, see Figure 2-9. Within the same pressure range the increase was 0-5%.

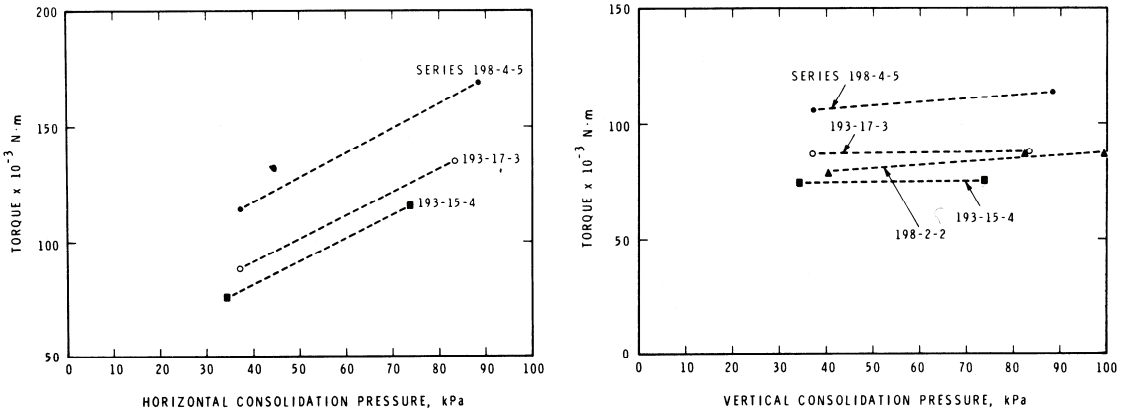

Figure 2-9 Measured torque versus horizontal consolidation pressure at constant vertical consolidation pressure and measured torque versus vertical consolidation pressure at constant horizontal pressure. (Law, 1979).

Law concluded that the shear strength from the vane tests is relatively insensitive to changes in the vertical consolidation pressure, but increases steadily with an increase in the horizontal and the all-around consolidation pressure.

Almeida and Parry (1983 and 1985) conducted vane, penetrometer and piezocone tests in reconstituted clay in a consolidometer to provide correlations between shear strength, cone resistance, overburden pressure and overconsolidation ratio (OCR), see also sections 2.2.1 and 2.6.4. Kaolin clay cakes were prepared at OCR values of 1, 3 and 10 and Gault clay at OCR values of 1, 1.9 and 7. Vane tests were performed at five depths for each applied pressure. The authors found, among other things, that the normalised, undrained shear strength increased with increasing OCR, that the increase was greater for Gault clay than for kaolin and that the variation in the vane shear strength with OCR for kaolin agrees with the undrained shear strength measured in isotropically consolidated triaxial tests in another study.

Aas et al. (1986) observed the influence of an overconsolidation ratio on the field vane strength and proposed an elaboration of the earlier correction curve (e.g. Bjerrum, 1973). Correlations were made with regard to plasticity index, field vane strength normalised to the *in situ* effective overburden stress, and whether the clay was considered to be "young, aged or overconsolidated". The field vane strength was compared to the average laboratory strength based on the average of triaxial compression, direct simple shear and triaxial extension tests. Data from a number of well-documented case records were used as an illustration of the applicability of the method.

Garga and Khan (1992) compared the undrained shear strength of an overconsolidated weathered crust ($K_0 > 1$), determined using the *in situ* field vane test, direct shear tests on horizontal and vertical specimens 60 mm square in cross section and 20.5 mm height and triaxial compression tests, isotropically consolidated and anisotropically consolidated to *in situ* stress state. The reason for the study was that several researchers had observed significantly higher values for the undrained shear strength (c_u) from field vane tests (FV) than from conventional laboratory tests in this type of soil. In the comparison, Garga and Khan (1992) separated the shear stress distribution on the cylindrical vertical surface from the horizontal (top and bottom) of the field vane. On the vertical surface they used the conventional assumption of a rectangular stress distribution. For the end stress distribution (top and bottom) they assumed plastic shear stress distribution, as shown in Figure 2-10, since the soil showed strain-softening behaviour in triaxial (CK_0UC) and direct shear tests.

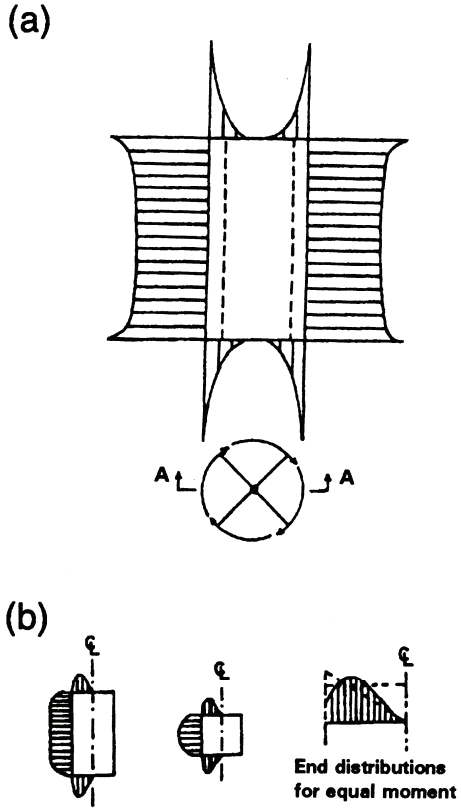

Figure 2-10 Stress distribution (from Donald et al. 1977 and Garga and Khan, 1992). Elastic (a) and plastic (b) shear stress distributions.

The undrained shear strength on the vertical surface was evaluated according to:

$$c_{uv} = \frac{M}{\pi D^3}\left(\frac{p_n}{p_n + K_s}\right)\mu_R \mu_D$$

The undrained shear strength on the end surfaces (top and bottom) was evaluated according to:

$$c_{uh} = \frac{M}{\pi D^3}\left(\frac{p_n K_s}{p_n + K_s}\right)\mu_R \mu_D$$

where μ_R and μ_D are correction factors for rate effect and disturbance due to vane insertion, respectively. The value of p_n for strain-softening soil was set at 7.27 from Figure 2-11. The coefficients of horizontal strength (K_s) at various depths were estimated from direct shear tests (DS). The tests were performed on samples oriented in two directions. The first types were conventional tests with the shear plane in the horizontal direction, where the applied normal stress was equal to the *in situ* vertical stress σ_{v0}'. The second type of test was conducted on samples with the shear plane in the vertical direction where the normal stress during shear was equal to σ_{h0}'. The strength anisotropy obtained from DS tests was assumed to be equal to that obtained from FV tests, i.e. $c_{uh}(FV)/c_{uv}(FV) = c_{uh}(DS)/c_{uv}(DS) = K_s$. The undrained shear strength from conventional analysis of the field vane test was also determined (i.e. $c_u = 0.86M/\pi D^3$ assuming uniform stress distributions and isotropic strength with no corrections).

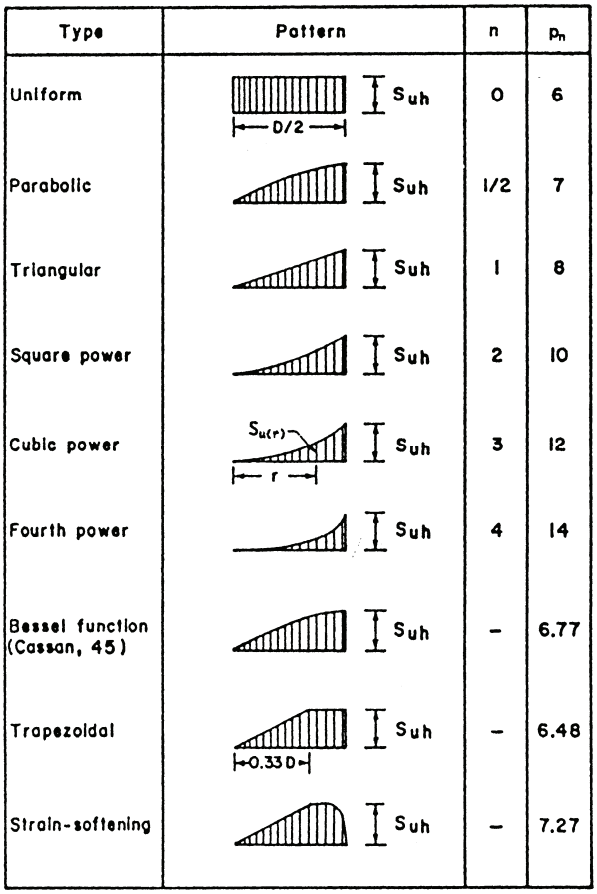

Figure 2-11 End shear stress distribution for rectangular vanes. The factor n is a coefficient that depends on the shape of the shear stress distribution and $p_n = 2(n+3)$ is the shear stress distribution factor for horizontal shear planes (from Silvestri and Aubertin, 1988).

The results from the field vane tests, the direct shear tests and the triaxial tests are shown in Figure 2-12. Garga and Kahn (1992) concluded that the undrained shear strength on the vertical plane c_{uv}(FV), within the crust depth, obtained from field vane tests (FV) is significantly higher than the undrained shear strength on horizontal planes c_{uh}(FV). This is to be expected for a soil with $K_0>1$ where the normal stress (σ_{h0}') on the vertical shearing face is greater than the normal stress (σ_{v0}') on the horizontal shearing face. They also point out that it is evident that the values of c_u(FV) obtained from conventional analysis are close to c_{uv}(FV) but are considerably higher than c_{uh}(FV). Furthermore, they observed that the values of c_{uv} obtained from FV and DS tests on samples with vertical shear planes could be expected to be similar, since the mode of failure on the vertical plane for both of the tests is similar. However, the match between the two values was not as close as between c_{uh}(FV) and c_{uh}(DS). Two reasons may explain that c_{uh}(DS) is less than c_{uh}(FV). Firstly, the lateral stresses cannot be imposed in a DS test and secondly, the specimens could

be easily disturbed, since the soil within the crust was loose, randomly microfissured and composed of small rounded nuggets easily broken into individual pieces.

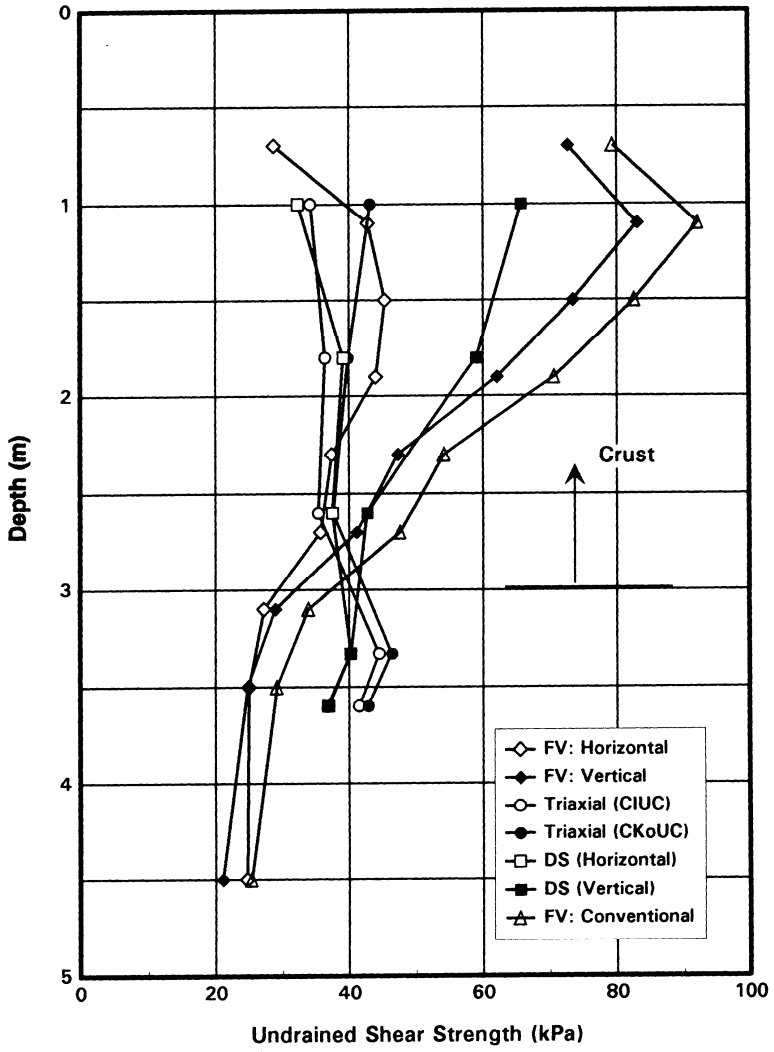

Figure 2-12 Undrained shear strength from field vane (FV), triaxial compression, and direct shear (DS) tests (Garga and Khan, 1992).

2.6.4 Effect of stress conditions on the piezocone shear strength

Cone penetration testing has over the last few decades been established as the most widely used *in situ* testing device for obtaining soil profiles worldwide. This has been achieved mainly by developing empirical correlation and soil classification charts. Good progress has also been made, albeit more slowly, in the understanding of the fundamental mechanics of the cone penetration tests under undrained conditions. The most widely used theoretical methods for analyses of cone penetration tests are (Yu and Mitchell 1998, Yu 2004):

1. Bearing capacity methods

2. Cavity expansion methods
3. Strain path methods
4. Finite element methods

Yu and Mitchell (1998) presented a brief review of these theories for analysis of cone penetration tests in low permeable clays and fully drained sands. They drew the following conclusions regarding cone penetration in low permeable clay:

1. Bearing capacity theories ignore soil compressibility and the influence of stress increase around the shaft of cone penetrometers and are therefore not representative of actual conditions, except perhaps for shallow foundations.
2. Cavity expansion theory provides a simple and yet reasonably accurate method for the analysis of cone resistance. This is because it accounts for soil compressibility (or dilatancy) and influence of stress build-up around the shaft of the cone penetrometer during the cone penetration process. The cavity expansion approach can be used for both clay and sand.
3. The strain path method has also been used with some success to analyse the cone penetration test in undrained clay. The cone factors obtained from the strain path method are approximate, as the equilibrium equations are not fully satisfied.
4. Because of the significant errors and numerical difficulties associated with collapse load calculations using displacement finite element methods, it is unlikely that the incremental finite element method will provide a completely satisfactory solution for cone penetration in soils.

While each of the above four theories may be used alone for cone penetration analysis, better predictions of the cone penetration mechanism may be achieved if some of them are used in combination (Yu, 2004).

The section below focuses on the influence of the initial stress conditions, and in particular horizontal stresses on the cone resistance and piezocone shear strength as described by some authors using the theories mentioned above.

Durgunoglu and Mitchell (1975) found that past studies of the failure mechanism associated with static penetration, both theoretical and experimental, involved mainly flat-ended penetrometers. The effect of penetrometer tip characteristics, as measured by the tip apex angle and surface roughness, on the failure mechanism had not been studied in detail. To provide additional information on the failure mechanism, with

particular reference to the influences of penetrometer tip characteristics, they carried out a series of model penetration tests in sand. They used wedge and cone-tipped penetrometers of different base apex angles (α = 15°, 30°, and 90°, where α is half the apex angle) and surface roughness. From the results of six model tests using wedge-shaped penetrometers, it was established, among other things, that a plane shear zone exists adjacent to the penetrometer base (AOC in Figure 2-13), and the topmost angle of this zone (γ) varies with base roughness. It was also established that there is a radial shear zone adjacent to the plane shear zone. Slip lines in this zone extended to the surface of the sand for the shallow depth (D/B<5) investigated. The authors' conclusion was that a failure surface as shown in Figure 2-13 closely represents the actual failure surface associated with wedge penetration, at least for shallow depths.

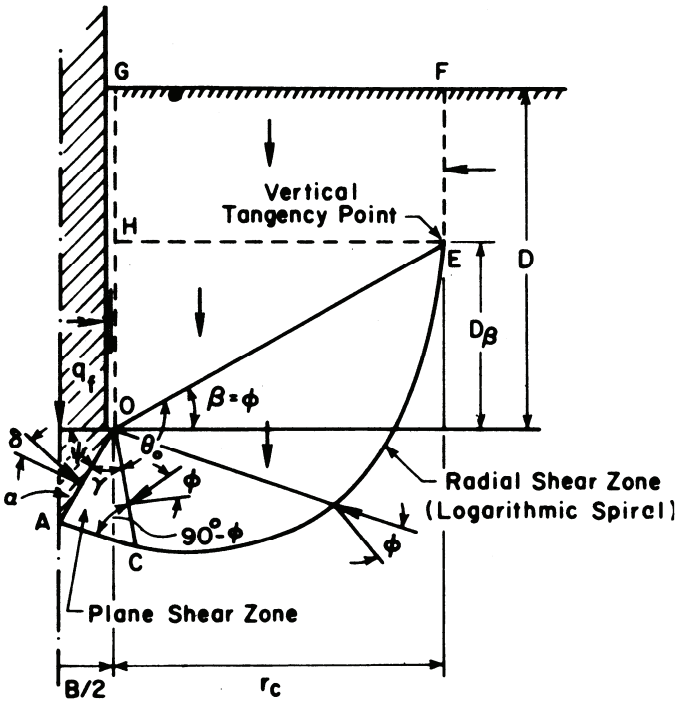

Figure 2-13 Proposed failure mechanism for wedge penetration at large relative depths (Durgunoglu and Mitchell, 1975).

The authors analysed the failure mechanism based on the general bearing capacity equation and the results from the model tests using an equilibrium analysis of the failure zone shown in Figure 2-13. They concluded that both theory and experiment have shown that the resistance to cone penetration into sand depends on cone geometry and size, surface roughness, soil strength parameters, soil compressibility, *in situ* lateral stress and penetration depth.

In describing point resistance of piles, Vesic (1975) stated that "classical" theories for the determination of the unit resistance (q_0), based on plasticity theory alone, should be considered inadequate and should be replaced by more refined, linear or non-linear elastoplastic theories. Classical theories present the solutions for q_0 in the well-known form:

$$q_0 = c_u N_c + q_v N_q \tag{2-1}$$

where c_u represents the strength intercept (cohesion) of the assumed straight-line Mohr envelope, q_v the effective vertical stress in the ground at the foundation level. N_c and N_q are dimensionless bearing capacity factors, related to each other by the equation:

$$N_c = (N_q - 1)\cot\varphi \tag{2-2}$$

According to Vesic (1975), at that time recent research showed beyond doubt that the point resistance is governed not by the vertical ground stress q_v but by the mean effective normal stress q_m, which is related to q_v by the expression:

$$q_m = \frac{1+2K_0}{3} q_v \tag{2-3}$$

where K_0 represents the coefficient of at-rest lateral pressure. The bearing capacity equation (2-1) should thus be used in the following revised form:

$$q_0 = c_u N_c^* + q_m N_q^* \tag{2-4}$$

where N_c^* and N_q^* are appropriate factors, still related to each other by equation (2-2) above. The computation of N_q^* can, in principle, be made by any of the established methods of analysis that take the soil deformability prior to failure into account. It is essential, however, that the computation be based on a realistic failure pattern. Vesic suggested that the value of N_q^* can be estimated by determining the ultimate pressure needed to expand a spherical cavity in an infinite soil mass. The effect of soil compressibility should be taken into consideration by introducing a rigidity index, I_r which is a function of Young's modulus, Poisson's ratio and the shear strength according to Mohr-Coulomb.

Baligh (1975) analysed the cone penetration test in two steps. First a complete solution for a simplified case was found, considering the cone as a symmetrical triangular wedge and with the assumption of a gap existing behind the wedge. Then an approximate solution was found interpreting the point resistance, q_c, considering it as the work done per unit area to push the cone a unit distance. The work could then be divided into two parts, where the first is the work done per unit area to push the cone tip a unit distance and the second is the work done per unit area per unit distance to expand a cylindrical cavity. The approximate solution includes the dependence of the rigidity index (I_r), the horizontal total stress, and the cone angle (2θ). The variation of $(q_c-\sigma_h)/c_u$ with I_r for different values of

the cone angle is shown in Figure 2-14. This equation assumes that the deformable material surrounding the wedge is isotropic, homogeneous, massless, rigid-perfect plastic and has a yield criterion which is independent of the hydrostatic pressure.

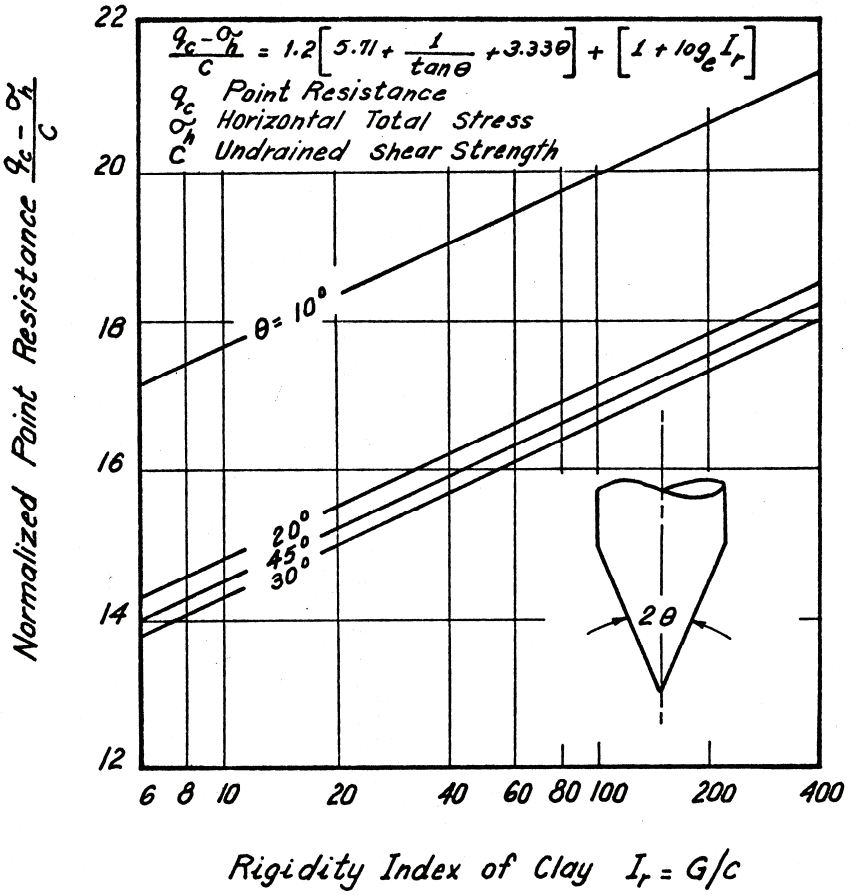

Figure 2-14 Effect of the clay rigidity index (I_r) and the cone angle (2θ) on penetration resistance (Baligh, 1975).

Konrad and Law (1987) proposed another method to determine the undrained shear strength from piezocone tests. In that method, it is considered that the cone is acted upon by a uniformly distributed normal soil pressure (σ_n), normal to the cone surface, and by a shear stress along the cone (τ), mobilised during penetration, as illustrated in Figure 2-15

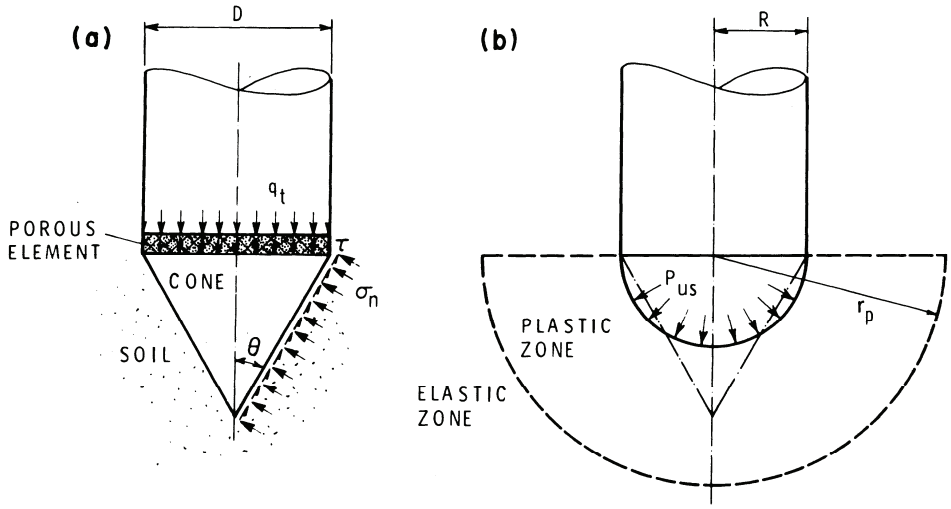

Figure 2-15 Assumptions for the Konrad and Law model: (a) Proposed stress field acting on cone; (b) expansion of spherical cavity (Konrad and Law, 1987).

Konrad and Law assumed that the unit shear stress at the cone-soil interface is a function of the normal total stress, the pore pressure in the failure zone, the friction angle (ϕ) and the friction factor for the soil acting on the cone surface (M). Force equilibrium at failure gives the relationship between the actual total cone resistance (q_t), σ_n and τ. Their next assumption was that σ_n is equal to the maximum internal pressure required to expand a spherical cavity. For the $\phi = 0$ case the solution is based on the assumptions that the soil is rigid-plastic in the plastic zone, no volume change in the plastic zone, linearly deformable soil in an elastic zone and homogeneous isotropic material. It is also assumed that prior to cavity expansion the entire soil mass has an isotropic total stress and that the soil is weightless. A formulation of the maximum internal pressure is made considering the Tresca yield criterion, i.e. independence of the hydrostatic pressure. The undrained shear strength mobilised during the penetration process is shown in a combination of these equations.

$$c_u = \frac{q_t - (1+F)\sigma_i + F\alpha u}{\frac{4}{3}(1+F)(\ln I_r + 1)}$$ where F is defined as $F = M \tan\phi'(\sigma_n - \alpha u)\cot\theta$

In the above equation σ_i is the initial total stress, α is a factor for increasing the measured pore water pressure (u) to obtain an approximation of the pore pressure in the failure zone, I_r is the rigidity index and θ is the apex angle (Figure 2-15). In this equation only q_t and u can be determined from the piezocone test. The other parameters need to be evaluated independently. The authors stated that the initial total stress σ_i must be

assumed to be spherical and therefore it should be approximated by the *in situ* total octahedral stress (σ_0), which requires the determination of both vertical and horizontal total stress. The proposed method was tested at three sites and the authors found that the profiles of undrained shear strength from the piezocone were in general agreement with those obtained from the vane test. The peak strength from CK_0U triaxial tests on Osterberg samples and on a block sample at one of the sites concurred well with the undrained shear strength from the piezocone. Among the results of strength interpretations based on other theories, Vesic's method and the proposed model yielded more or less the same results despite the fact that different failure surfaces were assumed in the models. The results from one of the test sites are shown in Figure 2-16.

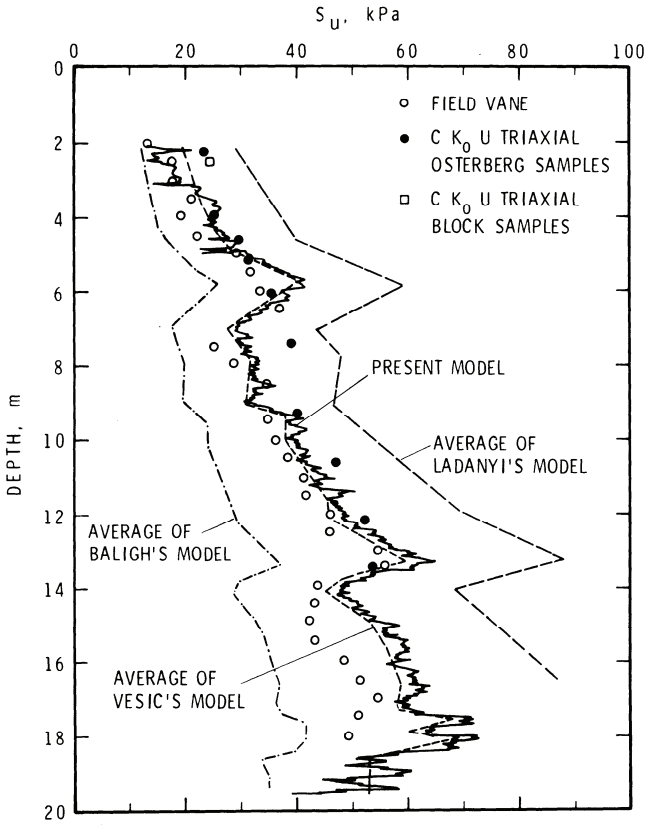

Figure 2-16 Strength profiles at the Gloucester site (Konrad and Law, 1987).

Teh (1987), Houlsby and Teh (1988) and Teh and Houlsby (1991) presented and elaborated on an analysis of the penetration of a piezocone into clay, followed by the pore pressure dissipation around the cone penetrometer. The analysis is based on the Strain Path Method, with additional details provided by large strain finite element analysis. The first phase of the analysis, which is of interest here, deals with the penetration of the piezocone into the clay, with the clay idealised as an incompressible elastic-perfect plastic (von Mises) material. Values of the cone factor N_{kt}

(defined as $(q_t-\sigma_{v0})/c_u$)) are derived. The authors stated that the penetration of the cone could be viewed as a steady state flow of soil passing a static penetrometer. From this flow pattern the complete history of strain for each soil element can be determined. Using appropriate initial stresses, together with the elastic-plastic constitutive laws, it is possible to calculate numerically the deviatoric stresses in the soil. The mean normal stresses may then be found by using one of the equilibrium relationships (radial or axial). The authors then found that the stresses did not exactly obey the other equilibrium relationship. Nevertheless, if the radial equilibrium equation is used to derive the mean stress, the inequilibrium can be shown to be relatively small and confined mainly to a very small region near the cone tip and a slightly larger region near the cone shoulder.

The authors showed the results of such calculations for cone factors for a 60° cone in a soil with an initially isotropic stress state. The variation in N_{kt} with rigidity index (I_r) showed the same trend as was predicted by the cavity expansion theory, see Figure 2-17. An equation for approximation of the values of N_{kt} was given. In the calculation no control was possible of the shear stress boundary condition on either the cone face or the shaft. The results were found to correspond to a specific cone roughness factor of approximately zero.

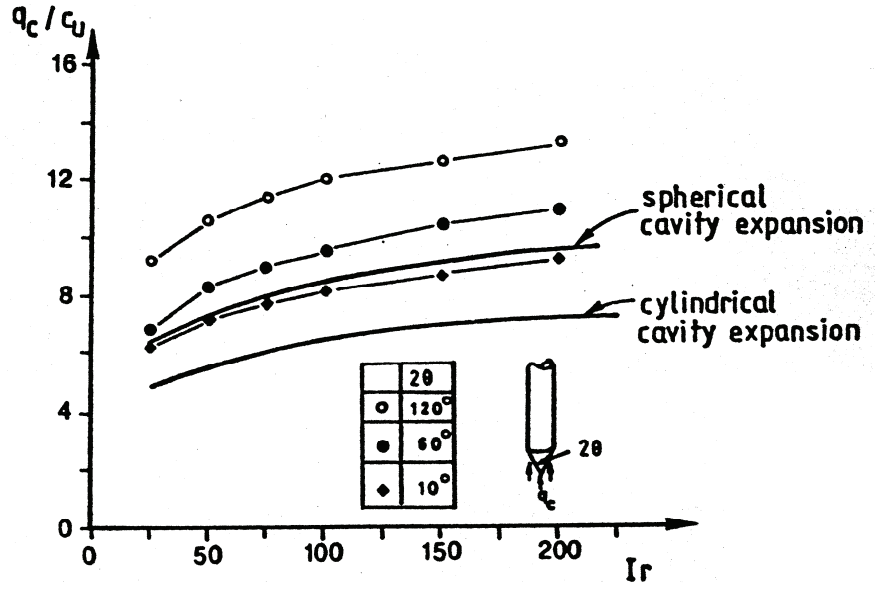

Figure 2-17 Variation in q_c with I_r (Teh, 1987).

The effect of initial stress anisotropy on the cone resistance was investigated by varying the *in situ* horizontal and vertical stresses. The stress distribution due to the penetration of a 60° cone for two sets of initial stress conditions was calculated. The initial stresses for the two cases were:

a) $\frac{\sigma_{h0}}{c_u} = 2.0 \qquad \frac{\sigma_{v0}}{c_u} = 3.5$

b) $\frac{\sigma_{h0}}{c_u} = 3.5 \qquad \frac{\sigma_{v0}}{c_u} = 2.0$

where σ_{v0} is the *in situ* vertical stress and σ_{h0} the *in situ* horizontal stress. In both cases the radial stress distribution was very similar. However, the axial stress in case (b) was considerably higher despite the fact that the initial vertical stress was lower. This higher axial stress component in case (b) led to higher computed factor N_{kt}. The calculation was repeated for other combinations of initial stresses. The initial stress state was characterised by a dimensionless factor Δ defined as $\Delta = (\sigma_{v0} - \sigma_{h0})/2c_u$ (where $-1 \leq \Delta \leq 1$). The calculated variation in N_{kt} with Δ could be approximated very closely by a straight line. The gradient of this line was found to be approximately -2, see Figure 2-18. This result indicated that q_t was almost independent of σ_{v0} and was affected mainly by the changes in σ_{h0}. It corresponded to $(q_t-\sigma_{h0})/c_u$ being almost constant rather than $(q_t-\sigma_{v0})/c_u$. However, since, σ_{h0} is not usually known accurately, the authors saw it as more practical to retain the use of the factor $N_{kt} = (q_t-\sigma_{v0})/c_u$, and to recognise the effect of the horizontal stress by modifying the equation for an approximation of N_{kt}.

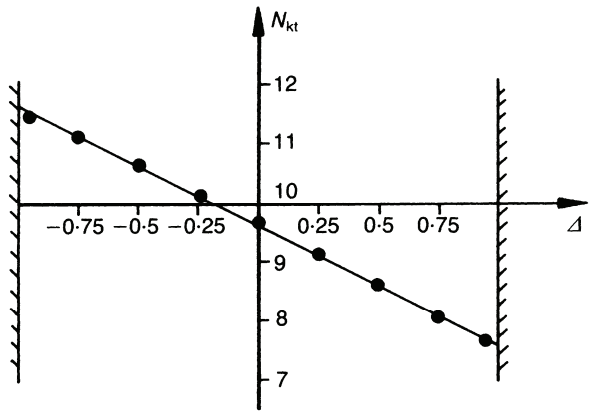

Figure 2-18 Variation of N_{kt} with Δ derived from the strain path method (Teh, 1987, Teh and Houlsby, 1991).

In an attempt to solve the inequilibrium problem of the strain path method, and still accounting for the effects of continuous penetration, a complementary finite element analysis was carried out. The results showed that for different combinations of initial horizontal and vertical stresses the same trend of N_{kt} with Δ as shown in Figure 2-18 was obtained, but with a slope of approximately −1.8 rather than -2.0.

The authors concluded that for a cone penetrating an elastic-perfect plastic material theoretical values of cone factors had been derived. The cone factor depends on:

- The rigidity index.
- The horizontal stress.
- Roughness of cone and shaft.

An approximate expression for the cone factor in terms of these parameters was also proposed: $N_{kt} = N_s\left(1.25 + \frac{I_r}{2000}\right) + 2.4\alpha_f - 0.2\alpha_s - 1.8\Delta$

Where α_f and α_s are roughness factors for cone and shaft respectively and N_s is the factor that appears in the spherical cavity expansion expression, i.e.

$N_s = \frac{4}{3}\left[1 + \ln(I_r)\right]$

Other authors have found similar expressions for the cone factor, which include the horizontal stresses, i.e. the Δ-term. Developing a novel finite element formulation for the analysis of steady state cone penetration in undrained clay using von Mises model, Yu et al. (2000) obtained a cone factor using the following equation $N_{kt} = 0.33 + 2\ln I_r + 2.37\alpha - 1.83\Delta$, where α is the cone and shaft roughness. Abu-Farsakh et al. (2003) simulated the cone penetration in clay numerically with a combined cavity expansion and finite element analysis using the modified Cam clay model. The cone factor thus obtained can be written $N_{kt} = 2.45 + 1.8\ln I_r - 2.1\Delta$.

The empirical approaches available for interpretation of the undrained shear strength, c_u, from piezocone test results can be grouped under three main categories (Lunne et al. 1997):

1. c_u estimation using "total" cone resistance
2. c_u estimation using "effective" cone resistance
3. c_u estimation using excess pore pressure

According to Lunne et al. (1997) an estimation of the undrained shear strength using total cone resistance is made from the equation:

$$c_u = \frac{(q_c - \sigma_{v0})}{N_k} \qquad (2\text{-}5)$$

or the modified and improved approach employing the cone resistance corrected for pore pressure effects, q_t, instead of measured cone resistance, q_c, (Campanella et al., 1982), which gives the equation:

$$c_u = \frac{(q_t - \sigma_{v0})}{N_{kt}} \qquad (2\text{-}6)$$

where $q_t = q_c + u(1\text{-}a)$

a = area ratio (constant for a specific cone)

Because of the significance of the stress conditions on the undrained shear strength, and the subsequent shear strength anisotropy, the values of these cone factors are dependent on which undrained shear strength is used as a reference value (the undrained shear strength from triaxial tests; from direct simple shear tests; from field vane tests or an average laboratory undrained shear strength). Over the years, a large number of studies have been performed to determine the N_{kt} factor. However, the reference method used may vary from one study to another.

To provide correlations between cone resistance, shear strength, overburden pressure and overconsolidation ratio, Almeida and Parry (1983 and 1985) conducted vane, penetrometer and piezocone tests in reconstituted clay in a consolidometer, see also sections 2.2.1 and 2.6.3. Kaolin clay slurry and Gault clay slurry were consolidated to 150 kPa and 126 kPa respectively. Tests were performed at the consolidation pressure (OCR = 1) and for the kaolin clay also at pressures corresponding to OCR = 3 and OCR = 10 and for Gault clay also at OCR = 1.9 and OCR = 7. The authors recognised, among other things, that for overconsolidation ratios greater than unity, the values of point resistance were not influenced very much by variations in the penetration rate between 1 and 20 mm/s, but for OCR equal to unity the point resistance was smaller at the rate of 1 mm/s than at 20 mm/s. At a penetration rate of 1 mm/s the modified N_{kt} values (using Equation 2-6) for kaolin increased from 6.8 to 13.6 with OCR increasing from 1 to 10. For Gault clay the modified N_{kt} values increased from 12.0 to 18.8 with OCR increasing from 1 to 7 at penetration rates of 4 to 6 mm/s.

Aas et al. (1986) presented cone factors, N_{kT}, estimated from piezocone tests, using Equation 2-6, at several well-documented test sites in Norway. The plasticity index at the test sites varied from 3% to 50%. The cone factor was correlated to the average laboratory undrained shear strength $c_{u,lab} = (c_{uc}+c_{ud}+c_{ue})/3$ where c_{uc}, c_{ud} and c_{ue} are the undrained shear strengths from triaxial compression, direct simple shear and triaxial extension tests respectively. The nine clay types investigated suggested a cone factor, N_{kT}, increasing linearly with the plasticity index, from 13±2 at $I_p = 0$ to 18.5±2 at $I_p = 50\%$.

La Rochelle et al. (1988) performed piezocone tests on three eastern Canadian clays. The clay deposits were chosen so as to cover a wide range of overconsolidation ratios as well as plasticity and liquidity indices normally encountered in the sensitive clay deposits of eastern Canada. The cone factor, N_{kt}, was computed using Equation 2-6 and the undrained shear strength based on the Nilcon field vane was used as a reference value. The N_{kt} value for the three sites ranged from 10 to 18 and they did not seem to increase with the overconsolidation ratio, which ranged from 1.2 to 50 for the three sites. The N_{kt} values were more or less constant and independent of the plasticity index, which ranged from 8 to 40 (liquid limit 31% to 66%).

Rad and Lunne (1988) studied available laboratory and piezocone penetration test data from 11 clayey soils from sites throughout the world (including seven sites from Norway or the North Sea). Undrained shear strength values used during the investigation were based on anisotropically or isotropically consolidated undrained compression triaxial tests. Although, the authors pointed out that the difference between the results of these tests was between 5% and 10%, they were used interchangeably without any corrections. In the study, possible correlations between piezocone test results and index soil properties, such as plastic limit (w_P), liquid limit (w_L), plasticity index (I_P), *in situ* water content (w_N), overconsolidation ratio (OCR) and sensitivity (S_t) were studied. Among these parameters, the authors found that for a given effective overburden stress, OCR was found to have the strongest influence on the piezocone test results. The N_{kt} values determined using Equation 2-6 above were found to vary between 8 and 29, increasing with increasing OCR.

Similarly, Powell and Quarterman (1988) studied data from well-documented test sites in the United Kingdom with London clay, Glacial till and Gault clay respectively. Based on undrained shear strengths from 38 mm triaxial compression tests and using Equation 2-6 above, the authors obtained N_{kt} values between 10 and 20 with a clear trend of increasing N_{kt} with increasing plasticity index. Based on 98 mm triaxial tests and plate tests higher N_{kt} values were obtained. This was explained by scale effects likely to be present in each deposit.

Senneset et al. (1989) proposed piezocone interpretation methods for Glava clay from the Trondheim region, Norway, an overconsolidated clay of medium to low sensitivity. The N_{kt} values were estimated using Equation 2-6 and undrained shear strength from CIU triaxial tests were used as the

reference strength. The samples were consolidated either to the present *in situ* stress level (σ'_{v0}-consolidated) or consolidated to or past the preconsolidation pressure (σ'_{c}-consolidated). Values of N_{kt} based on $c_{u,max}$ from σ'_{v0}-consolidated samples ranged from about 12 to 18. Corresponding values of N_{kt} based on the average peak shear stress from σ'_{c}-consolidated samples ranged from 7 to 10.

Using data from test fields in Sweden and Norway and based on the average undrained shear strength from active and passive triaxial tests and direct simple shear tests or, alternatively, direct simple shear tests together with corrected field vane tests, Larsson and Mulabdic (1991) found cone factors (N_{kt}) for normally consolidated and slightly overconsolidated clay varying between 14 and 20, with an average of 16.3 using Equation 2-6 above. The cone factors plotted against the liquid limit (w_L) revealed an increase of N_{kt} with a liquid limit, which could be written: $N_{kt} = 13.4 + 6.65 \cdot w_L$. In a study including overconsolidated clays from three sites in Sweden, Larsson and Åhnberg (2003) found that there was a need for an extra correction for overconsolidation. The authors proposed that the cone factor then should be written $N_{kt} = (13.4 + 6.65 \cdot w_L) \cdot (OCR/1.3)^{1-b}$.

The influence of the initial stress conditions on the piezocone test results has been observed in calibration chamber tests by Kurup (1993), Kurup et al. (1994) and Voyiadjis et al. (1994). They carried out miniature piezocone penetration tests on cohesive soil specimens in a calibration chamber system. Eight piezocone tests were conducted using four different specimens and factors such as soil type, stress history, penetration boundary conditions and filter locations were investigated. Of the four specimens three were isotropically consolidated and one specimen was anisotropically consolidated with a K_0-value of 0.52. The anisotropically consolidated specimen and two of the isotropically consolidated were normally consolidated and the third was overconsolidated with an OCR of 5. From the tests the N_{kt} factor has been determined using Equation 2-6 above. Reference c_u was determined from undrained triaxial compression tests. The authors observed that the empirical cone factor (N_{kt}) value for the isotropically consolidated specimens was higher than those for the anisotropically consolidated specimen, signifying the importance of the horizontal stress on N_{kt}.

Senneset et al. (1982) suggested that the undrained shear strength should be estimated using an effective cone resistance (q_e), where q_e is defined as the difference between the measured cone resistance (q_c) and pore pressure, measured immediately behind the cone (u_2). The procedure was applied to

available piezocone records and the parameter profiles obtained were compared with the corresponding laboratory results. Based on the effective values of $q_e = q_c - u_2$, the values of the corresponding effective cone factor, N_{ke}, were $N_{ke} = 9 \pm 3$.

Using the corrected cone resistance (q_t) the equation can be redefined as (Campanella et al., 1982):

$$c_u = \frac{q_e}{N_{ke}} = \frac{(q_t - u_2)}{N_{ke}}$$

Values of N_{ke} have been obtained in other studies. For example, Lunne et al. (1985) obtained for North Sea clays, N_{ke} values of 2 to 12, which appeared to correlate with the pore pressure parameter (B_q) whereas Robertsson et al. (1986) found N_{ke} values between 5 and 18 for clays in the Vancouver area with no correlation to B_q.

A number of relationships between generated excess pore pressure (Δu) and the undrained shear strength have been proposed, all of which have the form of:

$$c_u = \frac{\Delta u}{N_{\Delta u}} \qquad (\Delta u = u_2 - u_0)$$

Values of $N_{\Delta u}$ have been obtained in several studies. Among others, Lunne et al. (1985) obtained for North Sea clays $N_{\Delta u}$ values between 4 and 11 using triaxial compression strength as a reference strength. In these studies the filter was located at two different positions at the conical face of the tip. For three Canadian clays with overconsolidation ratios between 1.2 and 50, La Rochelle et al. found, $N_{\Delta u}$ values between 7 and 9. In this study the filter was located above the conical face of the tip and the Nilcon vane shear strength was used as a reference strength. Based on data from Swedish and Norwegian test fields, and for pore pressures measured at the conical face of tip, Larsson and Mulabdic (1991) found an average $N_{\Delta u}$ value of 16. For pore pressures measured above the conical face of the tip $N_{\Delta u}$ could be described as $14.1 - 2.8 \cdot w_L$. This relationship was found to be applicable to normally consolidated and only slightly overconsolidated homogeneous soil, since it was very sensitive to the overconsolidation ratio. The reference shear strength was obtained using corrected field vane tests and direct simple shear tests.

Karlsrud et al. (2005) compared piezocone test results from 17 sites with soft to medium stiff clays, a plasticity index from 10% to 50% and sensitivity from 3 to about 200, against undrained triaxial compression strength. The triaxial compression tests were carried out on high-quality block samples taken using a 250 mm block sampler. The piezocone undrained shear strength related to the pore pressure factor, $N_{\Delta u}$, the cone factor, N_{kt}, and the combined cone resistance and pore pressure factor, N_{ke}, were studied. The authors found that the measured excess pore pressure gave the best and most consistent correlation to the measured undrained shear strength and that the $N_{\Delta u}$, N_{kt} and N_{ke} values depended on the overconsolidation ratio, the plasticity index and the sensitivity.

3. EXPECTED INFLUENCE OF THE STRESS CONDITIONS ON THE UNDRAINED SHEAR STRENGTH (HYPOTHESIS)

Evaluation of the shear strength of clay from the piezocone and the field vane tests is to a large extent based on empirical relationships. For Swedish clays, the relationships commonly used are based on the stress distribution valid for horizontal ground and normally consolidated or slightly overconsolidated soil (Cadling and Odenstad, 1950, Larsson et. al., 1984, Larsson and Mulabdic, 1991). The relationship between the effective horizontal stresses and the effective vertical stresses then correspond to $K_{0(NC)}$ conditions. For these conditions the results from laboratory tests and field tests generally show good agreement.

Unloading of the soil results in a change of both the undrained shear strength and the relationship between the horizontal and the vertical stresses. At the same time, the relationship between the shear strengths measured using the different methods changes. During unloading of horizontal ground there is a fairly well-established pattern for the relationship between the vertical and the horizontal stresses. The change in the undrained shear strength measured after unloading appears to be larger when measured using direct simple shear tests in the laboratory than when measured using vane tests in the field, provided that the latter are not corrected for an overconsolidation ratio (e.g. Law, 1979, Jamiolkowski et al., 1985, Larsson and Åhnberg, 2003). Based on current experience, the results from the piezocone tests seem to exhibit behaviour similar to the field vane tests (e.g. Kurup et. al., 1994, Larsson and Åhnberg, 2003). The limited studies to be found dealing with how the various principal stresses influence the test results imply that the horizontal stress has a large influence on the results from vane tests and piezocone tests. Such an influence cannot be observed readily from the direct simple shear test results in the laboratory.

Natural slopes mainly have been formed in two different ways; either the soil has been deposited as inclined layers on inclined bedrock or the originally almost horizontal ground surface have been subjected to erosion. In natural slopes formed by erosion, the stress conditions are complex. Due to erosion, the horizontal stresses perpendicular to the direction of an eroding river have decreased substantially in the active zone, whereas the vertical stresses largely remain. At the same time, the vertical stresses in the passive zone have decreased greatly whereas the horizontal stresses have been reduced only to a very limited extent (e.g. Rankka, 1994). In

addition, the horizontal stresses in the clay slope are not equal along and across the direction of the eroding river. To assess the relevance of various methods for determining the undrained shear strength, it is important to know how the results are influenced by the actual stress conditions in the slope. When considering the actual stress conditions it is also important to know how a correction of the results should be made in order to give relevant values to be used in a slope stability analysis.

As described above, unloading of the soil results in a change in both the undrained shear strength and the relationship between the horizontal and the vertical stresses. The vertical stresses decrease after unloading. The horizontal stresses also decrease but not as much as the vertical stresses. On the other hand, unloading does not result in a change in the vertical and horizontal preconsolidation pressures. When the soil has relaxed and adapted to the new stress conditions after unloading, the undrained shear strength normally decreases slightly. The hypothesis to be tested in this study is that the undrained shear strengths measured with the field vane test and the piezocone test are mainly influenced by the horizontal stresses, both the preconsolidation pressures and the effective stresses in the horizontal direction. An unloading of the soil should then result in a smaller reduction in the undrained shear strength measured with field vane and piezocone tests compared to the direct simple shear test.

Both in the active zone at the crest of a slope and in the passive zone at the toe, the horizontal stresses are different in the direction perpendicular to an eroding river than along the river, as described above. It is difficult to model this situation in the laboratory (as well as with computer programs). The aim of this study has been to focus on the influence of the horizontal stresses perpendicular to the erosion river on the measured undrained shear strength. The hypothesis is that the undrained shear strength measured using the field vane test and the piezocone test in the active zone shows a different, possibly larger, reduction due to unloading than the corresponding undrained shear strength measured using direct simple shear tests. In the passive zone, the undrained shear strength measured using the field vane test and the piezocone test ought to be larger than the corresponding undrained shear strength measured using direct simple shear tests.

4. FIELD TESTS

4.1 Introduction

Slopes of particular interest in this project should have certain characteristics. They should be eroded from flat ground and consist of homogeneous clay without silt/sand layers. There should be clay up to the ground surface behind the crest of the slope. The slopes should have a low factor of safety but no stabilising measures should have been carried out. It should be possible to carry out field investigations at the toe of the slope, preferably without using a raft. In addition, it would be an advantage if the slope had already been well investigated, if earth pressure measurements had been carried out and if there was no quick clay.

Two test sites, both of which had most of the above-mentioned characteristics, were chosen for this project. Both test sites are located in the Göta Älv river valley. The Partille test site is situated east of Gothenburg on the shore of the Säveån river. The Slumpån test site is situated north of Gothenburg on the shore of the Slumpån river. Both rivers are feeder rivers to the main river, the Göta Älv. The locations of the test sites are shown in Figure 4-1.

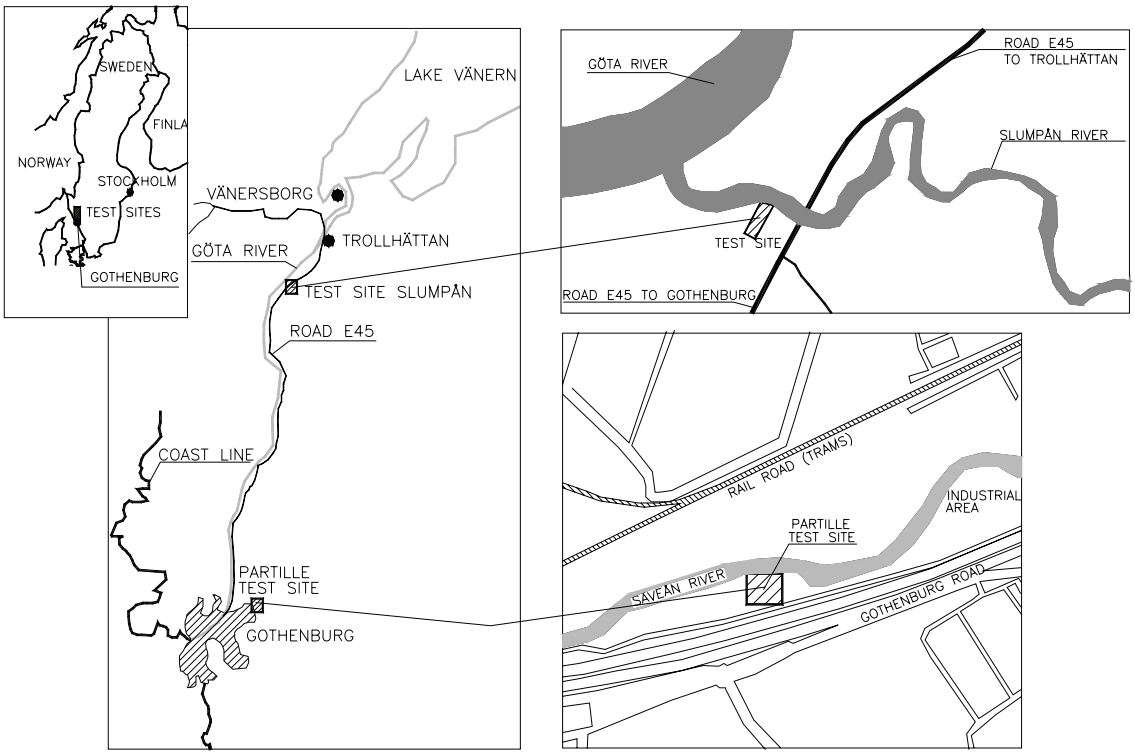

Figure 4-1 Locations of the test sites used in this project.

4.2 The Partille test site

The Partille test site is situated to the west of the municipality of Partille and 8 km east of Gothenburg. It is located on the south side of the Säveån river, which is a feeder river to the Göta Älv river. The test site is located below the highest coastline and less than 20 m above the present sea level. From the top of the slope to the river bottom, the fall in height is about 12 m. The inclination of the slope is about 15° in the lower half and about 5° in the upper half. A photo of the test site is shown in Figure 4-2.

Between 1989 and 1992, Rankka (1994) carried out a study of the slope at this test site. The purpose of that study at the Partille test site was to investigate the horizontal stress changes due to natural pore pressure and water level changes.

Figure 4-2 The Partille test site.

4.2.1 Geology

A description of the quaternary deposits along the Säveån river is found in Magnusson (1978). The soil consists of postglacial clay underlain by glacial clay and cohesionless soil on rock. Although there are some difficulties in determining the boundary between the glacial and postglacial clay deposits, the main part of the clay layers most likely consists of glacial clay. In conjunction with excavation work in central Partille, the postglacial clay was studied to depths of up to 4-4.5 m below the ground surface. The postglacial clay in the Partille area is rich in fossils. Along the Säveån river sediments of fine sand are to be found locally, probably formed by a combination of wave-washing and fluvial processes. A number of small slides have occurred along the river, probably due to the ongoing erosion process. Quick clay is commonly found in the area.

4.2.2 Site investigations

At the test site, Rankka (1994) carried out geotechnical investigations in one section at four different locations: point A close to the river, point B at the centre of the slope and points C and D above the crest. At points A and C the following tests were carried out: static penetration test, field vane tests, undisturbed sampling, pore pressure measurements with open system piezometers and measurements of horizontal pressure using total earth pressure cells (Glötzl type). At point C, pore pressures were also measured using closed piezometers at the same depths as the open systems. At points B and D pore pressure measurements using open system piezometers and measurements of horizontal pressure using total earth pressure cells were carried out. The investigation locations are shown in Figure 4-3.

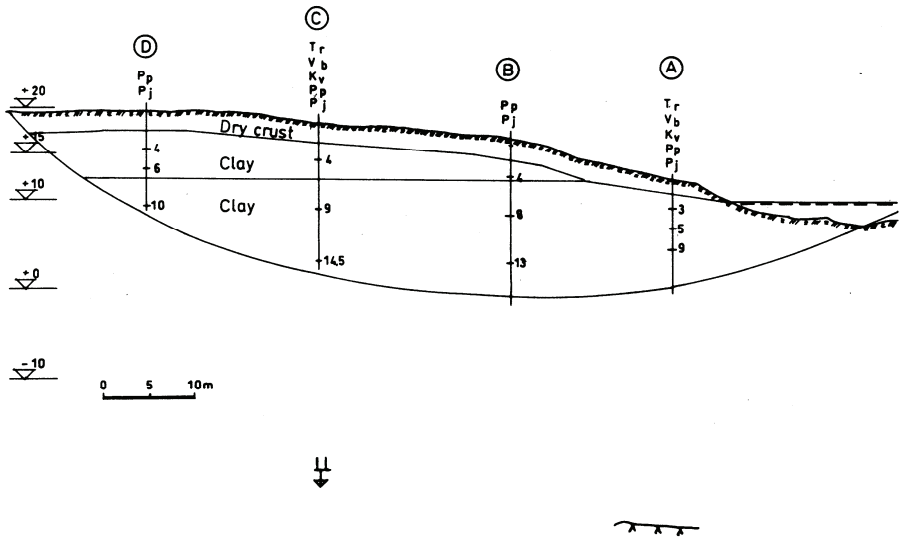

Figure 4-3 Geotechnical investigations in the study by Rankka (1994).

In the present study, investigations were carried out at two of the locations used by Rankka (1994), at one point close to the river (point A) and at one point above the crest (point D). At these two locations the following tests were carried out: piezocone test (CPTU), field vane tests, dilatometer tests, undisturbed sampling and pore pressure measurements with closed BAT piezometers. The piezometers were installed at a depth of about 3, 5 and 9 m at point A and at a depth of about 4, 9 and 14.5 m at point D. The location of the investigations in this study is shown in Figure 4-4.

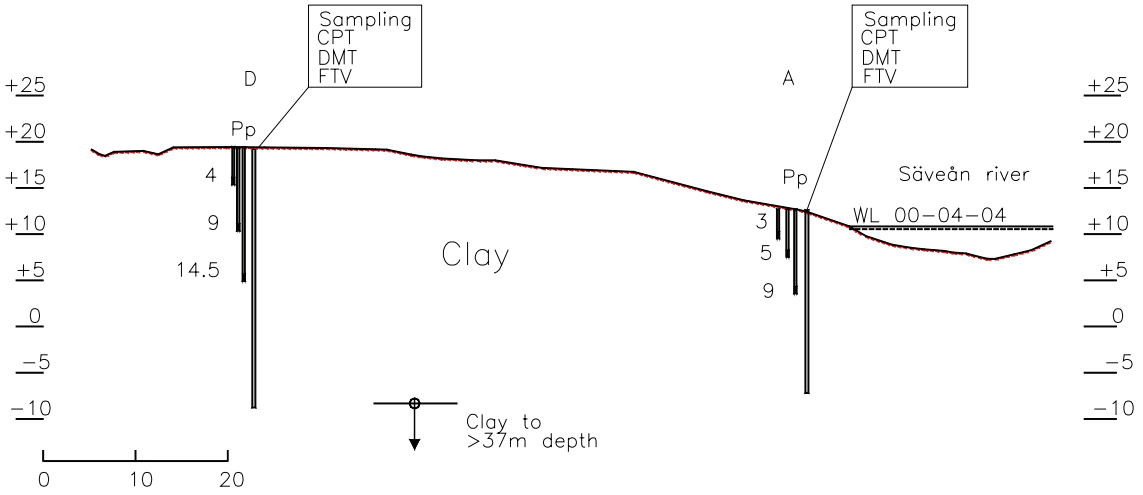

Figure 4-4 Geotechnical investigations in this study and the soil profile.

Routine analyses (bulk density, water content, liquid limit, undrained shear strength by fall cone test and sensitivity), CRS oedometer tests and direct simple shear tests were carried out on the undisturbed samples.

4.2.3 Geotechnical conditions

In the section studied, the depth to cohesionless soil is about 37 m at the toe of the slope and more than 37 m at the top. The upper 1-2 m consist mainly of dry crust underlain by soft clay with stains of sulphide and shells. The upper 2 – 4 m of the soft clay also have traces of roots.

The density, natural water content and liquid limit of the clay are shown in Figure 4-5. The water content and the liquid limit are almost equal. The effective strength parameters were determined by means of active, consolidated, undrained triaxial tests by Rankka (1994). The results indicated $c' \approx 5$ kPa and $\phi' \approx 30°$. The undrained shear strength is discussed and evaluated in Section 4.2.4 below.

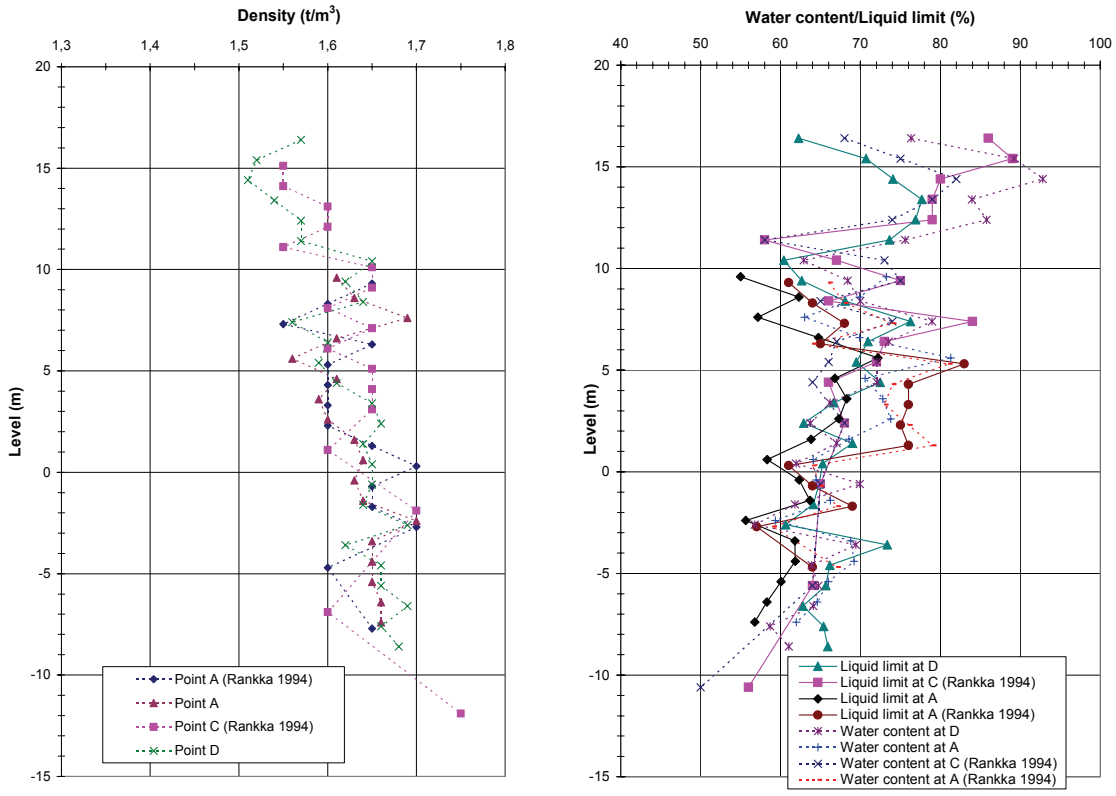

Figure 4-5 Density, natural water content and liquid limit of the soil.

In the present project, pore pressures were measured by means of six BAT piezometers placed in two groups, at points A and D. Measurements were carried out once; on March 30, 2000, see Figure 4-6. Pore pressure measurements at points A, B, C and D were carried out between November 1989 and September 1992 by Rankka (1994). The pore water pressure measurements, both in the present study and in the study by Rankka (1994), indicated behind the crest of the slope an almost hydrostatic pore water pressure from a groundwater table about 1 m below the ground surface. Close to the river the measurements indicated an almost hydrostatic pressure from a groundwater table about 0.5 m below the ground surface down to a level of +7.5 m and slightly higher than hydrostatic pressure for the deepest piezometer (level +3 m).

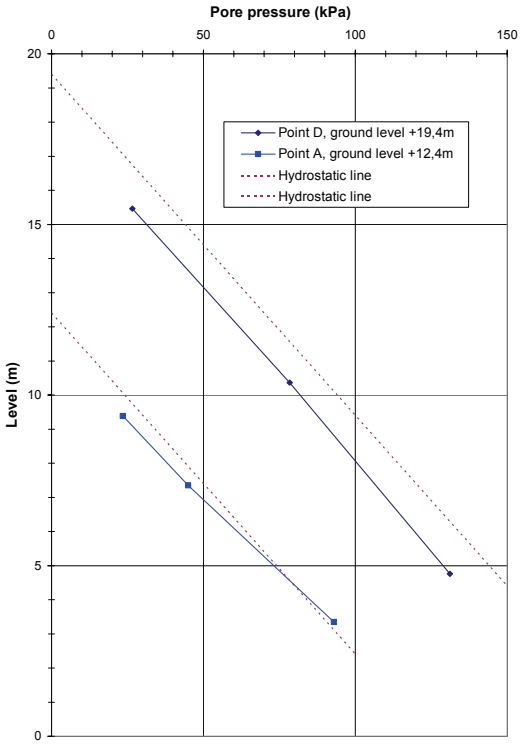

Figure 4-6 Pore water pressures measured May 30, 2000.

Vertical preconsolidation pressures determined by CRS oedometer tests are shown in Figure 4-7. Comparisons of the preconsolidation pressures measured in the passive zone close to the river and above the crest of the slope indicated that the clay could have been deposited with a difference in ground level at the end of deposition. The difference in ground level at deposition is then estimated to be about 2 m based on the preconsolidation pressures, i.e. the ground level at the present location of the Säveån river was +17.5 m after deposition. In the passive zone a number of stress path analyses have also been made using this assumption. However, there are no other indications of inclined layers. The water content and the liquid limit in the passive zone compared to those above the crest indicate horizontal ground level at deposition. It is more likely that the lower preconsolidation pressures are due to a gradually falling ground water level in the area above the crest up to the present conditions, and a ground water level at the ground surface in the area of the Säveån river before the erosion of the slope took place.

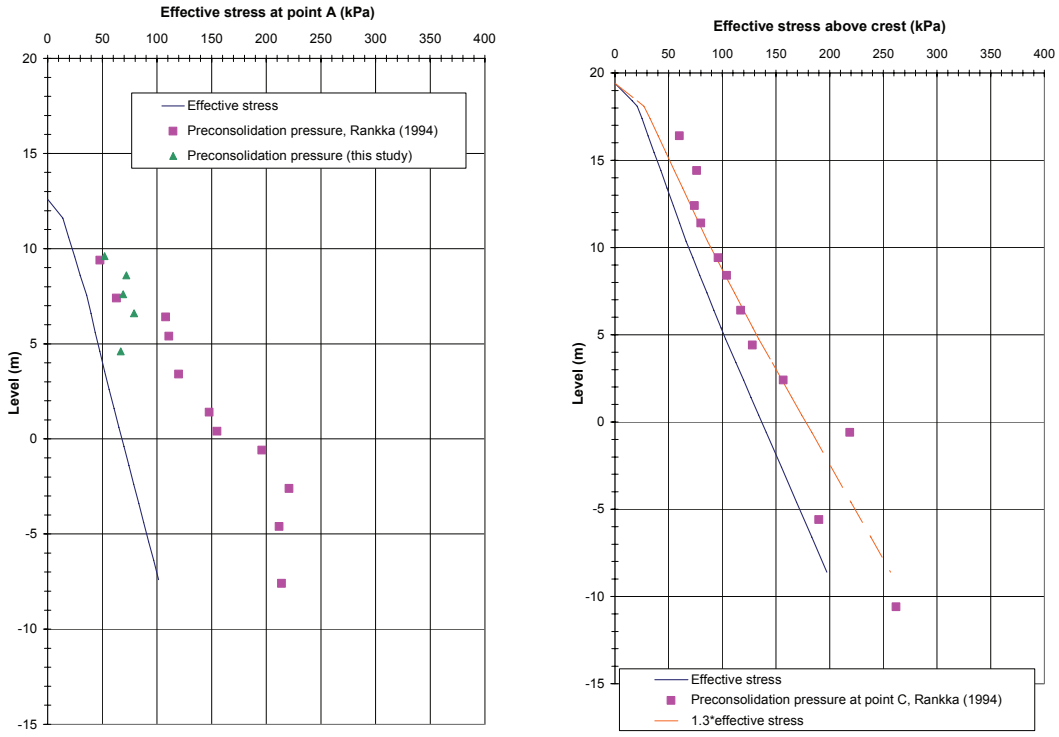

Figure 4-7 Effective vertical stress and preconsolidation pressures determined by CRS oedometer tests at point A and C.

4.2.4 Shear strength

The undrained shear strength has been determined by means of field vane tests and piezocone tests in the field and using direct simple shear tests and fall cone tests in the laboratory. The measured values from the field vane tests, the piezocone tests and the fall cone tests have been corrected with regard to the liquid limit (Figure 4-5).

Until recently, the evaluation of the undrained shear strength from the field vane test has been made according to empirical relationships as described in SGI Information 3 (Larsson et. al., 1984). Similarly, an evaluation of the undrained shear strength from piezocone tests has been made according to relationships described in SGI Report 42 and SGI Information 15 (Larsson and Mulabdic', 1991, Larsson, 1993). These relationships are based on data from normally consolidated and slightly overconsolidated soils. However, recent research (Larsson and Åhnberg, 2003) has shown that there is a need for an extra correction for overconsolidation in more overconsolidated soils (OCR > 1.5). In this study, an evaluation of the undrained shear strength from piezocone and field vane tests has been made using the new relationships, see also Section 2.3.1.

To assess the reasonableness of the evaluated undrained shear strengths, they have also been compared with the shear strength expected in clay with a corresponding loading history and consistency limits. The basis for this empirical shear strength is preconsolidation pressures, degree of overconsolidation and consistency limits. At the Partille test site, the empirical relationship described in SGI Information 3 (Larsson et. al., 1984) and in Commission on Slope Stability, (1995), has been used. However, this empirical relationship has been revised since the Partille test site was analysed. This is described in the updated version of SGI information 3 (Larsson et. al., 2007), where overconsolidation is also taken into account.

As the lower part of the slope (at point A and below the Säveån river) has been eroded from what was initially almost horizontal ground, the clay layers have a different loading history here compared with the upper parts of the slope (points C and D). Therefore, an evaluation of the measured shear strengths at point A has been separated from the evaluation of the measured shear strengths at points C and D. A compilation of all the shear strength data, related both to depth and related to level, clearly reveals that the best correlation is gained by plotting the data related to level. This is in agreement with the fact that the slope has been eroded from almost horizontal ground.

A comparison of the evaluated undrained shear strengths derived from field vane tests, piezocone tests, direct simple shear tests and fall cone tests at points C and D in the upper parts of the slope shows rather good agreement, see Figure 4-8. The largest difference can be observed in the evaluated shear strengths from the two series of fall cone tests, which are lower than the shear strengths evaluated from the other tests below about level +10. The difference increases with depth. Comparing the measured undrained shear strengths with the empirical shear strength, higher values are obtained using the empirical relationship. This difference also increases with depth. If the revised empirical relationship had been used (Larsson et. al., 2007), it would have resulted in slightly lower undrained shear strengths.

The undrained shear strength above the crest, where the ground level is between +18 and +19.5, can, under the dry crust, be described as constant 11.5 kPa between level +18 and +16, then increasing by 0.5 kPa/m to 12.5 kPa at level +14 and below level +14 increasing by 1.5 kPa/m, see Figure 4-8.

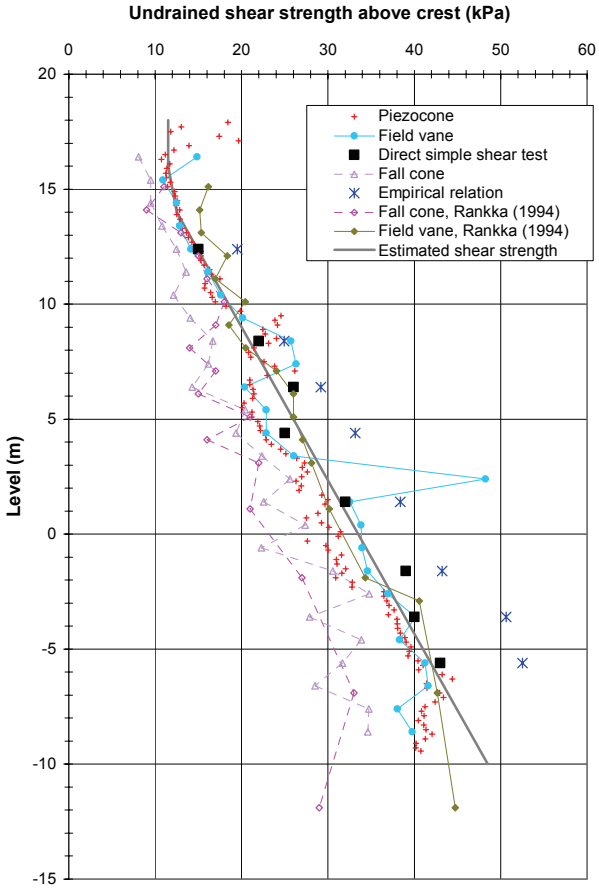

Figure 4-8 Undrained shear strength above the crest (at points C and D).

A comparison of the evaluated undrained shear strengths from field vane tests, piezocone tests, direct simple shear tests and fall cone tests at point A shows good agreement, see Figure 4-9. The results from the fall cone tests are also lower here than the shear strengths evaluated from the other tests. At this point they are lower below about level +5. Comparing the measured undrained shear strengths with the empirical shear strength, the agreement is good, except for levels above about +6, where the shear strength evaluated using the empirical relationship is lower.

The undrained shear strength at point A, where the ground level is about +12.5, can under the dry crust be described as 10.8 kPa at level +11 and thereunder increasing by 1.7 kPa/m, see Figure 4-9.

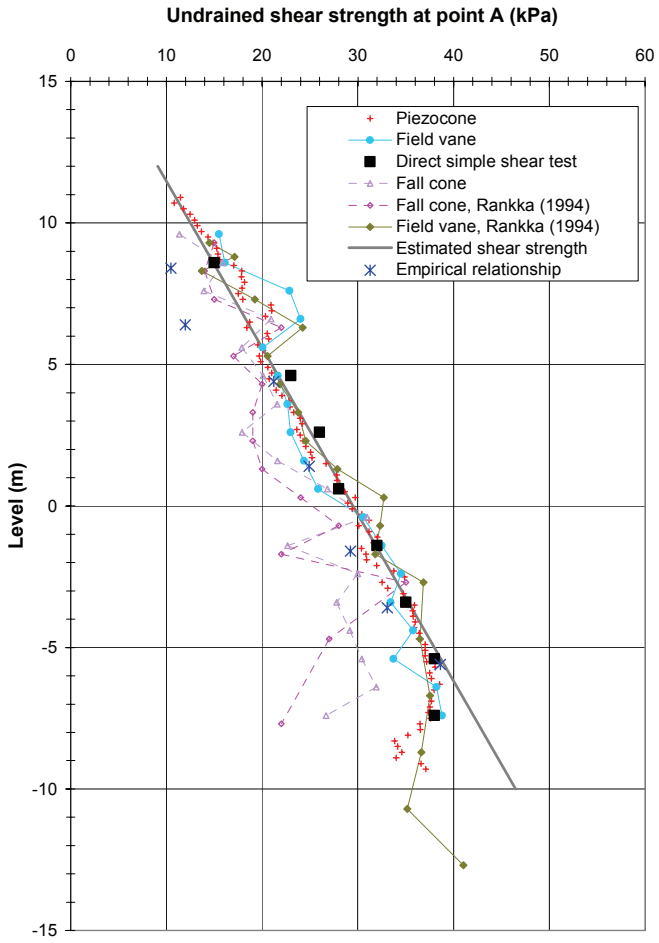

Figure 4-9 Undrained shear strength at point A (the toe of the slope).

To study how much the estimated shear strength, based on all shear strength determinations, could differ when the vane and piezocone shear strengths are calculated using the old (Larsson et. al., 1984, Larsson, 1993) and the new (Larsson and Åhnberg, 2003) relationships respectively, calculations based on the old relationships have also been carried out. Figure 4-10 shows a compilation of the undrained shear strengths at point A, where the measured shear strengths from the field vane tests and the piezocone tests have been calculated using the old relationships without correction for overconsolidation. It can be noted that agreement between the piezocone test, the field vane test and the direct simple shear test is better with the new relationship, which has an extra correction for overconsolidation. The undrained shear strength at point A could, based on the old evaluation of the piezocone and the field vane test together with the results from the direct simple shear tests, fall cone tests and empirical evaluation, be expressed as 12.3 kPa at level +11 and thereunder increasing by 1.65 kPa/m, Figure 4-10. The estimated undrained shear strength based

on the old relationship is in this case about 1 kPa higher than the undrained shear strength based on the new relationship.

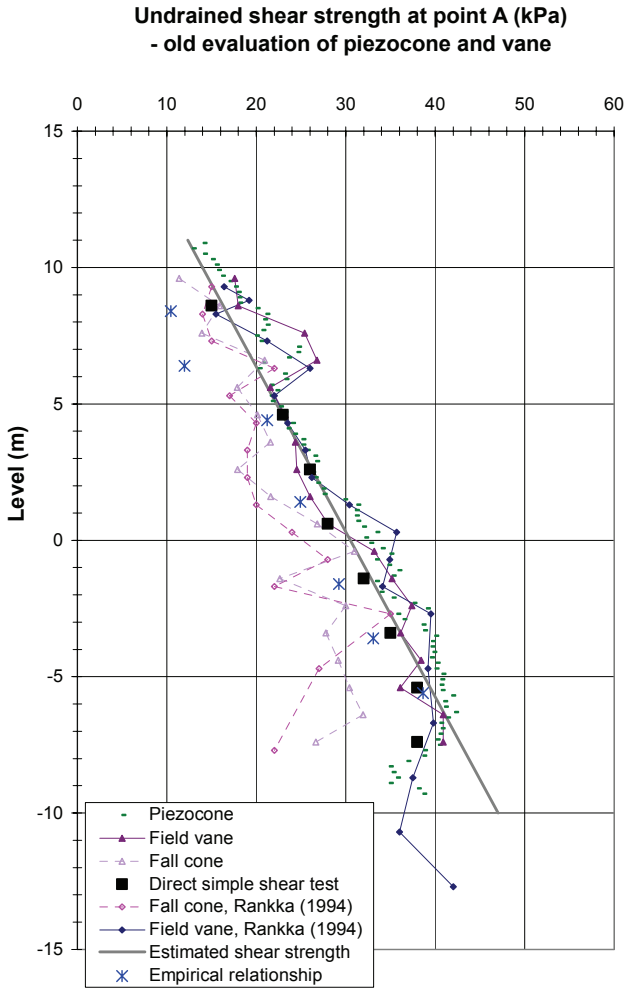

Figure 4-10 Undrained shear strength at point A (the toe of the slope) using the old evaluations of the piezocone and field vane strength (Larsson et. al., 1984, Larsson, 1993).

4.2.5 Stability analysis

4.2.5.1 *General*

Stability calculations have been carried out in accordance with the Swedish guidelines for slope stability investigations (Commission on Slope Stability, 1995). So-called limit equilibrium methods have been used. Calculations have been performed for circular slip surfaces using the Morgenstern-Price method and the computer program SLOPE/W. Calculations have been made with both undrained and combined analyses. The effect of anisotropy has been estimated by using the relationships

based on K_{0NC}, as described in the guidelines for slope stability investigations (Commission on Slope Stability, 1995).

4.2.5.2 *Basis for stability calculations*

The geometry of the slope has been determined by levelling. The bottom geometry of the Säveån river was determined by Rankka (1994) by sounding with a lead line.

As described in Section 4.2.3, the soil profile consists of soft clay to a depth of more than 37 m. The undrained shear strength of the clay has been estimated based on the results of the field and laboratory tests as described in Section 4.2.4, using the new evaluation of the piezocone and the field vane tests with the extra correction for overconsolidation. In parts of the slope where no investigations have been carried out, e.g. below the Säveån river, the shear strength estimation has been adapted to the probable loading history of the slope. The shear strength has thus been assessed to be slightly lower in the top clay layers below the Säveån river than at the same depth at point A, but with a slightly higher increase with depth. The undrained shear strength of the dry crust has been assumed to be 25 kPa. The geometry and the undrained shear strength of the calculated section are shown in Figure 4-11.

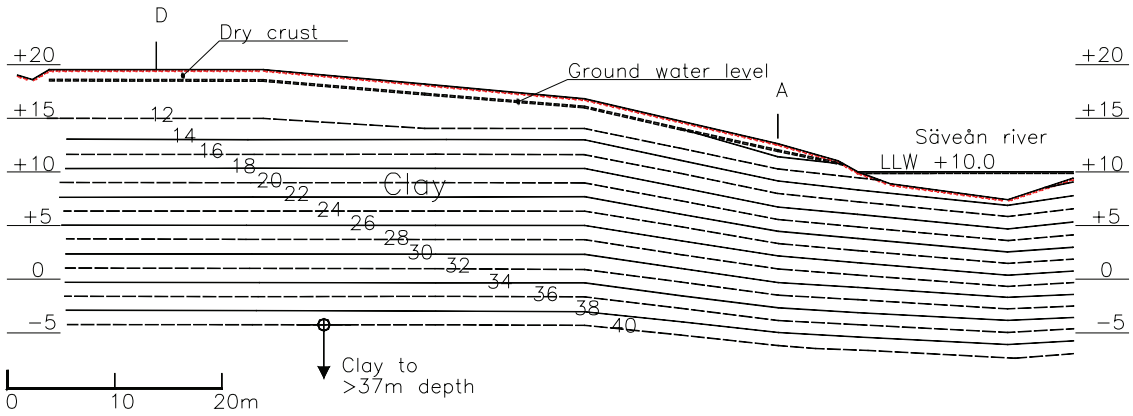

Figure 4-11 Geometry and assumed undrained shear strength in the calculated section.

The drained shear strength parameters of the clay have been estimated at c' = 5 kPa and ϕ' = 30º based on triaxial tests (from Rankka, 1994).

For an estimation of the anisotropy of the undrained shear strength of the clay according to the relationships in the guidelines for slope stability

investigations, a value of K_{0NC} = 0.65 has been used. The basis for this choice is the values of the liquid limit of the clay in the slope.

Hydrostatic pore water pressures have been used in the calculations, with a ground water level 1.5 m below the ground surface above the crest, and a ground water level at the ground surface at point A. The lowest water level (LLW) +10 of the Säveån river (from Rankka, 1994) was used in the calculations.

4.2.5.3 *Results of the calculations*

The stability of the slope has been calculated using undrained and combined analyses. Analyses have been carried out both with and without considering the anisotropy of the shear strength of the clay. In the calculated section of the slope using undrained analysis and without considering anisotropy, a factor of safety F_c = 1.11 was obtained (Figure 4-12). Using combined analysis the corresponding factor of safety was calculated to be F_k = 1.07 (Figure 4-13). Corresponding calculations considering anisotropy gave factors of safety F_c = 1.19 and F_k = 1.14.

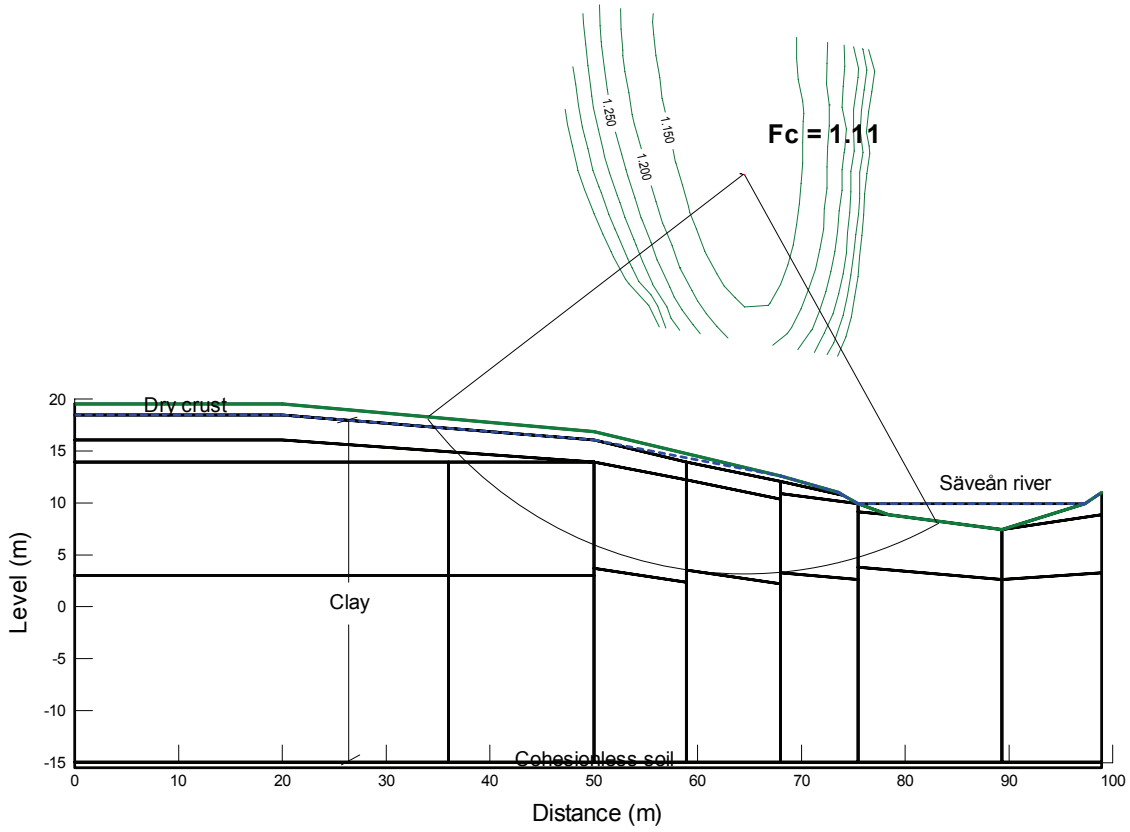

Figure 4-12 Most critical slip surface using undrained analysis.

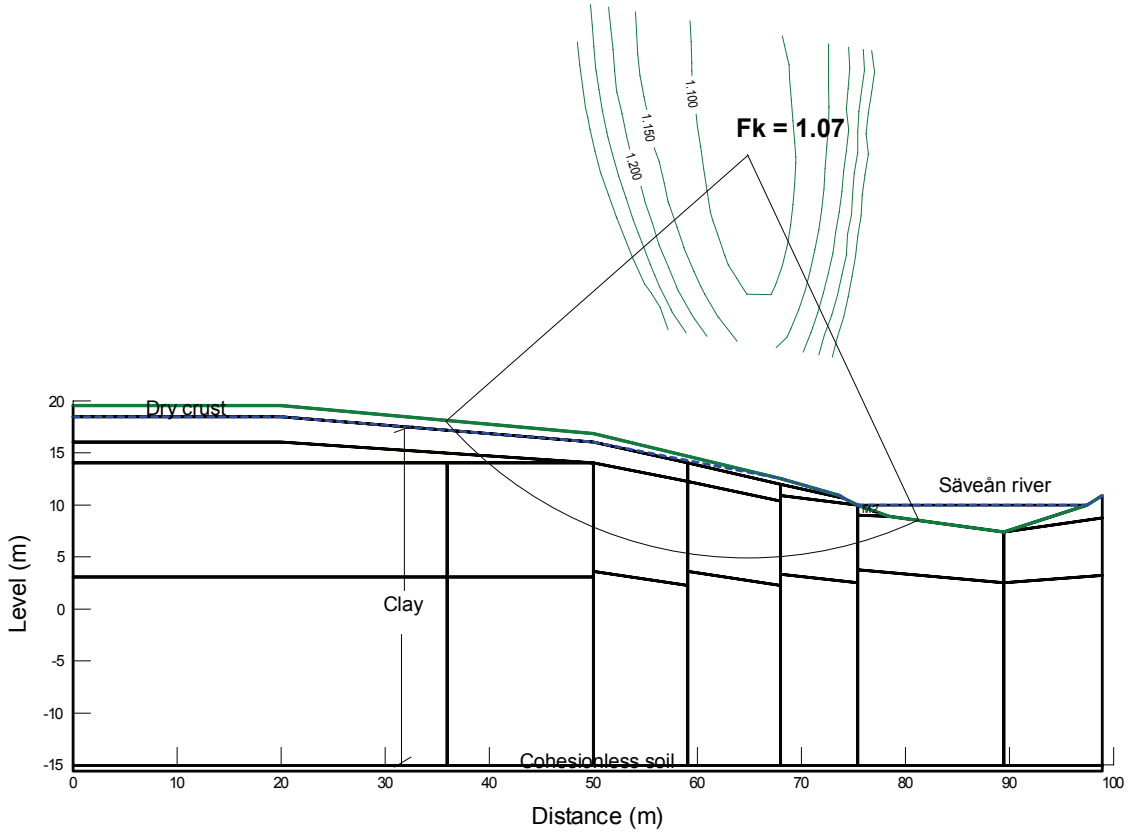

Figure 4-13 Most critical slip surface using combined analysis.

As a comparison, calculations were also carried out based on the calculated undrained shear strength from field and laboratory tests using the old relationship of the piezocone and the field vane tests (Figure 4-10), which were about 1 kPa higher at the toe of the slope. The factors of safety were then calculated to be $F_c = 1.12$ for the undrained analysis and $F_k = 1.08$ for the combined analysis (without considering anisotropy). For the Partille slope the revision of the relationships for calculation of the undrained shear strength from piezocone and field vane tests thus had, as expected, only a marginal effect on the calculated factors of safety. This is due to the fact that the soil in the Partille slope is not heavily overconsolidated and that direct simple shear tests were carried out in addition to the field tests. The revisions of the relationships of the piezocone and field vane strength have the greatest influence in heavily overconsolidated clays. The direct simple shear tests are considered to be a reliable method for determining the undrained shear strength and have thus a considerable influence when choosing the relevant undrained shear strength to be used in the analysis.

4.3 The Slumpån test site at Lilla Edet

The Slumpån test site is located about 8 km north of the municipality of Lilla Edet and 60 km north of Gothenburg. The test site is situated on the south side of Slumpån river, close to the mouth of the confluence with the Göta Älv river. The test site is located below the highest coastline and with the crest of the slope about 20 m above the present sea level. From the top of the slope to the river bottom, the height is about 21 m. The inclination of the slope is about 32º. A photo of the test site is shown in Figure 4-14.

Figure 4-14 The Slumpån test site

4.3.1 Geology

A description of the quaternary deposits along Slumpån is to be found in Fredén, 1984. The soil in the area consists mainly of glacial clay to great depths. North of Lilla Edet, glacial clay deposits with thicknesses close to 60 m are known. The glacial clay may be underlain by one to some metres of frictional soil. Here and there, sand and silt layers may be found embedded in the clay, in which artesian water pressures may occur. Artesian water pressures are known in the Slumpån valley. Thick layers of sand located high up in the soil profile are known at the confluence of the Slumpån and the Göta Älv and also at another place in the Slumpån valley (north of Fors church). The distribution of these layers is not known. In the Slumpån valley, postglacial silty clay is found on top of the glacial clay. The silty clay is important for the formation of gullies and layers several metres in thickness are known in the valley. The finer glacial clay, underlying the postglacial clay, is normally of a grey-blue colour with stripes of sulphide. Sulphide is formed in almost stagnant water deficient in oxygen. Areas of quick clay are known in the Slumpån valley. In the 1950s, the chloride contents in the clays in the Göta Älv valley were determined and used as an indicator of leaching. The majority of the upper

20-30 m of the clay deposits north of Lilla Edet was then found to be leached.

The river valleys of the Göta Älv and Slumpån are strongly marked by scars from erosion, landslides and gullies. Gullies in particular are frequently found in the Slumpån valley. Viberg (1982) mapped the landslide scars along Slumpån by means of aerial photograph interpretation. The age of the present landslide scars in the Slumpån valley are not known.

4.3.2 Site investigation

Site investigations were carried out at three locations on the slope, point A close to the river, point B at the crest and point C far behind the crest. At all locations piezocone tests (CPTU), field vane tests, undisturbed sampling and pore pressure measurements with closed BAT piezometers, were carried out. At points A and B dilatometer tests were also carried out. The piezometers were installed at depths of about 4, 9 and 15 m at point A, at about 6, 12, 21 and 28 m at point B and at about 4, 15 and 26.5 m at point C. The location of the investigations is shown in Figure 4-15.

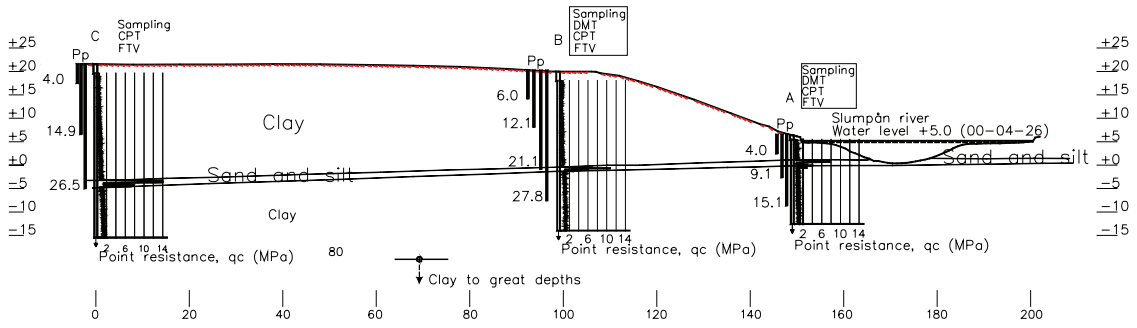

Figure 4-15: Geotechnical investigations and soil profile at the test site.

On the undisturbed samples routine analyses (bulk density, water content, liquid limit, undrained shear strength by fall cone test and sensitivity), CRS oedometer tests and direct simple shear tests were carried out.

4.3.3 Geotechnical conditions

Behind the crest in the section studied, the soil consists of clay to a depth of about 24 m (level -3 m), where there is a sand/silt layer with a thickness of about 1.5 – 2 m followed again by clay to a depth of more than 37 m. Geotechnical investigations have been carried out earlier down to a depth

of more than 60 m without reaching firm bottom layers (The Göta Älv Committee, 1962). At the toe of the slope beside the river, the depth to the sand/silt layer is about 5 m (level +1 m) and under the 1.5 – 2 m thick sand/silt layer there is clay to a depth of more than 19 m.

The upper 1 – 2 m of the soil profile consists mainly of dry crust underlain by soft clay with stains of sulphide. Above the sand layer, at a depth of 20 – 24 m at point C (level +1 to -3 m) and at a depth of 13–20 m at point B (level +7 to -1 m), the clay is highly sensitive with a sensitivity of $S_t > 200$ (quick clay). Also at point A the clay above the sand/silt layer, at a depth of 2–5 m (level +4 to +1 m) is highly sensitive ($30 < S_t < 65$). The slope geometry and location of the sand/silt layer are shown in Figure 4-15.

The density, natural water content and liquid limit of the clay are shown in Figure 4-16. According to old "rules of thumb" (Eriksson, 1996) a clay is normally consolidated or only slightly overconsolidated if the water content (w_N) is 5–10% higher than the liquid limit (w_L) and overconsolidated if the liquid limit is higher than the water content. For a quick clay the water content is much higher (often more than 20% higher) than the liquid limit (The Göta Älv Committee, 1962). These "rules of thumb" are well in accordance with the properties of the clay in the section studied.

On the basis of the liquid limit of the clay and the results of the piezocone tests, the clay above the sand/silt layer has been assessed as post-glacial clay and the clay under the sand/silt layer as glacial clay.

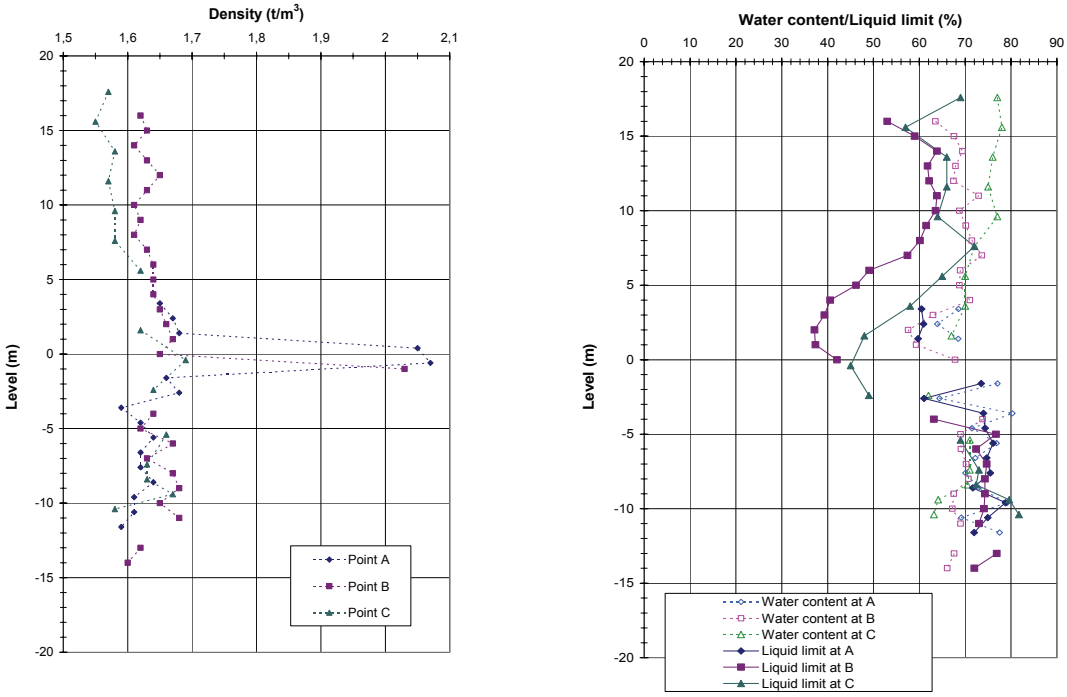

Figure 4-16: Density, natural water content and liquid limit of the soil.

Pore pressure measurements were carried out on three different dates at points A and B (22-5-2000, 21-8-2001 and 14-2-2002) and on two different dates at point C (21-8-2001 and 14-2-2002). Comparing these measurements, it was observed that the pore pressures for the highest situated piezometer were lower at the measurement made on 21-8-2001. For the deeper piezometers the pore pressures were fairly equal on all three occasions. The pore water pressure measurements indicate that at the crest and behind the crest, the pore water pressure is less than the hydrostatic pressure down to the sand/silt layer at about -3 m to ±0 m. This implies that behind the crest there is a downward groundwater flow from the ground surface towards the sand/silt layer. Under the sand/silt layer, at point B, the measurements indicate that the pore water pressures are hydrostatic or slightly higher. At point A the measurements indicate hydrostatic pore water pressures down to the sand/silt layer at about +1 m and thereunder slightly higher than hydrostatic pressure. This implies that at the toe of the slope there is a groundwater flow upwards, towards the sand/silt layer. The measurements show that the sand/silt layer is not free-draining. Pore pressures measured on 21-8-2001 are shown in Figure 4-17. It should be pointed out that the pore pressures at the highest located piezometer at point C indicate a ground water level slightly above the ground surface. It is not likely to have slightly artesian water pressures at a depth of 4 m. What is more likely at that depth is that the ground water level is below the

ground surface. The measured pore pressures at this level could possibly be due to a malfunctioning of the piezometer.

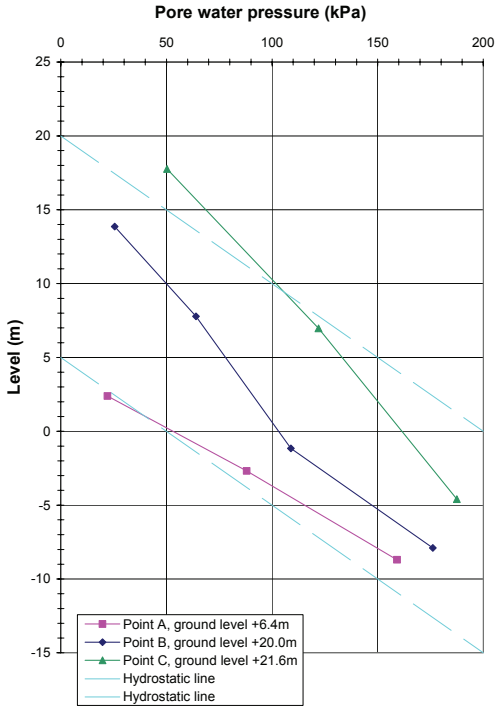

Figure 4-17: Pore water pressures measured on August 21, 2001.

Vertical preconsolidation pressures determined by CRS oedometer tests at points B and C are shown in Figure 4-18. The results show an overconsolidation ratio of 1.3, except for the clay under the sand/silt layer in point B, where the CRS oedometer tests indicate an overconsolidation ratio closer to 1.2. One reason for this may be that the high plastic (glacial) clay under the sand/silt layer has not developed high quasi-preconsolidation pressures with time in the same way as the (post-glacial) clay above the sand/silt layer with slightly lower plasticity (Larsson, 2007). Another reason could be that the pore water pressures under the sand/silt layer may previously have been higher than today and the effective stresses were then lower.

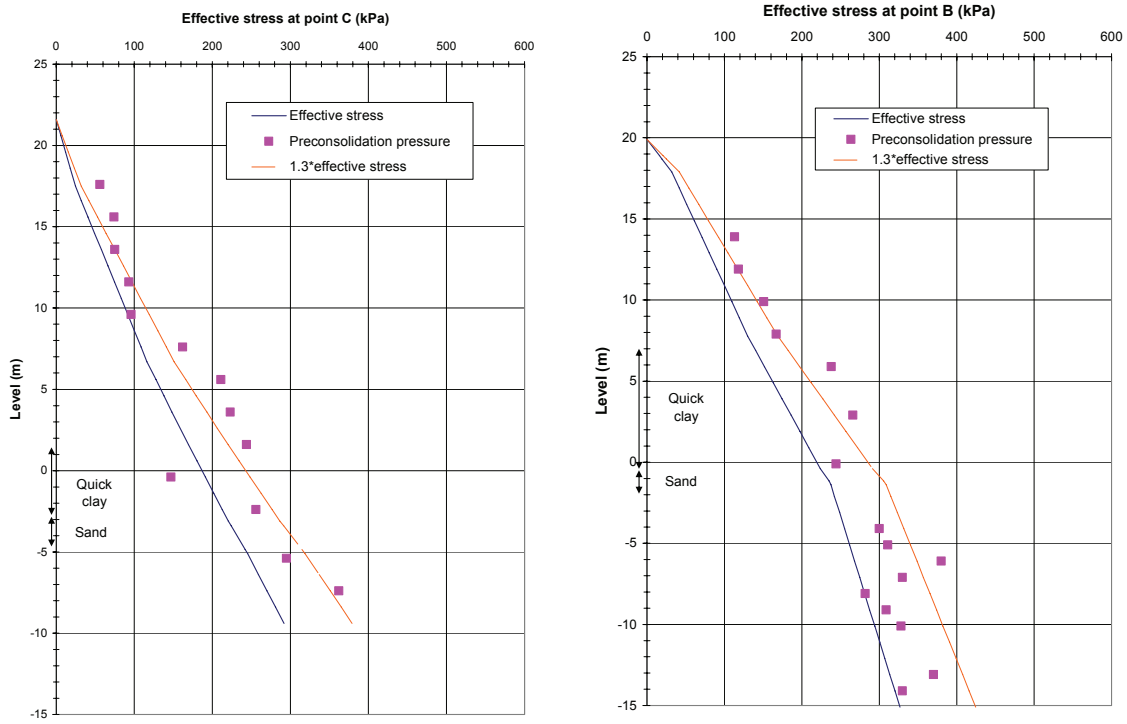

Figure 4-18: Effective vertical stress and preconsolidation pressures following CRS oedometer tests at points C and B

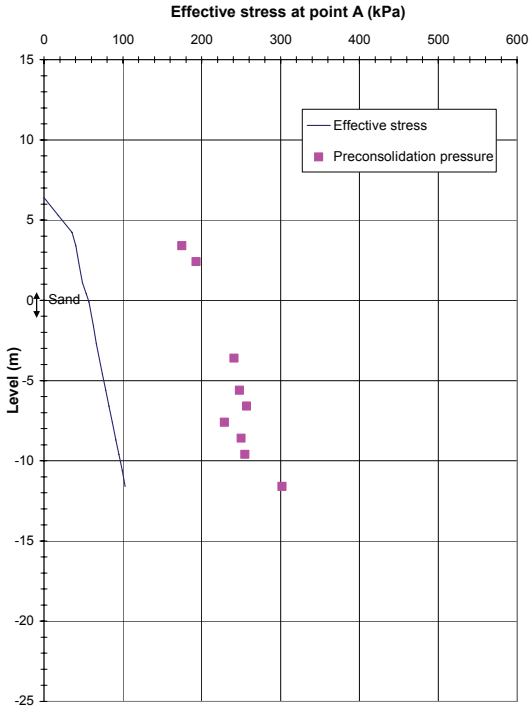

Figure 4-19: Effective vertical stress and preconsolidation pressures following CRS oedometer tests at point A.

Comparing the stress conditions at point C, behind the crest, and at point B at the crest the preconsolidation pressures and the present effective stresses are slightly higher at point B down to the sand/silt layer. The preconsolidation pressures at the toe of the slope, at point A (Figure 4-19), are slightly lower than at the same level below the crest at point B. The reason for this is most likely related to historical ground water conditions. Before Slumpån started to erode its course the pore pressures could be expected to have been hydrostatic from the ground surface. As the valley became deeper, the soil at the bottom became unloaded. At the same time the soil below and behind the crest consolidated for increasing effective stresses due to a lowered ground water level and decreasing pore pressures.

The sand/silt layer is slightly inclined, lower at point C (level -3 m) than at point A (level +1 m) (and even higher on the other side of Slumpån). As the consolidation process over time causes the sediments to compress and the total settlements to become larger for thick layers of sediments, the inclination indicates that at point C the bedrock is located deeper and the sediments are thicker, at least at deposition, than at point A.

4.3.4 Shear strength

The undrained shear strength has been determined by vane tests and piezocone tests in the field and by direct simple shear tests and fall cone tests in the laboratory. The measured values from the field vane tests, the piezocone tests and the fall cone tests have been corrected with regard to the liquid limit and the overconsolidation ratio (Figure 4-16).

An evaluation of the undrained shear strength from piezocone and field vane tests for the Slumpån test site has been made using the same relationships (Larsson and Åhnberg, 2003) as for the Partille test site, see Section 4.2.4. The evaluated shear strengths have also been compared with the shear strength to be expected in clay with the corresponding loading history and consistency limits. However, for the Slumpån test site the relationships in the updated version of SGI Information 3 (Larsson et. al., 2007), where overconsolidation is also taken into consideration, have been used.

The lower part of the slope (at point A and below the river) has most likely been formed by erosion processes as described in Section 4.3.1. The clay layers at point A thus have a different loading history than the upper parts of the slope (points B and C). As described previously, the historical pore

water pressure conditions could have been different in different parts of the slope, causing a variation in the preconsolidation pressures. This stress history of the slope is of importance for the undrained shear strength of the soil. Consequently, evaluation of the measured shear strengths at points A, B and C has been divided up. Compilation of all the shear strength data, both related to depth and related to level, clearly reveals that the best correlation is obtained by plotting the data related to the level. This is in agreement with the fact that the slope has been eroded from an almost horizontal or only slightly inclined ground surface.

As regards the ground conditions at the site, i.e. a sand/silt layer overlying a clay layer, certain aspects of the different methods used for determination of the undrained shear strength may be worth considering.

- The fall cone test is dependent on the quality of the samples and is from experience known to often give values that are too low at depths greater than 10 to 15 m.
- The field vane test carried out using equipment without protective casing (Geotech model, as used in this study) in this type of soil sequence (with a firm layer overlaying a loose layer) entails a risk that the firmer soil sticks to the vane during penetration into the looser soil, which will cause disturbance and a risk that the undrained shear strength is underestimated (Bergdahl, 1984, Larsson et. al., 1984).
- The piezocone test is also sensitive to soil sequences with firm layers overlaying very loose layers. The forces that arise in the firm layers may cause zero drift or hysteresis effects that influence the accuracy of the measurements in the underlying looser layers (Larsson, 1993). Furthermore, the test is sensitive to possible changes in temperature after the zero readings have been taken.

Comparing the evaluated, undrained shear strengths from field vane tests, piezocone tests, direct simple shear tests and fall cone tests at point C, behind the crest, the results show very good agreement to about level ±0, i.e. above the sand/silt layer, see Figure 4-20. However, the results from the fall cone tests are slightly lower than the results from the other tests. The empirical shear strength also shows quite good agreement with the measured undrained shear strengths. Below the sand/silt layer, from about level -5, the results from the piezocone tests and the direct simple shear tests show good agreement. The increase in the measured undrained shear strength with depth evaluated from these methods is also about the same as above the sand/silt layer. In contrast, the evaluated undrained shear strengths from the field vane tests and the fall cone tests are lower or much

lower than the measured undrained shear strength using the other methods. However, this is probably related to the limitations of the methods or equipment pointed out above. On the other hand, the empirical shear strength under the sand/silt layer is higher than all the measured shear strengths.

The undrained shear strength above the crest at point C, where the ground level is about +21.5, can, under the dry crust, be described as 14 kPa at level +20 and thereunder increasing by 0.8 kPa/m to 19.6 kPa at level +13, and then increasing by 2.1 kPa/m, see Figure 4-20.

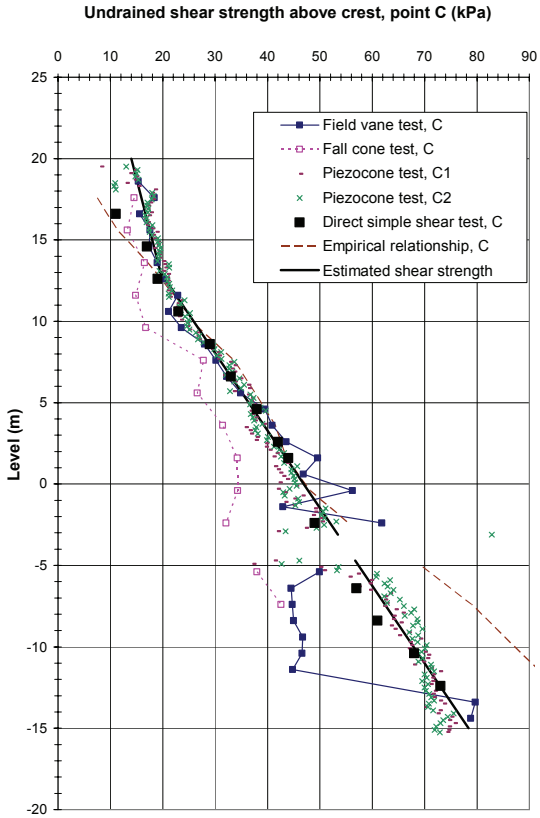

Figure 4-20: Undrained shear strength above the crest (at point C).

Comparing the evaluated undrained shear strengths from field vane tests, piezocone tests, direct simple shear tests and fall cone tests at point B, at the crest, there is a larger discrepancy between the methods, see Figure 4-21. Above the sand/silt layer, the measured undrained shear strengths from the direct simple shear tests, the field vane tests and the empirical shear strength show rather good agreement. The estimated undrained shear strengths from these methods are higher than the estimated shear strengths at point C, above the sand/silt layer, which is in accordance with the slightly higher preconsolidation pressures. In contrast, the results from the

piezocone tests and the fall cone tests are lower than the measured shear strengths using the other methods at point C. Under the sand/silt layer, the agreement between the methods is better. However, the results from the fall cone tests are lower and the empirical shear strength is higher than the estimated shear strengths. The estimated undrained shear strength below the sand/silt layer does not increase as much with depth as above the sand/silt layer. Nor does it appear to increase as much with depth as under the sand/silt layer at point C. One reason for this could be the influence of the eroded valley on the vertical stresses at depth at this point together with a different pore pressure gradient. Except for the results from the direct simple shear tests, it could also be related to the limitations of the methods as described above.

Attaching most importance to the results from the direct simple shear tests, the undrained shear strength at the crest at point B, where the ground level is about +19.5, can, under the dry crust, be described as a constant 23 kPa to level +14 and thereunder increasing by 1.25 kPa/m to 28 kPa at level +10. From level +10 the undrained shear strength increases by 2.3 kPa/m to 51 kPa at level ±0 and it then increases by 1.0 kPa/m, see Figure 4-21.

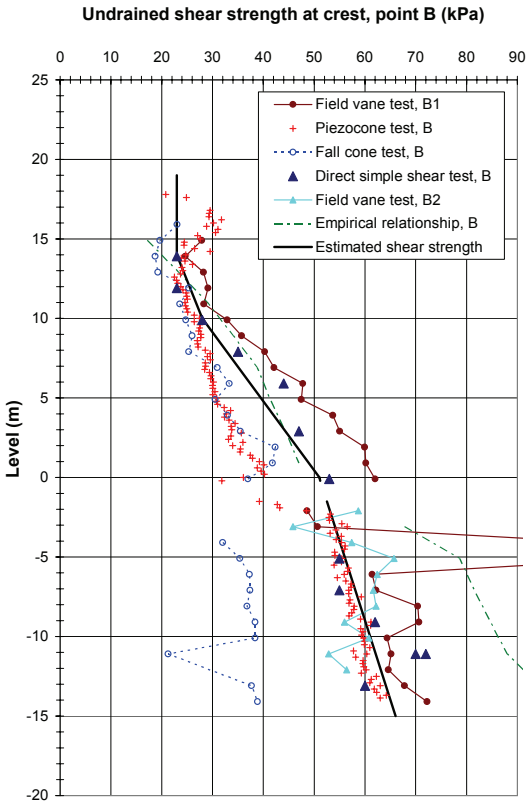

Figure 4-21: Undrained shear strength at the crest (at point B).

At point A close to the river, a comparison of the evaluated undrained shear strengths from field vane tests, piezocone tests, direct simple shear tests and fall cone tests show good agreement above the sand/silt layer, see Figure 4-22. The empirical shear strength also shows good agreement with the measured undrained shear strengths above the sand/silt layer. Below the sand/silt layer the results from the field vane tests, piezocone tests and the direct simple shear tests show a larger scatter but reasonable agreement. The results from the fall cone tests are lower than the results from the other tests and hardly increase at all with depth. Comparing the measured undrained shear strengths with the empirical shear strength, somewhat higher values are obtained with the empirical relationship.

The undrained shear strength at the toe of the slope, beside the river where the ground level is about +6.5, can under the dry crust be described as 26 kPa at level +5 and thereunder increasing by 2.2 kPa/m to 37 kPa at level ±0 and then increasing by 1.0 kPa/m, see Figure 4-22. The undrained shear strength at point A is lower than at the same levels at point C, behind the crest. It is natural that lower preconsolidation pressures and an unloading of the ground, due to an erosion process, result in lower undrained shear strengths.

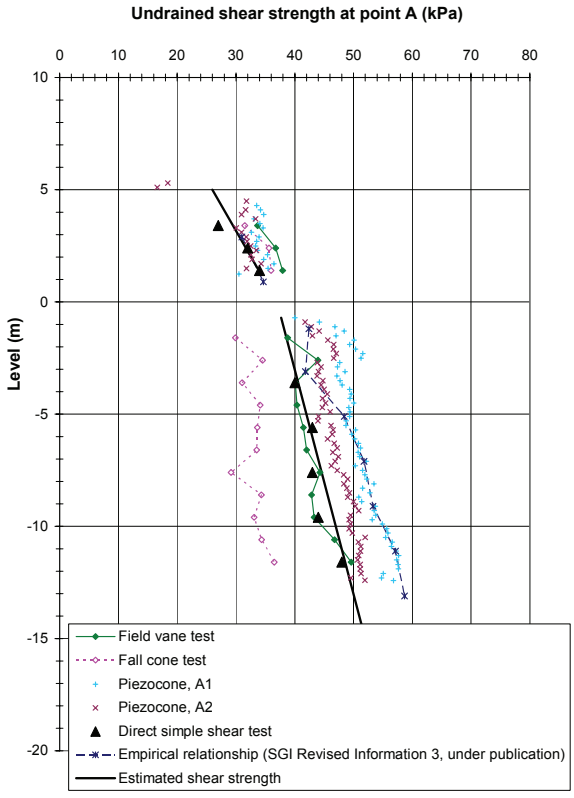

Figure 4-22 Undrained shear strength at point A (the toe of the slope).

To see how much the estimated shear strength (i.e. best estimate based on available data), could differ when the field vane and piezocone tests are evaluated with the old (Larsson et. al., 1984, Larsson, 1993) and new (Larsson and Åhnberg, 2003, Larsson et. al., 2007) relationships respectively also evaluations based on the old relationships, without correction for overconsolidation have been carried out. Figure 4-23 shows a compilation of the undrained shear strengths at point A, where the measured shear strengths from the field vane tests and the piezocone tests have been evaluated against the old relationships. Comparing the measured undrained shear strengths using the old and the new relationships for evaluation of the field vane and piezocone shear strength respectively, it can be noted that the agreement between the direct simple shear tests, the field vane tests and the piezocone tests is greatly improved with the new relationships (Figure 4-22). The results from the fall cone tests are also lowest with the old relationships. Using the old relationships, the scatter between all the results is quite equally distributed, whereas when using the new relationships the results from the direct simple shear tests, the field vane test and the piezocone tests show best agreement, along with the empirical shear strength.

Because of the even scatter between the results, it is rather difficult to make a best estimate of the undrained shear strength. Relying slightly more on the results from the direct simple shear tests, but still expecting the undrained shear strength to be somewhere in the middle of the results, the undrained shear strength at point A would have been described as 29 kPa at level +5 and thereunder increasing by 2.6 kPa/m to 42 kPa at level ±0 and then increasing by 0.87 kPa/m, see Figure 4-23. This undrained shear strength is about 2 to 5 kPa higher than the estimated undrained shear strength based on the new relationships.

In the evaluation, the results from direct simple shear tests have been assigned fairly considerable weight. The undrained shear strength evaluated from the direct simple shear tests is more than 2 kPa lower than the undrained shear strength evaluated from both the field vane tests and the piezocone tests using the old relationships. It was therefore considered relevant to also evaluate the undrained shear strength without support from the results from the direct simple shear tests. Assuming that the results from the field vane and the piezocone tests are equally reliable and the results from the fall cone tests are too low, the undrained shear strength would then have been described as 38 kPa at level +5 and thereunder increasing by 1.8 kPa/m to 47 kPa at level ±0 and then increasing by 0.8 kPa/m, see Figure 4-23. This undrained shear strength is about 7 to 12 kPa

higher than the undrained shear strength based on the new relationships for the field vane and piezocone shear strength together with the direct simple shear tests.

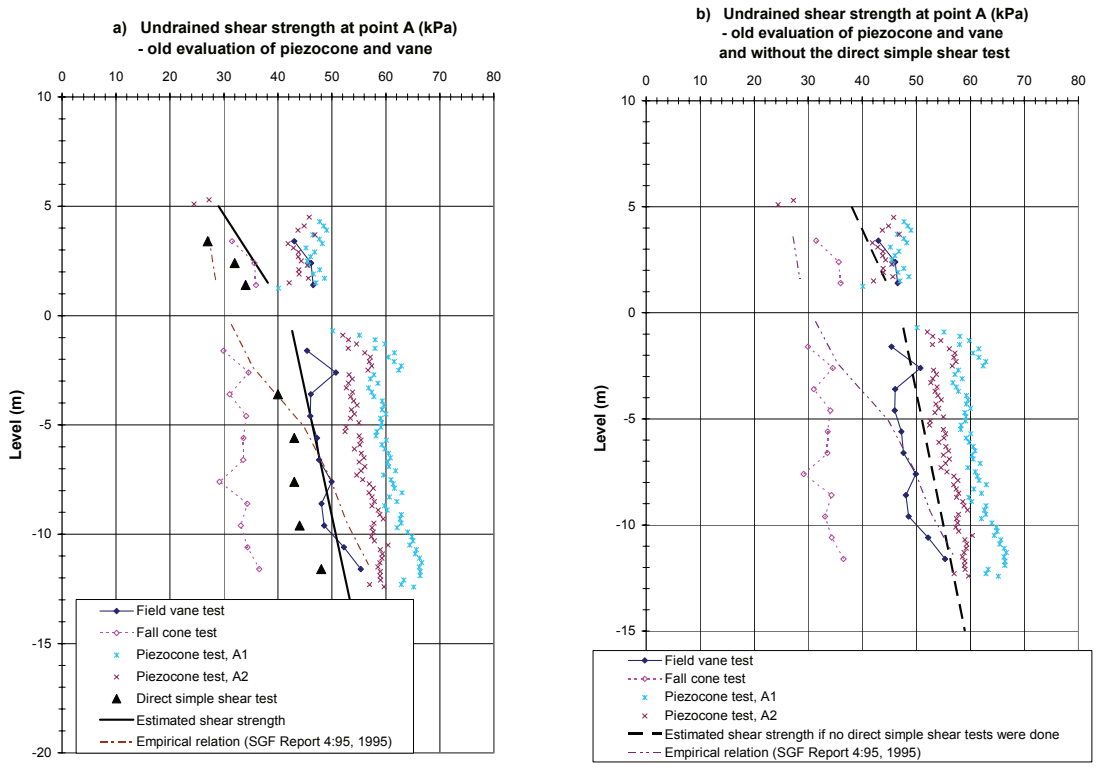

Figure 4-23 Estimation of undrained shear strength at point A (the toe of the slope) a) using the old evaluations of the piezocone and field vane test (Larsson et. al., 1984, Larsson, 1993) and b) using the old evaluations of the piezocone and field vane test and without support from the direct simple shear tests.

4.3.5 Stability analysis

4.3.5.1 *General*

Stability calculations have been carried out in accordance with the Swedish guidelines for slope stability investigations (Commission on Slope Stability, 1995). What are known as classical methods have been used. The calculations have been performed for circular slip surfaces using the Morgenstern-Price method and the computer program SLOPE/W. Analyses have been made with both undrained and combined analysis. The pore water pressure conditions have been defined as measured and deduced pressure at discrete points. The effect of anisotropy has been estimated by using the relationships based on K_{0NC}, as described in the guidelines for slope stability investigations.

4.3.5.2 *Basis for stability calculations*

The geometry of the slope has been determined by levelling. The bottom geometry of Slumpån has been determined by sounding with a lead line.

As described in Section 4.3.3, behind the crest the soil profile consists of clay to a depth of about 24 m (level -3 m), where there is a sand/silt layer with a thickness of about 1.5 – 2 m followed once again by clay to a depth of more than 37 m. The undrained shear strength of the clay has been estimated based on the results of the field and laboratory tests as described in Section 4.3.4, using the new evaluation of the piezocone and the field vane test with the extra correction for overconsolidation. Between the investigated points and in parts of the slope where no investigations have been carried out, e.g. under the river, the estimated shear strength has been adapted to the probable loading history of the soil. The undrained shear strength of the dry crust has been assumed to be 25 kPa. The geometry and the estimated undrained shear strength in the calculated section are shown in Figure 4-24.

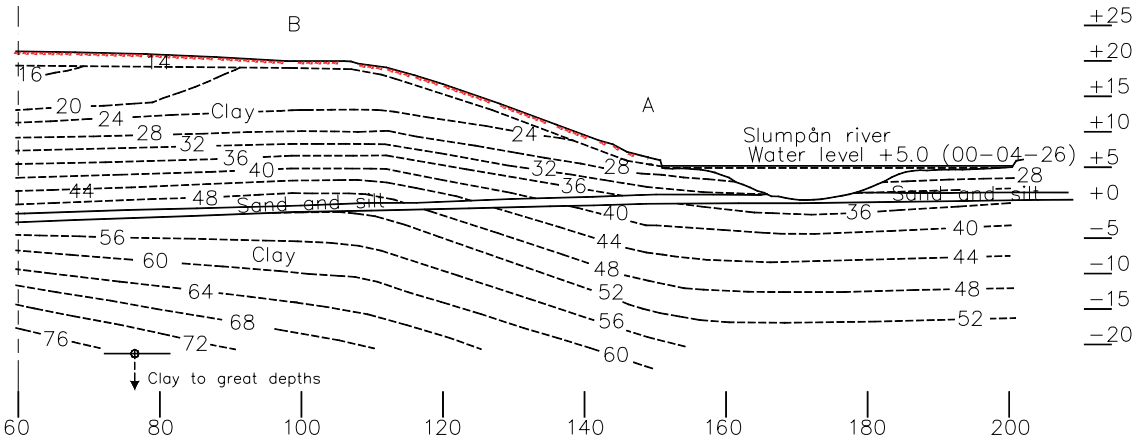

Figure 4-24 Geometry and assumed undrained shear strength of the calculated section.

Based on empirical experience, the drained shear strength of the clay has been assumed to be $c' = 0.1 \cdot c_u$ and $\phi' = 30°$. The friction angle of the sand/silt layer has been assumed to be $\phi' = 30°$. The friction angle estimated from the piezocone tests in the sandy part of the sand/silt layer was between 31° and 38°. A sensitivity analysis of the significance of the friction angle of the sand/silt for the overall stability of the slope has been carried out.

For estimation of the anisotropy of the undrained shear strength of the clay according to the relationships in the guidelines for slope stability

investigations, a value of K_{0NC} = 0.65 has been used. The basis for this choice is the values of the liquid limit of the clay in the slope.

The pore water pressure used in the calculations has been based on the pore water pressure measurements as described in Section 4.3.3. The pore water pressures between the locations of the pore water pressure measurements have been interpolated. The pore pressures in the soil under the river have been chosen at the same values as at point A. The water level measured in the river on 26-4-2000, level +5.0, was used in the calculations.

4.3.5.3 *Results of the calculations*

The stability of the slope has been analysed using undrained and combined analysis. Analyses have been carried out both with and without considering anisotropy of the shear strength of the clay. In the calculated section of the slope using undrained analysis and without considering anisotropy, a factor of safety F_c = 1.00 was obtained (Figure 4-25). With combined analysis the corresponding calculated factor of safety was F_k = 0.97 (Figure 4-26). Corresponding calculations taking into account anisotropy gave factors of safety of F_c = 1.08 and F_k = 1.05. Using a friction angle of 34º instead of 30º in the sand/silt layer had no significant impact on the results (F_c = 1.00 and F_k = 0.98 without considering anisotropy).

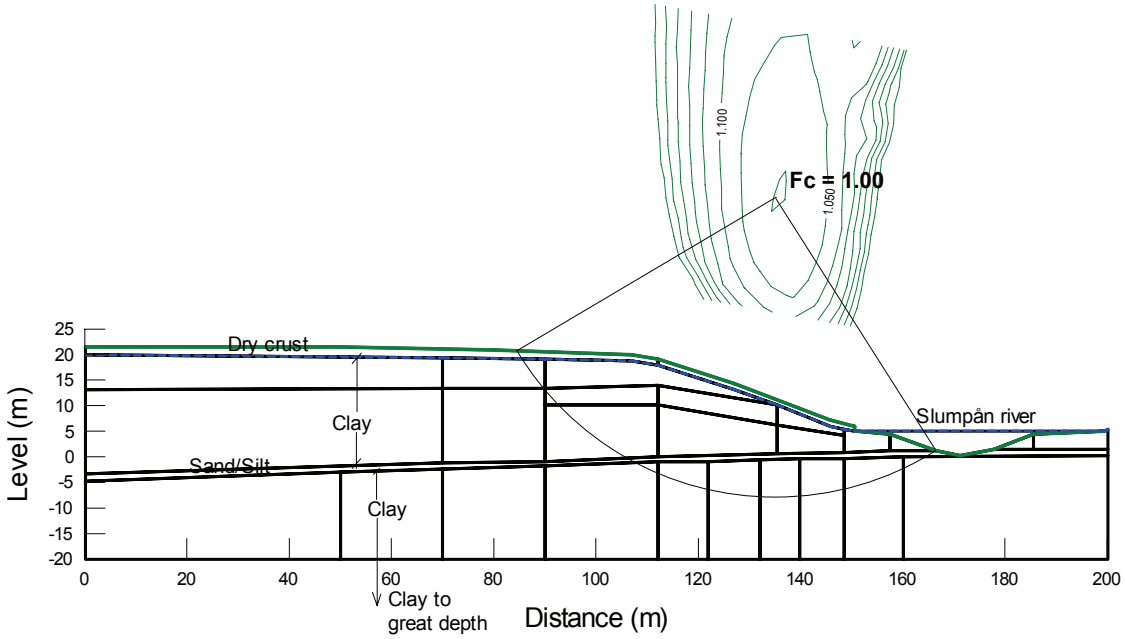

Figure 4-25 Most critical slip surface with undrained analysis.

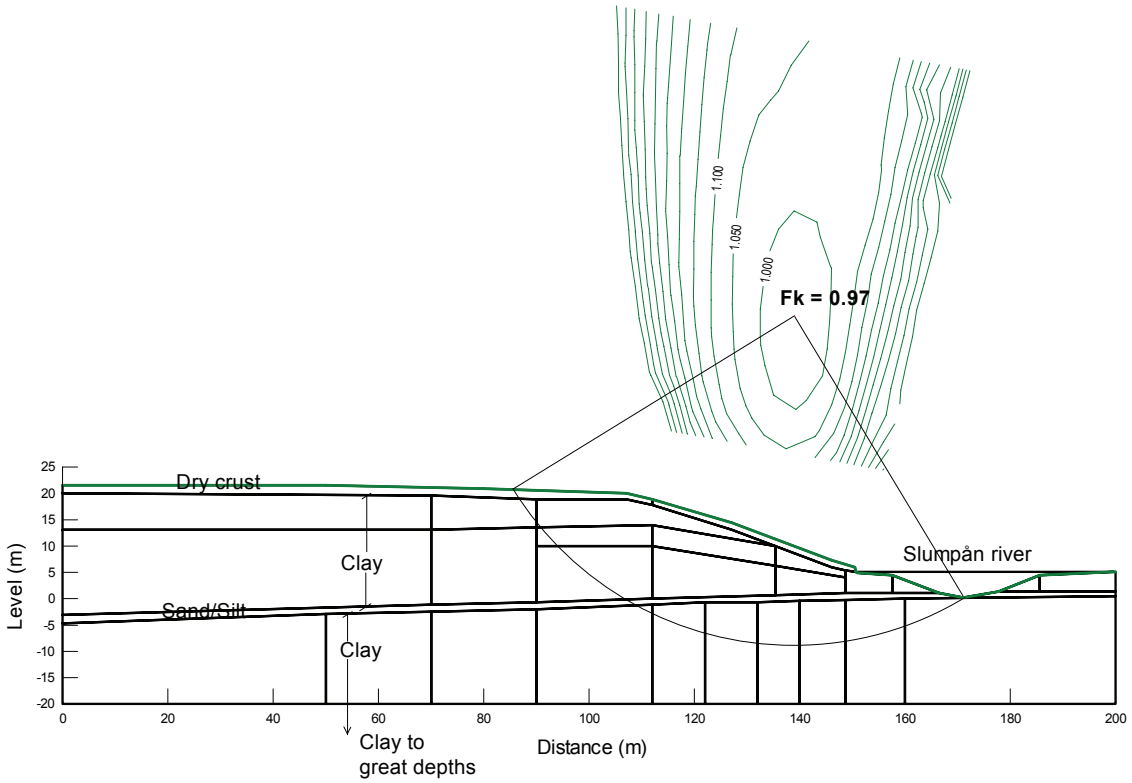

Figure 4-26 Most critical slip surface with combined analysis.

Additional calculations were also carried out for the Slumpån test site based on the estimated undrained shear strength from field and laboratory tests using the old evaluation of the piezocone and the field vane tests (Figure 4-23a). The factors of safety were then calculated at $F_c = 1.05$ for the undrained analysis and $F_k = 1.00$ for the combined analysis (without taking into account anisotropy). For the Slumpån slope the revision of the relationships for evaluation of the undrained shear strength from piezocone and field vane tests also only have a minor effect on the calculated factors of safety. This is due to the fact that the soil in most parts of slope is not heavily overconsolidated and that direct simple shear tests were carried out in addition to the field tests.

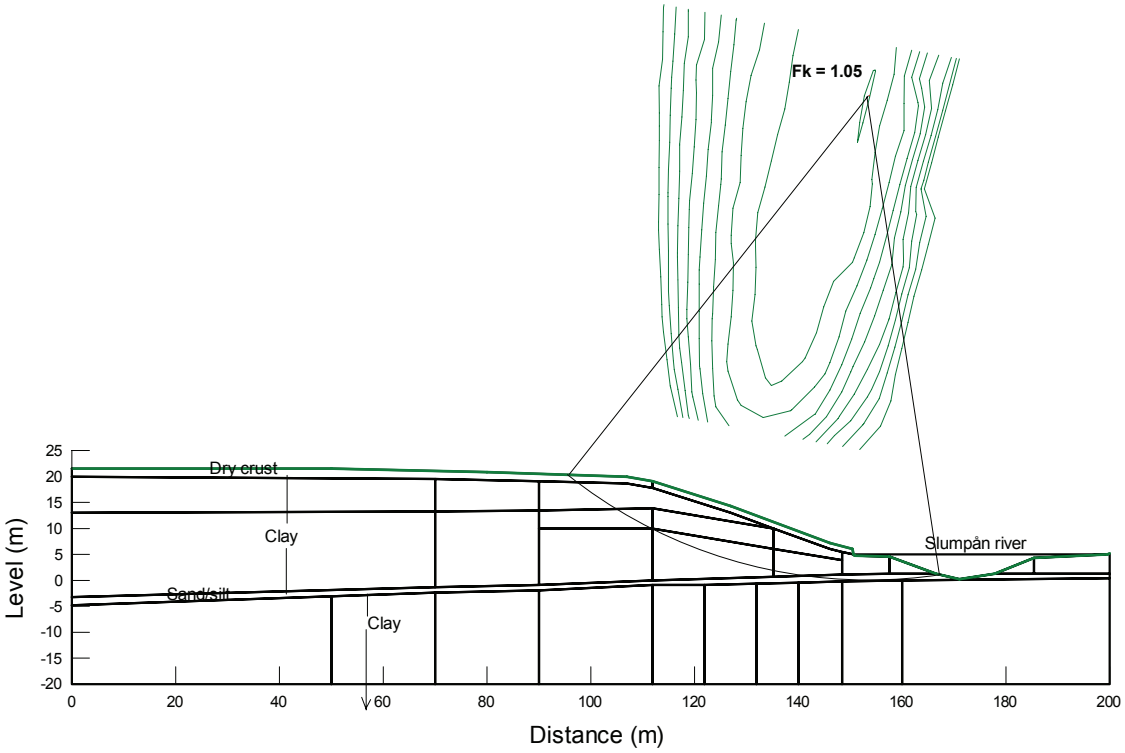

Figure 4-27 Most critical slip surface with combined analysis using the undrained shear strength based on the old relationships for the piezocone and field vane and without considering the direct simple shear tests.

Additional calculations were also carried out to show the effect on the stability of the slope if the undrained shear strength was estimated from the field vane and piezocone tests using the old evaluation, the empirical relationship and the fall cone test results, but without taking into account the direct simple shear tests (Figure 4-23 b). The factors of safety were then calculated at F_c = 1.08 for the undrained analysis and F_k = 1.05 for the combined analysis (without considering anisotropy), both analyses giving shallow critical slip surfaces passing through the sand/silt layer for more than 20 m close to the river. The most critical slip surface with combined analysis is shown in Figure 4-27. In this case, the assumed shear strength of the sand/silt layer significantly affects the calculated factor of safety. The critical slip surfaces for both undrained and combined analysis and with new and old relationships for evaluation of the piezocone and field vane tests in addition to the direct simple shear test results cross the sand/silt layer and extend at least 7 m beneath it (Figure 4-25 and Figure 4-26). The factor of safety for a similar slip surface, using the undrained shear strength estimated using the old evaluation of the field vane and piezocone tests without direct simple shear test results, was calculated at F_c = 1.10 with undrained analysis and F_k = 1.05 for combined analysis, which are 10% and 8% higher respectively than when using the new relationships.

5. MODEL TESTS

5.1 Scope of the tests

The model tests were conducted in order to study the effects of the ratio between horizontal and vertical stresses ($K = \sigma'_h/\sigma'_v$) on the undrained shear strength as determined using piezocone and vane tests under controlled conditions. The aim was to simulate the stress conditions in the active and passive zones of a slope as well as for horizontal ground surface. For each stress condition, model piezocone and vane tests were conducted and the cone resistance and penetration pore pressure were measured for the piezocone test and the torque for the vane test. The sleeve friction for the piezocone test was also registered but was not analysed as the cone manufacturer did not consider it to be sufficiently accurate (see Section 5.2.3.1 below). Furthermore, sleeve friction measurements are not used for evaluation of the undrained shear strength from piezocone tests.

In order to control the stress history of the clay specimens, each specimen was consolidated for stresses above its natural vertical and horizontal preconsolidation pressures. As a result, a new stress history for each specimen was created. All samples were taken from the upper part of the soil profile under the dry crust at the Partille test site.

The results of the model tests were compared with results from direct simple shear tests. Corrections were made according to the equation that describes how the undrained shear strength varies with the preconsolidation pressure and overconsolidation ratio (see Section 5.4.2 below).

5.2 Equipment

5.2.1 Sampler

To obtain clay samples that were large enough for the model tests and relatively easy to collect, a special sampler was designed and built. It consists of a steel cylinder, 900 mm long and with an inner diameter of 140 mm. It contains four PVC tubes with an inner diameter of 126 mm. The lengths of the PVC tubes are 200 mm (the upper tube including a filter), 300 mm (two sample tubes) and 100 mm (bottom tube). The two 300 mm tubes in the middle contain the clay samples to be used in the triaxial tests. A 66 mm long cutting edge is screwed onto the steel cylinder at the bottom. The PVC tubes are kept in place by the cutting edge and a shutter can be placed in front of the bottom PVC tube.

At the top, the steel cylinder is screwed onto a lid with a hollow rod in its centre, which can be connected to further extension rods for pushing down. On the upper part of the lid two clack valves are mounted to drain water from the tubes during sampling. There is also a smaller clack valve in the lid, which is connected to a thin, flexible plastic hose. The hose can be connected to a vacuum pump to exert suction on the upper end of the sample. This helps to retain the clay samples in the tubes during withdrawal of the sampler. A photograph of the sampler is shown in Figure 5-1.

Figure 5-1 Sampler constructed as part of the project.

5.2.2 Triaxial cells

Two types of triaxial cells were designed and built to carry out the model tests (Löfroth, 2002). The first type was used to consolidate clay specimens for isotropic stress conditions and for conditions with larger horizontal stress than vertical stress ($K \geq 1$). The second type was used to consolidate clay specimens for isotropic stress conditions or for stress conditions with higher vertical stress than horizontal stress ($K \leq 1$). Two cells of each type were built. The cells were designed for specimens with a height of 280 mm and a diameter of 126 mm.

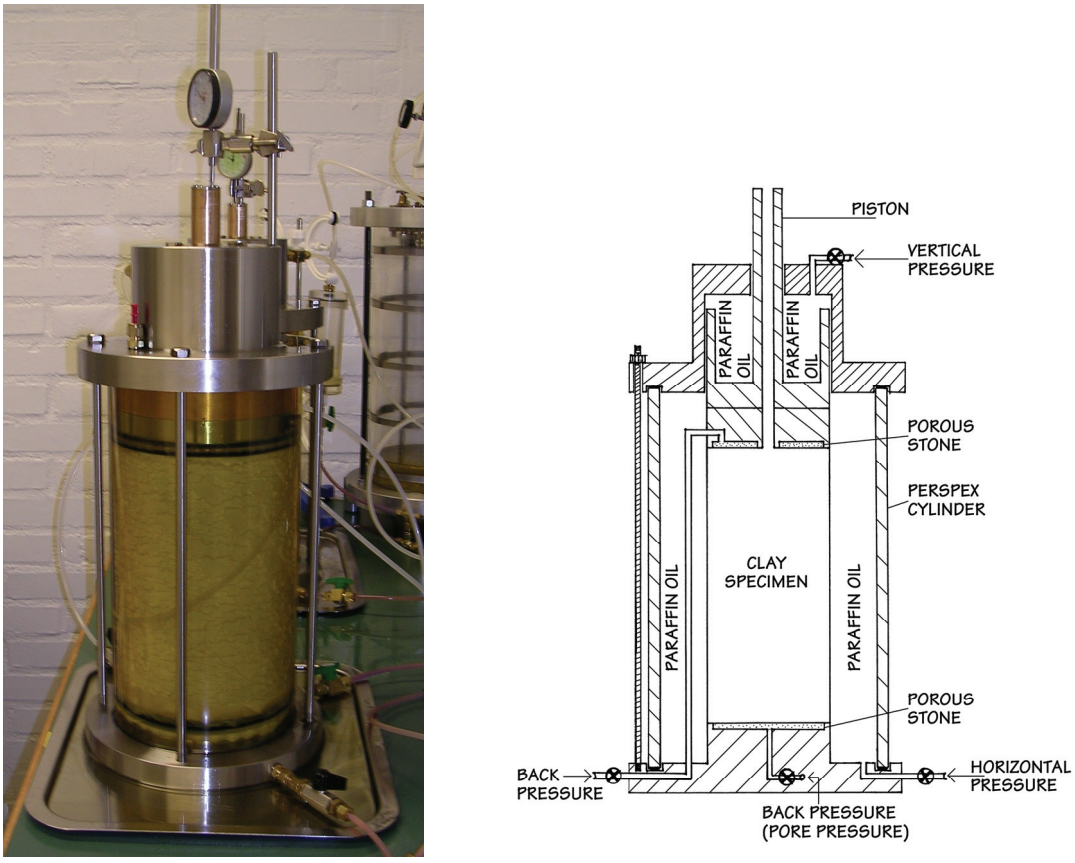

Figure 5-2 Triaxial cell for conditions with higher horizontal stress than vertical stress.

The first type of cell (Figure 5-2) consists of a round, steel-bottom plate and a cylinder with a lid and a piston. The bottom plate has a pedestal in its centre on which the clay specimen is placed as well as connections for controlling cell pressure and drainage and measurement of pore pressure. The pedestal has a diameter of 126 mm and a porous stone on top. The specimen is placed on the porous stone. The lower part of the piston, a 40 mm thick steel plate with a diameter of 126 mm and a porous stone at the bottom, was placed on top of the specimen. This plate also has a connection for drainage and measurement of pore pressure. A rubber membrane, held in place by o-rings at the pedestal and the piston, surrounds the specimen. A 380 mm high cylinder made of Plexiglas, with an inner diameter of 210 mm, is placed around this assembly. The lid, containing the upper part of the piston, is placed on top of the cylinder. The lid is made of steel and the upper part of the piston is made of brass. The upper part of the piston is bolted together through two small holes in the top of the lid with the lower part placed on top of the specimen. The centre of the piston is hollow. The lid and the piston are designed in such way that when the piston is inserted into the lid a pressure-tight chamber is formed in between, see Figure 5-2. In the lid there is a connection to control the pressure in the chamber.

The Plexiglas cylinder is filled with paraffin oil, through which the specimen is subjected to horizontal pressure. The chamber between the lid and the piston is also filled with paraffin oil, through which the specimen is subjected to vertical pressure. The vertical pressure on top of the specimen is thus separated from the horizontal pressure on its sides.

The second type of cell (Figure 5-3) also consists of a bottom plate and a cylinder with a lid and a piston. Where this type of cell differs from the first type is in the lid and the piston. The piston consists of a steel plate and a rod. The lid consists of a large steel plate with a hole in the centre with the piston rod passing through the hole. A steel frame is hung on the piston rod and weights can be applied to the lower part of the frame.

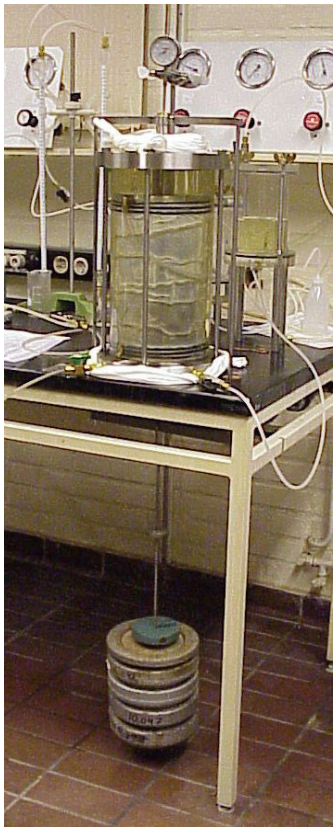

Figure 5-3 *Triaxial cell for conditions in which vertical stress is greater than horizontal stress (with and without weights).*

5.2.3 Mini-piezocone and vane

5.2.3.1 *Mini-piezocone*

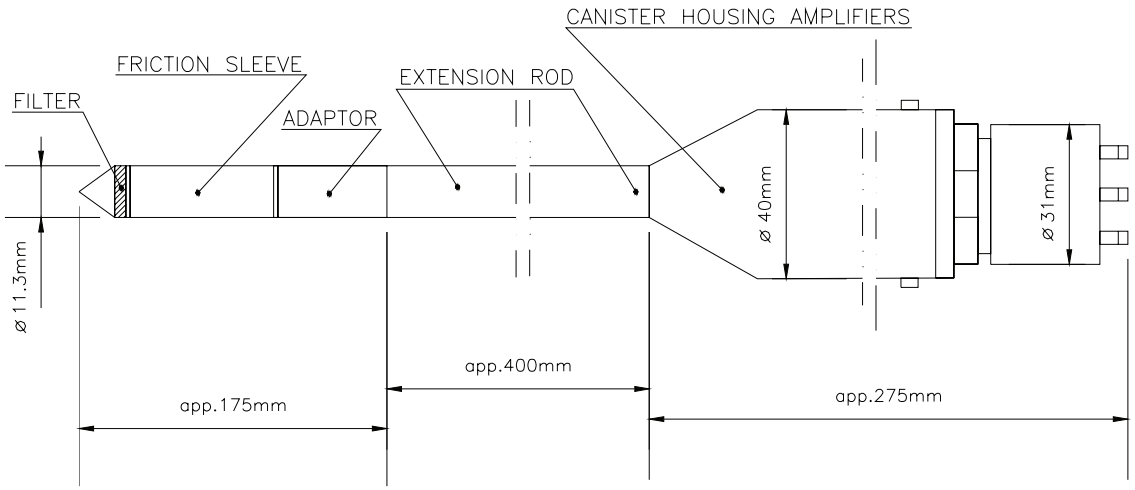

Figure 5-4 Mini-piezocone used in the model tests.

A mini-piezocone from Fugro Engineers BV was used in the model tests. The piezocone has a cone area of 100 mm^2 (diameter 11.3 mm), a friction sleeve with an area of 1500 mm^2 and a pore pressure transducer with a filter just behind the shoulder of the tip. The piezocone is equipped with amplifiers to enhance the output signals for further data acquisition. These amplifiers are located in a canister fitted to the top of the extension rod of the cone, see Figure 5-4. The length of the piezocone assembly is 575 mm from the tip to the amplifier.

The piezocone is a subtraction cone equipped with two load cells in series for the tip resistance (Q) and the tip resistance + sleeve friction (Q+F) respectively. The actual sleeve friction (F) is derived by subtraction i.e. F = (Q+F)-Q. The piezocone has been calibrated up to 20.0 MPa tip resistance and 1.5 MPa pore pressure by the manufacturer. As the desired calibrated tip resistance was 2 MPa, filtering has been used to reduce the noise of the signal. According to the manufacturer, the sleeve friction readings should be disregarded as not being sufficiently accurate.

According to the manufacturer, the quality of the data from the mini-piezocone is generally considerably lower than the data from larger probes. This is due to the miniature sensors being less stable than the larger ones. Thermal effects may cause zero drift and to minimise that effect two laboratory rooms with as stable conditions as possible were used. The probe generates heat itself and the measuring system needs to warm up for

a sufficient length of time. The mini-piezocone was therefore switched on in advance to reach a stable temperature before the tests started. Zero readings were also routinely taken before and after each test.

5.2.3.2 *Mini-vane*

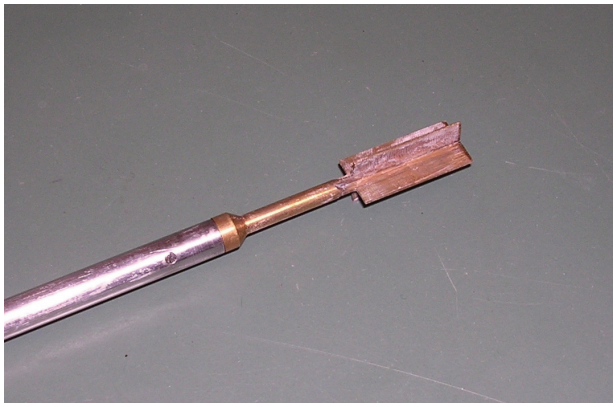

Figure 5-5 Mini-vane used in the model tests.

The mini-vane equipment was designed and built as part of the project. The mini-vane has the same ratio of height (H) to diameter (D) as the standard field vane (H/D = 2), the diameter is 10 mm and the height 20 mm. The first vane design had blades made of stainless steel with a thickness of 0.7 mm. The vane was fixed (screwed) to a rod with a diameter of 3 mm. To avoid friction between the rod and the clay and to ensure that the measured torque was generated only by rotation of the vane, the rod was surrounded by a protective casing with an inner diameter of 5 mm and an outer diameter of 6 mm.

However, this relatively simple design did not function as intended. Insertion of the vane generated torque, especially as the rod sometimes bent slightly during this operation. This pre-torque was not easily released. To avoid this problem a slip coupling was constructed between the rod, the protective casing and the vane. Nevertheless, the coupling did not function well together with the initial design of the equipment. Turning the vane generated a varying torque in the coupling or between the coupling and the protective casing. In addition, the vane turned slightly in the coupling during insertion. Thus, when the vane test was due to start there was sometimes no play in which to measure the initial torque. If the vane was turned in the opposite direction to generate play before pushing the vane down to the next test level, the vane came loose. In addition, when using a slip coupling the protective casing was no longer needed. It was therefore decided to construct a new vane.

The new design, which worked as intended, has the same vane dimensions but the blades were made of brass, see Figure 5-5. The vane stem has a diameter of 3.1 mm and a length of 19.6 mm. The upper end of the stem is fixed to a thicker rod of stainless steel with a diameter of 5.8 mm, through a tap and a slip coupling. The coupling has a play of 90°.

5.2.3.3 *Systems for pushing down the piezocone and vane*

A stand was built to accommodate the vane and the piezocone and to push them into the clay specimen in the cell. The stand is equipped with one motor to push down the vane or the cone with constant predetermined velocity and another for turning the vane at a constant rate of rotation, see Figure 5-6.

Figure 5-6 Stand built to accommodate the vane and the piezocone.

5.2.4 Data acquisition system

The computer program for measuring and steering the vane and piezocone tests was prepared by Peter Hedborg, Chalmers, using the program design tool Labview.

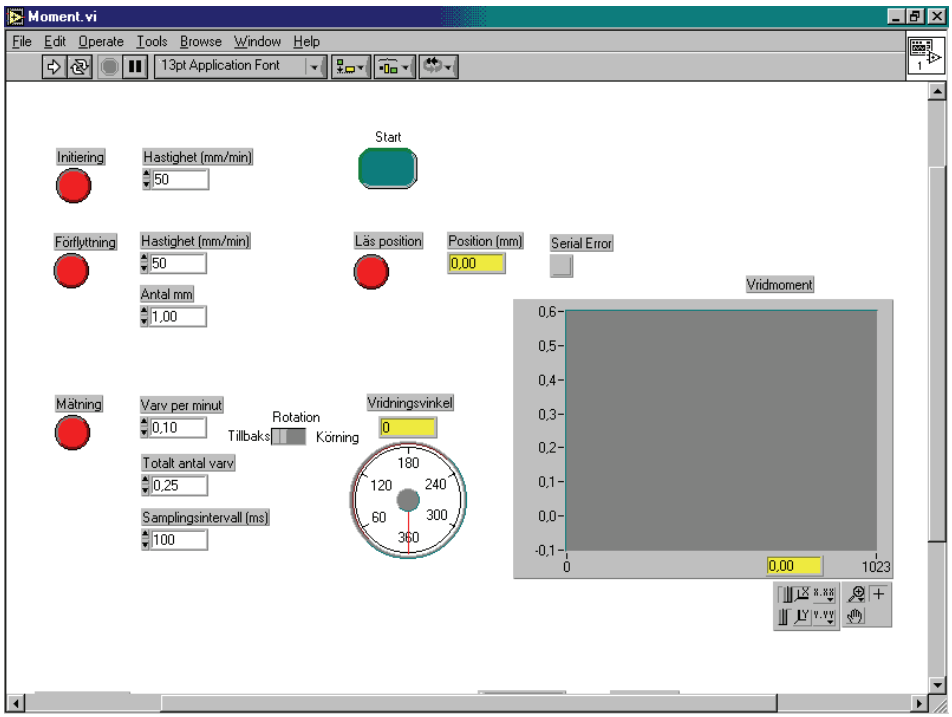

Figure 5-7 Control panel for the steering and measuring program for the vane tests.

The program is started by "clicking" the white arrow to the left in the program menu, see Figure 5-7. "Clicking" the button "initiering" (initiating), moves the equipment upwards. This movement is stopped by the contact breakers. The position is automatically set at zero after the initiation. The equipment is moved to the start position by "clicking" the button "förflyttning" (move), after specifying a distance (mm) and a velocity (mm/s). When the vane/piezocone has been moved to the start position, the measuring can start. For the piezocone, the velocity (mm/s), sampling interval (ms) and the total distance (mm) it should be driven are set. For the vane, rotations per minute, total number of rotations, sampling interval and the direction of the rotation are set. The position of the vane/piezocone tip is noted. To set the position at zero again, the equipment could be initiated a very short distance, e.g. 1-2 mm. The measuring is started by "clicking" the button "mätning" (measurement).

The torque for the vane or the cone resistance, the pore pressure and the sleeve friction for the piezocone are registered. At the same time, the position of the vane/piezocone tip at each single measurement is also

registered. These data are plotted on graphs in real time. When the measurements are terminated all data are saved in a file. The data can then be exported to other programs, e.g. Excel, for processing and presentation.

5.3 Test procedure

5.3.1 Sampling of clay

Before sampling, a hole is predrilled through the dry crust and down to the sampling level using a screw auger, 200 mm in diameter. The stem of the auger is hollow and above the flanges there are small holes drilled into the hollow stem. When the screw auger is withdrawn, air and/or water in the hole above the screw auger is sucked through the hollow stem. During withdrawal of the screw auger, any suction below the screw auger is equalised and the walls of the hole are thereby prevented from caving in.

With the sampler, samples from about 2 to 6 m depth are collected. When the starting level of the sampling is reached by predrilling, the sampler is installed at the bottom of the hole and pressed down at a rate of 7-8 mm/s. After the full stroke, the sampler is left in place for about 10 min, allowing the clay to stick to the inside of the tubes. The sampler is then withdrawn. If the clay is soft and/or highly sensitive, and there is a risk that the clay samples will tend to slide out, a vacuum pump is connected.

Some problems were encountered during testing of the equipment, which led to modifications. A major problem was that the clay samples did not remain in the tubes during withdrawal. The first modification was to install a shutter to keep the samples in place. However, this was not sufficient and a second clack valve connected to the flexible hose was installed. When this was connected to the vacuum pump during withdrawal of the sampler, the operation was successful.

Another problem was that the clack valves sometimes became partly clogged with clay and leaked during withdrawal. The negative pressures were then difficult to maintain and the samples slid out of the tubes. This problem was solved by installing two clack valves in series in the hollow push rod at some distance to the lid and a filter inside the lid.

The third initial problem was that the walls of the hole were unstable and debris covered the bottom of the predrilled hole. During sampling the upper part of the tube was filled with this partly remoulded clay. Drilling the

small venting holes in the hollow stem of the screw auger solved this problem and no suction occurred during its withdrawal.

5.3.2 Triaxial tests

5.3.2.1 *Calculations of deformations and time for consolidation*

Before starting the model tests, it was necessary to estimate the expected deformations of the specimens and time for consolidation. Other central questions were how to determine when the specimens had reached 90-95% consolidation and if there were any suitable ways to reduce the consolidation time. In order to clarify these questions, analytical and numerical calculations were made based on the properties of the clay at the Partille test site. Moreover, in the triaxial cells a consolidation test series was carried out on clay specimens from the Partille test site. These clay samples were taken at point A, close to the river, Säveån, Figure 5-20, Section 5.4.1.1 below.

To estimate the vertical and horizontal deformations of the specimens after consolidation past the preconsolidation pressure, results from CRS-oedometer tests on vertically oriented samples were used. As a simplification, the vertical and horizontal deformations were estimated based on the oedometer case in the vertical and horizontal directions. In Figure 5-8 the estimated vertical strains for varying effective vertical stresses on clay samples from depths of 4, 5 and 6 m at point A were plotted. Estimations of the horizontal strains were also made from these CRS test results, based on experience from oedometer tests on Bäckebol clay (Larsson 1981). This experience has shown that the modulus M_L in the horizontal direction (M_{LH}) is about 1.6 times higher than M_{LV}, the modulus in the vertical direction. The modulus number M' varies very little. On the other hand, the preconsolidation pressure in the horizontal direction (σ'_{ch}) is only about 70% of σ'_{cv}, the vertical preconsolidation pressure, or about $K_{0NC} \cdot \sigma'_{cv}$. The parameter σ'_L does not appear to be affected by sample orientation. Using these relationships for σ'_{ch} and M_{LH} together with the CRS oedometer curve from the vertically oriented samples gives strains for samples from a depth of 4 m, see Figure 5-8.

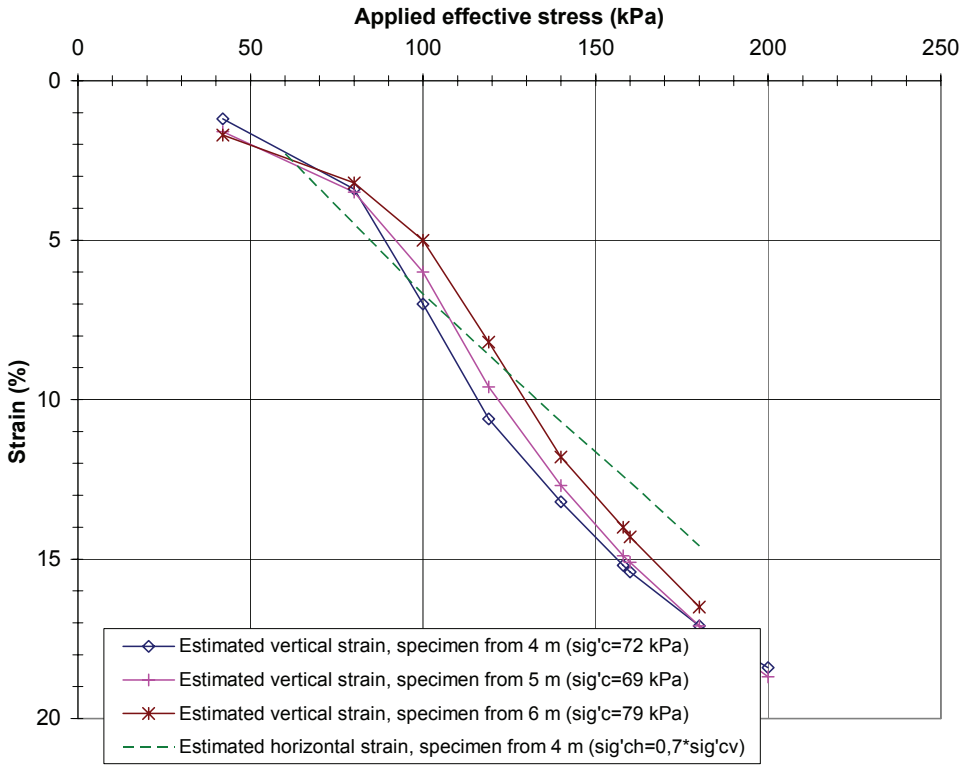

Figure 5-8 *Estimated vertical strains for increasing effective vertical stresses on clay samples from 4, 5 and 6 m depth and estimations of horizontal strains at increasing effective horizontal stresses in the oedometer case.*

To get an idea of the time required for 90% consolidation, the primary consolidation process in one dimension was first calculated analytically according to Terzaghi (1944). The properties of the clay at a depth of 4-5 m at point A (close to Säveån) were used ($c_{vv} \approx 3 \cdot 10^{-8}$ m^2/s). Assuming only radial drainage (in one dimension) gave a time for 90% consolidation of less than 1½ days. Assuming only vertical drainage gave a time for 90% consolidation of less than six days.

In addition, the consolidation process and the expected deformations were calculated using the computer program Embankco (Larsson et al. 1994), program version 1.02 CTH 960327. This program was developed for settlement analysis of compressible soil layers in the field and not for soil samples. However, describing the samples as a 0.3 m thick clay layer made it possible to model a K_{0NC} consolidation process for the case of drainage in the top and bottom of the samples. The parameters from CRS oedometer tests at depths of 4 and 5 m at point A were used in the calculations. (γ = 16 kN/m^3, σ'_c = 70-80 kPa, σ'_L = 106 kPa, M_L = 560 kPa, M' = 13.2, $k_i = 0.95 \cdot 10^{-9}$ m/s, $\beta_k = 4$. The modulus M_0, the swelling index (a_s) and the creep parameters α_{smax} and $\beta_{\alpha s}$ were chosen based on empirical experience as M_0 = 3750 kPa, a_s = 100, α_{smax} = 0.016 and $\beta_{\alpha s}$ = 0.41). Calculations were

made for applied effective pressures exceeding the preconsolidation pressure by 40 to 90 kPa. The corresponding total calculated deformations without creep were 22 to 42 mm, i.e. 7.3 - 14.0% strain. The calculated time for 90% consolidation, i.e. the time to obtain 90% of the total settlements, was six days. The calculated deformations corresponded well to deformations estimated directly from the CRS oedometer tests. The estimated time for 90% consolidation corresponded well to the simplified analytical calculation. Calculations, including creep effects, indicated that no significant extra creep deformation would occur before the time of 90% consolidation.

To decide how to run the tests, it was essential to investigate the influence of certain parameters on the consolidation process and to compare this with the test results. The parameters studied were: drainage conditions, sample size, modulus/permeability (c_v) and possible differences in horizontal and vertical permeability. For this study, Sadek Baker at Chalmers made finite element calculations using the computer program Plaxis, version 7. The following parameters were used in the calculations (Baker, 2003): linear elastic material model, isotropic consolidation, consolidation stress = 100 kPa, Poisson's ratio ν = 0.35, oedometer modulus M = 500 or 600 kPa (Young's modulus E = 310 or 370 kPa), permeability $k_v = 5 \cdot 10^{-9}$ or $6 \cdot 10^{-9}$ m/s and in one case $k_h = k_v/2$, specimen size 280 x 125 mm or 100 x 50 mm.

Calculations were made for the cases of drainage at the top and the bottom, radial drainage and drainage on all sides, see Table 5-1. It should be noted that the consolidation time for a specimen size of 280 x 125 mm will be about ten times less in the case of radial drainage than when drainage is only allowed at the top and bottom of the sample. This means about 33 hours instead of 16 days for a sample with $c_v = 3 \cdot 10^{-8}$ m^2/s and three hours instead of 39 hours for a sample with $c_v = 3 \cdot 10^{-7}$ m^2/s. The difference in the consolidation time in the case of drainage on all sides and radial drainage is comparatively small. According to the Plaxis calculations, for a sample with $c_v = 3 \cdot 10^{-8}$ m^2/s, the consolidation time when all sides drain will be 28 hours instead of 33 hours for radial drainage only.

Compared to ordinary size samples in triaxial tests (100 x 50 mm^2), the consolidation with radial drainage for 280 x 125 mm^2 samples will take about 33 hours instead of 5½ hours for a sample with $c_v = 3 \cdot 10^{-8}$ m^2/s. A 280 mm sample with $c_v = 3 \cdot 10^{-7}$ m^2/s will consolidate in 3½ hours instead of 30 minutes. A radial permeability of about half of the vertical permeability, $k_h = 3 \cdot 10^{-10}$ m/s in the case of $c_v = 3 \cdot 10^{-8}$ m^2/s ($k_v = 6 \cdot 10^{-10}$

m/s) will give about 30 hours' longer consolidation time, i.e. about twice the time of 33 hours for isotropic permeability. The consolidation times were evaluated according to the Casagrande method (see Section 5.3.2.2 below) and are summarised in Table 5-1.

Table 5-1 Results from the Plaxis calculations of the consolidation process.

	Consolidation time				
	Sample 280 x 125 mm^2				Sample 100 x 50 mm^2
Coefficient of consolidation	Drainage top and bottom	Drainage all sides	Radial drainage	Radial drainage $k_h = k_v/2$	Radial drainage
$c_v = 3 \cdot 10^{-8}$ m^2/s	16 days	28 hours	33 hours	63 hours	5½ hours
$c_v = 3 \cdot 10^{-7}$ m^2/s	39 hours	---	3½ hours	---	30 minutes

The relationships between degree of consolidation (U) and time factor (T) according to the Plaxis calculations were compared with the same relationships according to the analytical solutions. The time factor T is defined here as:

$$T_v = \frac{c_v \cdot t}{h^2}; \qquad T_r = \frac{c_v \cdot t}{r^2} \tag{5-1}$$

where h = the height of the sample, r = the radius of the sample

Several authors have studied vertical and radial consolidation, e.g. Terzaghi (1944), Silveira (1953) and Mc Kinlay (1961), but as consolidation is not a central part of this thesis their work is not described further. In the case of vertical drainage the Plaxis result was compared with the solution by Terzaghi (Terzaghi and Frölich 1936, Terzaghi 1944). The curves show quite good agreement, although the analytical curve is somewhat steeper than the Plaxis curve (Figure 5-9). In the case of radial drainage the Plaxis curve was compared with the analytical solution by Silveira (Silveira, 1953, Mc Kinlay 1961). In this case the curves have the same shape, but for the same degree of consolidation the time factor curves differ by about 3-5 times (Figure 5-10). For both cases the difference in the results is due to the different boundary conditions. The Plaxis calculations are conducted for isotropic consolidation, $\Delta\sigma_v = \Delta\sigma_h$ = constant, and the analytical

solutions are based on the oedometer case, $\Delta\sigma_v$ = constant, $\varepsilon_h = 0$ (see also Section 5.4.5 below).

Consolidation of clay specimens was also studied to gain an understanding of relevant times for consolidation and methods to evaluate the time for consolidation.

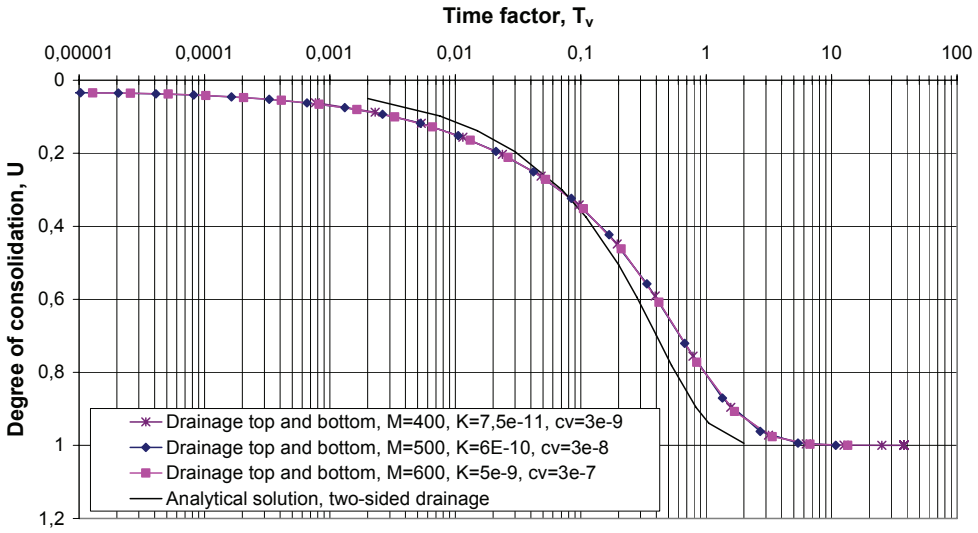

Figure 5-9 *Relationships between the degree of consolidation and the time factor for the model test specimens, drainage at the top and bottom, Terzaghi analytical solution and finite element calculations with Plaxis for isotropic consolidation (Baker, 2003).*

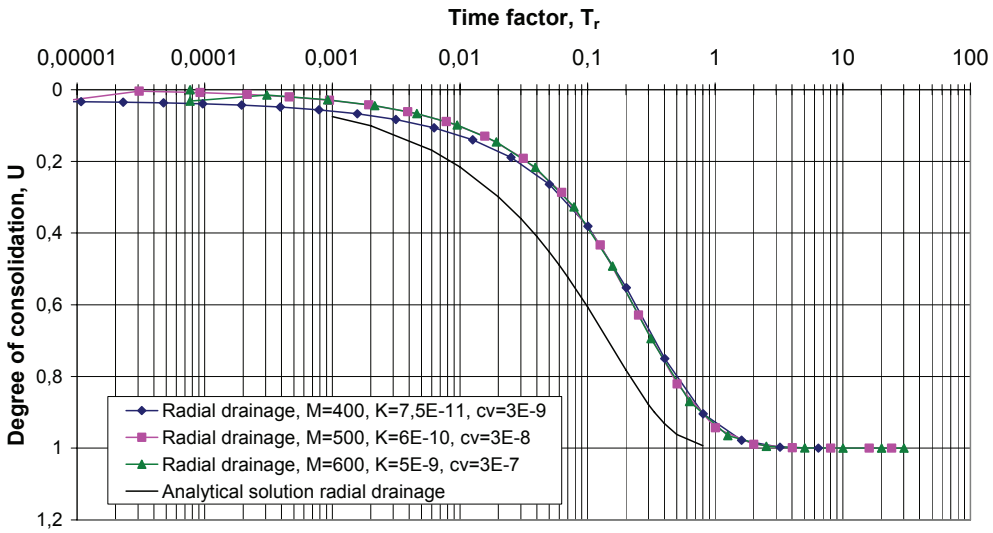

Figure 5-10 *Relationships between the degree of consolidation and the time factor for the model test specimens, radial drainage, analytical solution (Silveira, 1953, Mc Kinlay 1961) and finite element calculations with Plaxis for isotropic consolidation (Baker, 2003).*

Based on the calculations above it was decided to run the consolidation test series in the triaxial cells with radial drainage and drainage on all sides. Drainage at the top and bottom only was not considered relevant as the calculated time for consolidation was too long.

5.3.2.2 *Consolidation tests*

The consolidation test series was carried out to clarify the deformations, the time for consolidation and the best way to determine the time for end of primary consolidation. Specimens from a depth of 2-3 m at point A at the Partille test site (level about +10 m) (see Figure 5-20) were consolidated for stresses comparable to those at the level +7 m, i.e. 12.5 m below ground level (at point D) with an OCR of 1.4. The consolidation was carried out in four steps: 1. Approximately isotropic consolidation within the yield surface, i.e. without exceeding any preconsolidation pressure, 2. Consolidation approximately to the K_{0NC}-line within the yield surface, 3. Consolidation for increased vertical and horizontal stresses corresponding to K_{0NC}, and limited so as not to reach the failure line during the initial undrained state at stress application, 4. Consolidation in the same way to the final stress level. For two cells a 5th consolidation step was also carried out. The stress paths for the consolidation steps are shown in Figure 5-11 and the applied stresses are given in Table 5-2. In Figure 5-11, for cells 1 and 2, there is a discrepancy between the intended and the real stress paths. This is due to an error in applied vertical stress during the consolidation tests in cells 1 and 2, Table 5-2. This error was corrected before starting the "real" test series.

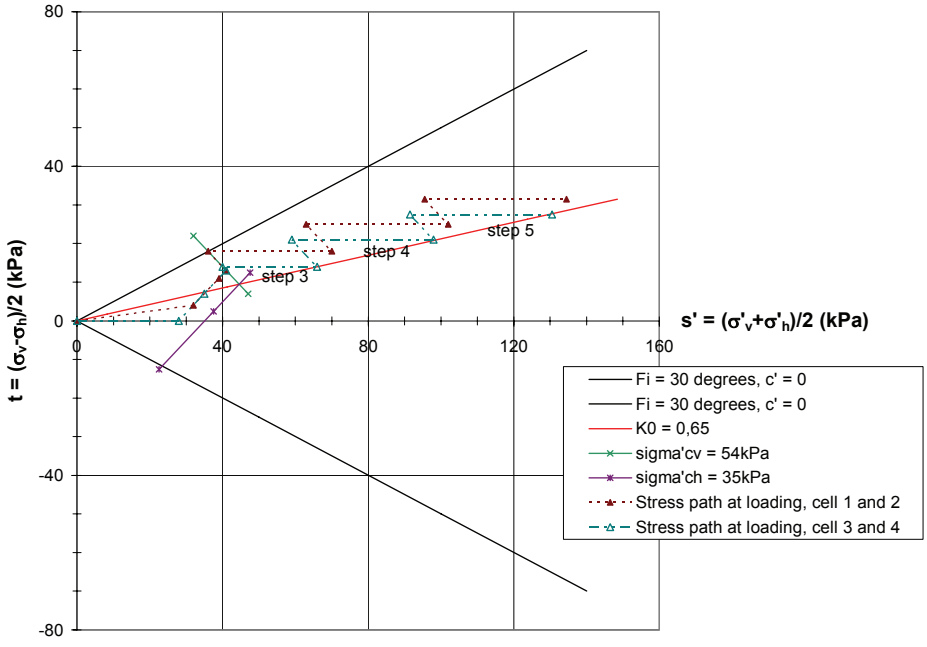

Figure 5-11 Stress paths for the consolidation steps.

Table 5-2 Stresses applied in the consolidation steps.

Load step	Effective vertical stress (σ'_v) kPa cells 1 and 2	Effective vertical stress (σ'_v) kPa cells 3 and 4	Effective horizontal stress (σ'_h) kPa all cells
1	36	28	28
2	50	42	28
3	88	80	52
4	127	119	77
5	166	158	103

One specimen was consolidated in each of the four triaxial cells. Cells 1, 3 and 4 had only radial drainage whereas cell 2 had drainage on all sides. The drains on the sides of the specimens consisted of two layers of filter paper. Vertical slots of 10 – 20 mm were cut in the filter paper to facilitate deformation. At the top and bottom, cells 1, 3 and 4 had first one plastic film to prevent drainage from the ends and then two layers of filter paper to let drainage water from the sides to continue on to the porous stones. Cell 2 had only two layers of filter paper on the top and bottom. During consolidation, the vertical deformations and the amount of pore water pressed out of the specimens were registered at predetermined intervals.

The time for 100 % consolidation was evaluated according to the Taylor and Casagrande methods. These methods were developed for incremental oedometer tests, for samples with a typical height of 20 mm, with drainage at one or two ends, and they give the mean degree of consolidation. Since consolidation of the current specimens was in three dimensions, both the vertical deformations and the volume of water pressed out of the specimens were plotted against the square root of time and the logarithm of time. The times for consolidation for the first three load steps were evaluated from all four plots. In the first load step, the specimens consolidated relatively quickly. The evaluated consolidation times varied between five hours and one day. The second step was close to the preconsolidation pressure and, probably therefore, the required S-shape for the Casagrande evaluation only appeared in one case. The third step showed a large span of evaluated consolidation times, varying between eight hours and almost seven days.

Comparing the two methods, the Taylor method had some notable disadvantages, especially for the third load step beyond the preconsolidation pressure. The first step in the method is to draw the straight line which best fits the early portion of the deformation versus the

square root of the time curve. The third consolidation step showed curves that bent off quite early, thus making it difficult to determine any straight portion, and gave much shorter consolidation times than the Casagrande method. Moreover, the "secondary" strain measured at the end of the consolidation step was in three cases 50-100% of the strains evaluated at 100% consolidation according to Taylor (maximum consolidation time about two days). The Casagrande method (maximum consolidation time about five days) gave "secondary" strains after 100% consolidation, which in all cases were 15–35% of the strains evaluated at 100% consolidation. During consolidation step 3, each specimen was allowed to consolidate for about 29 days in total. The strains after 100% consolidation according to the Casagrande method were considered to be more relevant. A comparison of the two methods using the consolidation curve from one of the Plaxis calculations (Section 5.3.2.1 above) also showed "secondary" strains after 100% consolidation that were larger using the Taylor method than the Casagrande method. In this case the strains after 100% consolidation were about 22% using the Taylor method and about 2% using the Casagrande method.

Using the Casagrande method, it was also easier to observe directly when 100% consolidation was about to be reached, as the curve then showed a distinct change in inclination. The Casagrande method was therefore chosen to evaluate the time for consolidation. However, it should be noted that the load steps must be of a certain magnitude to ascertain the required S-shape to be obtained. This is usually done by doubling the load, as in an incremental oedometer test (Mesri 1974 and 1977, Larsson 1981). In the present consolidation tests each load step was smaller than a doubling of the load. Comparing the log time – vertical deformation and the log time – volume change curves, the time for consolidation evaluated using the Casagrande method was about the same in most cases. A problem with the log time – volume change curve was that the accuracy of the volumetric readings was less than that of the deformation readings. In some cases the curves did not become S-shaped and, possibly due to gas bubbles in the system, indentations in the curve could suddenly appear .

The evaluated times for consolidation of the specimens in steps 3 and 4 are given in Table 5-3. The curve for the specimen in cell 1, load step 3, has no significant bend, and the preconsolidation pressure may not have been exceeded sufficiently. Except for this cell, the consolidation times for step 3 are in the same range. For consolidation step 4 the difference is greater. What is also worth noticing is that there is a significant difference in consolidation time between steps 3 and step 4. The value of c_v decreases

considerably from the preconsolidation pressure, σ'_c, to a minimum at σ'_L and thereafter it only increases slightly. This will give shorter times for consolidation in step 3. In addition, in load step 4 the consolidation was significantly faster for the specimen with drainage all around. This was not the case for load step 3. A possible reason for this could be that the filter papers on the sides of the specimens had become clogged.

Table 5-3 Evaluated times for consolidation of the specimens in step 3 and 4.

	Consolidation time			
	Cell 1: radial drainage	Cell 2: drainage all sides	Cell 3: radial drainage	Cell 4: radial drainage
Load step 3	(11 days)	4½ days	2 days	3½ days
Load step 4	15 days	7 days	28 days	(25½ days)
Load step 5 (geotextile)	14 days	---	14 days	---

To investigate this, a 5th load step was added for two of the cells. The specimens were taken out of the cells and a layer of geotextile with oblique slots was added outside the filter papers. The 5th step was smaller in relation to the previous stresses than the 4th step (Table 5-2). The consolidation still showed S-shaped log time – deformation curves, though not as pronounced as for load step 4. The consolidation times were in one case about the same and in one case half of the consolidation time for load step 4 (Table 5-3 and Figure 5-12). It was then decided to use two filter papers and one geotextile with oblique slots around the specimens in the tests. The time for consolidation with drainage all around was not expected to be much shorter than for radial drainage. Consequently, there would be no obvious advantage in using all-around drainage. On the other hand, since consolidation with radial drainage gives the same preconsolidation pressure in each vertical section, i.e. along the vertical section for the piezocone and the vane tests, radial drainage only was preferable.

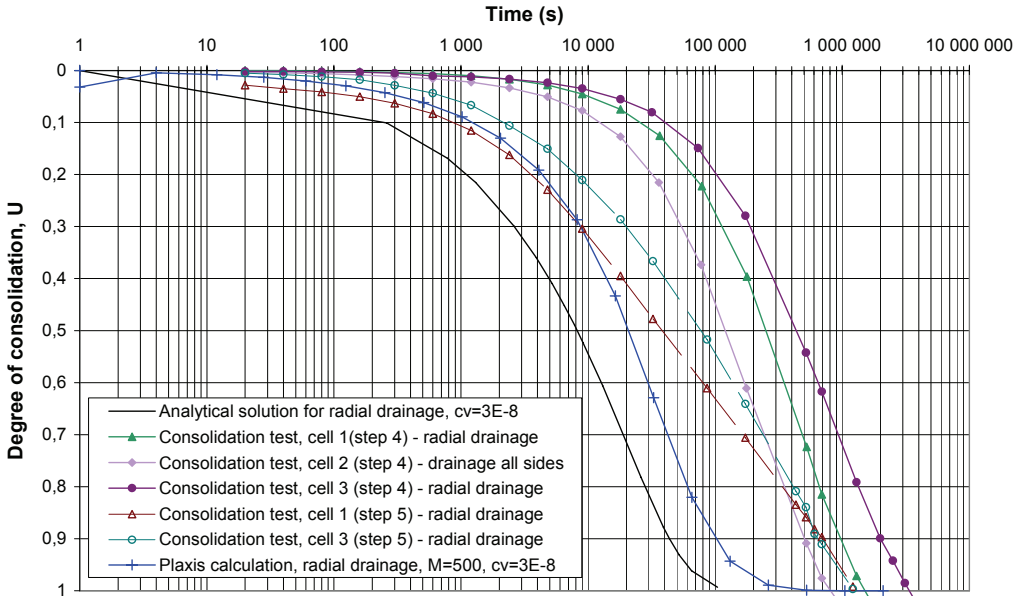

Figure 5-12 Time for consolidation curves for the consolidation test specimens, load steps 4 and 5 compared with the analytical solution for radial drainage (Silveira, 1953, Mc Kinlay, 1961) and finite element calculations with Plaxis (Baker, 2003).

Based on the measured deformations and volume changes during each consolidation step, the strains after consolidation were calculated. These strains are given in Table 5-4. The maximum strain at the end of step 4 is equal to vertical deformations of 35 mm, which is acceptable for the equipment.

Table 5-4 Strains after the end of primary consolidation of the specimens

	Strains cell 1 (%)		Strains cell 2 (%)		Strains cell 3 (%)		Strains cell 4 (%)	
Load step	Vertical	Radial	Vertical	Radial	Vertical	Radial	Vertical	Radial
1+2	1.5	2.6	3.2	6.7	2.2	1.3	0.2	0.07
1+2+3	4.0	5.8	8.5	6.7	5.5	1.8	0.9	0.3
1+2+3+4	7.1	9.2	12.4	6.7	7.6	2.1	2.6	1.2
1+2+3+4+5	8.5	-	-	-	9.4	-	-	-

The Taylor and Casagrande methods were developed for incremental oedometer tests where small specimens are used. Because of the rather large size of the specimens in the current tests, the consolidation process takes much longer time. The specimens may thus have been subjected to creep effects. As a result, measured preconsolidation pressures from CRS-tests conducted on small samples from the consolidated large clay

specimens may differ from the mean effective stresses the specimens have been subjected to, as creep will increase the preconsolidation pressure.

CRS-tests were carried out on small samples from two of the specimens in the consolidation test. Two samples from one of the specimens were tested in a climate chamber at +8°C. The estimated preconsolidation pressures were around $\sigma'_c \approx 200$ kPa, i.e. about 35 kPa higher than the applied vertical stress of 166 kPa. One small sample from the other specimen was tested at a temperature of 20°C, i.e. the same temperature as in the room where the consolidation tests were carried out. The preconsolidation pressure was estimated to $\sigma'_c = 124$ kPa, i.e. about the same as the applied vertical stress of 127 kPa. A CRS-test carried out at lower temperature than the storing temperature will result in a higher preconsolidation pressure (Tidfors, 1987, Tidfors & Sällfors, 1989, Eriksson, 1989, Leroueil and Marques, 1996). The approximately 20% higher preconsolidation pressure measured in the tests at 8°C corresponds roughly to what could be expected due to temperature effects (Eriksson, 1989, Leroueil and Marques, 1996). However, as the CRS curves were rather flat, it was also difficult to estimate accurately the preconsolidation pressure.

5.3.2.3 *Basis for choice of test procedure*

The time for consolidation according to the Plaxis calculations was compared with the test results from load step 3 where the filters apparently functioned as intended. It was concluded that in all cases the consolidation took longer in the tests than what was calculated. The difference in the consolidation time for the case with drainage all around compared with only radial drainage is insignificant, both in the tests and as calculated.

The vertical strains obtained in the consolidation tests were compared with the vertical strains from the CRS oedometer tests. The vertical strains of the specimens in the cells were in the range 1/4 to 2 times the strains from the CRS test results, with strains in two of the specimens in the same range as the CRS test results, see Figure 5-13. In the tests, radial strains should occur during the first step with isotropic consolidation. During the other three steps, with consolidation corresponding to K_{0NC}, ideally no radial strains should occur. Based on the volume change measurements, however, radial strains were observed during all four steps. The reasons for this may be sample disturbance, uncertainties in measurement of the pore water pressed out from the specimens and that consolidation during steps 2 to 4 differs slightly from consolidation corresponding to K_{0NC}. The K_{0NC} value

was also estimated from empirical relationships and may have been slightly overestimated.

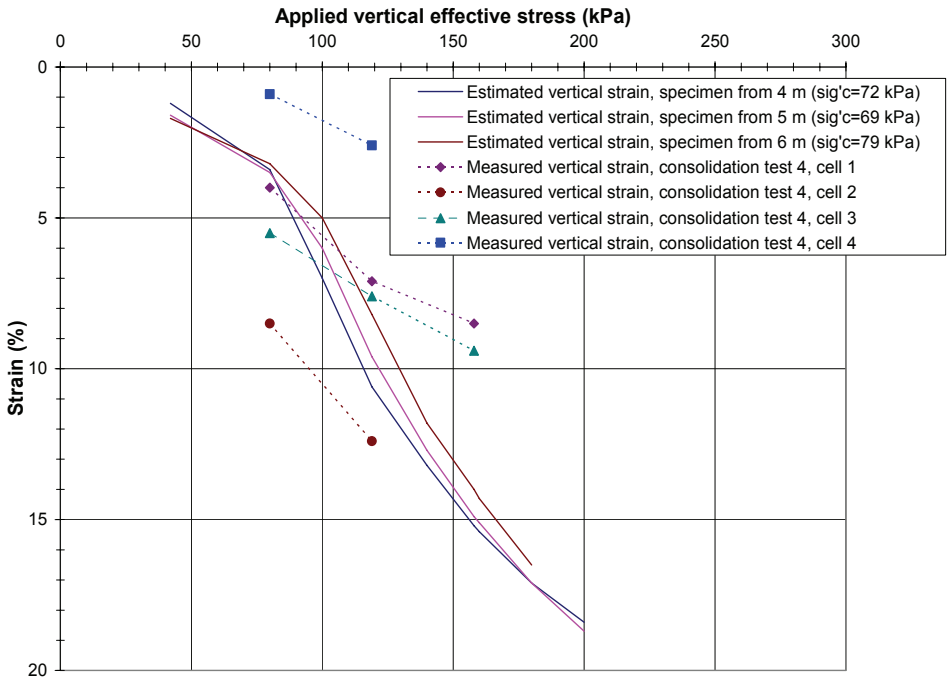

Figure 5-13 Vertical strains obtained in the consolidation tests compared with vertical strains from the CRS oedometer tests.

Based on the calculations and the consolidation tests, the following conclusions were drawn and decisions made:

- The consolidation strains for the maximum effective stresses are acceptable for the equipment.
- To shorten the consolidation time, load step 4 could start before consolidation of step 3 is completed.
- The Casagrande method and the log time – deformation curve should be used for evaluation of the time for 100% consolidation.
- Radial drainage should be used in the tests.
- Two layers of filter paper and one of geotextile with oblique slots should be used as drains around the specimens.

5.3.2.4 *Preparation of specimens and cells*

Mounting of the specimens in the special triaxial cells is mainly carried out in the same way as in ordinary triaxial cells. The porous stones are cleaned in an ultrasonic bath and treated by vacuum to dispose of air, before they are placed in the bottom pedestal and the lower part of the piston respectively. Inclined drains consisting of two layers of filter paper strips

and one strip of geotextile are applied on the perimeter of the specimen. The top and bottom ends of the specimen are covered with sheets of plastic to allow only radial drainage. Sheets of filter paper and geotextile are applied between the plastic covers and the pedestal and piston to provide a drainage connection between the filter stones and the drains at the perimeter of the specimen. A hole is cut at the centre of the plastic, paper and geotextile sheet on top of the specimen to allow the piezocone and the vane to penetrate later on. The specimen is then mounted in the cell as described in Section 5.2.2.

Before mounting the piston, a piece of plastic is fastened in the bottom of the hole in the piston by means of a flange and screws. When the piston and the cell lid are in place, the hole in the piston is filled with water and another lid is applied on top of the hole. This prevents clay from being squeezed up into the hole when the specimen is loaded.

5.3.3 Mini-piezocone and vane tests

5.3.3.1 *Calibration of piezocone*

To check and ensure the accuracy of the results of the tests, it was considered prudent to calibrate the equipment before and after each test series. Procedures for calibration of the piezocone and the vane were therefore established and equipment required for the calibrations was designed and produced. In principle, the procedures used for the calibration of the piezocone are the same as for the field piezocone (SGF, 1993, report 1:93E). The procedure for calibration of the vane is described in Section 5.3.3.2 below.

In a piezocone test, the cone resistance, the sleeve friction and the pore pressure are measured. In this case, the sleeve friction is not used, as the sleeve friction readings are not considered reliable enough. In addition, the sleeve friction is not used in the evaluation of the undrained shear strength. The calibration is carried out in two steps. First, loads are placed on top of the cone to calibrate the cone resistance. A calibration chamber is then used to calibrate the pore pressure, the area factors and the internal friction (Figure 5-14). An adapter was designed to apply the loads on the cone tip (Figure 5-15). It consists of a plate attached to a tube with an inner diameter slightly larger than the diameter of the piezocone. This adapter, made of brass, is slid over the piezocone, which is turned upside down, and the tip of the cone enters a conical seat in the plate at the closed end of the tube. Loads can then be applied on the plate. During this operation, it is

checked that the piezocone is vertical and that the adapter hangs freely on the tip of the cone, i.e. that the end of the tube does not touch the side of the piezocone. The calibration chamber consists of a Plexiglas tube, which can be connected at one end to a regulated air pressure supply. At the other end, the piezocone can be inserted and locked in place using an airtight seal at this end of the tube.

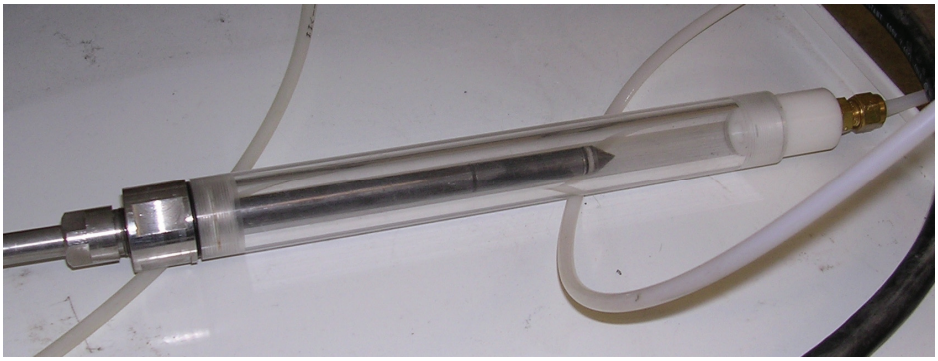

Figure 5-14 Calibration chamber used to calibrate the pore pressure, area factors and internal friction.

Figure 5-15 Adapter for calibration of the piezocone with loads.

Calibration of the piezocone with loads is carried out as follows. At first the output voltage without load is measured and the measuring range is adjusted. As there may be a zero drift, the output voltage must be measured before and after each loading cycle. A rough calibration is then made from zero to 300 N, in steps of 20 or 40 N, first loading and then unloading. After that, a fine calibration is made in the same way from zero to 10 N, in steps of 0.5 or 1 N. Both calibrations are plotted on the same type of graph

with applied load versus measured signal. Such a graph for the rough calibration is presented in Figure 5-16. It should be checked that the relationship is a straight line and that loading up and down gives practically the same values, i.e. that the hysteresis is negligible. The calibration factor is then determined and given as input in the computer program for the measurements. A new loading and unloading cycle is performed and the force registered by the measuring program is checked.

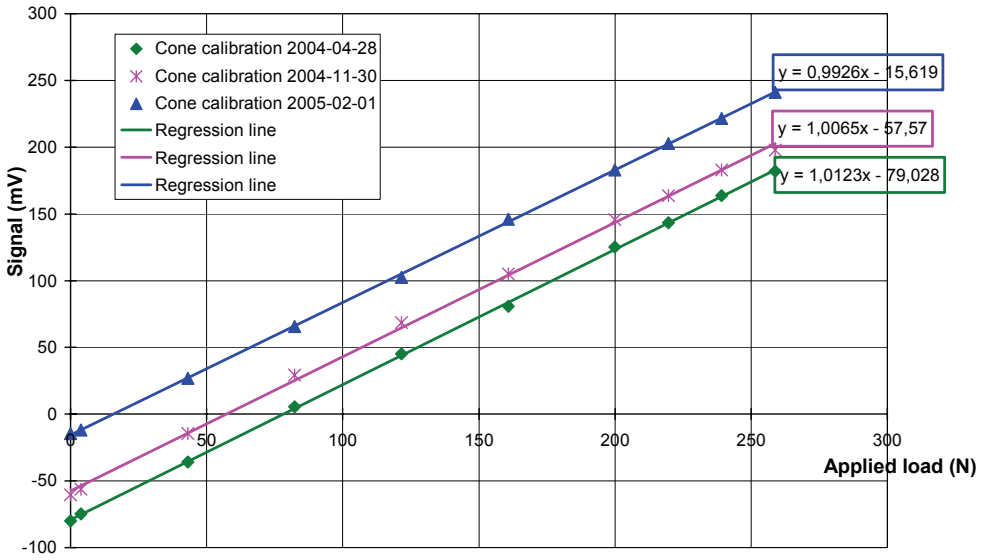

Figure 5-16 Results from calibration of the piezocone with loads (rough calibration).

In the calibration chamber, the signals from the transducers for cone resistance and pore pressure are calibrated against applied air pressure in the chamber. The pore pressure measurements are calibrated and checked in the same way as the cone resistance, but with applied air pressure instead of an applied load. This calibration is made from zero to 350 kPa, in steps of 20 or 50 kPa. The determined calibration factor for the pore pressure is given as input in the computer program for the measurements. A new loading and unloading cycle is carried out and the pore pressure registered by the program is checked. From this loading and unloading cycle the values of the area factor *a* and internal friction *Oc* are determined by plotting the applied air pressure versus registered pressure on the cone tip (the registered cone resistance) (SGF, 1993, report 1:93E). The area factor *a* is determined from the inclination of this line, and the inner friction *Oc* is determined from the intersection of the linear relationship and the abscissa at zero chamber pressure, i.e. atmospheric pressure, see Figure 5-17. In Figure 5-17 the registered pressure on the cone tip at zero chamber pressure differs from zero, as the cone tip load cell was normally not set at zero at the start of the calibrations. Due to inner friction the relationship between

chamber pressure and registered cone resistance is not always a straight line. For this piezocone, however, it turned out that the internal friction is negligible.

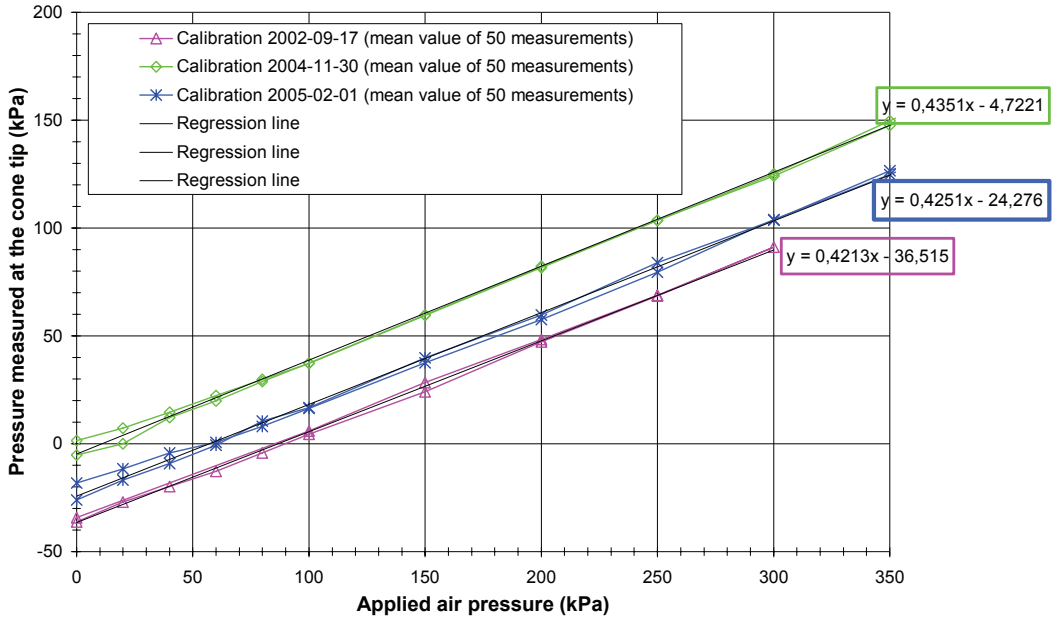

Figure 5-17 Results from calibration of the piezocone in the calibration chamber.

As also pointed out by the manufacturer, careful control of ambient temperatures is required as thermal effects can cause zero drift. Therefore, a temperature calibration was carried out to determine how variations in temperature influence the results of the test. Tests were made by inserting the piezocone in water baths. The water temperatures were kept at about 10, 20 and 30ºC. The piezocone was held in each water bath for 12 - 15 minutes and readings were taken after 5, 8, 10 and 12 minutes. Table 5-5 shows the start and end temperatures and the corresponding cone resistance and pore pressure readings.

Table 5-5 Start and end temperatures and the corresponding cone resistance and pore pressure for the temperature calibration.

Water bath No. (start/end)	Temperature start	Cone resistance (kPa)	Pore pressure (kPa)
1: start	9°	97	64
1: end	11°	99	64
2: start	20°	98	64
2: end	20°	97	65
3: start	33°	94	64
3: end	30°	92	60

It is seen that a variation in temperature has some influence on the measured signals although these variations are small for the cone resistance and pore pressure and are of no practical importance for the calculated shear strengths. No additional temperature calibrations were therefore considered necessary. However, a temperature change during a test can still cause errors. To obtain as good results as possible, laboratory rooms with as stable conditions as possible (temperature of about 20°) were used and zero readings were taken before and after each test.

5.3.3.2 *Calibration of vane*

For calibration of the vane equipment, the electric motor and the torque transducer are fixed horizontally in a tube with the axis of the transducer slightly protruding out of the tube, see Figure 5-18. The centre of the lever is attached to the axis in such way that the lever itself does not produce any torque. The lever is supplied with loading plates at both ends and torque can be applied in both directions by putting weights on these plates. At the start of the calibration, the lever is set in a vertical position. Loads are applied on the lower plate and the axis and lever are rotated slowly. The maximum signal when the lever is almost horizontal is recorded. Depending on the amount of torque applied to the transducer, the amount of rotation around the axis needed to reach maximum signal differs slightly. In all other respects, the procedure follows the same principle as for calibration of the cone resistance and the pore pressure. The equipment and method of calibration follow the recommendations from the manufacturer of the torque transducer. Apart from torque, the loading also introduces forces other than pure torque to the axis and transducer. However, it has been ascertained that these do not significantly affect the measurements.

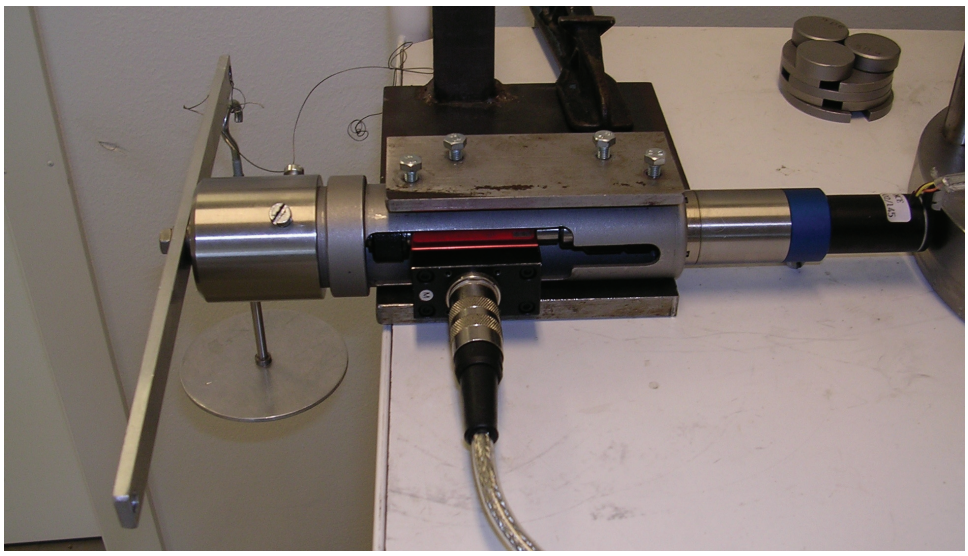

Figure 5-18 Equipment for calibration of the vane.

5.3.3.3 *Piezocone and vane test*

Before the start of a test, be it a piezocone or a vane test, the drainage lines for the pore water are closed. The small lid on top of the hollow piston is removed and the plastic plug in the bottom of the hollow piston is penetrated using a sharp rod. The stand for the piezocone or the vane is mounted on top of the cell and the piezocone or vane is attached to the stand, sees Figure 5-19.

In the piezocone test, the filter is cleaned in a supersonic bath and then kept saturated by keeping the cone and filter in a water bath under vacuum for at least one hour before the test. The electronics in the piezocone are switched on well in advance of the test so that the temperature of the equipment is stable when the test starts. A zero reading is taken as close to the start of the test as possible. The piezocone is lowered to the start position, just above the upper end of the specimen. The penetration velocity, the sampling interval and the depth to which the piezocone should be driven are adjusted in the program. The piezocone is pushed down at a rate of 30 mm/min (0.5 mm/s), which is a practical value and a rough scaling from the penetration rate for the field piezocone. The piezocone test is started and the cone resistance and pore pressure are registered in the data acquisition system. A zero reading is also taken after the test in each cell.

Also in the vane test, a zero reading is taken just before the start of the test. The vane is then inserted at the first test level. The turning velocity, the sampling interval and the number of rotations are adjusted in the program. The vane is turned at a speed of 0.03 turns per minute. This speed is based

on the recommended standard for field vane tests (SGF, 1993, report 2:93), where the speed should be chosen to provide failure within 2 to 4 minutes. As for the field vane test, there should be a waiting time of about 5 minutes before starting the test, after the vane has been pushed to the test level (SGF, 1993, report 2:93). The vane test is then started and the data acquisition system registers the rotation and torque at pre-set time intervals. A new zero reading is taken when the tests at the chosen levels in each cell have been conducted.

Figure 5-19 Model test equipment ready for a piezocone test.

5.4 Model tests for Partille conditions

5.4.1 Choice of stress combinations

In this project, influences of the stress conditions in slopes on the measured shear strengths are studied. It is therefore essential to assess the stress situation (vertical, horizontal and shear stresses) in various parts of the slope being studied. The stress conditions in the active and passive zones are of particular interest. The vertical stresses are calculated as the overburden pressure. The horizontal stresses are more difficult to estimate.

The horizontal stresses in the Partille slope have been estimated using measurements and stress path analyses. These results are used as a basis for the choice of applied stresses in the model test series.

5.4.1.1 *Measured horizontal stresses*

In a study of horizontal stresses and pore pressures in slopes Rankka (1994) measured horizontal stresses using total earth pressure cells and pore pressures using piezometers in the Partille slope between November 1989 and September 1992. The instruments were placed in four groups and at three depths in each group. At the toe (group A) the instruments were placed at a depth of 3, 5 and 9 m, in the middle (groups B and C) at a depth of 4, 8 and 13 m and 4, 9 and 14.5 m respectively, and at the crest (group D) at a depth of 4, 6 and 10 m, see Figure 5-20.

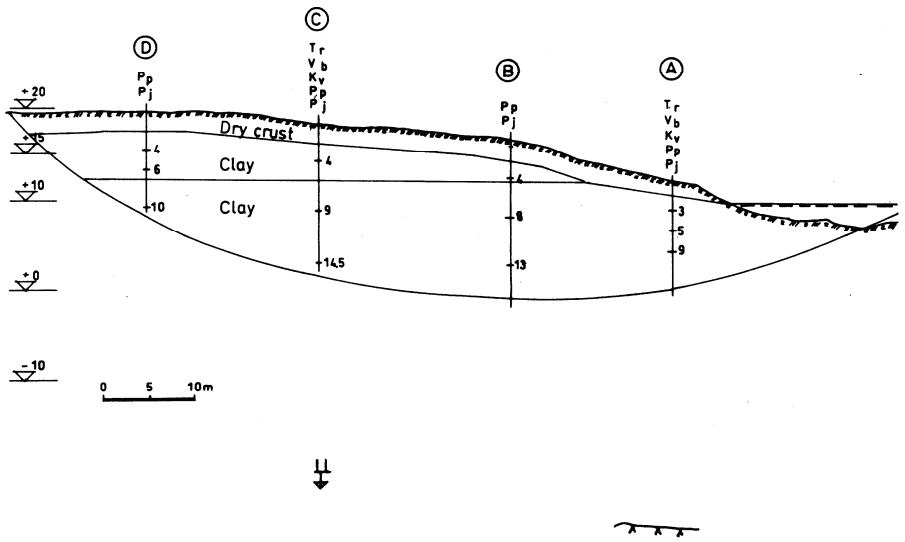

Figure 5-20 Instrumentation of the Partille slope (Rankka, 1994).

According to Rankka the coefficients of earth pressure (K values) based on effective stresses are higher in the passive zone (group A) than at the other locations although the variation with time is large. Drops in the K values have thus been measured during dry periods and rises during wet periods. The measurements show a variation in the passive zone (group A) of K values from about 0.8 to 1.0. In the middle of the slope, at group B, the measured K values are around 0.9 to 1.0 at a depth of 4 m and around 0.4 to 0.5 at a depth of 8 and 13 m. In group C the variations are mainly between 0.5 and 0.8. Behind the crest (group D) the measured K values vary between around 0.3 and 0.6.

Dilatometer tests carried out as part of the present study in March 2000, in the passive zone (group A) and at the crest (group D), indicated K values between 0.9 and 1.2 in group A and 0.6 and 0.8 in group D. It can be noted that the K values from the dilatometer tests generally are higher than the K values from the total earth pressure cells. However, the relationship used for evaluation of K from the dilatometer tests normally gives values of ±25% of the reference values (Larsson, 1989). The earth pressure cell values are within this range.

5.4.1.2 *Predicted horizontal stresses using stress path analysis*

Stresses and K-values were estimated at certain levels in four sections. One section at the bottom of the river and one section below group A on the shore (level +11 m) were studied in the passive zone. In the active zone, one section above group B, in the middle of the slope (level +17 m), and one section in group D, at the crest of the slope, were studied, see Figure 5-20. The principal stresses were assumed to act in the vertical and horizontal directions, i.e. a possible change in orientation of the principal stresses was not taken into consideration. Only the horizontal stresses perpendicular to the slope were considered. Perpendicular to the slope is here defined as the direction from crest to toe or from toe to crest.

Determination of $K_{0(NC)}$ for the conditions beneath a flat ground surface was done using an empirical relationship presented by Larsson (1977), which gave a starting value of $K_{0(NC)}$. To estimate the K_0 value after long-term adjustments for ageing and possible stress variations, i.e. after a long period of erosion and ground water level changes causing equal unloading over the whole area up to today's upper ground level, the relationship proposed by Schmidt (1967) was used. Since there is no possibility of separating overconsolidation caused by ageing, for which no empirical relationships for the development of K_0 exist, and those caused by unloading, the entire overconsolidation was assumed to be caused by the latter. Thus, the calculated values were assumed to correspond to the stress situation in all parts of the slope before erosion of the Säveån valley took place.

For determinations of $K_{0(NC)}/K_0$ as described above the following relationships were used. Larsson (1977) found that for Scandinavian inorganic clays $K_{0(NC)}$ could roughly be expressed as:

$$K_{0NC} = 0.31 + 0.71 \cdot (w_L - 0.2) \qquad (5\text{-}2)$$

For soils that are overconsolidated due to unloading, Schmidt (1967) formulated the expression: $K_0 = K_{0NC} \cdot OCR_v^{\sin 1.2\phi}$, which for a Scandinavian clay with ϕ' = 30° becomes:

$$K_0 = K_{0NC} \cdot OCR_v^{0.6} \qquad (5\text{-}3)$$

The value of K_{0NC} for consolidation of the specimens for the model tests was set at 0.65, using equation 5-2 above and determinations of the liquid limit (w_L) on undisturbed samples from the Partille site.

To simulate the stress situation in the passive zone, at the bottom of the river and on the shore, two different assumptions were made. One assumption was that the magnitude of the horizontal stresses remained roughly unchanged after erosion to the slope profile of today. This was one of the conclusions reached by Rankka (1994). The other assumption was that the horizontal stresses increased slightly after erosion, i.e. the small decrease in horizontal stress due to vertical unloading was compensated by an increase in horizontal stress due to the lower factor of safety. In the analyses this was calculated with an increase of 10 kPa in horizontal stress through the whole soil profile. However, this assumption resulted in stresses above the previous horizontal preconsolidation pressure. This means that the horizontal preconsolidation pressure should have increased compared to the situation during deposition and that considerable horizontal movement should have occurred. If this were the case, the empirical relationships are no longer valid.

Simulation of the possible stress situation in the active zone has been made taking limiting values of the conjugate stress ratio, K, into consideration (Chowdhury, 1978). For a uniform natural slope K is defined as $K = \sigma_\beta/\sigma_v$, where $\sigma_v = \gamma z \cos\beta$ and $\sigma_\beta = K\gamma z \cos\beta$, γ is the unit weight of the soil and β is the inclination of the slope, see Figure 5-21. For a soil mass with a horizontal surface as well as a sloping surface the value of K must be between the earth pressure coefficients, K_a and K_p ($K_a < K < K_p$). For a sloping soil mass with inclination β and c' = 0, the earth pressure coefficients may be calculated using the following equations:

$$K_a = \frac{\cos\beta - \sqrt{\cos^2\beta - \cos^2\phi'}}{\cos\beta + \sqrt{\cos^2\beta - \cos^2\phi'}} \qquad K_p = \frac{1}{K_a} \qquad (5\text{-}4)$$

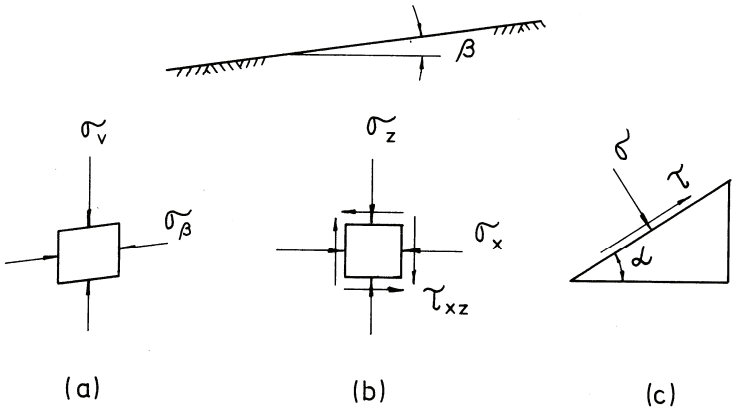

Figure 5-21 Stresses within a long uniform natural slope (a) conjugate stresses (b) normal and shear stresses on an element (c) stresses on a plane at any arbitrary inclination (Chowdhury, 1978).

The Partille slope has an inclination of about 15° and a friction angle in the clay, $\phi' = 30°$, giving values of the earth pressure coefficients $K_a = 0.39$ and $K_p = 2.56$.

Figure 5-22 shows the K-values in the passive zone estimated through dilatometer tests, Glötzl cell measurements and stress path analysis based on an empirical approach (using Equations 5-2 and 5-3). The corresponding values for horizontal ground are shown in Figure 5-23.

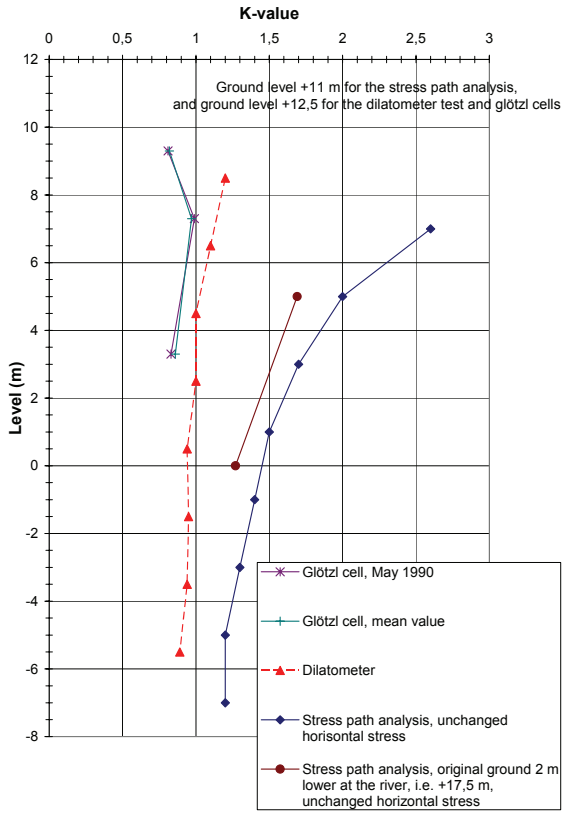

Figure 5-22 Estimated K-values in the passive zone (on the river side).

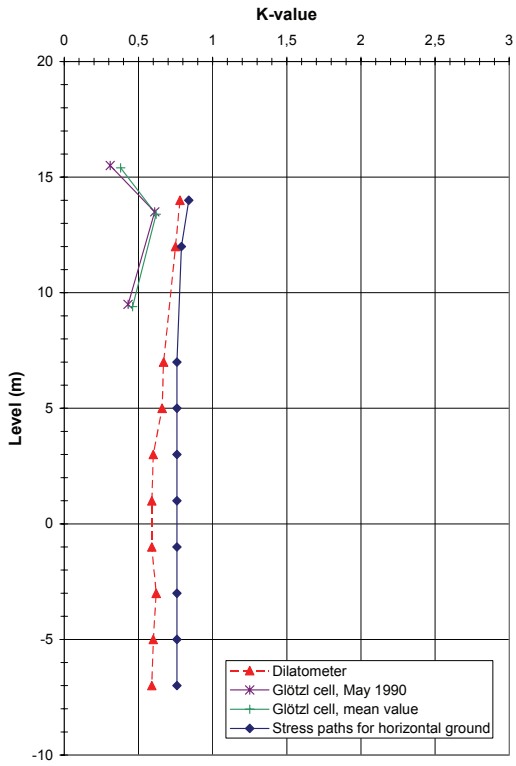

Figure 5-23 Estimated K-values for horizontal ground.

These comparisons were used as a basis for the choice of applied stresses in the model test series.

5.4.2 Test series

As mentioned earlier, the model tests were conducted in order to study the effect of various stress conditions on the shear strength calculated from piezocone and vane tests. The aim was to simulate realistic conditions in an eroded clay slope and to include the variations in stress conditions that may occur in a soil mass involved in a slope stability problem. The results were compared with results from direct simple shear tests using the equation that describes how the undrained shear strength varies with preconsolidation pressure and overconsolidation ratio, see Equation 5-7 below.

From the start, the aim was to carry out model tests for stress conditions equal to those in the passive and active zones of the slope, as well as for horizontal ground. However, only the stresses perpendicular to the slope (see Section 5.4.1.2) were to be considered. The tests should also be carried out at stress conditions corresponding to two different levels in the ground, one level close to the surface in the passive zone and one level deeper

down. The aim was to simulate the conditions in the slope as close as possible. To estimate relevant horizontal stresses (and relevant K_0-values) at various locations and depths in the slope, stress path analyses and previous measurements were used (see Section 5.4.1).

The following conditions were considered to be relevant for the studied slope at Partille:

- Ground level +19.5 m in the active zone (behind the crest) and +8.5 m in the passive zone (at the toe of the slope).
- $K_{0(NC)} = 0.65$
- Overconsolidation ratio OCR = 1.4 in the active zone and on horizontal ground. In the passive zone the overconsolidation ratio has been assumed to be OCR = 3.5 on both levels.
- Two different levels in the soil profile, one corresponding to a level just below the ground surface in the passive zone and one deeper down.
- A common preconsolidation pressure on each stress level in all zones and one representative value of the vertical pressure corresponding to the active zone and one value of the vertical pressure corresponding to the passive zone for each level.
- A range of K_0-values in the active zone: From $K_0 = 0.8$ (change of K_0 from $K_{0(NC)}$ due to changes in OCR over time from 1.0 to 1.4, owing to e.g. ground water level changes and ageing) to $K_0 = 0.4$ (decreased horizontal pressure, i.e. K-value close to the active earth pressure coefficient).
- A range of K_0-values in the passive zone: From $K_0 = 2.0$ (unchanged horizontal pressure) to $K_0 = 1.0$ (decreased horizontal pressure). The same K_0 – value has been assumed for both levels.

The above conditions for the model tests resulted in the following stress conditions in the model tests that were intended to correspond to the level +7 m (the highest level, close to the ground surface in the passive zone):

Preconsolidation stresses: $\sigma'_{cv} = 119$ kPa, $\sigma'_{ch} = 77$ kPa, $K_{0(NC)} = 0.65$

Initial stresses during the model tests:

Test condition 7-1:	$\sigma'_v = 85$ kPa,	$\sigma'_h = 68$ kPa,	$K_0 = 0.8$
Test condition 7-2:	$\sigma'_v = 34$ kPa,	$\sigma'_h = 68$ kPa,	$K_0 = 2.0$
Test condition 7-3:	$\sigma'_v = 34$ kPa,	$\sigma'_h = 34$ kPa,	$K_0 = 1.0$
Test condition 7-4:	$\sigma'_v = 85$ kPa,	$\sigma'_h = 34$ kPa,	$K_0 = 0.4$

The initial stresses during the model tests for the test conditions 7-1 to 7-4, are shown in a s-t stress diagram in Figure 5-24. Also an additional test (7-

5) and isotropic tests (ISO1-ISO3), defined on the following pages, are shown in Figure 5-24. In the s-t stress diagram s and t stand for:

$$s = \frac{\sigma'_v + \sigma'_h}{2} \qquad \text{mean effective stress} \qquad (5\text{-}5)$$

$$t = \frac{\sigma'_v - \sigma'_h}{2} \qquad \text{shear stress} \qquad (5\text{-}6)$$

where σ'_v = vertical effective stress [kPa]
σ'_h = horizontal effective stress [kPa]

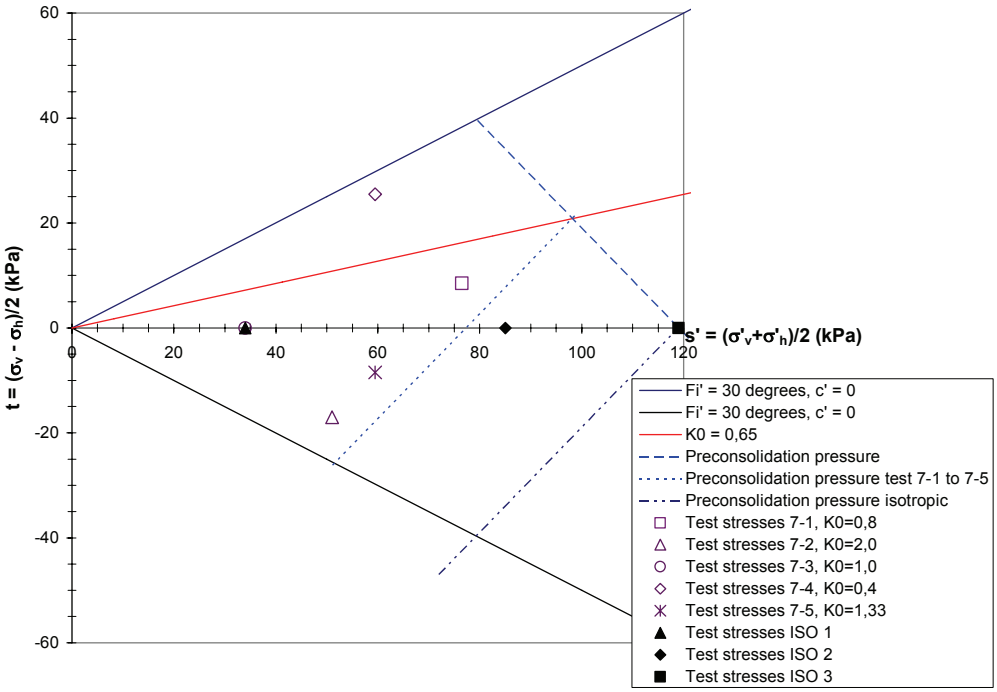

Figure 5-24 Initial stresses during the model tests for test conditions 7-1 to 7-5 and ISO1 to ISO3.

The model tests intended to correspond to the level ±0 m were given the following stress conditions:

Preconsolidation stresses: σ'_{cv} = 182 kPa, σ'_{ch} = 118 kPa, $K_{0(NC)}$ = 0.65

Initial stresses during the model tests:

Test condition 0-1:	$\sigma'_v = 130$ kPa,	$\sigma'_h = 104$ kPa,	$K_0 = 0.8$
Test condition 0-2:	$\sigma'_v = 52$ kPa,	$\sigma'_h = 104$ kPa,	$K_0 = 2.0$
Test condition 0-3:	$\sigma'_v = 52$ kPa,	$\sigma'_h = 52$ kPa,	$K_0 = 1.0$
Test condition 0-4:	$\sigma'_v = 130$ kPa,	$\sigma'_h = 52$ kPa,	$K_0 = 0.4$

The initial stresses during the model tests for the test conditions 0-1 to 0-4, are shown in an s-t stress diagram in Figure 5-25.

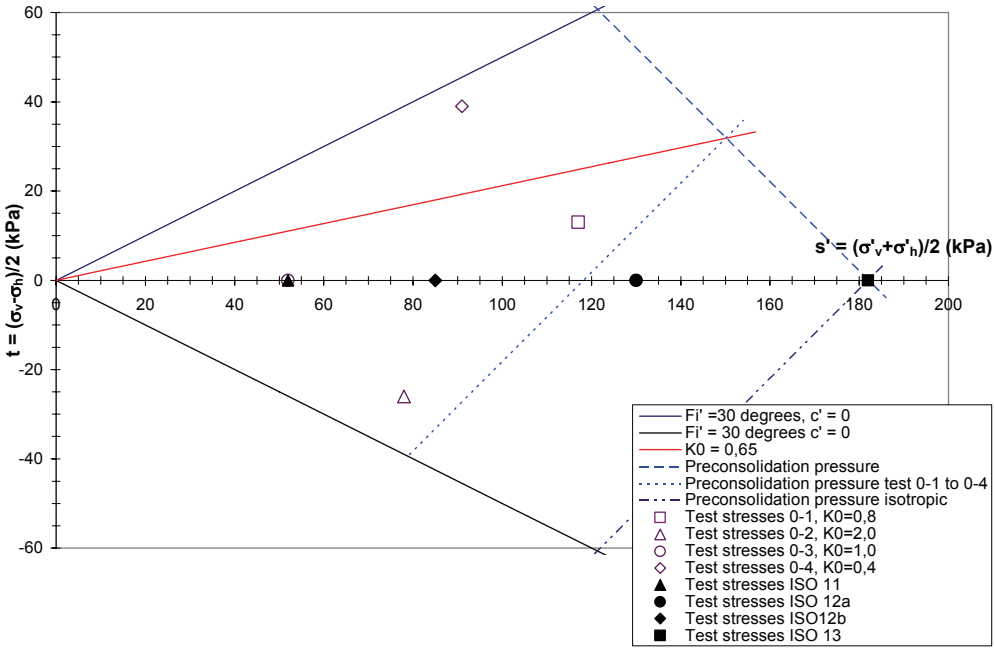

Figure 5-25 *Initial stresses during the model tests for test conditions 0-1 to 0-4 and ISO11 to ISO13.*

After the first test series was completed, it was decided to complement with two isotropically consolidated test series; one with isotropic preconsolidation stresses corresponding to the vertical preconsolidation pressure at level +7 m and one with isotropic preconsolidation stresses similarly corresponding to level ±0 m. The following test conditions were used:

- The preconsolidation stresses for the isotropic tests were equal to the vertical preconsolidation stresses in the $K_{0(NC)}$-consolidated tests.
- Tests were carried out for three different stress combinations:
  - one test at the preconsolidation stresses (OCR = 1)
  - one test with an overconsolidation ratio corresponding to OCR = 1.4
  - one test with an overconsolidation ratio corresponding to OCR = 3.5.

The isotropic model tests corresponding to the level +7 m had the following test conditions:

Preconsolidation stresses: σ'_{cv} = 119 kPa, σ'_{ch} = 119 kPa, $K_{0(NC)}$ = 1.0

Initial stresses during the model tests:
Test condition ISO 1: σ'_v = 34 kPa, σ'_h = 34 kPa, K_0 = 1.0
Test condition ISO 2: σ'_v = 85 kPa, σ'_h = 85 kPa, K_0 = 1.0
Test condition ISO 3: σ'_v = 119 kPa, σ'_h = 119 kPa, K_0 = 1.0

The consolidation stresses for the isotropic tests corresponding to the level +7 m, ISO 1 to ISO 3, are shown in Figure 5-24.

The isotropic model tests corresponding to the level ±0 m had the following test conditions:

Preconsolidation stresses: σ'_{cv} = 182 kPa, σ'_{ch} = 182 kPa, $K_{0(NC)}$ = 1.0

Initial stresses during the model tests:
Test condition ISO 11: σ'_v = 52 kPa, σ'_h = 52 kPa, K_0 = 1.0
Test condition ISO 12a: σ'_v = 130 kPa, σ'_h = 130 kPa, K_0 = 1.0
Test condition ISO 13: σ'_v = 182 kPa, σ'_h = 182 kPa, K_0 = 1.0

The initial stresses during the model tests for the isotropic tests corresponding to the level ±0 m, ISO 11 to ISO 13, are included in Figure 5-25.

In addition to the tests described above, two extra tests were carried out. Due to a calculation error one extra test with preconsolidation stresses corresponding to the level +7 m was carried out and due to an unloading error an extra isotropic test with preconsolidation stresses corresponding to the level ±0 m was carried out. These tests had the following initial stresses during the model tests:

Test condition 7-5: σ'_v = 51 kPa, σ'_h = 68 kPa, K_0 = 1.33
Test condition ISO 12b: σ'_v = 85 kPa, σ'_h = 85 kPa, K_0 = 1.0

These initial stresses during the model tests are included in Figure 5-24 and Figure 5-25 respectively.

According to empirical experience, an equation that describes how the undrained shear strength varies with the preconsolidation pressure and overconsolidation ratio can be written (e.g. Ladd et. al., 1977 and Jamiolkowski et al., 1985):

$$\frac{c_u}{\sigma'_{cv}} = a \cdot OCR_v^{b-1} \tag{5-7}$$

The average value of a = 0.22 is often used for the case of direct simple shear. The b factor is normally between 0.75 and 0.85 in both triaxial tests and direct simple shear tests and is normally set at 0.8 according to this empirical experience (Larsson and Åhnberg, 2003). In Swedish clays it has been found that the a-factor is a function of the liquid limit (Larsson, 1980). For the clay in Partille the a-factor should not differ significantly from the average value.

In order to compare the results of the model tests using Equation 5-7 the a-factor and b-factor for the Partille clay were determined using the SHANSEP procedure (Ladd & Foot, 1974). In the test series the clay specimens were loaded to 2.5 times the preconsolidation pressure. Thereafter, unloading was carried out to overconsolidation ratios of 1.5, 2.0, 2.5, 3.5, 4.5 and 6.5 and direct simple shear tests were conducted. This procedure reflects well loading above the natural preconsolidation pressure and thereafter unloading as carried out for the specimens in the model tests. A test series according to a slight modification of the SHANSEP procedure (normally used in Scandinavia) was also carried out. In this test series, the clay specimens were loaded to the natural preconsolidation pressure *in situ* and thereafter unloaded to different overconsolidation ratios, (see Section 5.4.6 below).

5.4.3 Test procedures

To reach the preconsolidation pressures corresponding to levels ±0 m and +7 m for the $K_{0(NC)}$-consolidated tests, the consolidation was carried out in four steps (described more in detail in Section 5.3.2.2 above). A K_0-consolidated test here refers to a test where a specimen is consolidated to given stresses corresponding to those in the field. A K_0-test, on the other hand, implies a test with no horizontal strain. The consolidation stresses for the consolidation steps are given in Table 5-6 and the final consolidation stresses are shown in Figure 5-24 and Figure 5-25 above. The pressures for the first consolidation step were kept for one day before applying the next step and the same was also done for the second consolidation step. The

pressures for the third consolidation step were kept for about four days. For the fourth consolidation step, the time – deformation curve was plotted and the time for 100% consolidation was evaluated using the Casagrande method. To determine the appropriate duration of consolidation step 3, the deformations for the third consolidation step were also followed during the first test series, and the time – deformation curves plotted. Based on these results, a duration of 3 – 4 days for consolidation step 3 was considered sufficient.

When roughly 100% consolidation had been reached during the fourth consolidation step, unloading to the final consolidation stresses was carried out in one step. These stresses were applied for 1-2 days in most cases. The further deformation process during the unloading stage was not followed although the total strains were noted.

Table 5-6 Consolidation stresses at preconsolidation of the specimens in the $K_{0(NC)}$-consolidated model tests.

Consoli-dation step	Consolidation stresses, level +7 m		Consolidation stresses, level ±0 m		Both stress levels
	Effective vertical stress (σ'_v) kPa	Effective horizontal stress (σ'_h) kPa	Effective vertical stress (σ'_v) kPa	Effective horizontal stress (σ'_h) kPa	Pore pressure (u) kPa
1	30	30	30	30	30
2	46	30	46	30	60
3	75	49	91	59	100
4	119	77	182	118	100

The isotropically consolidated tests were preconsolidated using two consolidation steps. The consolidation stresses for the isotropically consolidated tests are given in Table 5-7. The deformations were followed and the time – deformation curves were plotted for both steps and the time for 100% consolidation was evaluated according to the Casagrande method. When 100% consolidation had been reached during the second consolidation step, unloading to the final consolidation stresses was carried out in one step. For the latest conducted test series the heave during unloading was also monitored and the time – heave curve for the unloading plotted. The unloading period lasted for 1-2 days in most cases.

Table 5-7 Consolidation stresses at preconsolidation of the specimens in the isotropically consolidated model tests.

Consoli-dation step	Consolidation stresses, level +7 m		Consolidation stresses, level ±0 m		Both stress levels
	Effective vertical stress (σ'_v) kPa	Effective horizontal stress (σ'_h) kPa	Effective vertical stress (σ'_v) kPa	Effective horizontal stress (σ'_h) kPa	Pore pressure (u) kPa
1	70	70	90	90	60
2	119	119	182	182	100

For each test condition, a piezocone test and a series of vane tests were to be carried out along the central line of the specimens and a direct simple shear test was to be carried out on a sample taken along the central line of the specimen. To accomplish this, two cells were used for tests under each test condition. Four cells, two for $K_0 \geq 1.0$ and two for $K_0 \leq 1.0$ were constructed, and tests under two test conditions could be carried out at the same time. In each testing round four specimens were normally preconsolidated and unloaded to stresses corresponding to two different test conditions.

The first test series was performed in such a way that one piezocone test and one vane test was carried out in the specimen in the first cell. In the specimen in the second cell, two vane tests were carried out and one sample was taken for the direct simple shear test and trimmed by hand. However, during these first test series the vane equipment did not function satisfactorily and a new vane equipment was constructed (see Section 5.2.3.2 above). The results from the first test series also revealed that the clay in the upper 40 – 50 mm was softer than in the rest of the specimen. The following test series were then carried out in such a way that of the two specimens with the same test conditions, the piezocone was driven to 120 mm depth in the first specimen. The remaining 100 – 120 mm of the specimen was left for the direct simple shear test sample. In the second specimen, four vane tests were conducted at a depth of 70, 120, 170 and 220 mm (lower edge of the vane).

The piezocone and the vane equipment were calibrated just before the tests in each testing round and then again directly after the tests.

After the tests, the triaxial cells with the specimens were dismantled and samples were taken from the outer parts of the specimens for routine

analyses (bulk density, water content, liquid limit and undrained shear strength as determined by the fall cone test) and CRS-oedometer tests. The CRS-oedometer tests were carried out on samples oriented in two directions, one on a sample cut out vertically and one on a sample cut out horizontally.

5.4.4 Results of the routine analyses and CRS oedometer tests

The results from the routine analyses showed quite a large scatter. One reason could be that the natural clay is not homogeneous. The model test samples have been taken from a depth of 2 to 6 m around point A at the Partille test site, see Figure 5-20. There is a variation in the properties of the natural clay *in situ* at these depths. The bulk density varies between 1.55 and 1.68 t/m^3, the water content varies between 64 and 81% and the liquid limit varies between 55 and 76%. Another reason could be related to the dismantling of the specimen. It should be remembered that first the whole specimen is taken out from the cell and it is no longer under pressure. The small samples are then cut out from the outer parts of the specimen where the properties could differ slightly from those at the centre. A piston sampler tube was used to cut out the samples. To visualise the scatter and to see if some trend can be observed, the results were plotted against the mean preconsolidation stress of the specimens.

In Figure 5-26 the bulk density is plotted against the mean preconsolidation stress. Although there is a large scatter, the tendency is an increase in the bulk density with increased mean preconsolidation stress, which is reasonable.

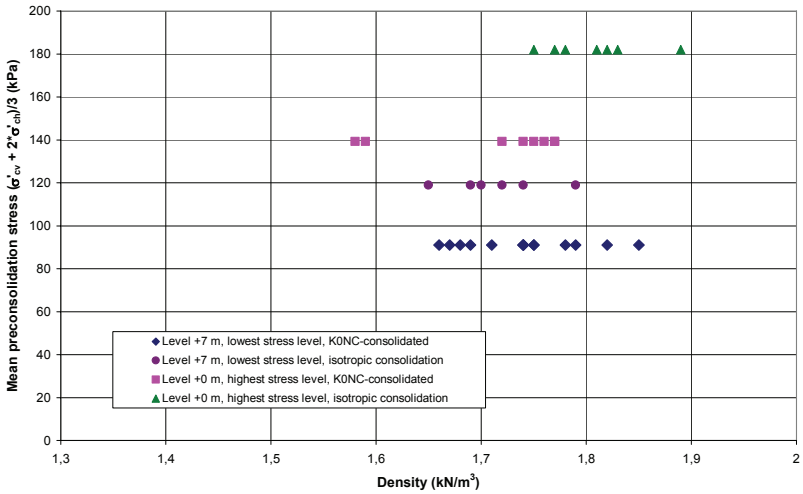

Figure 5-26 Measured bulk density of the specimens after the model tests.

In Figure 5-27 the water content and the liquid limit are plotted against the mean preconsolidation stress. It can be seen that there is a tendency towards decreased water content with increased mean preconsolidation stress whereas the liquid limit is fairly constant. Compression of the soil above the preconsolidation pressure should normally lead to a decrease in the water content and so this is as expected. The increasing consolidation stresses also change the water content from being at or above the liquid limit to being lower than this value. This is also as to be expected.

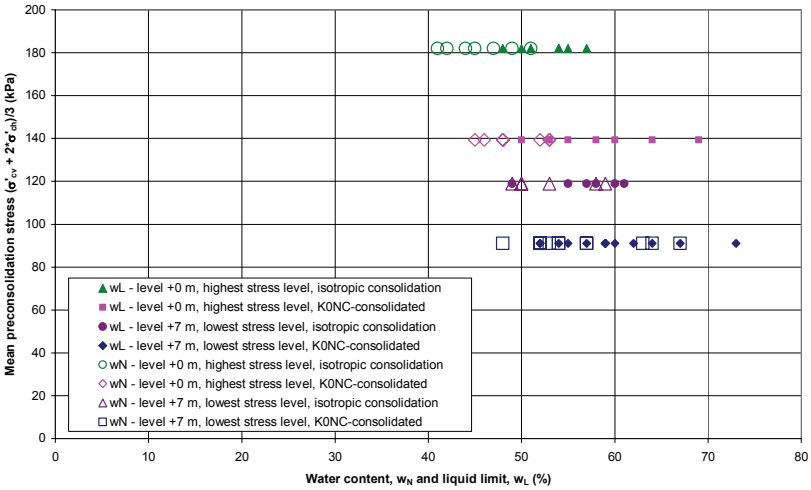

Figure 5-27 Measured water content and liquid limit of the specimens after the model tests.

Figure 5-28 shows the undrained shear strength of the specimens determined using a fall cone test. Despite the large scatter a clear trend towards increased undrained shear strength with increased mean preconsolidation stress can be observed.

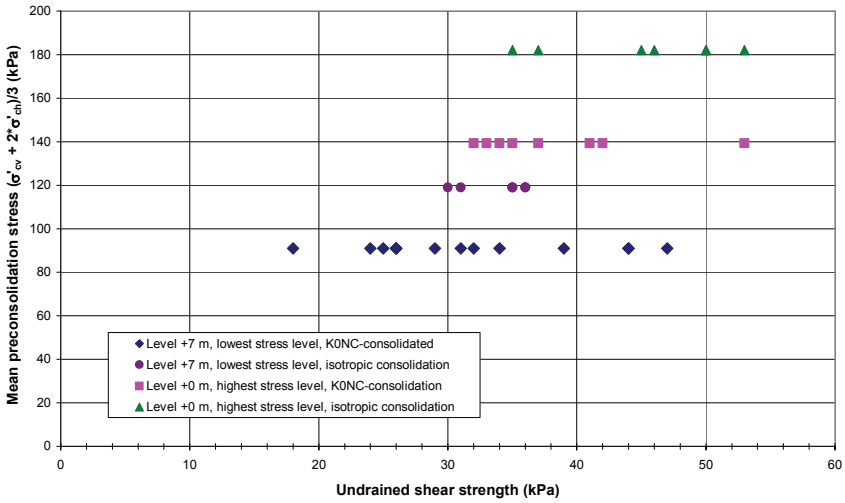

Figure 5-28 Undrained shear strength of the specimens after the model tests determined using a fall cone test.

The results of the CRS oedometer tests, both in the vertical and in the horizontal direction, show an even larger scatter than the results from the routine analyses. The stress-strain curves from the CRS oedometer tests are all very flat, as is usually the case for a very young clay, and they do not show the typical distinct bend at the preconsolidation pressure. This is believed to depend on the very short time (compared to naturally deposited clay) the "new" preconsolidation pressures have acted. It has been rather difficult to evaluate the preconsolidation pressure from these flat curves, which could be one reason for the large scatter in the estimated preconsolidation pressures. It can also be related to disturbance effects from the dismantling of the sample and the sampling and the preparation of the oedometer specimen. In Figure 5-29 the vertical preconsolidation pressures estimated from the CRS oedometer tests have been plotted against the vertical pressure applied to the specimens. Correspondingly, in Figure 5-30 the horizontal preconsolidation pressure estimated from the CRS oedometer tests has been plotted against the horizontal pressure applied to the specimens. It can be noticed that most of the estimated preconsolidation pressures are lower than the applied stresses, which indicates a considerable disturbance and is contradictory to the outer parts of the specimens, which have a slightly higher preconsolidation pressure due to creep effects.

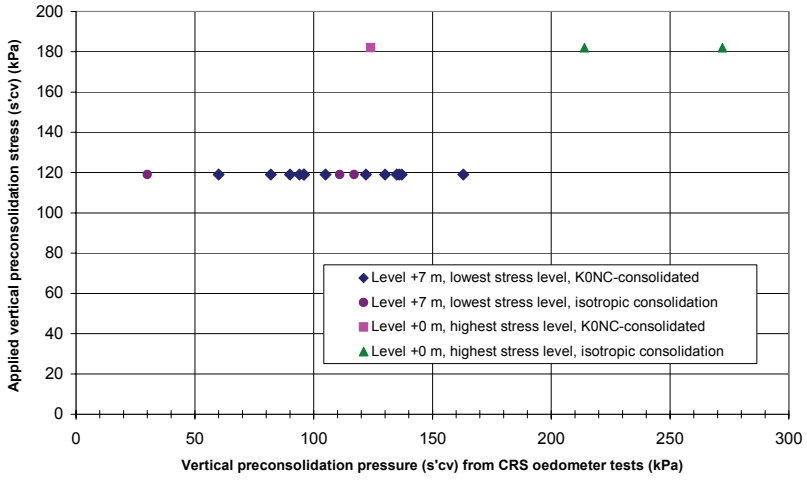

Figure 5-29 Vertical preconsolidation pressure estimated from the CRS oedometer tests plotted against the vertical stress applied to the specimens.

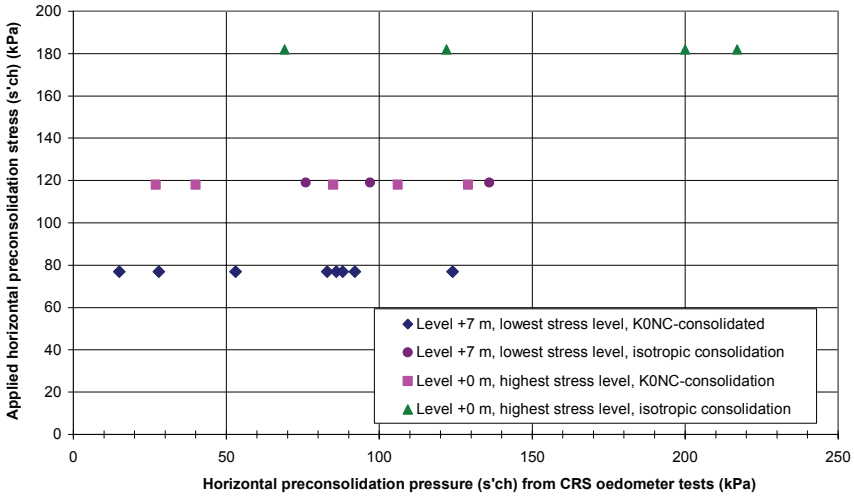

Figure 5-30 Horizontal preconsolidation pressure estimated from the CRS oedometer tests plotted against the horizontal stress applied to the specimens.

5.4.5 Results of the measurements during consolidation of the specimens

As described previously, consolidation of the specimens for the anisotropically consolidated tests for an *in situ* stress state ($K_{0(NC)}$) were carried out in four steps with radial drainage and for the last consolidation step the time – deformation curve was plotted. These curves were compiled for both consolidation stress levels and compared with the analytical solution for radial drainage (Silveira, 1953, McKinlay, 1961) and with the results of finite element analyses.

The finite element calculations were carried out by Per-Evert Bengtsson, SGI, using the computer program Plaxis, version 8. The following parameters were used in the calculations (Bengtsson, 2007): linear elastic model, applied pressure = 100 kPa, Poisson's ratio ν = 0.35, oedometer modulus M = 500 kPa (Young's modulus E = 310 kPa), permeability $k_v = k_h = 5 \cdot 10^{-9}$ m/s, sample size 280 x 125 mm^2 and radial drainage. Two different boundary conditions were used in the calculations: no lateral strain allowed (the oedometer case, $\Delta\sigma_v$ = constant, $\varepsilon_h = 0$,) and lateral strain accepted (isotropic consolidation, $\Delta\sigma_v = \Delta\sigma_h$ = constant). As the specimens are anisotropically consolidated for an *in situ* stress state ($K_{0(NC)}$) and not isotropically consolidated, a calculation with Plaxis was also carried out with anisotropic conditions ($K_{0(NC)}$ stress state; $\Delta\sigma_v$ = 100 kPa and $\Delta\sigma_h$ = 65 kPa). This results in a rather large initial deformation. In reality, a much larger modulus is valid for the initial phase than for the deformation caused by consolidation. Therefore, the elastic deformation

has been disregarded and only the deformation during consolidation was plotted. The time factor – degree of consolidation curve is then practically identical to the corresponding curve calculated with isotropic consolidation. The analytical solution is based on the oedometer case.

During consolidation of the specimens in the triaxial cells, lateral extension is possible. However, the specimens are consolidated anisotropically with the intention of imitating $K_{0(NC)}$-conditions, which implies no or insignificant lateral strain. Therefore, the relationships between the degree of consolidation and the time factor for the specimens were compared with the relationships between the degree of consolidation and the time factor calculated with boundary conditions in accordance with the oedometer case as well as isotropic consolidation. To be able to make this comparison, the measured time – deformation curves for the specimens were plotted as time factor versus degree of consolidation (deformation/total deformation). The time factor for water flow in the radial direction (see equation 5-1) was calculated using the coefficient of consolidation c_{vv} (vertical compression, vertical flow) calculated from CRS oedometer tests at the same strain as measured after consolidation of the specimens. The coefficient of consolidation was then estimated at $c_{vv} = 3 \cdot 10^{-8}$ m/s^2. Ideally, the coefficient of consolidation to be used should be c_{vh} (vertical compression, horizontal flow). Several researchers (Larsson, 1981, Tavenas et. al., 1983, Leroueil et. al., 1990) have shown that the permeability of homogeneous soft marine clays is practically isotropic and remains so for strains up to at least about 25%, independent of the type of compression applied. As the measured strains of the specimens during consolidation are less than about 13% for these specimens, the values of c_{vv} and c_{vh} should be fairly equal. Estimation of the coefficient of consolidation c_{vv} has also been made from CRS-oedometer tests on samples taken after consolidation of the specimen and after the tests, for the highest stress condition. It was then estimated at $c_{vv} \approx 5.3 \cdot 10^{-8}$ m/s^2 (mean value).

In Figure 5-31 the results of the consolidation of the specimens from the test series with the lower consolidation stresses are plotted together with results from the Plaxis calculations and the analytical solution. Correspondingly, in Figure 5-32 the results of the consolidation of the specimens from the test series with the higher consolidation stresses are plotted together with results from the Plaxis calculations and the analytical solution.

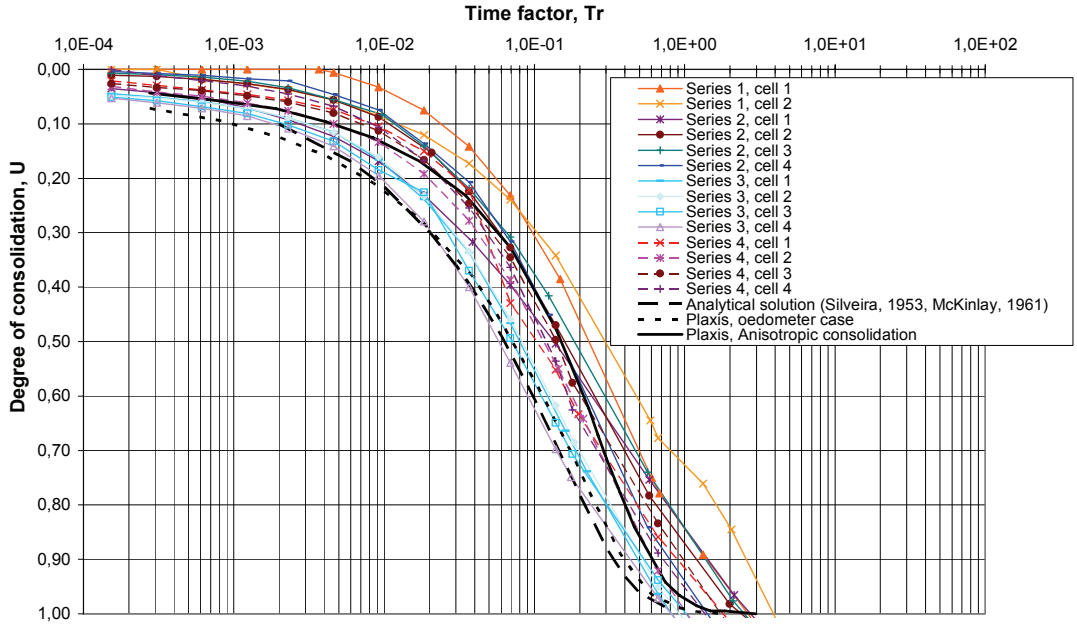

Figure 5-31 *Relationships between the degree of consolidation and the time factor for the model test specimens consolidated for the lower consolidation stresses (load step 4), radial drainage, analytical solution (Silveira, 1953, McKinlay, 1961) and finite element calculations with Plaxis for the oedometer case and anisotropic consolidation (Bengtsson, 2007).*

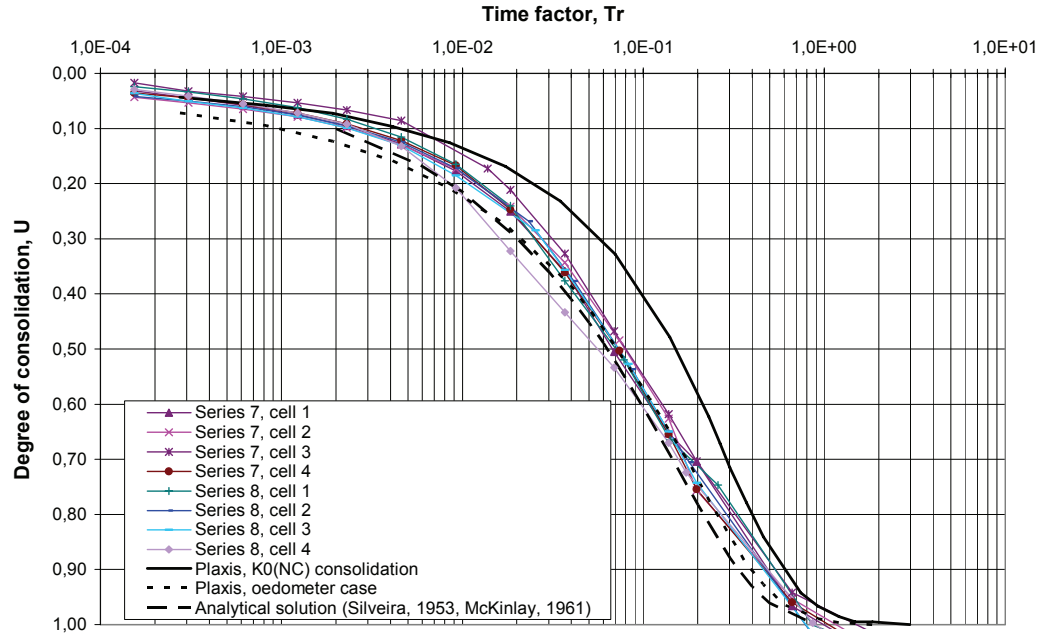

Figure 5-32 *Relationships between the degree of consolidation and the time factor for the model test specimens consolidated for the higher consolidation stresses (load step 4), radial drainage, analytical solution (Silveira, 1953, McKinlay, 1961) and finite element calculations with Plaxis for the oedometer case and anisotropic consolidation (Bengtsson, 2007).*

In Figure 5-31 and Figure 5-32 it can be seen that the relationships between the degree of consolidation and the time factor for the model test specimens consolidated for the lower stress level show a larger scatter than the corresponding relationship for the specimens consolidated for the higher consolidation stresses. One reason for this may be that the lower stress level is close to the preconsolidation pressure of the original clay, where the modulus of the clay changes (decreases drastically). The coefficient of consolidation varies accordingly (as the permeability only changes gradually) and could be different for each specimen consolidated to the lower stress level. For the highest consolidation stresses, the stress level is so high that the compression modulus has started to increase again, which normally also leads to a slight increase in the coefficient of consolidation. Another reason could be variations in the c_{vv} value of the clay. Both the permeability and the modulus of the clay vary with the water content, or really with the pore volume of the sample. The CRS-oedometer tests carried out for the highest stress level after consolidation of the specimens and after the tests, showed quite a large variation in the c_{vv} value.

Although there is a larger scatter in the relationships between the degree of consolidation and the time factor for the model test specimens consolidated for the lower stress level, the shape of the curves is rather similar. Comparing the curves for the higher stress level with the calculated curves, the shape of the curves is close to the calculated curves for the oedometer case. This could be an indication that the specimens are consolidated similar to the $K_{0(NC)}$ – conditions, i.e. $\varepsilon_h = 0$. However, as no measurements of the radial deformation were made, it cannot be verified that no radial strain has occurred during consolidation.

To gain an idea of the magnitude of eventual radial strain of the specimens during consolidation for the *in situ* stress state (K_{0NC}), calculations of the radial deformation of the specimens during consolidation have been done according to the theory of elasticity. The radial strain can then be written:

$$\varepsilon_r = \frac{2}{E}\left[\Delta\sigma'_r - \upsilon\left(\Delta\sigma'_v - \Delta\sigma'_r\right)\right] \qquad (5\text{-}8)$$

In the calculations, the applied effective consolidation stresses from load step 3 to load step 4 for the higher stress level have been used, $\Delta\sigma'_v = 91$ kPa, $\Delta\sigma'_r = 59$ kPa. The calculations have been made based on Young's modulus (E), either calculated from measured vertical deformation (see Figure 5-33) or calculated from the oedometer modulus estimated from CRS oedometer tests on clay from the specimens after the model tests. Poisson's ratio $\nu = 0.3$ has been used. These calculations indicate a radial

deformation of the specimens during consolidation of around 5 to 15 mm, and thus not $\varepsilon_h = 0$ as for the oedometer case. However, such large deformations were not observed during consolidation of the specimens.

It can be noted that all the degree of consolidation – time factor curves are fairly close to the curves from the finite element calculations with Plaxis and the analytical solution (Silveira, 1953, Mc Kinlay, 1961), indicating that a reasonable estimate of the settlement process for the model test specimens is given using the permeability and modulus from the CRS oedometer tests.

To visualise the difference in time for end of primary consolidation and deformation due to variations in soil properties between the specimens, the measurements during consolidation of the specimens from the test series with the higher consolidation stresses are plotted as time versus deformation in Figure 5-33.

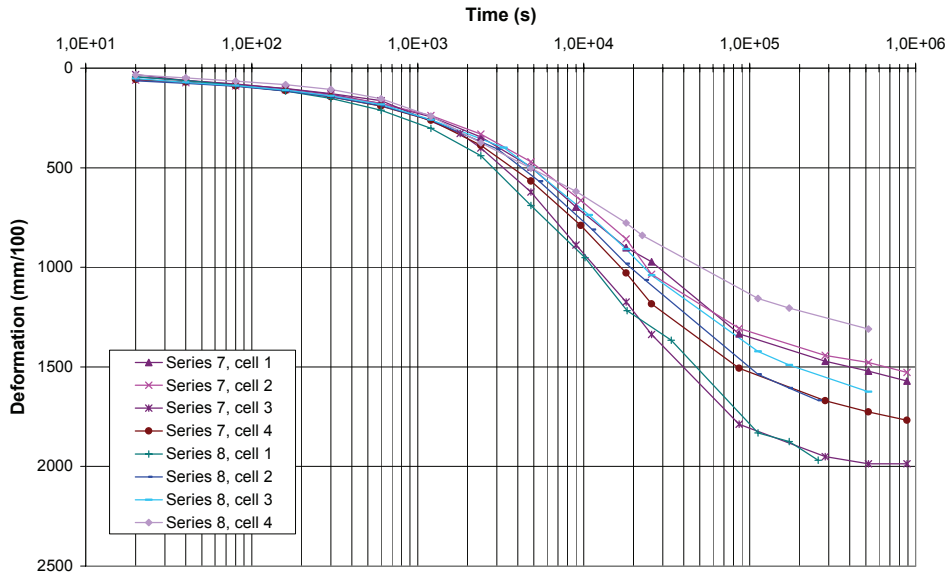

Figure 5-33 Relationships between deformation and consolidation time for the model test specimens consolidated for the higher consolidation stresses (load step 4).

When the specimens had reached the final preconsolidation stresses, they were unloaded to the final consolidation stresses. Measurements of the swelling in the vertical direction were then carried out 1-2 days after unloading. The compression in the vertical direction due to stress changes in all directions is, according to the elasticity theory, for the triaxial case written:

$$\varepsilon_v = \frac{1}{E}\left[\Delta\sigma'_v - 2\upsilon \cdot \Delta\sigma'_r\right] \quad (5\text{-}9)$$

In Figure 5-34 the negative strain in the vertical direction (swelling) was, accordingly, plotted against the combined changes in effective stress in all directions. Poisson's ratio ν = 0.3 has been used. The results indicate that there is a relationship between the vertical strain and the combined effective stress changes in all directions. Corresponding diagrams with strain plotted versus change in vertical effective stress or mean effective stress do not show relationships that are as good.

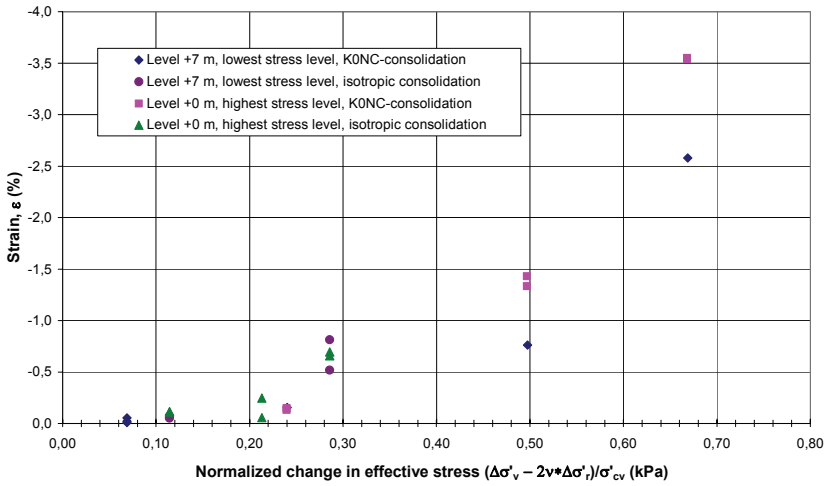

Figure 5-34 Vertical swelling of the specimens due to unloading from the preconsolidation stresses to the final consolidation stresses plotted versus the normalised combined change in effective stress in all directions.

5.4.6 Results of the direct simple shear tests

As described in Section 5.4.2, direct simple shear tests on specimens from the Partille test site were carried out to compare the results of the model tests with the equation that describes how the undrained shear strength varies with preconsolidation pressure and overconsolidation ratio. The results from the direct simple shear tests consolidated for effective stresses 2.5 times the natural preconsolidation pressure and then unloaded to various OCRs according to the SHANSEP procedure, can be described using the general Equation 5-7 above. The calculated factors *a* and *b* are then 0.22 and 0.81 respectively, see Figure 5-35, i.e. very close to the empirical values (a = 0.22 and b = 0.8, Section 5.4.2 above). The results from the direct simple shear tests on specimens consolidated just below the natural preconsolidation pressure and then unloaded to various OCRs gave *a* and *b* factors of 0.22 and 0.88 respectively, i.e. an a-factor very close to the empirical value and a slightly higher b-value than the empirical value.

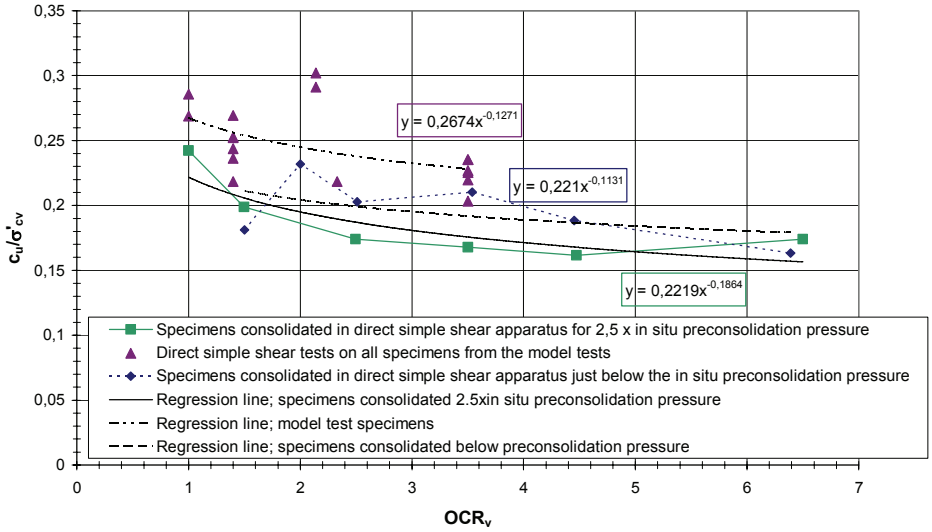

Figure 5-35 Results from direct simple shear tests on specimens according to the SHANSEP procedure and on specimens from the model tests. Tests were performed using specimens from the Partille test site.

The results from the direct simple shear tests on clay from the specimens in the model tests show a considerable scatter. These results also appear to be described roughly with the general equation and the calculated factors then become about a = 0.27 and b = 0.87 respectively, see Figure 5-35, i.e. slightly higher values than the empirical values. However, due to the scatter, the relationship cannot be considered significant. It should also be noted that the specimens consolidated for the model tests do not have the same boundary conditions as the specimens consolidated in the direct shear apparatus. According to empirical relationships, (Larsson, 1977), the a-factor for specimens consolidated for K_{0NC} = 0.65, as for the model tests, is about 0.25, whereas the empirically used a-factor of 0.22 corresponds to a K_{0NC}-value of about 0.55. Isotropically consolidated specimens, K_{0NC} = 1.0, empirically correspond to an a-factor of about 0.33.

In Figure 5-36 the results from the isotropically consolidated specimens and the K_{0NC}-consolidated specimens for the model tests have been separated. In correspondence with the empirical relationships, this results in the highest value of the a-factor for the isotropically consolidated specimens, a ≈ 0.28, thereafter a ≈ 0.24 for the specimens consolidated for K_{0NC} = 0.65. The lowest a-factor, a ≈ 0.22, is accordingly obtained for the specimens consolidated in the direct shear apparatus (K_{0NC} probably ≈ 0.55). However, these relationships cannot be considered more than indicative due to the scatter. The b-factor also varies, b ≈ 0.85 for the isotropically consolidated specimens, b ≈ 0.95 for the K_{0NC} = 0.65

consolidated specimens and b ≈ 0.81 for the specimens consolidated in the direct shear apparatus. However, there are no empirical relationships known that cover how the decrease in shear strength with OCR changes with the value of K_0 during consolidation.

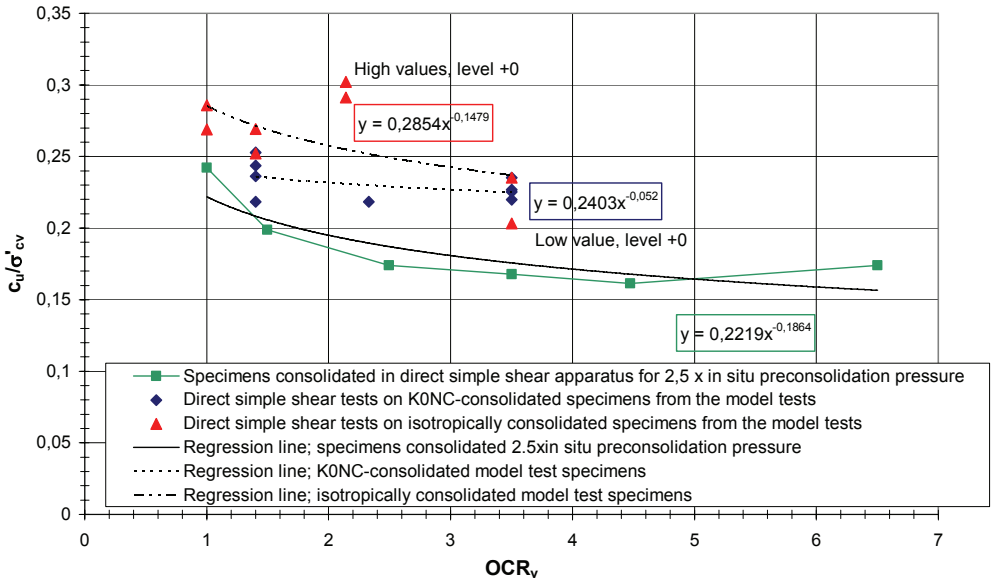

Figure 5-36 Results from direct simple shear tests on specimens according to the SHANSEP procedure and on specimens from the model tests. Tests were performed on specimens taken from the Partille test site.

Tests were also carried out according to the SHANSEP procedure on specimens from the Slumpån test site. The results from the direct simple shear tests on specimens consolidated for effective stresses 2.5 times the natural preconsolidation pressure and then unloaded to various OCRs according to the SHANSEP procedure, give calculated factors *a* and *b* of 0.21 and 0.79 respectively, i.e. very close to the empirical values, see Figure 5-37. The results from the direct simple shear tests on specimens consolidated just below the natural preconsolidation pressure and then unloaded to various OCRs gave *a* and *b* factors of 0.24 and 0.80 respectively, i.e. also close to the empirical values.

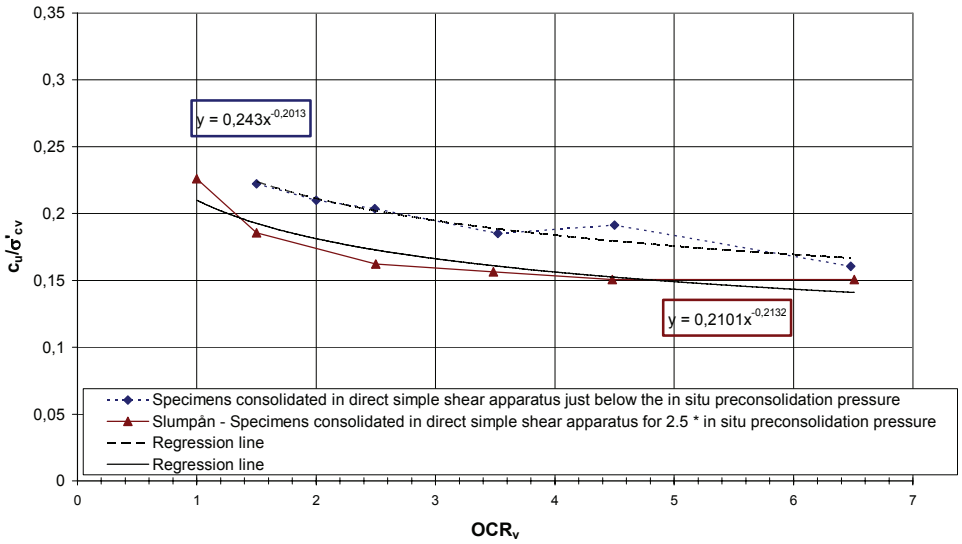

Figure 5-37 Results from direct simple shear tests on specimens according to the SHANSEP procedure and according to the modified SHANSEP procedure. Tests were performed on specimens from the Slumpån test site.

5.4.7 Results of the vane tests

The results of the vane tests, plotted as torque against depth, for consolidation stresses corresponding to level +7 m are presented in Figure 5-38 and the results of the vane tests for consolidation stresses corresponding to level ±0 m are presented in Figure 5-39. It can be noted that the measured torque at depths of 70 and 220 mm for some of the tests diverge more than the torque at depths of 120 and 170 mm and are thereby considered to be less representative. Therefore, only the results from the depths 120 and 170 mm were used in the analysis. The results from the isotropically consolidated test specimen with OCR 1.0 (level +7 m) show a rather high torque at depths of both 70 and 120 mm compared to the other tests and to the results at depths of 170 and 220 mm. This high torque is considered to be less representative and consequently the result from the depth of 120 mm is not included in the analysis.

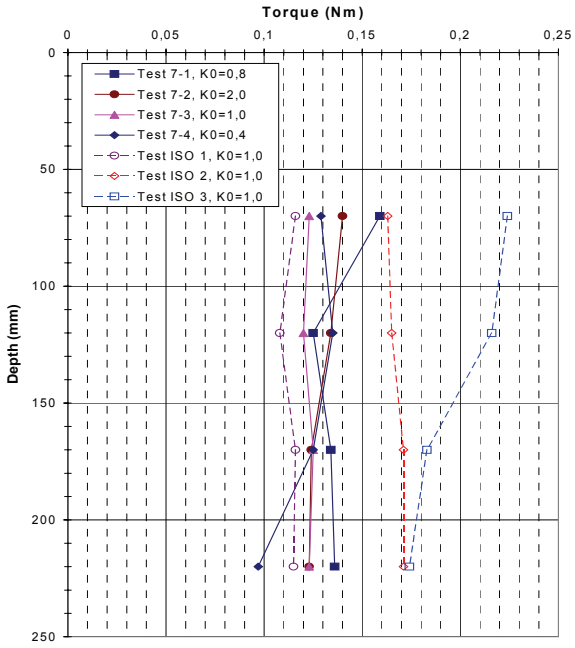

Figure 5-38 Results of the vane tests 7-1 to 7-5 and ISO1 to ISO3.

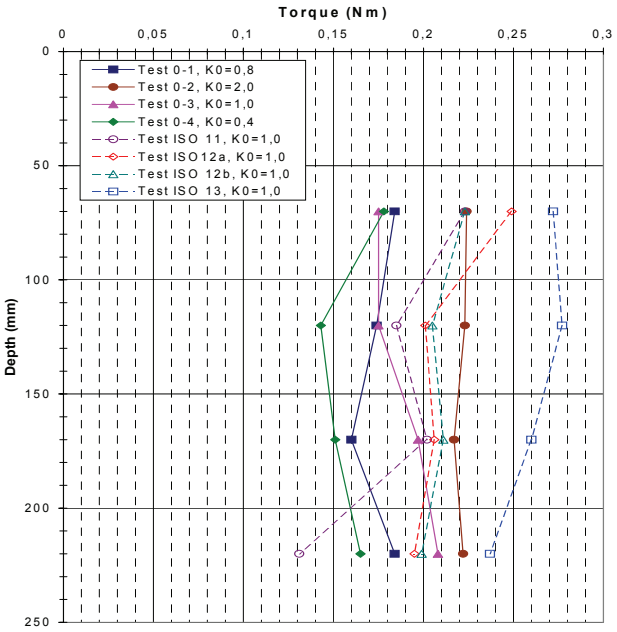

Figure 5-39 Results of the vane tests 0-1 to 0-4 and ISO11 to ISO13.

One purpose of the analysis is to try to evaluate whether it is the horizontal stresses, the vertical stress or a weighted stress that has the main influence on the vane test results. Therefore, the results were normalised against the horizontal preconsolidation pressure, the vertical preconsolidation pressure and a weighted preconsolidation pressure: 1/7 of the vertical preconsolidation pressure and 6/7 of the horizontal preconsolidation

pressure. The weighted stress is generally believed to best reflect the influence of horizontal and vertical preconsolidation pressure on the undrained shear strength determined using the vane test (Bjerrum, 1973). Another purpose of the analysis is to study the possible effect of the overconsolidation ratio in various directions (and consequently also the influence of the consolidation stresses in these directions). The normalised shear strength was therefore plotted against the horizontal, vertical and mean or weighted OCRs. A relationship for the data was drawn in each diagram using the least squares method, power function.

It is believed that the OCR corresponding to the most influencing preconsolidation pressure was the main influence on the vane test results. Consequently, if the horizontal preconsolidation pressure is the main influencing stress on the vane shear strength, then the OCR in the horizontal direction should also be the main influence on the vane shear strength, see also Section 2.6.3.

These relationships were compared with the empirical equation that describes how the undrained shear strength varies with preconsolidation pressure and overconsolidation ratio: $\frac{c_u}{\sigma'_{cv}} = a \cdot OCR_v^{b-1}$ (Equation 5-7, Section 5.4.2 above). The normally used values of 0.22 for the a-factor for direct simple shear and 0.8 for the b-factor were applied. These values were also calculated for the actual clay from the direct simple shear tests consolidated according to the SHANSEP procedure (Section 5.4.6 above).

It should be remembered that the empirical relationship above was developed from laboratory tests comparing the strength of specimens consolidated for the same relationship between vertical and horizontal stresses i.e. the same K-condition and unloaded to various overconsolidation ratios with a slight change in the K-conditions. For direct simple shear tests the empirical relationship corresponds to specimens consolidated and sheared under K_0- conditions (in active triaxial tests the specimens were consolidated and tested under K_0 conditions or under isotropic conditions, according to the literature). The strength comparisons were between specimens with different vertical OCRs and only this OCR value was considered.

In the model tests the specimens are either anisotropically consolidated for K_{0NC} conditions and unloaded to different K_0 conditions, between $K_0 = 0.4$ and $K_0 = 2.0$, or isotropically consolidated and unloaded to isotropical conditions. Hence, if the horizontal preconsolidation pressures have an

influence on the shear strength determined using the vane (or the piezocone) it should be possible to detect this, comparing the various plots of the model test results with the empirical relationship.

The empirical relationship is based on normalisation of the undrained shear strength against the vertical preconsolidation pressure. To be able to also compare this empirical equation with the model test results normalised against the horizontal preconsolidation pressure or the weighted preconsolidation pressure, the empirical equation was converted to be valid for these conditions. This was achieved by using the empirical relationships described below.

Combining Equation 5-7 (above) with the relation $K_{0NC} = \frac{\sigma'_{ch}}{\sigma'_{cv}}$ gives for normalisation against the horizontal preconsolidation pressure:

$$\frac{c_u}{\sigma'_{ch}} = \frac{0.22}{K_{0NC}} \cdot OCR_v^{-0.2} \qquad (5\text{-}10)$$

For normalisation against the weighted preconsolidation pressure, a combination of Equation 5-7, Section 5.4.2 above and 5-10 (above) results in the following expression:

$$\frac{c_u}{\left(0.14\sigma'_{cv} + 0.86\sigma'_{ch}\right)} = \frac{0.22 \cdot OCR_v^{-0.2}}{0.14 + 0.86K_{0NC}} \qquad (5\text{-}11)$$

The undrained shear strength normalised against the vertical, the horizontal or the weighted preconsolidation pressure was plotted against the vertical, the horizontal and the mean or the weighted overconsolidation ratio. The vertical OCR was converted using the following relationships:

$$\sigma'_h = K_0 \cdot \sigma'_v \;; \qquad K_0 = K_{0NC} \cdot OCR_v^{0.6} \;; \qquad OCR_h = \frac{\sigma'_{ch}}{\sigma'_h}$$

$$OCR_{mean} = \frac{OCR_v + 2OCR_h}{3} \;; \quad OCR_{weighted} = \frac{OCR_v + 6OCR_h}{7}$$

To illustrate how the shape of the empirical relationship changes when plotted against the horizontal OCR instead of the vertical OCR, the relationship is plotted against both the vertical and the horizontal OCR in Figure 5-40. It can be seen that the normalised shear strength decreases more rapidly with increasing horizontal OCR than with increasing vertical

OCR. This is due to the fact that the horizontal stresses do not decrease as quickly with increasing OCR_v as the vertical stresses under unloading in K_{0NC}-conditions. A low b-factor gives a more rapid decrease than a high b-factor. Normalisation against the horizontal OCR instead of the vertical OCR also means that the a-factor in the equation is multiplied by $1/K_{0NC}$. This change in the empirical relationship is also shown in Figure 5-40.

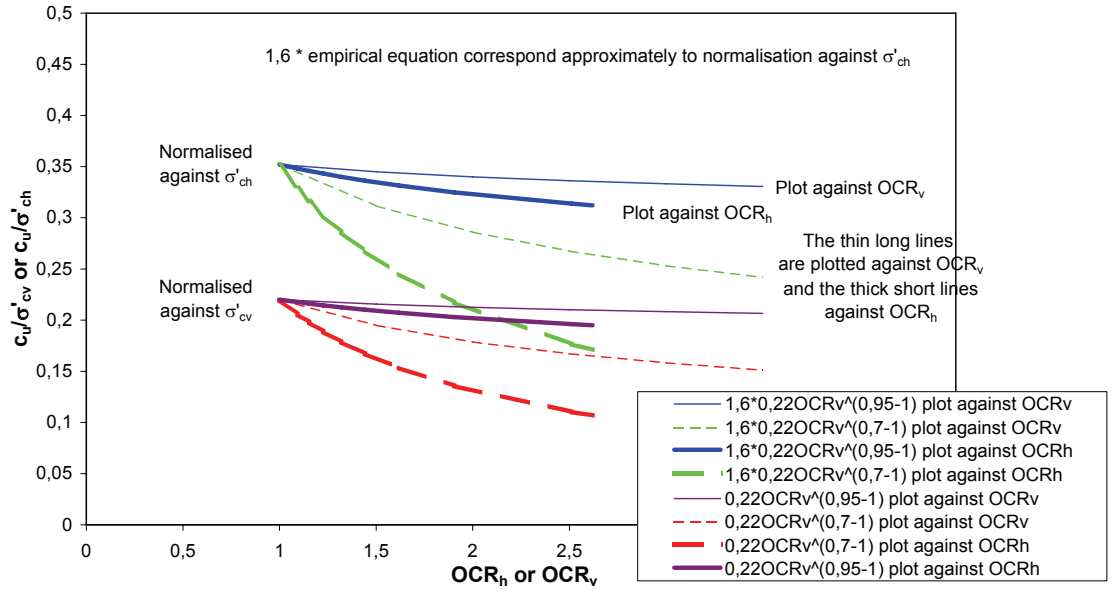

Figure 5-40 Variation in the empirical relationship when the shear strength is normalised against vertical or horizontal preconsolidation pressure and plotted against the vertical or horizontal OCR.

Thus, normalisation of the empirical shear strength against the horizontal (or the weighted) preconsolidation pressure instead of the vertical preconsolidation pressure gives a higher value for the normalised shear strength although it only moderately changes the shape of the empirical relationship. However, normalising the shear strength from the model test results against the horizontal (or the weighted) preconsolidation pressure instead of the vertical preconsolidation pressure changes significantly the relationship between the K_{0NC}-consolidated and the isotropically consolidated specimens in the plots.

Independent of how the normalisation of the vane model test results is done, a considerable scatter in the data can be observed. The amount of data from the model tests is also limited. It is therefore not possible to obtain highly significant relationships in any of the plots (R^2 between 0.1 and 0.4). However, the significance is enhanced considerably when the

shear strength is normalised against the horizontal preconsolidation pressure or the weighted average preconsolidation pressure compared to against the vertical preconsolidation pressure. Figure 5-41 and Figure 5-42 show the vane shear strength normalised against the horizontal preconsolidation pressure and plotted against the OCR in the horizontal direction for the tests at depths of 120 and 170 mm respectively. To compare the relationships from the vane test data with the empirical equation, the level of the equation data was raised to the starting level of the relationship of the shear strength data using a multiplier: $\frac{c_u}{\sigma'_{cv}} = x \cdot a \cdot OCR_v^{b-1}$ The multiplier x is influenced by factors such as the liquid limit, the rate of rotation, the $K_{0(NC)}$, the vane size etc. For the tests at a depth of 120 mm, the relationship coincides fairly well with the empirical equation. For the tests at a depth of 170 mm there is a larger scatter.

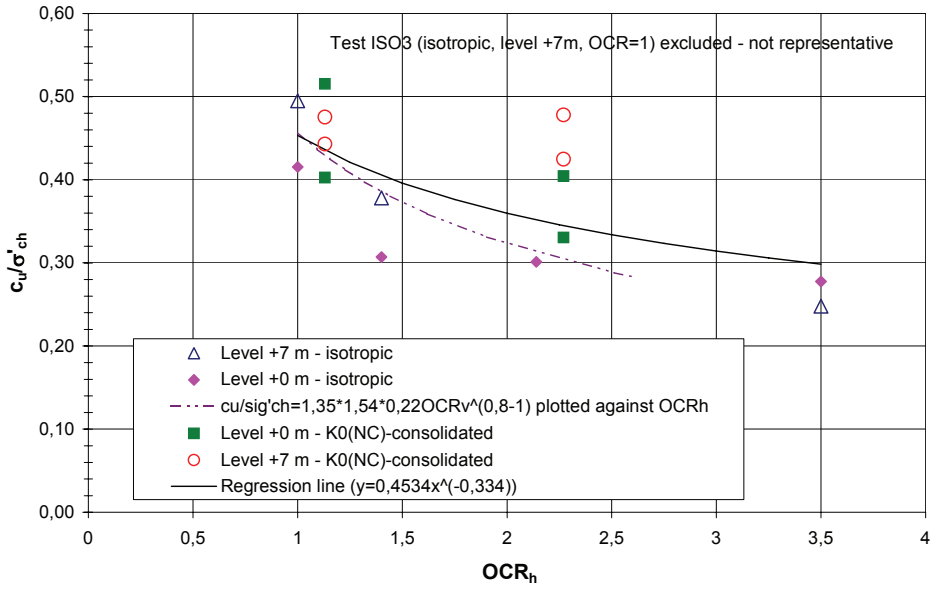

Figure 5-41 The vane shear strength measured at a depth of 120 mm normalised against the horizontal preconsolidation pressure and plotted against the OCR in the horizontal direction.

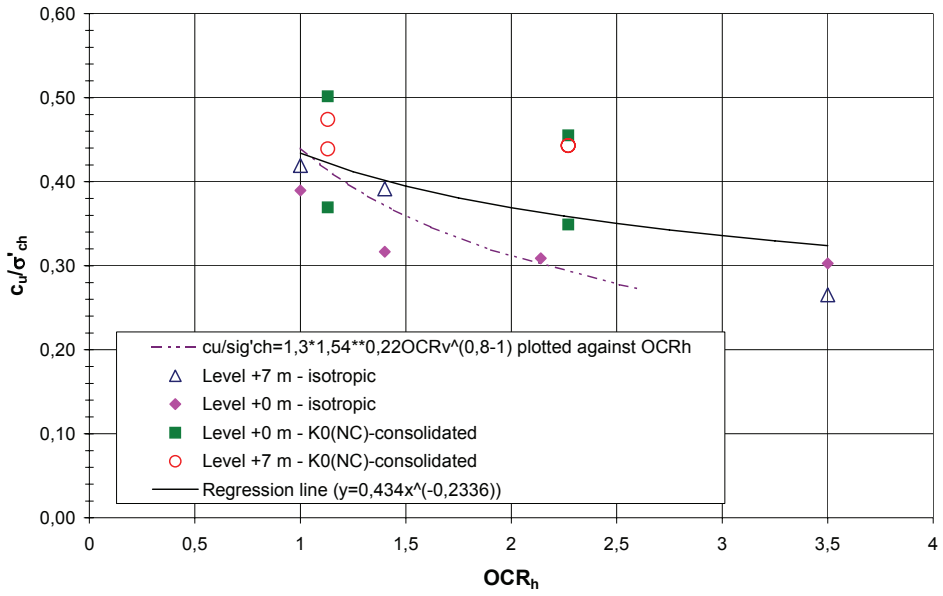

Figure 5-42 The vane shear strength measured at 170 mm depth normalised against the horizontal preconsolidation pressure and plotted versus the OCR in the horizontal direction.

Figure 5-43 and Figure 5-44 show the vane shear strength normalised against the weighted preconsolidation pressure and plotted against a weighted OCR for the tests at depths of 120 and 170 mm respectively. The results are rather similar to the results from the normalisation against the horizontal preconsolidation pressure. The discrepancy is slightly smaller for the data at depths of both 120 and 170 mm between the empirical equation and the relationship of the vane test data and the significance is about the same. As the weighted preconsolidation pressure is close to the horizontal preconsolidation pressure it is not surprising that the results are similar. The vane shear strength normalised against the weighted preconsolidation pressure and plotted against a horizontal OCR gives a slightly higher significance, but then the discrepancy between the empirical equation and the relationship of the vane test data is slightly larger.

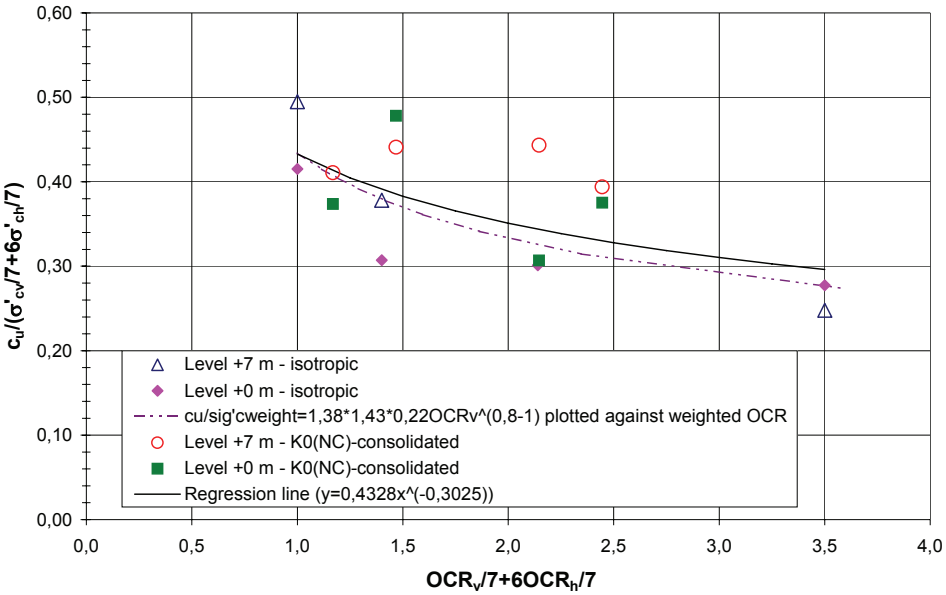

Figure 5-43 The vane shear strength measured at a depth of 120 mm and normalised against the weighted preconsolidation pressure and plotted against the weighted OCR.

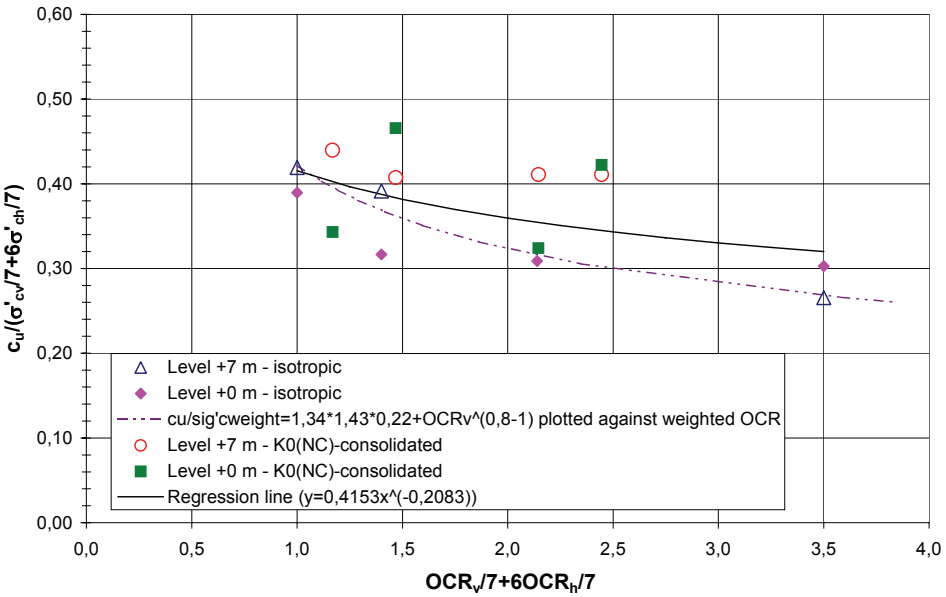

Figure 5-44 The vane shear strength measured at a depth of 170 mm and normalised against the weighted preconsolidation pressure and plotted against the weighted OCR.

The relationship of vane shear strength normalised against the vertical preconsolidation pressure and plotted against the OCR in the vertical

direction gives a close correlation with the empirical equation although the significance of the relationship is very low, see Figure 5-45 and Figure 5-46. It is therefore not relevant to draw any definite conclusions from this correlation.

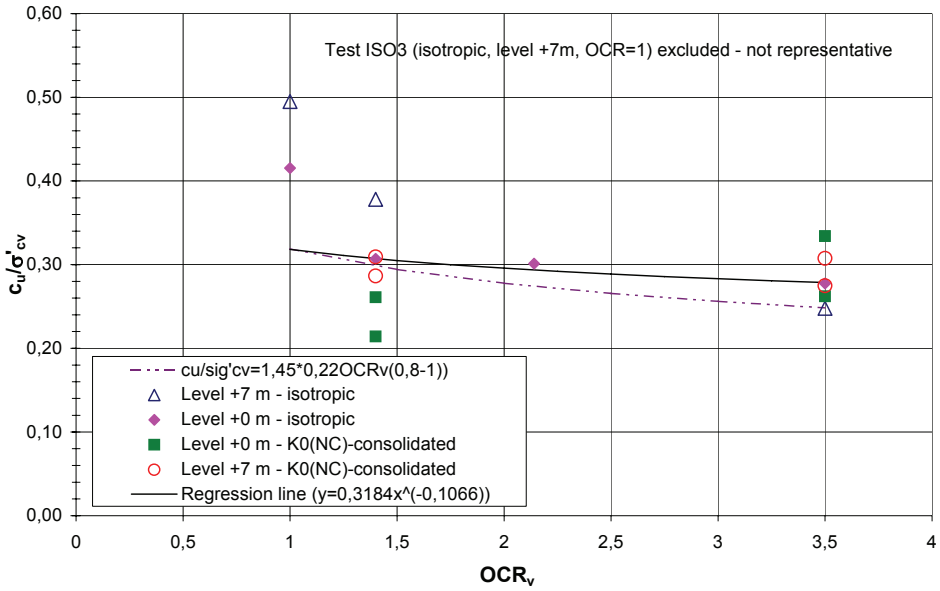

Figure 5-45 The vane shear strength measured at a depth of 120 mm and normalised against the vertical preconsolidation pressure and plotted against the OCR in the vertical direction.

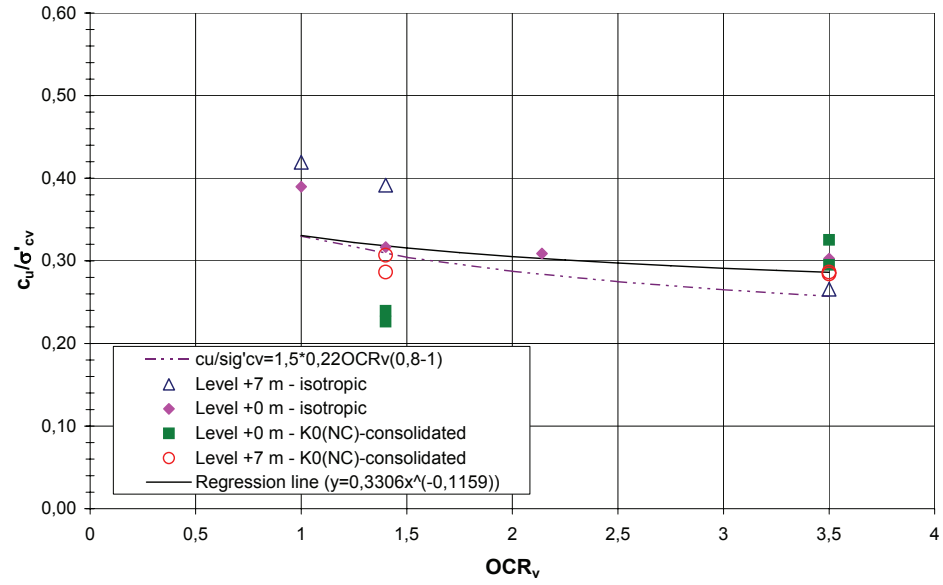

Figure 5-46 The vane shear strength measured at a depth of 170 mm and normalised against the vertical preconsolidation pressure and plotted against the OCR in the vertical direction.

The results from this analysis of the data indicate that there is influence from the horizontal preconsolidation pressure and the OCR in the horizontal direction on the vane shear strength. However, as the relationship for the vane test data cannot be considered quite significant, this conclusion is tentative.

The coefficient of variation for both the vane shear strength and the normalised vane shear strength for the data with OCR in the same range is between 0.15 to 0.25. This is in the lower interval of the coefficient of variation for the soil parameter undrained shear strength, which is 0.1 to 0.5 according to Lumb (1974). However, the undrained shear strength of the clays in the western part of Sweden normally shows a coefficient of variation of 0.1 to 0.15, which is slightly lower than the coefficient of variation for the shear strength determined in the tests in this study.

Regardless of whether the data is normalised against the vertical, horizontal or weighted preconsolidation pressure and plotted against the vertical, horizontal or weighted OCR, the relationships from the model test results do not decrease quite as much as the empirical equation, see Figure 5-41 – Figure 5-46. This is in agreement with field vane data from several sites presented by Jamiolkowski et. al. (1985). The b-value from field vane tests at six of nine sites was larger than 0.9. Larsson and Åhnberg (2003) also present field vane test results from three Swedish test sites with high overconsolidation ratios where the observed b-factors are between 0.88 and 1.12. This indicates that unloading has a greater influence on the direct simple shear test results than on the vane test results.

The best significance and the best correlation with the empirical equation are obtained by plotting the model test results from the isotropically consolidated specimens only, see Figure 5-47 and Figure 5-48. As the empirical equation should not correspond to isotropic conditions, the reason for this is possibly that the use of fewer data generates fewer assumptions and errors. In this case normalisation against the horizontal, weighted and vertical preconsolidation pressures gives the same result, as the vertical preconsolidation pressure is equal to the horizontal preconsolidation pressure in the isotropically consolidated tests results. The data for the empirical equation is also equal in these three cases as the normalisation against the horizontal or weighted preconsolidation pressure is obtained by multiplying the empirical equation by an additional/larger x factor (see equation above).

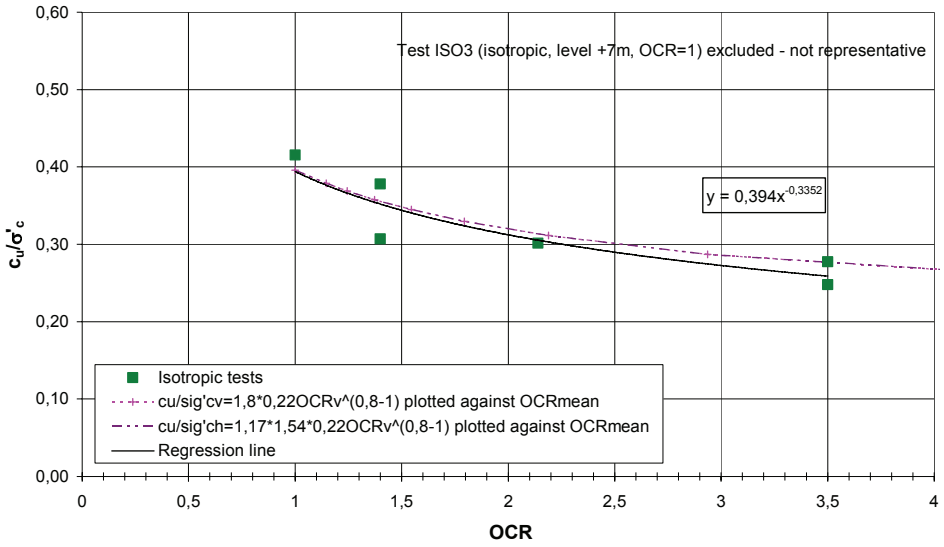

Figure 5-47 The vane shear strength measured at a depth of 120 mm for the isotropically consolidated specimens normalised against the OCR.

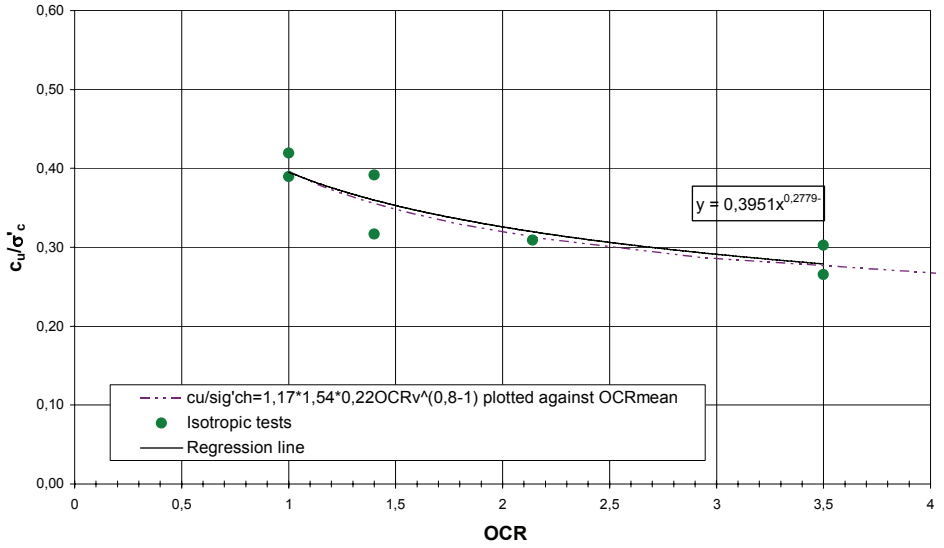

Figure 5-48 The vane shear strength measured at a depth of 170 mm depth for the isotropically consolidated specimens normalised against the OCR.

No correction of the results from the field vane tests for overconsolidation has traditionally been made in Sweden. However, Larsson and Åhnberg (2003) propose that for evaluation of the undrained shear strength from vane tests an extra correction, μ_{OCR}, should be applied in addition to that which in Sweden is made on the basis of the liquid limit of the soil. This correction is proposed to be $\mu_{OCR} \approx OCR^{-0,15}$. As the ordinary correction

with respect to the liquid limit is based on soils with an overconsolidation ratio of about 1.3, the corrections for overconsolidation up to this value can be assumed to be included. The correction then becomes: $\mu_{OCR} \approx \left[\frac{OCR}{1.3}\right]^{-0.15}$.

This means that the uncorrected undrained shear strength value measured using the field vane test does not decrease as much with the vertical OCR as the empirical equation implies.

5.4.8 Results of the piezocone tests

The results of the piezocone tests for consolidation stresses corresponding to level +7 m are presented in Figure 5-49 and the piezocone test results for consolidation stresses corresponding to level ±0 m are presented in Figure 5-50. It can be noted that all the piezocone tests in the K_{0NC}-consolidated specimens, level +7 m, give almost the same value of the net cone resistance (q_T-σ_{v0}). However, the results differ for the isotropic tests. For the tests in the specimens consolidated for stresses corresponding to level ±0 m the results show a larger scatter. The value of (q_T-σ_{v0}) from the test in the isotropically consolidated specimen, consolidated at the highest stresses and an OCR of 3.5, is so low that it is not considered to be representative. Therefore, it is not included in the analysis.

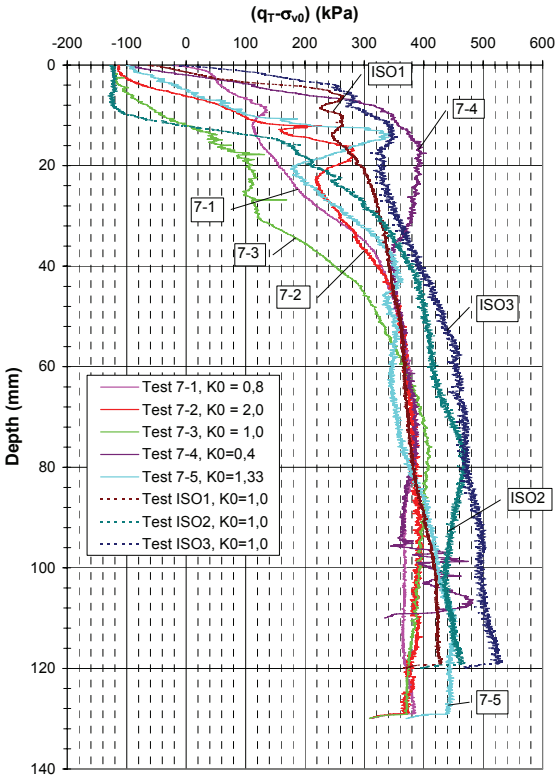

Figure 5-49 Results of piezocone tests 7-1 to 7-4 and ISO1 to ISO3.

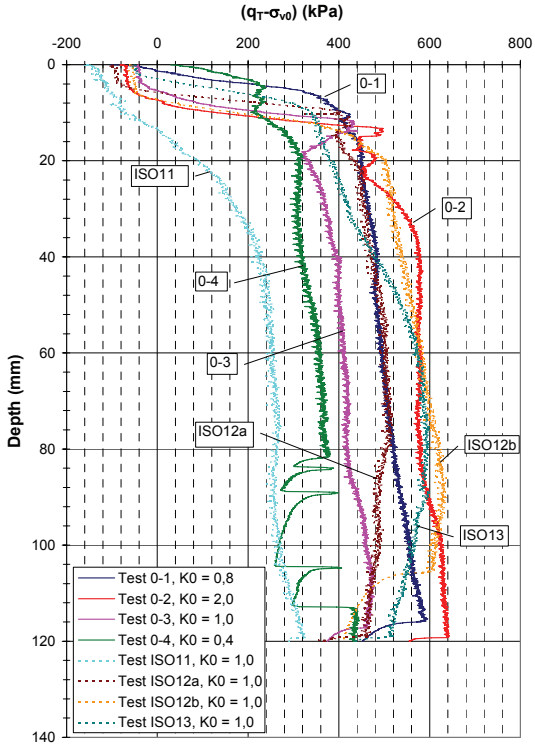

Figure 5-50 Results of piezocone tests 0-1 to 0-4 and ISO11 to ISO13.

The basis for correlating the net cone resistance from the piezocone test to the undrained shear strength was, apart from empirical correlations, been theoretical analyses using bearing capacity methods, cavity expansion methods (cylindrical expansion or/and spherical expansion), strain path methods, and finite element methods or a combination of these methods, see Section 2.6.4. According to these theories the net cone resistance and correspondingly the calculated undrained shear strength should be governed by either the horizontal stresses or both the horizontal and the vertical stresses. Evaluation of the undrained shear strength from piezocone tests is normally made using the equation: $c_u = \frac{q_T - \sigma_{v0}}{N_{kt}}$. The cone factor N_{kt} varies depending on what shear strength it is referred to, i.e. the active shear strength, the shear strength at direct simple shear or some other case (see Section 2.6.4). However, the focus in this study is to see which stresses exert most influence on the net cone resistance (q_T-σ_{v0}). Therefore, (q_T-σ_{v0}) has been normalised against the horizontal preconsolidation pressure, the vertical preconsolidation pressure and the mean preconsolidation pressure. To see the effect of the overconsolidation ratio (OCR), the normalised net cone resistance was plotted against the horizontal, vertical or mean overconsolidation ratio. It is believed that the OCR corresponding to the most influencing preconsolidation pressure exerts most influence on the piezocone test results. Consequently, if the mean preconsolidation pressure exerts most influence on the shear strength then the mean OCR should also exert most influence on the shear strength calculated from the piezocone.

To compare these relationships with the empirical equation that describes how the undrained shear strength varies with preconsolidation pressure and overconsolidation ratio: $\frac{c_u}{\sigma'_{cv}} = a \cdot OCR_v^{b-1}$ (Equation 5-7, Section 5.4.2 above) it is necessary to include a cone factor, N_{kt}. In the empirical curves in the diagrams, c_u in the equation was multiplied by N_{kt}. The empirical relationship of N_{kt} corresponding to the shear strength at direct simple shear for Swedish slightly overconsolidated clays: $N_{kt} = 13.4 + 6.65 \cdot w_L$, where w_L is the liquid limit in decimals (Larsson and Mulabdic, 1990) was used. This cone factor can thus vary between 14 and 20 with an average of 16.3 for inorganic clays. The value of w_L is chosen as a mean value of w_L for the model tests, which gives $N_{kt} \approx 17$. In the empirical equation for undrained shear strength in clay, which is used for the comparison, the normally used values of 0.22 for the a-factor for direct simple shear and 0.8 for the b-factor were applied. These values were also calculated for the actual clay

from the direct simple shear test consolidated according to the SHANSEP procedure (Section 5.4.6 above).

The empirical relationship is based on a normalisation of the undrained shear strength against the vertical preconsolidation pressure. To be able to compare this empirical equation also with the model test results normalised against the horizontal preconsolidation pressure or the mean preconsolidation pressure, the empirical equation was converted in order to be valid for these conditions. This has been accomplished by using empirical relationships as described below.

Combining equation 5-7 with the relationship $K_{0NC} = \frac{\sigma'_{ch}}{\sigma'_{cv}}$ gives for normalisation against the horizontal preconsolidation pressure: $\frac{c_u}{\sigma'_{ch}} = \frac{0.22}{K_{0NC}} \cdot OCR_v^{-0.2}$ (Equation 5-10, Section 5.4.7 above). For normalisation against the mean preconsolidation pressure, a combination of Equation 5-7 and 5-10 results in the following expression:

$$\frac{c_u}{\left(0.33\sigma'_{cv} + 0.67\sigma'_{ch}\right)} = \frac{0.22 \cdot OCR_v^{-0.2}}{0.33 + 0.67K_{0NC}} \qquad (5\text{-}12)$$

The net cone resistance normalised against the vertical, the horizontal or the mean preconsolidation pressure has been plotted against the vertical, horizontal or mean overconsolidation ratios. The vertical OCR has been converted using the following relationships:

$$\sigma'_h = K_0 \cdot \sigma'_v \;; \qquad K_0 = K_{0NC} \cdot OCR_v^{0.6} \;; \qquad OCR_h = \frac{\sigma'_{ch}}{\sigma'_h}$$

$$OCR_{mean} = \frac{OCR_v + 2OCR_h}{3};$$

It can be noted that the scatter of the data from the piezocone tests is greater than for the vane tests. As a result, the significance of the relationships is considerably lower than for the vane tests. The significance is actually very low for all the piezocone plots (R^2 between 0.02 and 0.1). There is no great difference whether the net cone resistance is normalised against the horizontal, vertical or mean preconsolidation pressure.

In an attempt to detect a correlation, the plots with the net cone resistance normalised against the horizontal, vertical or mean preconsolidation

pressure, each plotted against the horizontal, vertical or mean OCR, were compared. This comparison gives no indication that any of the normalised plots should correlate better with the empirical equation than the other. It can also be noted that in general the results of the vane tests correlate better with the empirical equation than the results from the piezocone tests, in addition to having better significance. Comparing the trends of the normalised net cone resistance against OCR, it can be noted that a plot against the vertical OCR gives unchanged or increased normalised net cone resistance with OCR. A plot against the mean OCR gives an unchanged or slightly decreased normalised net cone resistance with OCR and a plot against the horizontal OCR gives a decrease with OCR. However, as the empirical equation also shows the largest decrease with horizontal OCR it is not possible to draw any conclusions from this either. In all the plots, the empirical equation shows a larger decrease with OCR than the results from the piezocone tests. Figure 5-51, Figure 5-52 and Figure 5-53 show the net cone resistance normalised against the horizontal preconsolidation pressure and plotted against the horizontal OCR, the vertical preconsolidation pressure plotted against the vertical OCR and the mean preconsolidation pressure plotted against the mean OCR.

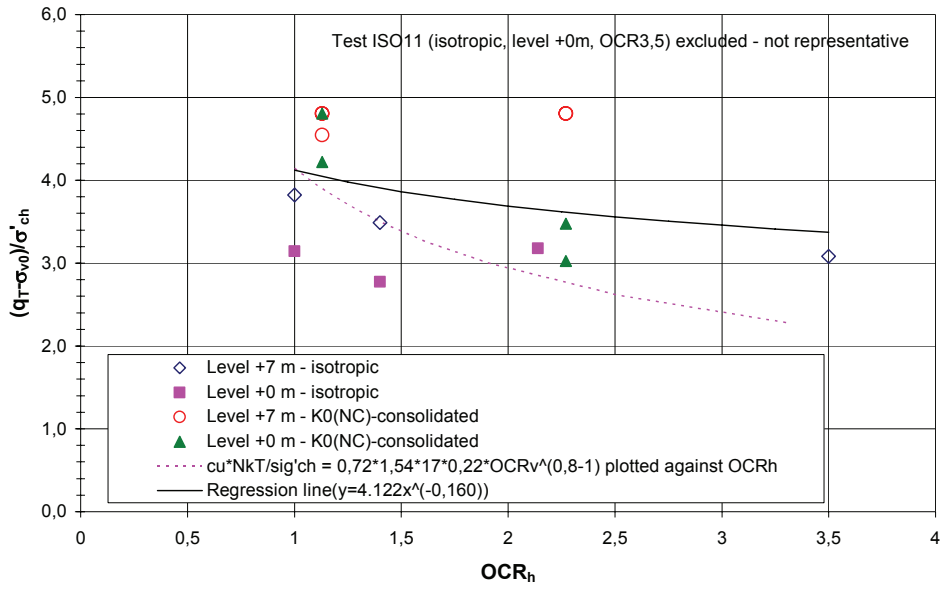

Figure 5-51 The net cone resistance normalised against the horizontal preconsolidation pressure and plotted against the OCR in the horizontal direction.

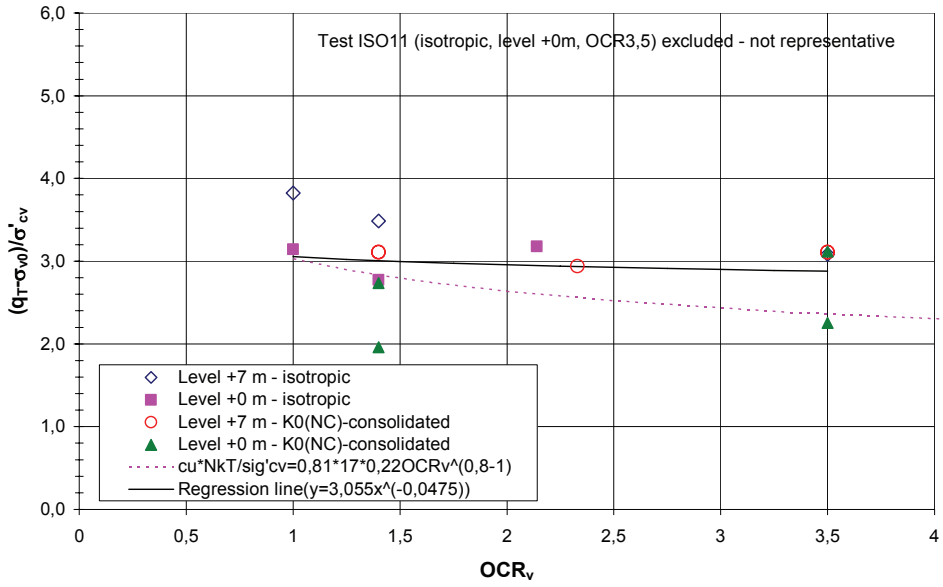

Figure 5-52 The net cone resistance normalised against the vertical preconsolidation pressure and plotted against the OCR in the vertical direction.

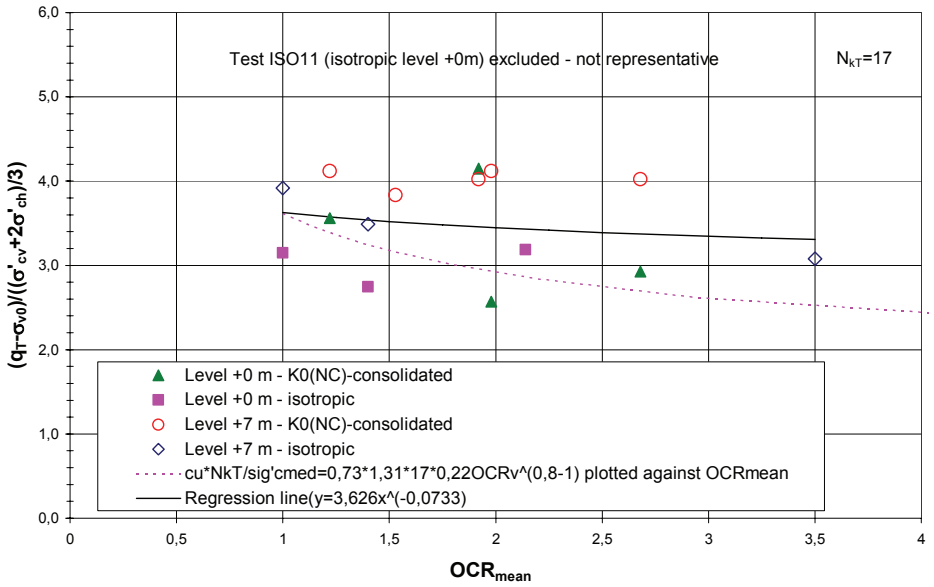

Figure 5-53 The net cone resistance normalised against the mean preconsolidation pressure and plotted against the mean OCR.

Plotting only the data from the tests with consolidation stresses corresponding to the level +7 m gives slightly better significance, Figure 5-54 (and the level ±0 m gives lower significance). Then only half the data is used and there is still no great difference in the scatter of the data between the normalisation against the horizontal stresses, the vertical

stresses or the mean stress. Plotting the data from the isotropic tests shows hardly any increase in the significance compared to the plots with all the data and best significance, Figure 5-55. What can be distinguished from these diagrams is that the normalised net cone resistance appears to decrease slightly with the overconsolidation ratio, but much less than the empirical equation.

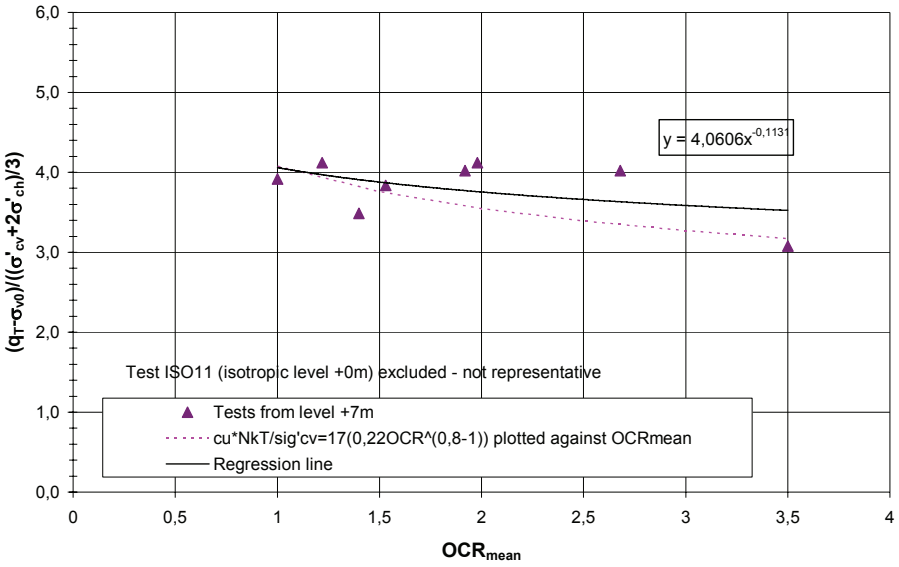

Figure 5-54 The net cone resistance for the tests with consolidation stresses corresponding to the lowest stress level (+7 m) normalised against the mean preconsolidation pressure and plotted against the mean OCR.

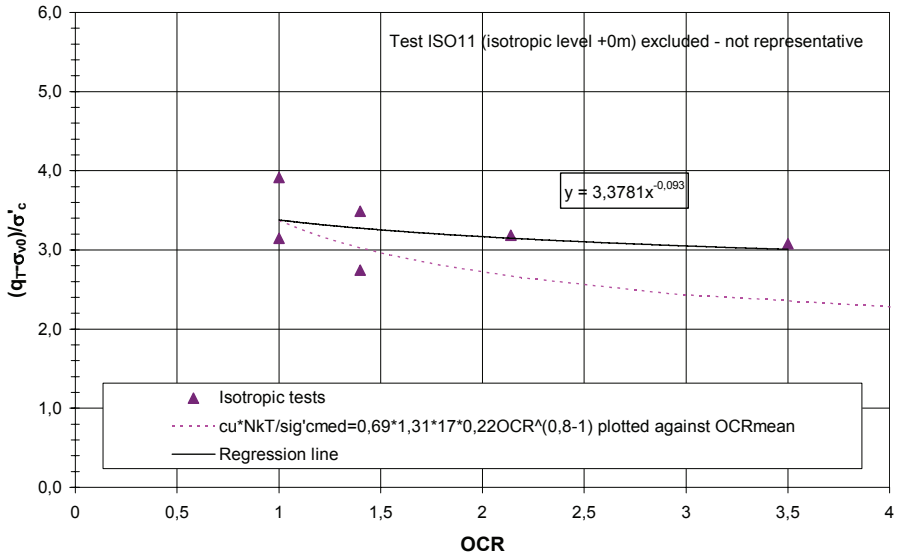

Figure 5-55 The net cone resistance for the isotropically consolidated specimens normalised against the preconsolidation pressure and plotted against the OCR.

What can also be noted is that two of the results from the direct simple shear tests from the series on isotropically consolidated specimens, level ±0 m, show the same tendency as the corresponding results from the piezocone test. The result of the test with OCR = 2.14 is rather high and the result of the test with OCR = 3.5 is too low (excluded from the evaluation), see Figure 5-56, below and Figure 5-36 in Section 5.4.6. As both the direct simple shear tests and the piezocone tests were carried out on the same specimen, this gives an indication that the shear strength of these specimens was too high or too low respectively.

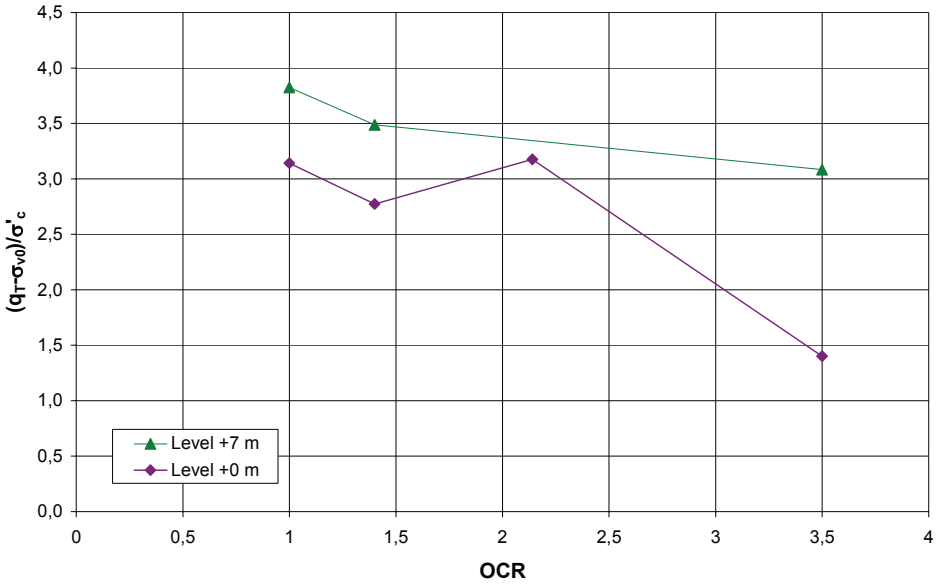

Figure 5-56 *The net cone resistance for all the isotropically consolidated specimens and with the two stress levels separated normalised against the preconsolidation pressure and plotted against the OCR.*

Looking at the relationship between the net cone resistance and the preconsolidation pressure, the significance is greatly enhanced. The best correlation is obtained for the net cone resistance plotted against the mean preconsolidation pressure and against the horizontal preconsolidation pressure. The net cone resistance plotted against the mean preconsolidation pressure is shown in Figure 5-57. The relationship between the net cone resistance and the preconsolidation pressure is between 3.0 and 3.7 with the lowest value for the vertical preconsolidation pressure ($\sigma'_{cv} = \frac{q_T - \sigma_{v0}}{3.0}$). This is in the same range as Demers and Leroueil (2002) found on 31 Quebec clays when comparing the net cone resistance and the preconsolidation pressure measured using oedometer tests in the laboratory. Leaving out two

of the sites, their relationship can be expressed as: $\sigma'_{cv} = \frac{q_T - \sigma_{v0}}{3.4}$. The variation in the factor for these 29 sites was then between 2.9 and 4.5. It is also in the same range as the clear correlation between the net cone resistance and the preconsolidation pressure on Scandinavian clays (SGI and NGI data) found by Larsson and Mulabdic (1991). This correlation can be expressed as:

$$\sigma'_{cv} = \frac{q_T - \sigma_{v0}}{3.43} \tag{5-13}$$

or

$$\frac{q_T - \sigma_{v0}}{\sigma'_{cv}} = 1.21 + 4.4 \cdot w_L \tag{5-14}$$

If consideration is given to the liquid limit the relationship becomes $\sigma'_{cv} \approx \frac{q_T - \sigma_{v0}}{3.7}$ for the clay in the model tests.

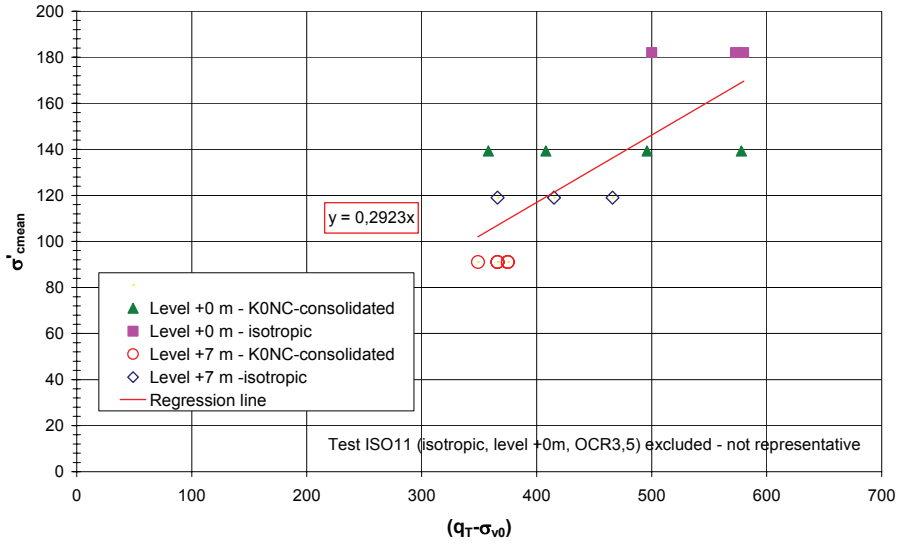

Figure 5-57 The net cone resistance plotted against the mean preconsolidation pressure.

Based on the results alone, it is not possible to determine whether it is the horizontal, the vertical or the mean preconsolidation pressure that exerts most influence on the net cone resistance. This is because of the low significance and the difficulty distinguishing the type of plot that best correlates with the empirical equation. However, according to the above-mentioned theories (Section 2.6.4) the net cone resistance should be governed by either the horizontal stresses or both the horizontal and the vertical stresses. Consequently, normalisation against the horizontal or the

mean preconsolidation pressure should theoretically give the best correlation.

It may be possible to estimate the influence of the horizontal or the vertical preconsolidation pressure using empirical data from earlier studies. Combining the two Equations 5-2 and 5-14 above gives an expression for the relationship between the net cone resistance and the horizontal preconsolidation pressure:

$$\frac{q_T - \sigma_{v0}}{\sigma'_{ch}} = \frac{1.21 + 4.4 \cdot w_L}{0.31 + 0.71 \cdot (w_L - 0.2)} \qquad (5\text{-}15)$$

In Figure 5-58 the net cone resistance is normalised against the vertical preconsolidation pressure and the horizontal preconsolidation pressure respectively and plotted against the liquid limit using equations 5-14 and 5-15. It is clearly seen that there is hardly any change in the net cone resistance normalised against the horizontal preconsolidation pressure with the liquid limit, whereas the net cone resistance normalised against the vertical preconsolidation pressure is a clear function of the liquid limit. This indicates that the net cone resistance is primarily dependent on the horizontal preconsolidation pressure and appears to be a more or less direct function of this.

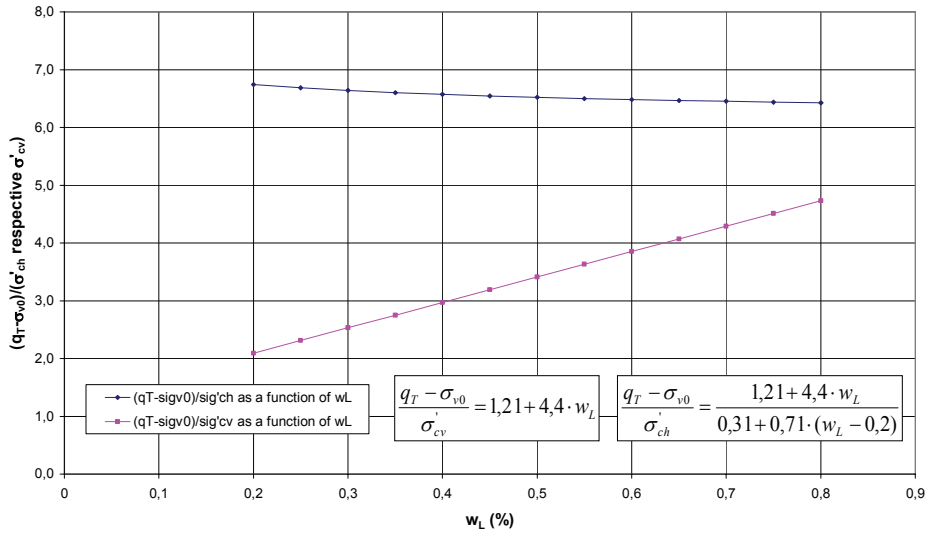

Figure 5-58 The net cone resistance normalised against the horizontal preconsolidation pressure and the vertical preconsolidation pressure respectively and plotted against the liquid limit.

Larsson and Åhnberg (2003) propose a revised calculation method for the undrained shear strength considering the overconsolidation ratio as follows:

$$c_u = \frac{q_T - \sigma_{v0}}{13.4 + 6.65 w_L} \left[\frac{\sigma'_{cv}}{1.3 \sigma'_{v0}} \right]^{b-1} . \qquad (5\text{-}16)$$

This calculation is an elaboration of the calculation method proposed by Larsson and Mulabdic (1991):

$$c_u = \frac{q_T - \sigma_{v0}}{13.4 + 6.65 w_L} \qquad (5\text{-}17)$$

which does not take the overconsolidation ratio into account. The revised calculation method indicates that the calculation by Larsson and Mulabdic, (1991) gave undrained shear strength values that were too high for OCRs significantly larger than 1.3. The aim is that with the revised method the undrained shear strength calculated using the piezocone test should decrease as much with the vertical OCR as the empirical equation implies.

The coefficient of variation for both the shear strength and the normalised shear strength calculated from the piezocone test for the data with OCR in the same range is between 0.15 and 0.25. This is in the lower interval of the coefficient of variation for the soil parameter undrained shear strength, which according to Lumb (1974) is 0.1 to 0.5. However, the undrained shear strength of the clays in the western part of Sweden normally show a coefficient of variation of 0.1 to 0.15, which is slightly lower than the coefficient of variation for the shear strength determined in the tests in this study.

6. ANALYSIS OF FIELD TEST RESULTS BASED ON THE RESULTS OF THE MODEL TESTS

6.1 Analysis procedure

The results of the model tests described in the previous chapter indicate that there is an influence of the horizontal preconsolidation pressure and the OCR in the horizontal direction in the field vane test results. Even though it is not possible to ascertain whether it is the horizontal, vertical or mean preconsolidation pressure that has most influence on the net cone resistance in piezocone tests based on the model test results alone, the influence of the horizontal preconsolidation pressure could be estimated by using empirical data from earlier studies.

The purpose of the analysis presented in this chapter is to predict the undrained shear strength from the field vane test and the piezocone test at the toe of the test site slopes based on the results of the model tests and the stress conditions in the slopes. The field tests performed far behind the crest of the slope are used as references as they correspond to almost horizontal ground conditions. From the results of the model tests, the best correlations found for undrained shear strength and stress history are used. Thus, for the model vane, the regression line for the vane shear strength normalised against the weighted preconsolidation pressure and plotted against the weighted OCR is used. The mean value of the regression line for the tests at a depth of 120 and 170 mm in the test specimens has been used. For the model piezocone, the regression line for the net cone resistance normalised against the horizontal preconsolidation pressure and plotted against the horizontal OCR is used. The model test regression lines used in the analysis are shown in Figure 6-1 and Figure 6-2.

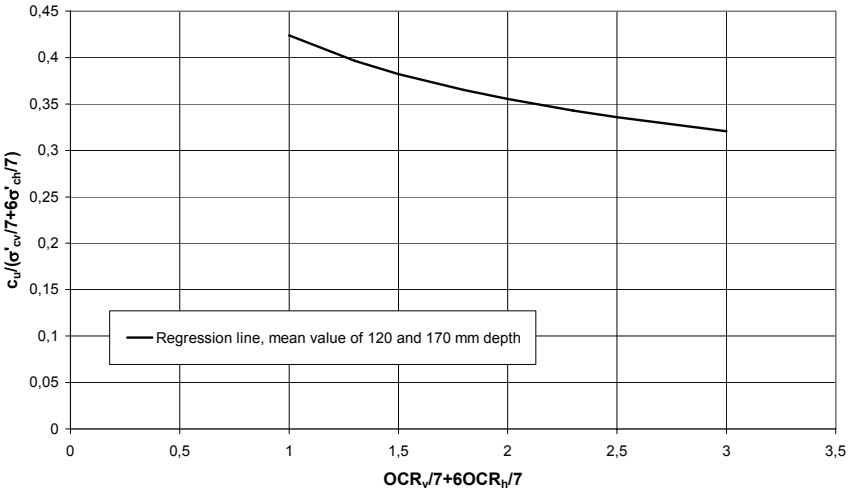

Figure 6-1: Regression line for the mean value of the shear strength measured by the model vane at a depth of 120 and 170 mm, normalised against the weighted preconsolidation pressure and plotted against the weighted OCR.

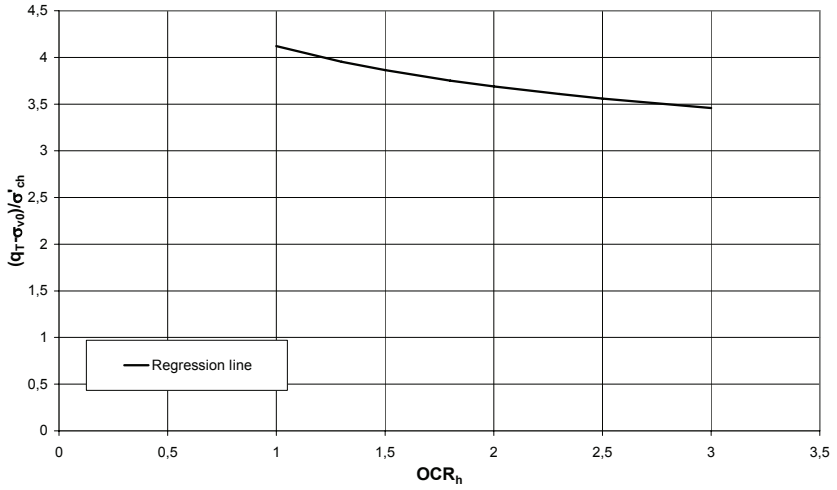

Figure 6-2 Regression line for the net tip resistance measured by the model piezocone normalised against the horizontal preconsolidation pressure and plotted against the horizontal OCR.

The following procedure is used in the analysis:

- The results from field vane tests and piezocone tests behind the crest of the slope are plotted against the depth. The old relationship for evaluation of the undrained shear strength with no correction for overconsolidation are used (no difference to the new relationship since $OCR_v \approx 1.3$). The calculated undrained shear strength is corrected with regard to the liquid limit.
- The values of the undrained shear strength thus determined are normalised against the weighted preconsolidation pressure at the test

level for the field vane and the horizontal preconsolidation pressure at the test level for the piezocone. The vertical preconsolidation pressure ($\sigma'_{cv\text{-}crest}$) has been determined using CRS oedometer tests. The corresponding horizontal preconsolidation pressure has been estimated from $\sigma'_{cv\text{-}crest}$ and K_{0NC}, where K_{0NC} has been estimated empirically from Equation 5-2, Section 5.4.1.2.

- This normalised field shear strength value has been used to calibrate the model test regression line to the field tests, i.e. to give the right starting point for the "field test" regression curve. Consideration has been given to the fact that the overconsolidation ratio for the thus normalised field shear strength value is slightly greater than one.
- When the model test regression curve has in that way been adapted to the ratio between the shear strength and the weighted/horizontal preconsolidation pressure in the field, the undrained shear strength at the toe of the slope can be determined from this new regression line. The input are the vertical preconsolidation pressure at the toe ($\sigma'_{cv\text{-}toe}$) evaluated on the basis of CRS oedometer tests, the horizontal preconsolidation pressure at the toe (from $\sigma'_{cv\text{-}toe}$ and K_{0NC} or from CRS oedometer tests on horizontally oriented specimens) and the horizontal effective stress. The horizontal effective stress has been estimated on the basis of dilatometer tests, empirical experience and at Partille also finite element calculations and measurements by Glötzl cells.

6.2 The Partille test site

6.2.1 Stress conditions

At the Partille test site the vertical preconsolidation pressure at point D, above the crest of the slope ($\sigma'_{cv\text{-}crest}$) (Section 4.2.2, Figure 4-4) was estimated from CRS oedometer tests (Section 4.2.3) to $1.3 \cdot \sigma'_{v0}$. The horizontal preconsolidation pressure was estimated from $\sigma'_{cv\text{-}crest}$ and K_{0NC} as described in Section 6.1 above. The horizontal effective stress at point D, horizontal ground, was estimated using the effective vertical stress at point D and K_{0rb} from the empirical equation (Schmidt, 1967):

$$K_{0rb} = K_{0NC} \cdot OCR_v^{\sin 1.2 \cdot \phi'} \qquad (6\text{-}1)$$

For $\phi' = 30^o$ and $OCR_v = 1.3$ this gives a horizontal overconsolidation ratio, $OCR_h = 1.11$ and a weighted overconsolidation ratio, $OCR_{weighted} = 1.14$ at point D.

At the toe of the slope, point A, the vertical preconsolidation pressures have been estimated from CRS oedometer test results ($\sigma'_{cv\text{-}toe}$) (Section 4.2.3). The horizontal preconsolidation pressure has been estimated from $\sigma'_{cv\text{-}toe}$ and K_{0NC} as described in Section 6.1 above. The effective horizontal stresses at point A have been estimated based on dilatometer tests, Glötzl cell measurements (Rankka, 1994), finite element calculations and empiricism combined with a statement by Rankka (1994), Figure 6-3.

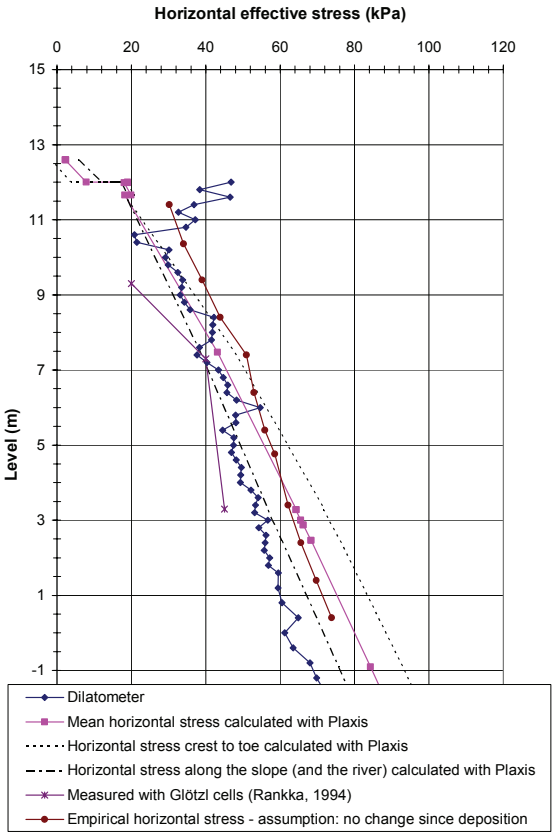

Figure 6-3: Horizontal effective stresses at the toe of the slope (point A).

In her dissertation Rankka (1994) states that "the effective horizontal stresses at a given height above sea level were almost the same independent of in which part of the slope the measurements were made". This indicates that erosion has not caused a significant change in the effective horizontal stresses. The empirical horizontal effective stresses in Figure 6-3 have been estimated based on this statement and with the assumption of a ground level at deposition as at point D, a groundwater level at the ground surface and K_{0NC} estimated from Equation 5-2, Section 5.4.1.2.

Finite element calculations for estimation of the effective horizontal stresses have been carried out by Per-Evert Bengtsson, SGI, using the computer program Plaxis, Version 8. The following parameters were used

in the calculations (Bengtsson, 2007): drained material model according to Mohr-Coulomb, friction angle ϕ = 30º, effective cohesion c' = 1 kPa at level +19.5 increasing by 0.15 kPa/m, dilatancy angle = 0, Young's modulus E = 2500 kPa at level +19.5 increasing by 375 kPa/m i.e. E = $250c_u$, Poisson's ratio ν = 0.30, two clay layers with a density of 1.6 t/m^3 in the upper layer and 1.65 t/m^3 in the lower layer.

During the analysis of the model test data it was seen that the horizontal preconsolidation pressure had quite a considerable influence on the calculated undrained shear strength. To improve the accuracy in the estimation of the horizontal preconsolidation pressures, it was decided to run some CRS oedometer tests on horizontally oriented specimens. The samples available were ordinary 50 mm piston samples taken at the start of the project. It is not possible to trim out a 20 mm high, 50 mm diameter horizontal specimen from these samples. Therefore, the CRS oedometer equipment was modified so that samples 40 mm in diameter could be tested. As the samples were eight years old, it was uncertain whether their quality was such that they could be used and provide reliable results. The water content of each sample to be used was therefore determined and compared with the water content at the time of sampling, i.e. eight years earlier.

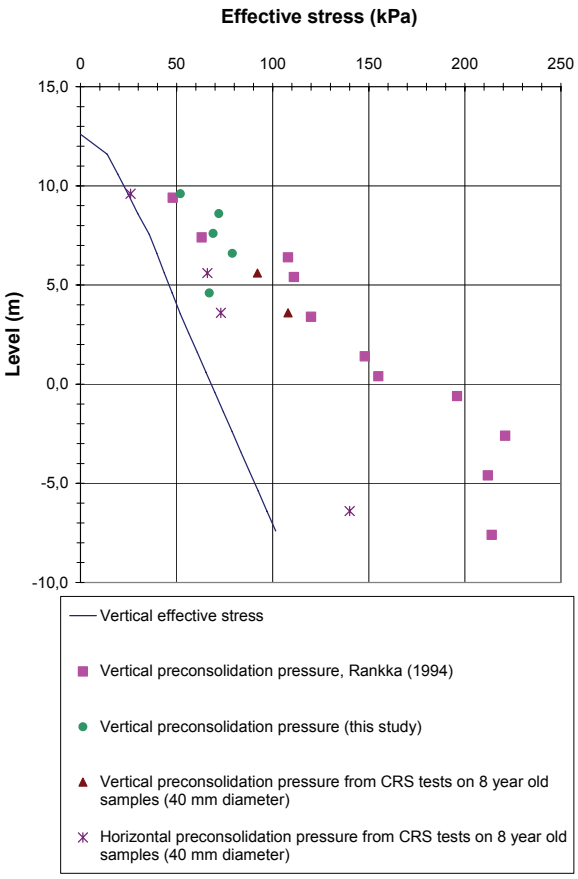

Figure 6-4 Results of CRS oedometer tests on vertically and horizontally oriented specimens from point A at the Partille test site.

Specimens from four levels at point A at the Partille test site were tested. The water contents in these samples appeared to have diminished slightly during these eight years. To verify the relevance of the results, vertically as well as horizontally oriented specimens were trimmed out and tested. The results of these new CRS oedometer tests as well as earlier CRS oedometer tests are shown in Figure 6-4. It can be seen that the new CRS oedometer tests on vertically oriented 40 mm diameter specimens give the same or only slightly lower preconsolidation pressures than the earlier tests. The $K_{0(NC)}$ estimated from the new CRS oedometer tests are about the same as the empirical values. The empirical values of $K_{0(NC)}$ at a depth of between 3 and 19 m are mainly between 0.58 and 0.71 and the $K_{0(NC)}$ estimated from the new CRS oedometer tests are between 0.68 and 0.74.

6.2.2 Undrained shear strength based on vane model tests

The undrained shear strength at point D, above the crest, calculated using the old relationships based on normally consolidated or slightly overconsolidated soil from the field vane tests and corrected with regard to

the liquid limit can be described as 14 kPa down to level +13.5 and thereunder increasing by 1.3 kPa/m, Figure 6-5.

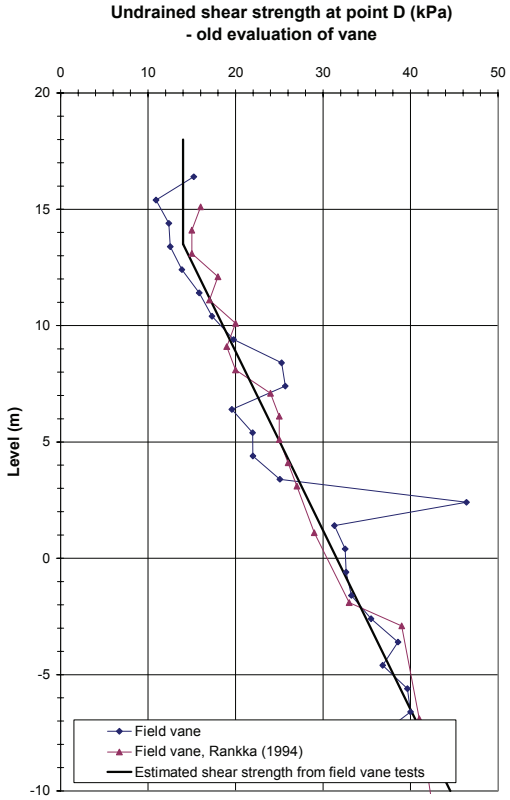

Figure 6-5: Undrained shear strength above the crest from the field vane test.

This estimated undrained shear strength has been normalised against the weighted preconsolidation pressure and plotted against the weighted OCR, see Figure 6-7. The weighted preconsolidation pressure is defined as:

$$\sigma'_{c-weighted} = \frac{\sigma'_{cv} + 6\sigma'_{ch}}{7} \tag{6-2}$$

The normalised undrained shear strength decreases slightly with depth, see Figure 6-6. Ideally, the undrained shear strength should be governed directly by the weighted preconsolidation pressures and the weighted OCR and the value of the normalised undrained shear strength should be the same at each level. The reason for the discrepancy could be that the undrained shear strength calculated from the field vane test does not increase as much with depth as it ought to. This is indicated by the estimation of the undrained shear strength based on the gathered field and laboratory tests together with empiricism, which results in a slightly higher increase in the undrained shear strength with depth compared to that measured by the field vane (see Section 4.2.4).

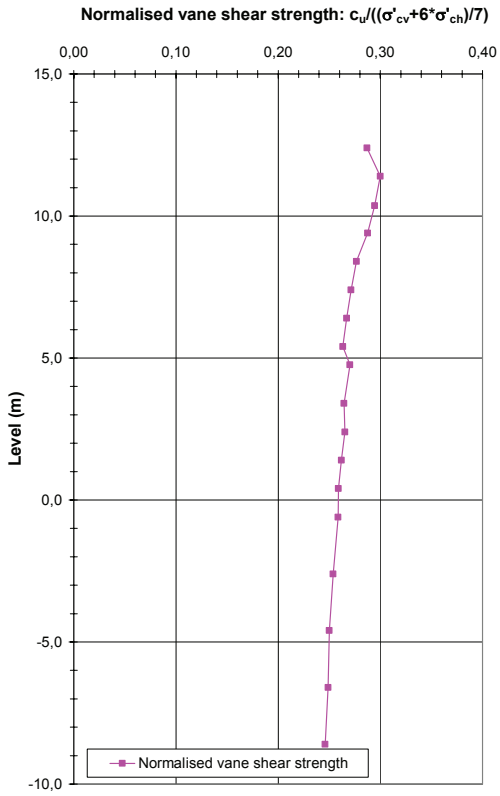

Figure 6-6 Normalised vane shear strength from the field vane test above the crest.

For comparison, the undrained shear strength was also calculated from the field vane test results at point D without the correction for the liquid limit. However, this resulted in a larger decrease with depth of the normalised undrained shear strength.

The regression line calibrated for the mean normalised undrained shear strength is shown in Figure 6-7. In the analysis, both the mean value of all values of the normalised undrained shear strength between level +13.5 and -8.5 and the mean values of smaller groups of separate values, i.e. the mean values of separate values from levels with nearly the same normalised undrained shear strength between level +13.5 and -8.5 grouped together separately, have been used to calibrate the model vane regression line to the field data.

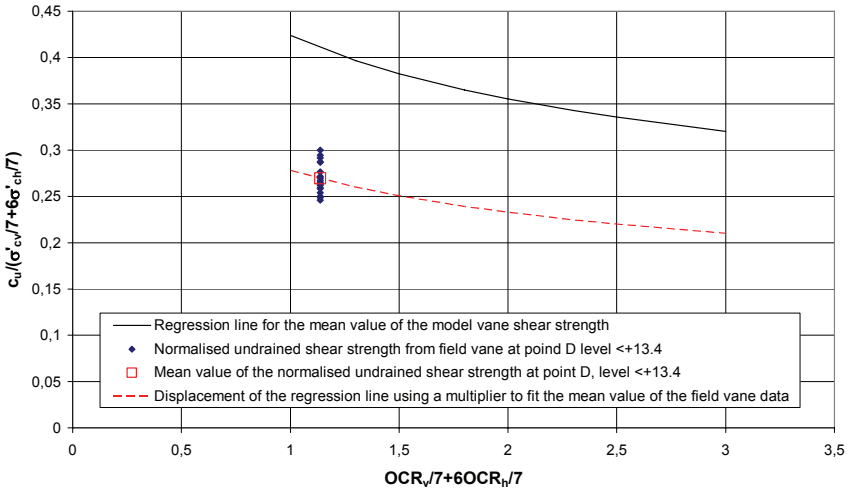

Figure 6-7: Displacement of the model vane regression line to fit the normalised field vane shear strength.

The undrained shear strength at the toe of the slope, point A, calculated using the undrained shear strength at point D together with the parallel displaced model vane regression line based on mean values and the weighted preconsolidation pressures and overconsolidation ratios at point A is presented in Figure 6-8. The use of the mean values of smaller groups of separate values instead of the mean value of all values of the normalised undrained shear strength gives a slightly more varied curve and slightly higher values in the upper part of the soil profile. Variations in the horizontal stresses have a minor influence on the calculated undrained shear strength. The horizontal preconsolidation pressures have a greater influence. As estimation of horizontal preconsolidation pressures has so far been limited to the use of empiricism together with vertical preconsolidation pressures based on CRS test results, some CRS oedometer tests on horizontally oriented specimens were carried out to verify the empirical values, see Section 6.2.1 above.

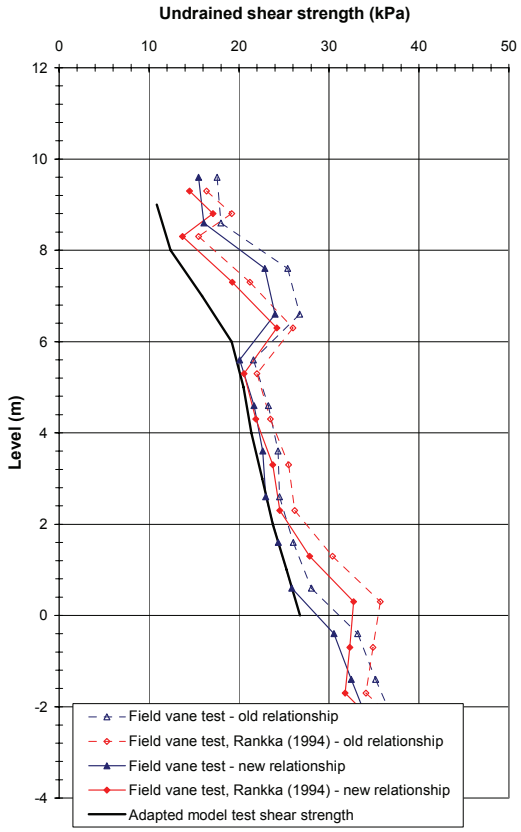

Figure 6-8: Undrained shear strength calculated from the model vane test results compared with calculated field vane test results.

In Figure 6-8 the undrained shear strength calculated from the adapted model test results is compared with the undrained shear strength calculated with the old relationships, which are based on normally consolidated and slightly overconsolidated soils (Larsson et. al., 1984) and the undrained shear strength calculated using the new relationships, which have an extra correction for overconsolidation (Larsson & Åhnberg, 2003). It can be seen that the undrained shear strength calculated from the adapted model test results corresponds rather well with the new relationship, except for the upper 3 m of the soil profile where the adapted model test results are lower. This indicates that there is a need for an extra correction of the field vane test results for overconsolidation. It also indicates that even though the field vane test results are mainly governed by the horizontal preconsolidation pressure a correction based on vertical preconsolidation pressures also gives quite good correspondence with the adapted model test results.

Estimation of the undrained shear strength from the adapted model test results and based on vertical preconsolidation pressures from the old CRS oedometer tests and horizontal preconsolidation pressures from the new CRS oedometer tests gave almost the same value for the undrained shear

strength. However, for levels between +4 and +7 in the upper part of the soil profile the values of the undrained shear strength were 1 – 2 kPa lower.

6.2.3 Undrained shear strength based on piezocone model tests

The undrained shear strength at point D, above the crest, calculated using the old relationships from the piezocone test and corrected with regard to the liquid limit can be described as 11 kPa at level +15 and thereunder increasing by 1.2 kPa/m.

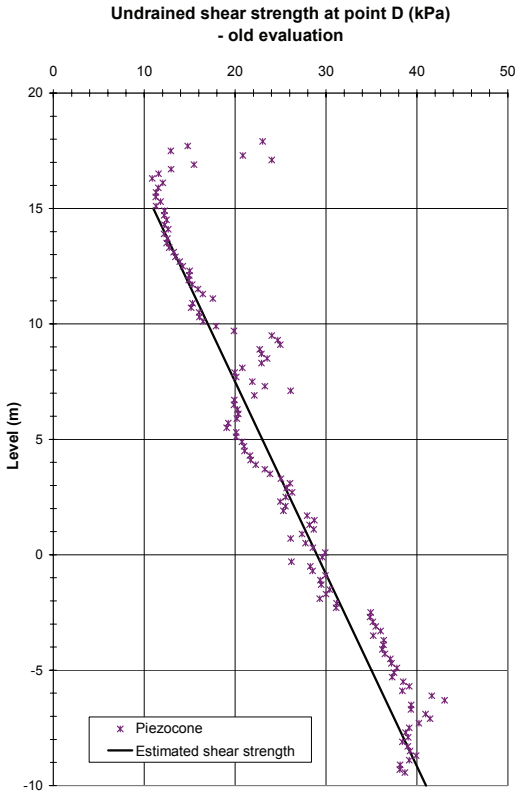

Figure 6-9: Undrained shear strength above the crest from the piezocone test.

This estimated undrained shear strength has been multiplied by the cone factor (N_{kT}) and then normalised against the horizontal preconsolidation pressure and plotted against the horizontal OCR, see Figure 6-11. The cone factor has been assumed to be $N_{kT} = 17$ as a mean value of the model tests (see Section 5.4.8). The normalised net tip resistance obtained decreases slightly with depth, see Figure 6-10. Ideally, if the net tip resistance is governed directly by the horizontal preconsolidation pressures and the horizontal OCR, the value of the normalised net tip resistance should be the same at each level. The reason for the discrepancy could be that the undrained shear strength calculated from the piezocone test does not increase quite as much with depth as it ought to (similar to the results from the field vane test). This is also indicated by the estimation of the undrained

shear strength based on both field and laboratory tests together with empiricism, which results in a slightly higher estimated increase of the undrained shear strength with depth (see Section 4.2.4).

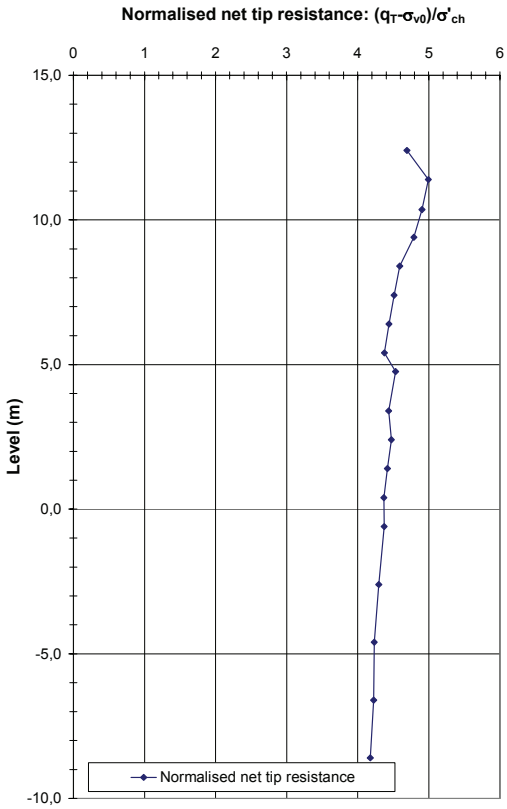

Figure 6-10 Normalised net tip resistance from piezocone test above the crest.

The regression line calibrated for the mean normalised net tip resistance is shown in Figure 6-11. In the analysis, the same procedure as for the vane model tests was used to calibrate the model piezocone regression line to the field data, i.e. both the mean value of all values of the normalised undrained shear strength between level +13.5 and -8.5 and the mean value of smaller groups of separate values.

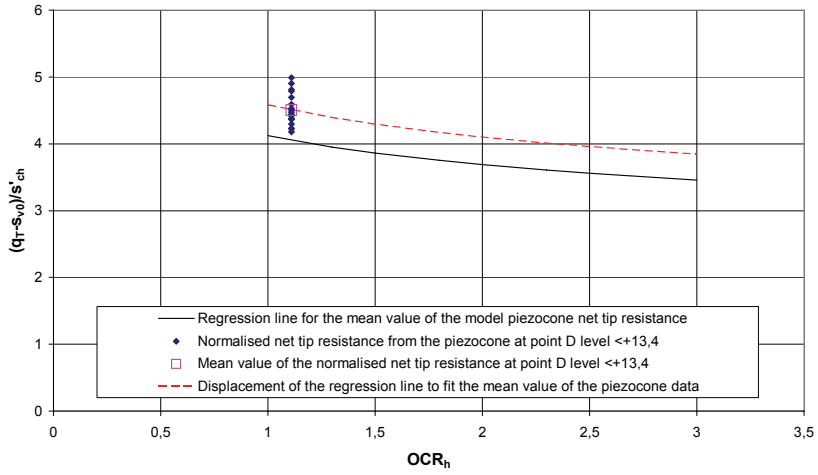

Figure 6-11: Displacement of the model piezocone regression line to fit the normalised piezocone net tip resistance.

The undrained shear strength at the toe of the slope, point A, was calculated using the undrained shear strength at point D together with the displaced model piezocone regression line for the net tip resistance based on mean values and the horizontal preconsolidation pressures and overconsolidation ratios at point A. Once again, the cone factor of N_{kT} = 17 was used, this time to translate the net tip resistance to an undrained shear strength. The calculated undrained shear strength is presented in Figure 6-12. As for the field vane test, the horizontal preconsolidation pressures have an obvious influence on the calculated data. The use of the mean values of smaller groups of separate values instead of the mean value of all values produces hardly any difference in the calculated undrained shear strength.

As for the vane tests, estimation of horizontal preconsolidation pressures have been based on empiricism and vertical preconsolidation pressures from CRS oedometer results together with some CRS oedometer tests on horizontally oriented specimens, see Section 6.2.2 above.

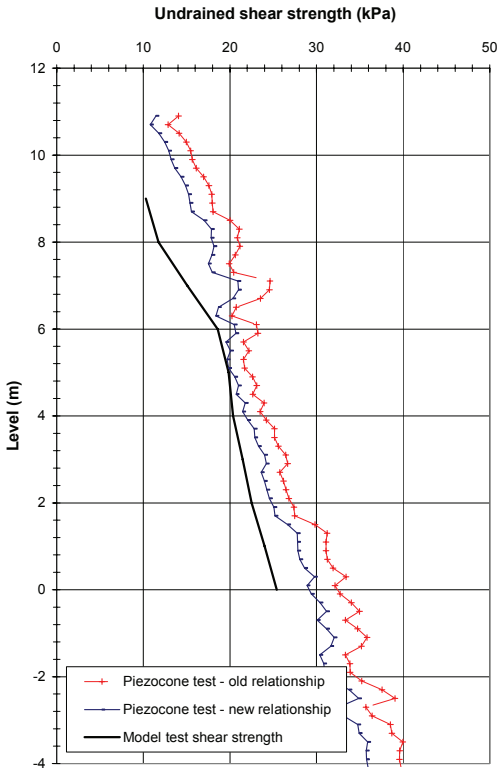

Figure 6-12: Undrained shear strength calculated from the model piezocone test results compared with calculated field piezocone test results.

In Figure 6-12 the undrained shear strength calculated from the model tests is compared with the undrained shear strength calculated from the field tests with the old relationships, which are based on normally consolidated and slightly overconsolidated soils (Larsson et. al., 1984) and the undrained shear strength calculated with the new relationships, which have an extra correction for overconsolidation (Larsson & Åhnberg, 2003). It can be seen that the undrained shear strength calculated from the model tests is also lower than the undrained shear strength based on the new relationship, especially in the upper part of the soil profile. It is considerably lower than that based on the old relationship. Estimation of the undrained shear strength from the adapted model test results and based on vertical preconsolidation pressures from the CRS oedometer tests and horizontal preconsolidation pressures from the new CRS oedometer tests produced almost the same values. However, between levels +5 and +7 m in the upper part of the soil profile the values of the undrained shear strength were 1 – 2 kPa lower.

That the undrained shear strength calculated from the model tests is considerably lower than the undrained shear strength based on the old relationship indicates that there is a need for an extra correction of the

piezocone test for overconsolidation. The fact that it is also lower than the undrained shear strength based on the new relationship indicates that this correction should possibly be even greater than that in the new relationship. However, it should be borne in mind that the piezocone model test data show quite a large scatter and consequently have a very low significance. This conclusion is therefore only tentative.

6.3 The Slumpån test site at Lilla Edet

6.3.1 Stress conditions

At the Slumpån test site the vertical preconsolidation pressure at point C, above the crest of the slope ($\sigma'_{cv\text{-}crest}$) (Section 4.3.2, Figure 4-15) was estimated from CRS oedometer tests (Section 4.3.3) to $1.3 \cdot \sigma'_{v0}$ above the sand/silt layer and $1.2 \cdot \sigma'_{v0}$ below the sand/silt layer. The horizontal preconsolidation pressure was estimated from $\sigma'_{cv\text{-}crest}$ and K_{0NC} as described in Section 6.1 above. The horizontal effective stress at point C, horizontal ground, was estimated using the effective vertical stress at point C and K_{0rb} from the empirical equation (Schmidt, 1967):

$$K_{0rb} = K_{0NC} \cdot OCR_v^{\sin 1.2 \cdot \phi'} \qquad (6\text{-}3)$$

For $\phi' = 30^o$ and $OCR_v = 1.3$ this gives a horizontal overconsolidation ratio, $OCR_h = 1.11$ and a weighted overconsolidation ratio, $OCR_{weighted} = 1.14$ above the sand/silt layer at point C. For $\phi' = 30^o$ and $OCR_v = 1.2$ below the sand/silt layer the corresponding horizontal overconsolidation ratio is $OCR_h = 1.08$ and the weighted overconsolidation ratio, $OCR_{weighted} = 1.10$

At the toe of the slope, point A, the vertical preconsolidation pressures have been estimated from CRS oedometer test results ($\sigma'_{cv\text{-}toe}$) (Section 4.3.3). The horizontal preconsolidation pressure has been estimated from $\sigma'_{cv\text{-}toe}$ and K_{0NC} or from CRS oedometer tests on horizontally oriented specimens as described in Section 6.1 above. The effective horizontal stresses at point A have been estimated based on dilatometer tests and empiricism combined with a statement by Rankka (1994), see Section 6.2.1 above, and the assumption of a ground level at deposition as at point C, a groundwater level at the ground surface and K_{0NC} estimated from Equation 5-2.

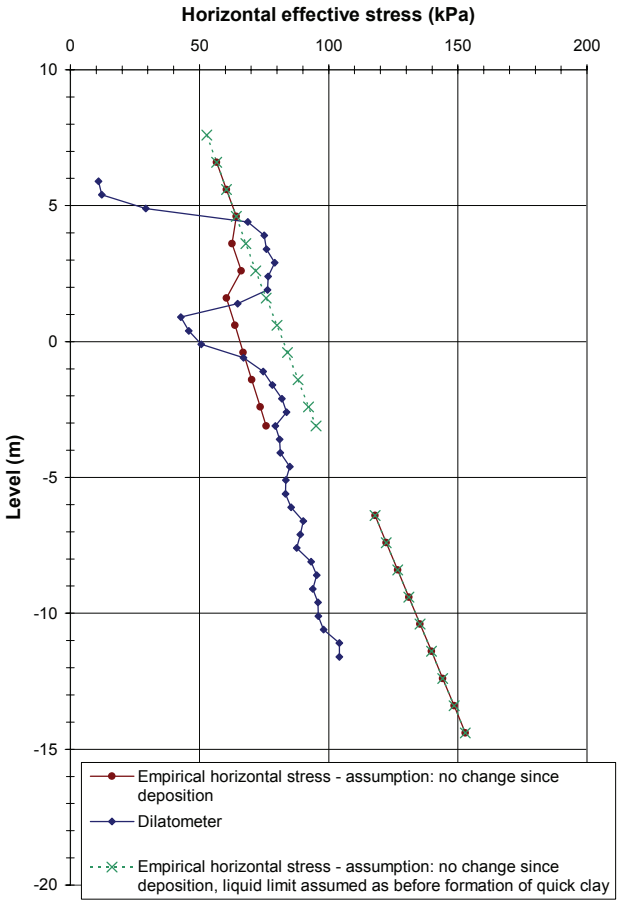

Figure 6-13 Horizontal effective stresses at the toe of the slope (point A).

To be able to carry out the CRS oedometer tests on horizontally oriented specimens, new samples from five levels at point A were taken at the Slumpån test site. To obtain reliable results both vertically and horizontally oriented specimens were trimmed out and tested at each level. The results of these new CRS oedometer tests as well as earlier CRS oedometer tests are shown in Figure 6-14. Although the results from the tests on vertical specimens show some scatter, they are close to the results from the earlier tests. The $K_{0(NC)}$ estimated from the new CRS oedometer tests are about the same as the empirical values. $K_{0(NC)}$ values from the results of the CRS oedometer tests are between 0.62 and 0.75 (depth of 8 to 14 m). The empirical values of $K_{0(NC)}$ at the corresponding levels are between 0.61 and 0.70.

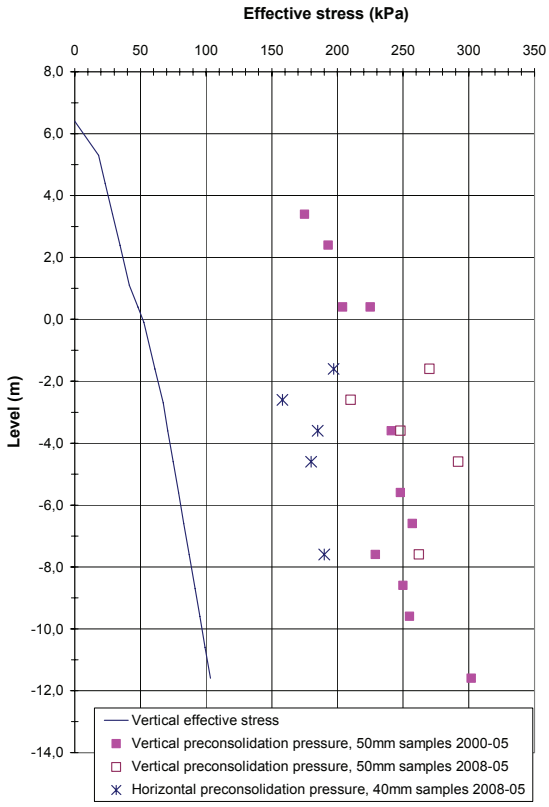

Figure 6-14 Results of CRS oedometer tests on vertically and horizontally oriented specimens from point A at the Slumpån test site.

6.3.2 Undrained shear strength based on vane model tests

The undrained shear strength at point C, above the crest, calculated using the old relationships based on normally consolidated or slightly overconsolidated soil from the field vane tests and corrected with regard to the liquid limit can be described as 15 kPa at level +19 and thereunder increasing by 0.67 kPa/m to 19 kPa at level +13 and then increasing by 2.21 kPa/m, Figure 6-15. The low, undrained shear strength directly beneath the sand layer (below level -5) is probably related to the limitations of the method or equipment as discussed in Section 4.3.4.

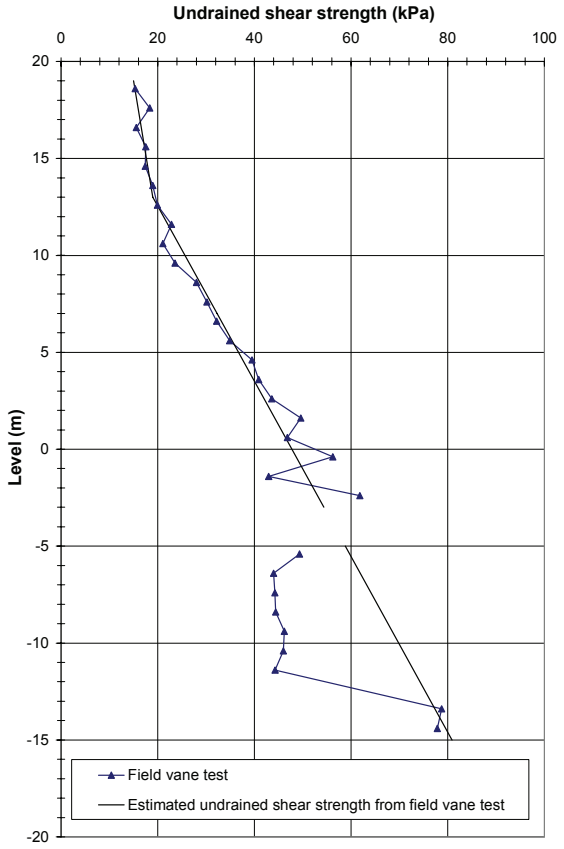

Figure 6-15 Undrained shear strength above the crest from field vane test.

This estimated undrained shear strength has been normalised against the weighted preconsolidation pressure and plotted against the weighted OCR, (Equation 6-2) and is presented in Figure 6-17.

The normalised undrained shear strength decreases slightly with depth and there is a larger decrease from above the sand/silt layer to below it, see Figure 6-16. Ideally, the undrained shear strength should be governed directly by the weighted preconsolidation pressures and the weighted OCR and the value of the normalised undrained shear strength should be the same at each level. The reason for these discrepancies could be that the undrained shear strength calculated from the field vane test does not increase as much with depth as it ought to and that the increase should be different above and below the sand layer.

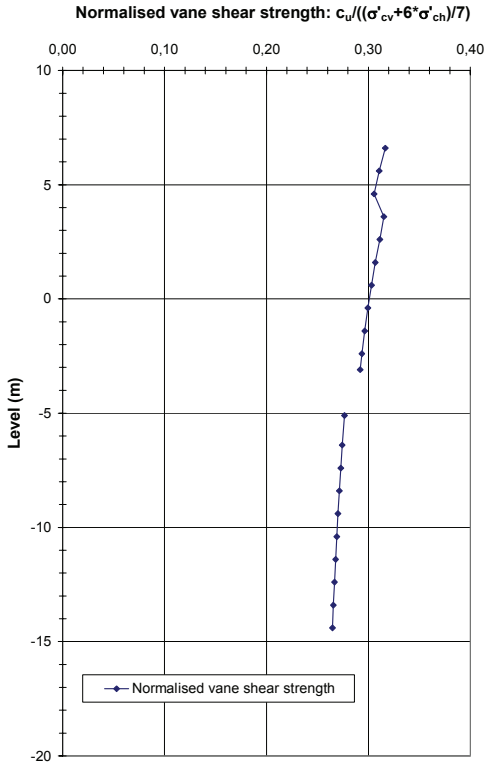

Figure 6-16 Normalised vane shear strength for field vane test above the crest.

The regression line calibrated for the mean normalised undrained shear strength is shown in Figure 6-17. In the analysis, the mean value of all values of the normalised undrained shear strength above the sand layer and below the sand layer has been used to calibrate the model vane regression line to the field data.

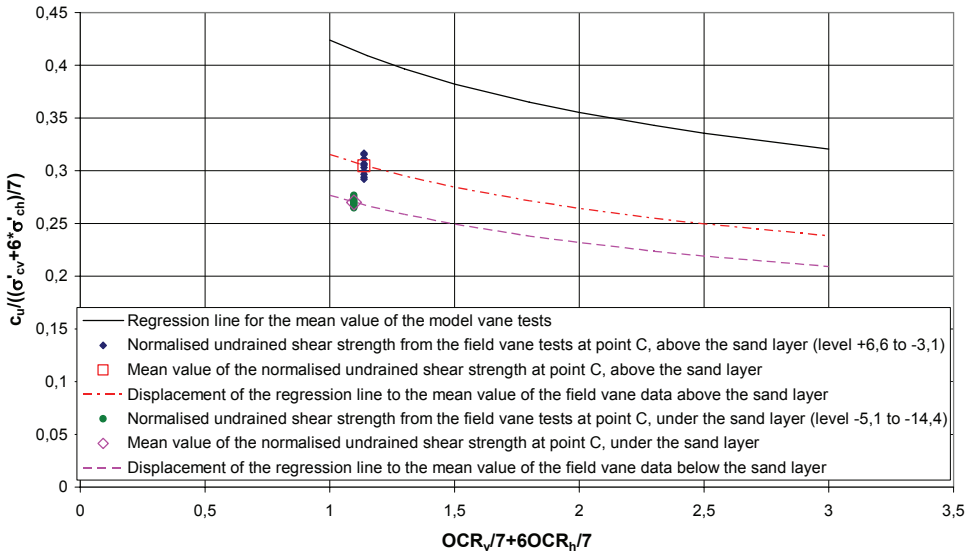

Figure 6-17 Displacement of the model vane regression line to fit the normalised field vane shear strength.

The undrained shear strength at the toe of the slope, point A, calculated using the undrained shear strength at point C together with the displaced model vane regression lines based on mean values above and below the sand/silt layer and the weighted preconsolidation pressures and overconsolidation ratios at point A is presented in Figure 6-18. The undrained shear strength calculated from the adapted model test results is compared with the undrained shear strength calculated using the old relationships based on normally consolidated and slightly overconsolidated soils (Larsson et. al., 1984) and the undrained shear strength calculated using the new relationships that have an extra correction for overconsolidation (Larsson & Åhnberg, 2003). Above the sand layer the undrained shear strength from the adapted model test results are lower than the undrained shear strength based on the relationship with a correction for overconsolidation. Below the sand layer, the undrained shear strength calculated from the adapted model test results corresponds quite well with the relationship that has a correction for overconsolidation. Compared to the undrained shear strength calculated using the old relationship based on normally and slightly overconsolidated soil the undrained shear strength from the adapted model test results are considerably lower. Using the same vertical preconsolidation pressures, but the horizontal preconsolidation pressures from the CRS oedometer tests (see Section 6.3.1) gives 2 to 3 kPa higher undrained shear strength from level -2 to -9, increasing with depth. The results are still lower than the undrained shear strength based on the old relationships.

Thus, in correspondence with the Partille test site, these results also imply a need for an extra correction of the field vane test results for overconsolidation. Furthermore, it implies that a correction based on vertical preconsolidation pressures gives quite good correspondence with the adapted model test results, even though the field vane test results are governed mainly by the horizontal preconsolidation pressure.

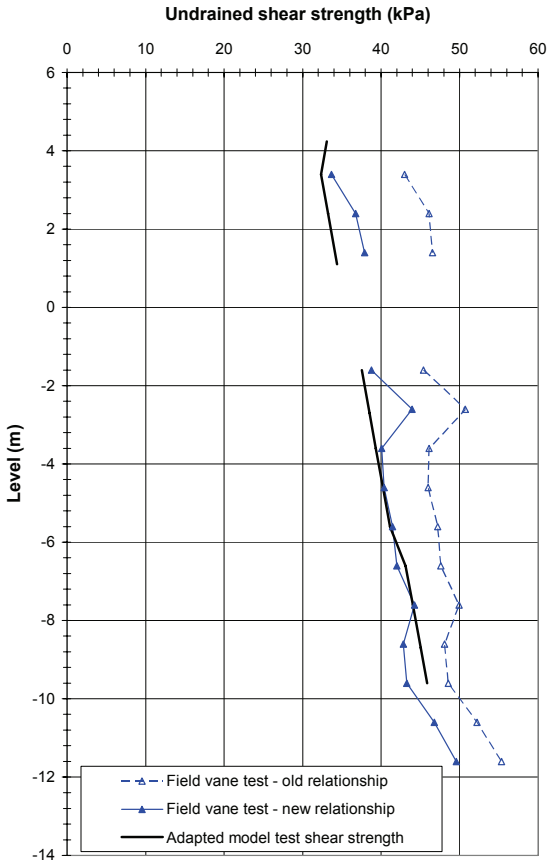

Figure 6-18 Undrained shear strength calculated from the model vane test results compared with calculated field vane test results.

6.3.3 Undrained shear strength based on piezocone model tests

The undrained shear strength at point C, above the crest, calculated using the old relationships from the piezocone test and corrected with regard to the liquid limit can be described as 14 kPa at level +20 and thereunder increasing by 0.88 kPa/m to 21 kPa at level +12 and then increasing by 2.07 kPa/m, see Figure 6-19.

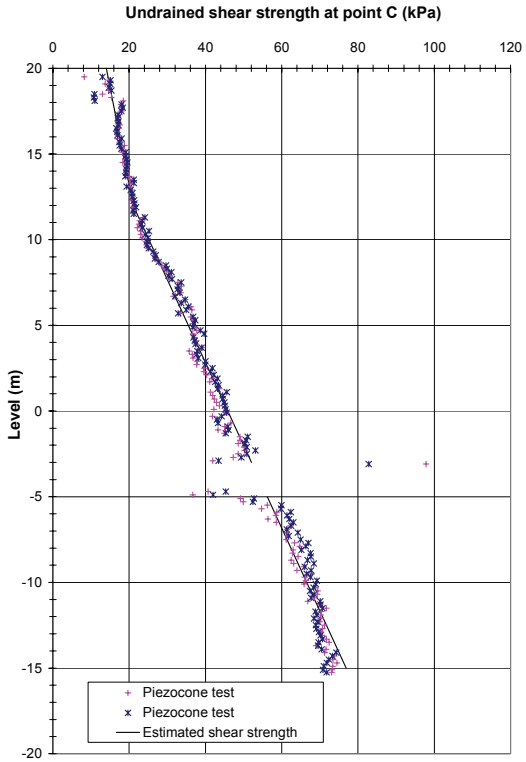

Figure 6-19: Undrained shear strength above the crest from piezocone test.

This estimated undrained shear strength has been multiplied by the cone factor (N_{kT}) and then normalised against the horizontal preconsolidation pressure and plotted against the horizontal OCR, see Figure 6-21. The cone factor has been assumed as $N_{kT} = 17$ as a mean value of the model tests (see Section 5.4.8). The normalised net tip resistance obtained decreases slightly with depth and as for the normalised vane shear strength, there is a slightly larger decrease from above to below the sand/silt layer, see Figure 6-20. Ideally, if the net tip resistance were governed directly by the horizontal preconsolidation pressures and the horizontal OCR, the value of the normalised net tip resistance should be the same at each level. The reason for this discrepancy could be that the undrained shear strength calculated from the piezocone test does not increase quite as much with depth as it ought to and that the increase should be different above and below the sand layer (similar to the results from the field vane test).

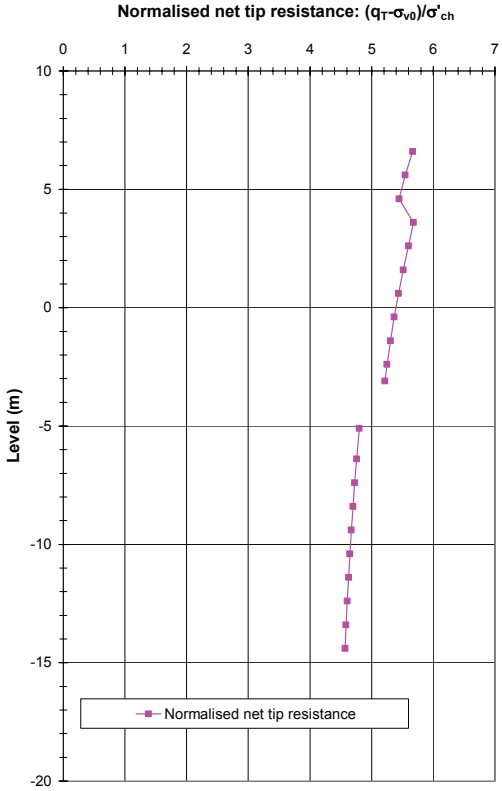

Figure 6-20 Normalised piezocone shear strength from the piezocone test above the crest.

The regression line calibrated for the mean normalised net tip resistance is shown in Figure 6-21. In the analysis, the mean value of all values of the normalised undrained shear strength above the sand/silt layer and below the sand/silt layer have been used to calibrate the model piezocone regression line to the field data.

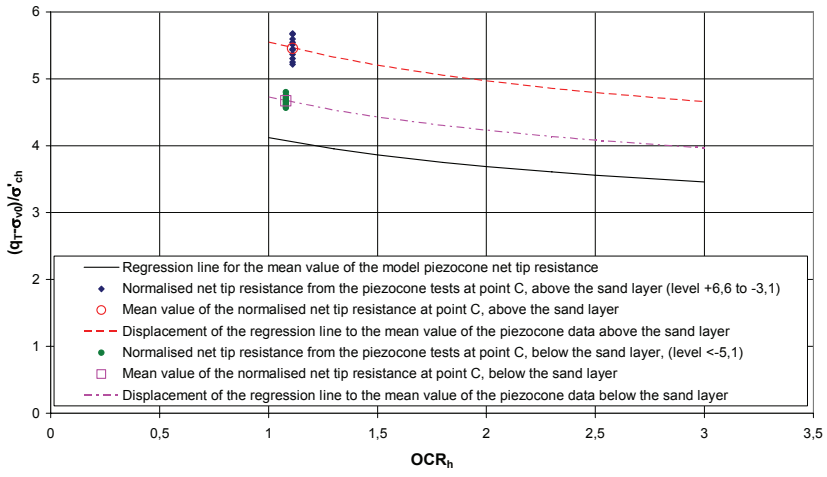

Figure 6-21 Displacement of the model piezocone regression line to fit the normalised piezocone net tip resistance.

The undrained shear strength at the toe of the slope, point A, has been calculated using the undrained shear strength at point C together with the displaced model piezocone regression line for the net tip resistance based on mean values above and below the sand/silt layer and the horizontal preconsolidation pressures and overconsolidation ratios at point A. To translate the net tip resistance to an undrained shear strength, the cone factor $N_{kT} = 17$ was again used.

In Figure 6-22 a comparison is made between the undrained shear strength calculated from the model tests, the undrained shear strength calculated from the field tests with the old relationships based on normally consolidated and slightly overconsolidated soils (Larsson et. al., 1984) and the undrained shear strength calculated using the new relationships, which have an extra correction for overconsolidation (Larsson & Åhnberg, 2003). Above the sand/silt layer, the undrained shear strength calculated from the model tests is about the same as the undrained shear strength based on the relationship that has a correction for overconsolidation. Below the sand/silt layer the undrained shear strength calculated from the model tests is lower than this relationship. It is considerably lower than the undrained shear strength based on the old relationship both above and below the sand/silt layer. Using the same vertical preconsolidation pressure but the horizontal preconsolidation pressure from the CRS oedometer tests gives 2 to 4 kPa higher undrained shear strength between level -2 to -9, increasing with depth. This gives about the same values of the undrained shear strength as the lowest values of the piezocone tests (piezocone test A2) calculated with the relationship with a correction for overconsolidation.

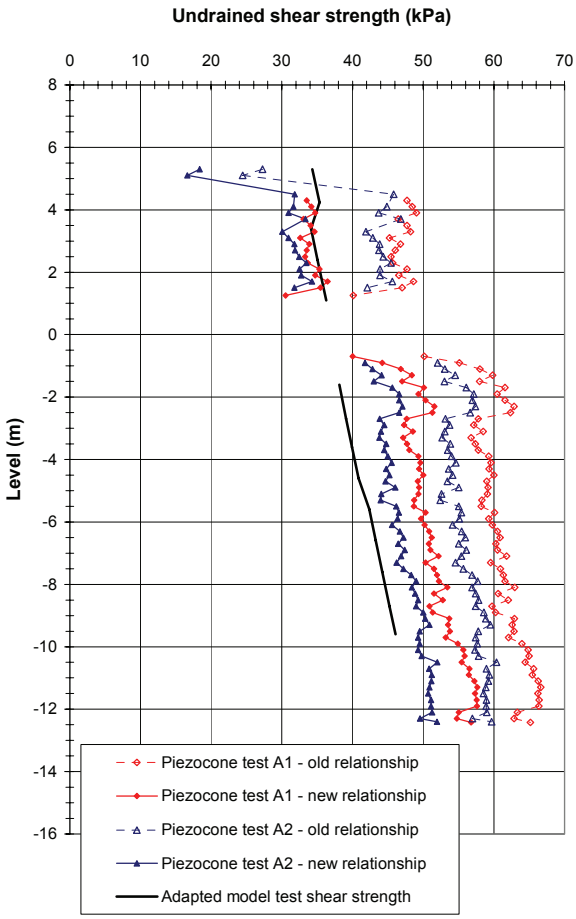

Figure 6-22 Undrained shear strength calculated from the model piezocone test results compared with calculated field piezocone test results.

In correspondence with the results from the Partille test site, the results imply a need for an extra correction of the piezocone test for overconsolidation. Possibly this correction should be even greater than that in the new relationship. However, there is quite a large scatter in the piezocone model test data and consequently the relationships have a very low significance. In addition, the use of results from a few CRS oedometer results on horizontally oriented specimens from the toe of the slope reveals the importance of the horizontal preconsolidation pressures in the evaluation. More CRS oedometer tests on horizontal specimens, both above the crest and at the toe of the slope, would give a better estimate of the undrained shear strength from the model test results. This conclusion is therefore only tentative.

7. DISCUSSION, CONCLUSIONS AND FUTURE RESEARCH

7.1 Influence of stress conditions

The stress conditions in an aged or overconsolidated soil are in every direction composed of both the preconsolidation pressures (the largest effective stresses the soil has been subjected to and possibly some extra consolidation due to ageing or creep effects) and the effective stresses acting today in the direction in question. Both types of stresses and the relationship between them are important to the value of the undrained shear strength of soils. According to the hypothesis of this study, the horizontal effective stresses have a greater influence on the field vane and piezocone test results than the vertical stresses. During and after unloading, the horizontal effective stresses do not decrease as much as the vertical effective stresses. Thus, unloading of the soil should result in a smaller reduction in the undrained shear strength measured using these tests than when using, for example, the direct simple shear test, at least for the vane strength and most likely also for the piezocone strength.

7.1.1 Influence of stress conditions on the vane test results

One purpose of the analysis was to try to evaluate which stress had the main influence on the vane shear test results. Therefore, the results were normalised against the horizontal preconsolidation pressure, the vertical preconsolidation pressure and a weighted preconsolidation pressure: 1/7 of the vertical preconsolidation pressure and 6/7 of the horizontal preconsolidation pressure. The weighted pressure is believed to best reflect the influence of horizontal and vertical preconsolidation pressure on the undrained shear strength determined by the vane shear test (Bjerrum, 1973).

Another purpose of the analysis was to study the possible effect of the overconsolidation ratio in various directions (and consequently also the influence of the consolidation stresses in these directions). The normalised shear strength was therefore plotted against the horizontal, vertical or weighted OCRs. A relationship for the data was drawn in each diagram. The relationships were compared with the empirical equation that directly or indirectly describes how the undrained shear strength varies with preconsolidation pressure and overconsolidation ratio (Equation 5-7, Section 5.4.2). The empirical values of 0.22 for the *a*-factor for direct simple shear and 0.8 for the *b*-factor were applied.

The results from the analysis of the vane data indicate that there is a major influence of the horizontal preconsolidation pressure and the OCR in the horizontal direction on the vane test results. However, the amount of data is limited and a considerable scatter in the data can be observed. The relationship for the vane test data cannot be considered quite significant, which is why this conclusion is tentative.

Regardless of whether the data is normalised against the vertical, horizontal or weighted preconsolidation pressure and plotted against the vertical, horizontal or weighted OCR, the results from the model tests do not decrease quite as much with OCR as the empirical equation, which is based on direct simple shear tests. This indicates that unloading, i.e. a decrease in the vertical effective stresses, has a greater influence on the direct simple shear test results compared to the vane test results and that the calculation of the results from the vane test should be dependent on the OCR.

7.1.2 Influence of stress conditions on the piezocone test results

The scatter of the data from the piezocone tests is greater than for the vane tests. As a result, the significance of the relationships is considerably lower than for the vane tests. The significance is actually very low for all the piezocone plots. There is no great difference whether the net cone resistance is normalized against the horizontal, vertical or mean preconsolidation pressure. Therefore, based on the results from this study alone it is not possible to ascertain whether it is the horizontal, the vertical or the mean preconsolidation pressure that has the greatest influence on the net cone resistance.

However, it may be possible to estimate the influence of the horizontal or the vertical preconsolidation pressure using empirical data from earlier studies by combining the empirical equation for estimation of K_{0NC} for Scandinavian inorganic clays (Equation 5-2, Larsson, 1977) and the empirical equation for the correlation between the net cone resistance and the preconsolidation pressure in Scandinavian clays (Equation 5-13, Larsson and Mulabdic', 1991). It can then clearly be seen that there is hardly any change in the net cone resistance normalised against the horizontal preconsolidation pressure with the liquid limit, whereas the net cone resistance normalised against the vertical preconsolidation pressure is a clear function of the liquid limit. This indicates that the net cone resistance is primarily dependent on the horizontal preconsolidation pressure and appears to be more or less a direct function of this.

Regardless of whether the data is normalised against the vertical, horizontal or mean preconsolidation pressure and plotted against the vertical, horizontal or mean OCR, the empirical equation based on direct simple shear tests shows a larger decrease with OCR than the results from the piezocone tests. This indicates that unloading has a greater influence on the direct simple shear test results than on the piezocone test results and that the evaluation of the results from the piezocone test should also be dependent on the OCR.

7.2 Practical implications

7.2.1 Undrained shear strength and stability based on empirical relationships for piezocone and field vane test

In Chapter 4, calculations of stability for the slopes at Partille and at Slumpån were carried out using the undrained shear strength at the toe of the slope calculated with the (old) relationships for the piezocone and field vane test without a correction for overconsolidation, which are based on normally consolidated and slightly overconsolidated clays (Larsson et. al., 1984, Larsson and Mulabdic, 1991) and with the (new) relationships which have an extra correction for overconsolidation (Larsson and Åhnberg, 2003). At Partille, estimation of the undrained shear strength from all field and laboratory tests together with the empirical relationship and using the relationships for the piezocone and field vane tests without correction for OCR shows only marginal difference compared with the use of all data using the relationships with a correction for OCR (1 kPa higher). At Slumpån, the undrained shear strength estimated from all field and laboratory tests together with the empirical relationship and with the relationships for the piezocone and field vane tests without correction for OCR is slightly higher than when using the relationships with a correction for OCR (2 – 5 kPa higher). Without support from the direct simple shear tests the corresponding estimated undrained shear strength in the passive zone at Slumpån is 7 – 12 kPa higher. For both the Partille and the Slumpån slopes using the relationships for the calculation of the undrained shear strength from piezocone and field vane tests with correction for OCR only had a minor effect on the calculated factors of safety (<5% lower with the new relationships) compared to the relationships without correction for OCR. Calculating the stability at Slumpån using the estimated undrained shear strength with the old relationships without support from the direct simple shear tests gave a 8 – 10% higher factor of safety.

This indicates that for these types of slopes, with slightly overconsolidated clay behind the crest and overconsolidated clay at the toe of the slope, using the new corrections for overconsolidation when calculating the undrained shear strength from the piezocone and field vane test has a certain but limited influence on the calculated factor of safety of the slope.

7.2.2 Undrained shear strength in the *in situ* slopes based on the model tests

The undrained shear strength calculated from the field vane tests and the piezocone tests at the toe of the test site slopes were also predicted based on the results of the model tests and the stress conditions in the slopes. The field tests performed far behind the crest of the slope were used as references as they correspond to almost horizontal ground conditions.

The undrained shear strength at the toe of the slopes calculated from the adapted model test results is compared with the undrained shear strength calculated with the relationships without correction for overconsolidation, which are based on normally consolidated and slightly overconsolidated soils and the undrained shear strength calculated with the relationships that have an extra correction for overconsolidation. This calculation was done for both the field vane tests and the piezocone tests.

For the Partille test site, the undrained shear strength calculated from the adapted model test results for the field vane test corresponds quite well with the new relationship with a correction for overconsolidation, except for the upper 3 m of the soil profile where the adapted model test results are lower. For the Slumpån test site the undrained shear strength from the adapted model test results are lower than the undrained shear strength based on the new relationship above the sand layer. Below the sand layer, the undrained shear strength calculated from the adapted model test results corresponds quite well with the relationship that has a correction for overconsolidation.

This indicates that there is a need for an extra correction of the field vane test results for overconsolidation. It also indicates that even though the field vane test result is mainly governed by the horizontal preconsolidation pressure a correction based on vertical preconsolidation pressures also gives fairly good correspondence with the adapted model test results.

For the piezocone test at the Partille test site, it can be seen that the undrained shear strength calculated from the model tests is lower than the

undrained shear strength based on the relationship that has a correction for OCR, especially in the upper part of the soil profile. It is considerably lower than that based on the relationship without a correction for OCR. At the Slumpån test site the undrained shear strength calculated from the model tests is in the lower range of the undrained shear strength from the piezocone tests based on the relationship which has a correction for overconsolidation.

This indicates that there is also a need for an extra correction of the piezocone test results for overconsolidation. That the estimated strength also is lower than the undrained shear strength based on the relationship that has a correction for OCR indicates that this correction could possibly be even greater than that in the current correction for OCR. However, it should be borne in mind that the piezocone model test data show a large scatter and consequently have a very low significance. This conclusion is therefore only tentative.

7.3 Possible reasons for discrepancies in the model test results

The samples taken in the Partille slope for the model tests were taken from a depth of 2 to 6 m in the upper part of the soil profile under the dry crust at point A. Routine analyses on ordinary 50 mm samples from these depths show variations in bulk density from 1.55 to 1.69 t/m^3, variations in water content from 63 to 74% and variations in liquid limit from 55 to 68%, which can be considered as fairly large for clays in the western part of Sweden.

The best would have been if routine analyses had been done on clay from each large sample to be used for the model tests. In that way the variations in the properties of the soil to be used in the tests would have been documented. As in principle the whole large sample was used in the test this was not possible and even if it had been possible, this would not have covered variations within each sample. The routine analyses of clay taken after the tests from the specimens used in the model tests also showed quite a large scatter in all determined properties, i.e. bulk density, water content, liquid limit and shear strength from fall cone tests. However, these properties should differ from the original and among themselves as the samples are consolidated to two different stress levels and thereafter unloaded to various K_0-conditions. So, this is not a very representative

indication. It can be assessed that the tested material, although relatively homogeneous, was not quite ideal.

It was observed that the shear strength for two of the results from direct simple shear tests on specimens used in the model tests show the same tendency as the corresponding results from the piezocone test in the same specimen (one rather high and one too low). This indicates that the shear strength of these two specimens was too high and too low respectively. Consequently, part of the scatter in the results is in no doubt caused by differences in the properties of the specimens.

The coefficient of variation for both the shear strength and the normalised shear strength calculated from the vane and the piezocone model tests for the data with OCR in the same range are between 0.15 and 0.25. The undrained shear strength of the clays in the western part of Sweden normally show a coefficient of variation of 0.1 to 0.15, which is lower than the coefficient of variation for the test results in this study. The scatter cannot be explained only by variations in the natural properties even if this could be a part of the explanation.

According to the manufacturer of the piezocone, the accuracy of the data from the mini-piezocone is, in general, considerably less than of those from larger probes. This is due to the miniature sensors, being less stable than larger ones. In addition, it was not possible to calibrate the cone for the required tip resistance of 2 MPa obtaining the desired output voltage of 2000 mV without an unacceptable signal-to-noise ratio. The cone was calibrated for a tip resistance of 20 MPa and the noise was reduced by filtering. This resulted in a lesser accuracy than what was actually desired.

7.4 Experiences from construction of the equipment

The main, but not very surprising experience from construction of the equipment, both the sampler, the triaxial cells and the mini-vane is that it is not possible to arrive at properly functioning equipment at the first design and construction. There is always some part of the construction that does not work as intended and some aspect that has been overlooked in the design. Using newly designed and built equipment over a longer period, as between 2002 and 2005 for the model tests, provides opportunities for small, continuous improvements over time.

7.5 Experiences from consolidation of specimens

Comparisons between the compiled consolidation curves of the specimens for the fourth load step, the analytical solution for radial drainage and the results of finite element analyses show that the shape of the consolidation curves is close to the calculated curves for the oedometer case. This indicates that the consolidation of the specimens is in accordance with the boundary conditions for the oedometer case ($\Delta\sigma_v$ = constant, $\varepsilon_h = 0$), which in turn indicates that the specimens are consolidated similar to the K_0 – conditions prevailing in the field.

All the degree of consolidation – time factor curves are fairly close to the curves from the finite element calculations with Plaxis and the analytical solution (Silveira, 1953, Mc Kinlay, 1961), indicating that a reasonable estimate of the settlement process for the model test specimens is given using the permeability and modulus from the CRS oedometer tests.

Measurements of swelling during unloading from the final preconsolidation stresses to the final consolidation stresses indicate that there is a relationship between the vertical strain and the combined effective stress changes in all directions. The shape of the curve is comparable with the unloading curve in an oedometer test.

7.6 Experiences from other laboratory tests

7.6.1 Experiences from the direct simple shear tests

Direct simple shear tests on specimens from the Partille test site were carried out to compare the results of the model tests with the equation that describes how the undrained shear strength varies with preconsolidation pressure and overconsolidation ratio (Equation 5-7, e.g. Ladd et. al. 1977). These tests show that regardless of whether the specimens are consolidated to 2.5 times the natural preconsolidation pressure according to the SHANSEP procedure and then unloaded to various OCRs or whether the specimens are consolidated just below the natural preconsolidation pressure and thereafter unloaded, the results are similar and the calculated *a* and *b* factors are close to the empirical values. This indicates that the undrained shear strength for the young clay created by loading the model test specimens above the natural preconsolidation pressure varies with preconsolidation pressure and overconsolidation ratio roughly in the same way as a natural, aged clay.

7.6.2 Experiences from the CRS oedometer tests

As the stress-strain curves from the CRS oedometer tests on clay from the model test specimens were all very flat and did not show the typical distinct bend at the preconsolidation pressure, it was rather difficult to estimate the preconsolidation pressure from these tests. This indicates that the CRS oedometer test may not be the best method to determine the preconsolidation pressure for young clay, or that young clay does not have such pronounced stress-strain behaviour as older clay have.

Preconsolidation pressures determined by CRS oedometer tests on horizontal 40 mm samples at both test sites show good agreement with horizontal preconsolidation pressures estimated empirically using Equation 5-2. This indicates that the empirical equation gives a fairly good estimation of the horizontal preconsolidation pressure.

7.7 Advantages/disadvantages of laboratory versus field studies

This study reveals some advantages and disadvantages when trying to simulate field conditions in the laboratory. As this study focuses on the influence of the stress conditions, the great advantage of laboratory tests is that the stress conditions acting on the clay can be fully controlled. There is thus a possibility to measure directly a response to a combination of applied stresses. On the other hand, the stress conditions acting in the field are somewhat uncertain. Even if the stresses can be controlled in the laboratory it is not certain that these correspond exactly to the stresses acting in the field. In addition, in a triaxial cell it is not possible to simulate different horizontal stresses in different directions as is the case in natural slopes. Another disadvantage is that the homogeneity of the clay plays a greater role when the test equipment is scaled down compared to the field equipment; in this case the standard field vane and the piezocone. In addition, miniature electrical sensors are often less accurate than larger ones. However, trying to study the effect of horizontal stresses on the piezocone and field vane test in the field implies that both the influencing parameters and the responses to these parameters are uncertain. It is the author's belief that this is most often an even greater disadvantage. One problem in this study was that it has been impossible to calculate all the parameters without using empiricism. Doing a similar study in the field would include even more empiricism as evaluation of parameters from the equipment used in the field is largely based on empirical relationships.

7.8 Future research

The study by Larsson and Åhnberg (2003) indicates that there is a need for an extra correction for overconsolidation ratio when calculating the undrained shear strength from field vane and piezocone tests, and the authors propose a correction based on the vertical OCR. This study indicates that the results of field vane and piezocone tests are dependent of the horizontal stresses and the overconsolidation in the horizontal direction. Comparisons of the results from these two studies show that even though the field vane and piezocone test results are mainly governed by the horizontal preconsolidation pressure and overconsolidation, a correction based on vertical preconsolidation pressures and overconsolidation gives fairly good correspondence. Slope stability calculations for the studied test sites show that this correction is of limited importance for the calculated stability of the studied slopes. However, even if slopes with low overconsolidation ratio, such as Partille and Slumpån, are only moderately affected, the calculated stability for slopes with higher overconsolidation ratios will be affected more by a revision of the undrained shear strength. Therefore, a sensitivity analysis for slopes with higher overconsolidation ratios ought to be carried out. In that way the risk that investigated slopes classified as having sufficient factors of safety in fact have too low a factor of safety is eliminated.

REFERENCES

Aas, G. (1965). A study of the effect of vane shape and rate of strain on the measured values of *in situ* shear strength of clay. International conference on soil mechanics and foundation engineering, 6. Proceedings, Vol 1, pp141-145. Toronto.

Aas, G, Lacasse, S, Lunne, T and Høeg, K. (1986). Use of in situ tests for foundation design on clay. ASCE Geotechnical Special Publication 6, pp 1-30. Proceedings of In Situ '86. Blacksburg.

Abu-Farsakh, M, Tumay, M, and Voyiadjis, G. (2003). Numerical parametric study of piezocone penetration test in clays. ASCE International Journal of Geomechanics, Vol 3, No 2, pp 170-181.

Almeida, MSS, and Parry, RHG. (1983). Tests with centrifuge vane and penetrometer in a normal gravity field. Technical Report, SOILS TR 141, Cambridge University.

Almeida, MSS, and Parry, RHG. (1985). Small cone penetrometer tests and piezocone tests in laboratory consolidated clays. Geotechnical Testing Journal, Vol. 8, No 1, pp 14-24.

Anderson, WF, Pyrah, IC and Fryer, SJ. (1991). A clay calibration chamber for testing field devices. Geotechnical Testing Journal, Vol. 14, No 4, pp 440-450.

Baker, S. (2003). Personal communication.

Baligh, MM. (1975). Theory of deep site static cone penetration resistance. Massachusetts Institute of Technology. Civil Engineering Department. Report; R75-56. Cambridge MA.

Bengtsson, P-E. (2007). Personal communication.

Bergdahl, U. (1984). Geotekniska undersökningar i fält. Geotechnical field investigations (In Swedish). Swedish Geotechnical Institute. SGI Information No 2, Linköping.

Bjerrum, L. (1967). Engineering geology of Norwegian normally-consolidated marine clays as related to settlements of buildings. Norwegian Geotechnical Institute. Publication No 71, Oslo.

Bjerrum, L. (1973), Problems of soil mechanics and construction on soft clays and structurally unstable soils (collapsible expansive and others). International conference on soil mechanics and foundation engineering, 8. Proceedings, Vol. 3, pp 111-190, General Report, Session 4. Moscow.

Cadling, L. and Odenstad, S. (1950). The vane borer. Swedish Geotechnical Institute. Proceeding No 2. Stockholm.

Campanella, R.G, Gillespie, D and Robertsson, P.K. (1982). Pore pressure during cone penetration testing. European symposium on penetration testing, 2. ESOPT-II, Proceedings, Vol. 2. pp 507-512. Amsterdam.

Commission on Slope Stability (1995). Anvisningar för släntstabilitetsutredningar. Guidelines for slope stability investigations (In Swedish). Royal Academy of Engineering Science, Commission on Slope Stability. Report 3:95, Linköping.

Demers, D. and Leroueil, S. (2002). Evaluation of preconsolidation pressure and the overconsolidation ratio from piezoconc tests of clay deposits in Quebec. Canadian Geotechnical Journal, Vol. 39, No 1, pp 174-192, Canada.

Donald, IB, Jordan, DO, Parker, RJ and Toh, CT. (1977). Vane test: a critical appraisal. International conference on soil mechanics and foundation engineering, 9. Proceedings, Vol. 1. Tokyo.

Durgunoglu, HT, Mitchell, JK. (1975). Static penetration resistance of soils, 1: Analysis. Conference on in situ measurement of soil properties, North Carolina State University, Raleigh, NC. Proceedings, Vol. 1, pp 151-171.

Eriksson, LG. (1989). Temperature effects on consolidation properties of sulphide clays. International Conference on Soil Mechanics and Foundation Engineering, 12, Proceedings, Vol. 3, s 2087-2090, Rio de Janeiro.

Eriksson, L. (1996). Personal communication.

Fredén, C. (1984). Beskrivning till jordartskartan Vänersborg SO. Description of the Quaternary map Vänersborg SO (In Swedish). Swedish Geological Survey. Serie Ae, No 48. Stockholm.

Garga, VK. Khan, MA. (1992). Interpretation of field vane strength of an anisotropic soil. Canadian Geotechnical Journal. Vol. 29, nr 4, pp 627-637.

Göta-älv Committee (1962). Rasriskerna i Götaälvdalen – Betänkande angivet av Götaälvkommittén. The risk of landslides in the Göta-älv Valley – Report from the Göta-älv Committee (In Swedish). Statens offentliga utredningar, SOU 1962:48, Stockholm.

Helenelund, KV. (1977). Methods for reducing undrained shear strength of soft clay. Swedish Geotechnical Institute. SGI Report 3. Linköping.

Houlsby, GT and Teh, CI. (1988). Analysis of the cone penetration test by the strain path method. International conference on numerical methods in geomechanics, 6, Innsbruck, April 1988. Proceedings, Vol. 1. pp 397-402.

Huang, A-B, Holtz, RD, Chameau, J-L. (1988). A calibration chamber for cohesive soils. Geotechnical Testing Journal. Vol. 11, No 1, pp 30-35.

Jamiolkowski, M, Ladd, CC, Germaine, JT and Lancellotta, R. (1985). New developments in field and laboratory testing of soils. International conference on soil mechanics and foundation engineering, 11, Proceedings, Vol. 1, s 57-153. San Francisco.

Karlsrud, K, Lunne, T, Kort, D.A and Strandvik, S. (2005). CPTU correlations for clays. International conference on soil mechanics and geotechnical engineering, 16. Proceedings, Vol. 2. pp 693-702. Osaka.

Kenney, TC, and Landva, H. (1965). Vane-triaxial apparatus. International conference on soil mechanics and foundation engineering, 6. Proceedings, Vol. 1. pp 269-272. Montreal.

Konrad, JM and Law, KT. (1987). Undrained shear strength from piezocone tests. Canadian Geotechnical Journal. Vol 24, No 3, pp 392-405.

Kurup, PU. (1993). Calibration chamber studies of miniature piezocone penetration tests in cohesive soil specimens. Diss. Louisiana State University. Baton Rouge.

Kurup, PU, Voyiadjis, GZ and Tumay, MT. (1994). Calibration chamber studies of piezocone test in cohesive soils. ASCE. Journal of Geotechnical Engineering, Vol 120, No 1, pp 81-107.

Lacasse, S. and Lunne, T. (1988). Calibration of dilatometer correlations. International symposium on penetration testing, 1. ISOPT-1. Proceedings Vol. 1, pp 539-548. Orlando, Florida.

Ladd, CC. and Foot, R. (1974). New design procedure for stability of soft clays. ASCE Journal of the Geotechnical Engineering Division. Vol 100, No GT7, pp 763-786.

Ladd, CC, Foott, R, Ishihara, K, Schlosser, F and Poulos, HG. (1977). Stress-deformation and strength characteristics. International conference on soil mechanics and foundation engineering, 9, Proceedings, Vol. 2, pp 421-494. Tokyo.

La Rochelle, P, Zebdi, P.M, Leroueil, S, Tavenas, F and Virely, D. (1988). Piezocone tests in sensitive clays of eastern Canada. International symposium on penetration testing, 1. ISOPT-1. Proceedings Vol. 2, pp 831-841. Orlando, Florida

Larsson, R. (1977) Basic behaviour of Scandinavian soft clays. Swedish Geotechnical Institute, Report No 4. Linköping.

Larsson, R. (1980). Undrained shear strength in stability calculation of embankments and foundations on soft clays. Canadian Geotechnical Journal. Vol. 17, No 4, pp 591-602. Canada.

Larsson, R. (1981). Drained behaviour of Swedish clays. Swedish Geotechnical Institute, Report No 12, Linköping.

Larsson, R, Bergdahl, U and Eriksson, L. (1984). Utvärdering av skjuvhållfasthet i kohesionsjord. Evaluation of shear strength in cohesive soils with special reference to Swedish practice and experience. Swedish Geotechnical Institute. SGI Information 3 or 3E, Linköping.

Larsson, R. (1989). Dilatometerförsök (Dilatometer tests) (In Swedish). Swedish Geotechnical Institute, Information No 10, Linköping.

Larsson, R and Sällfors, G. (1985) Automatic continuous consolidation testing in Sweden. ASTM Special Technical Publication; 892. pp 299-328.

Larsson, R and Eskilsson, S. (1989). Dilatometerförsök i lera. Dilatometer tests in clay (In Swedish). Swedish Geotechnical Institute. Varia 243, Linköping.

Larsson R and Mulabdic' M. (1991). Piezocone tests in clay. Swedish Geotechnical Institute, Report No 42, Linköping.

Larsson, R., Bengtsson, P-E. and Eriksson, L. (1994). Settlement prognoses for embankments on loose fine-grained soil. Swedish Geotechnical Institute, Information No 13E, Linköping.

Larsson, R. (2001). Personal communication.

Larsson, R. and Åhnberg, H. (2003). Long-term effects of excavations at crests of slopes. Swedish Geotechnical Institute, Report No 61, Linköping.

Larsson, R. (2007). Personal communication.

Larsson, R, Sällfors, G, Bengtsson P-E, Alén, C, Bergdahl, U, Eriksson, L. (2007). Utvärdering av skjuvhållfasthet i kohesionsjord. Evaluation of shear strength in cohesive soil (In Swedish). Swedish Geotechnical Institute. Revision of SGI Information No 3, Linköping.

Law, KT, Bozozuk, M, and Eden, WJ. (1977). Measured strengths under fills on sensitive clay. International conference on soil mechanics and foundation engineering, 9. Proceedings Vol. 1, pp187-192. Tokyo.

Law, KT. (1979). Triaxial-vane tests on a soft marine clay. Canadian Geotechnical Journal, Vol. 16, No 1, pp 11-18.

Leroueil, S, Bouclin, G, Tavenas, F, Bergeron, L. and La Rochelle, P. (1990). Permeability anisotropy of natural clays as a function of strain. Canadian Geotechnical Journal, Vol. 27, No 5, pp 568-579.

Leroueil, S. Marques, M.E.S. (1996). State of the art: Importance of strain rate and temperature effects in geotechnical engineering. American Society of Civil Engineers, ASCE. Geotechnical Special Publication 61. New York.

Lumb, P. (1974). Application of statistics in Soil Mechanics, I.K. Lee (editor), Soil Mechanics – New Horizons, Butterworth & Co (publishers) Ltd.

Lunne, T, Christoffersen, HP, and Tjelta, TI. (1985). Engineering use of piezocone data in North Sea clays. International conference on soil mechanics and foundation engineering. Proceedings, Vol. 2. pp 907-912. San Francisco.

Lunne, T, Robertsson, PK, and Powell, JJM. (1997). Cone penetration in geotechnical practice. Blackie Academic and Professional. London.

Löfroth, H. (2002). Model and field tests to study influence of stress conditions on measured shear strength. Proceedings of the International symposium on identification and determination of soil and rock parameters for geotechnical design, PARAM 2002, pp 69-75. Paris.

Magnusson, E. (1978). Beskrivning till jordartskartan Göteborg SO. Description of the Quaternary map Gothenburg SO (In Swedish). Swedish Geological Survey. Serie Ae, No 26. Stockholm.

Marchetti, S. (1980) In Situ Tests by Flat Dilatometer. Journal of the Geotechnical Division, ASCE, Vol. 106. GT 3. pp 299-321.

Mayne, PW. (1988). Determining OCR in clays from laboratory strength. ASCE, Journal of Geotechnical Engineering. Vol. 114, No 1.

Mc Kinlay, D.G. (1961). A laboratory study of rates of consolidation in clays with particular reference to conditions of radial pore water drainage. Proceedings of the 5th International Conference on Soil Mechanics and Foundation Engineering, Vol. 1, pp 225-228.

Mesri, G. and Rokhsar, A. (1974). Theory of consolidation for clays. ASCE, Journal of the Geotechnical Engineering Division, Vol. 100, No GT8, 1974.

Mesri, G. and Godlewski, M. (1977). Time and stress-compressibility interrelationship. ASCE, Journal of the Geotechnical Engineering Division, Vol. 103, No GT5, 1977.

Pilot, G. (1972). Study of five embankment failures on soft soils. Proceedings, ASCE Specialty conference on performance of earth and earth-supported structures, Purdue University, Lafayette, IN, Vol. 1, (Part 1) pp 81-99.

Powell, JJM, and Quarterman, RST. (1988). The interpretation of cone penetration tests in clays, with particular reference to rate effects. International symposium on penetration testing, 1. ISOPT-1. Proceedings Vol. 2. pp 903-910. Orlando, Florida

Powell , JJM, and Uglow, IM. (1988). Marchetti dilatometer testing in UK soils. International symposium on penetration testing, ISOPT-1. Proceedings Vol.1. pp 555-562. Orlando, Florida.

Rad, NS, and Lunne, T. (1988). Direct correlations between piezocone test results and undrained shear strength of clay. International symposium on penetration testing, 1. ISOPT-1. Proceedings Vol. 2. pp 911-917. Orlando, Florida.

Rankka, K. (1994). In situ stress conditions across clay slopes – A study comprising seven test sites. Diss. Chalmers University of Technology. Dept. of Geotechnical Engineering. Gothenburg.

Robertson, PK, Campanella, R.G, Gillespie, G, and Grieg, J. (1986). Use of piezometer cone data. ASCE Geotechnical Special Publication 6, pp 1263-1280. Proceedings of In Situ ’86. Blacksburg.

Rosenfarb, JL, and Krizek, RJ. (1978). Directional vane strengths for different clay fabrics and stress conditions. Soils and Foundations. Vol. 18, No 3, pp 1-11.

Senneset, K, Janbu, N, and Svanø G. (1982). Strength and deformation parameters from cone penetration tests. European symposium on penetration testing, 2. ESOPT-II. Proceedings Vol. 2. pp 863-870. Amsterdam.

Senneset, K. Sandven, R, and Janbu, N. (1989). Evaluation of soil parameters from piezocone tests. Transportation Research Record 1235. pp 24-37. Washington.

Silveira, I. (1953). Consolidation of a cylindrical clay sample with external radial flow of water. Proceeding of the 3rd International Conference on Soil Mechanics and Foundation Engineering, Vol. 1, pp 55-56.

Silvestri, V, and Aubertin, M. (1988). Anisotropy and in-situ vane tests. ASTM. Special Technical Publication; STP 1014, pp 88-103.

Smith, MG. (1993). A laboratory study of the Marchetti dilatometer. Diss. University of Oxford.

Swedish Geotechnical Institute (SGI). (1970). Reducering av skjuvhållfasthet med avseende på finlekstal och sulfidhalt. Reduction in shear strength with reference to liquid limit and sulphide content (In Swedish). Summary from technical meeting 1969-12-11.

Swedish Geotechnical Society. (1993). Recommended standard for cone penetration test. Swedish Geotechnical Society, Report No 1:93E, Linköping.

Swedish Geotechnical Society. (1993). Recommended standard for field vane shear test. Swedish Geotechnical Society, Report No 2:93E, Linköping.

Swedish Geotechnical Society. (2004). Direct simple shear test – an instruction (In Swedish). Note 2:2004. Linköping.

Sällfors, G. (1975) Preconsolidation pressure of soft, high-plastic clays. Diss. Chalmers University of Technology. Dept. of Geotechnical Engineering. Gothenburg.

Tavenas, F, Leblond, P, Jean, P. and Leroueil, S. (1983). The permeability of natural soft clays. Part II: Permeability characteristics. Canadian Geotechnical Journal, Vol. 20, No 4, pp 645-660.

Taylor, D. (1942). Research on consolidation of clays. Massachusetts Institute of Technology. Dept. of Civil and Sanitary Engineering. Serial 82.

Teh, CI. (1987). Analytical study of the cone penetration test. Diss. University of Oxford.

Teh, CI, and Houlsby, GT. (1991). Analytical study of the cone penetration test in clay. Geotechnique, Vol. 41, No 1, pp 17-34.

Terzaghi, K. (1944). Theoretical soil mechanics. Chapman and Hall. New York.

Tidfors, M. (1987). Temperaturens påverkan på leras deformationsegenskaper – en laboratoriestudie (The influence of temperature on the deformation properties of clay – a laboratory study) (In

Swedish). Diss. Dept. of Geotechnical Engineering. Chalmers University of Technology. Gothenburg.

Tidfors, M, Sällfors, G. (1989). Temperature effect on preconsolidation pressure. ASTM Geotechnical Testing Journal, Vol. 12, No 1, pp 93-97.

Torstensson, B-A. (1973). Kohesionspålar i lös lera. En fältstudie i modellskala. (Friction piles in soft clay. A field study in model scale) (In Swedish). Dept. of Geotechnical Engineering. Chalmers University of Technology. Gothenburg.

Vesic, AS. (1975). Principles of pile foundation design. (Lecture 1-2). Duke University. Soil Mechanics. Series nr 38. Boston.

Viberg, L. (1982). Kartering och klassificering av lerområdens stabilitetsförutsättningar. Mapping and classification of stability prerequisites of clay areas (In Swedish). Swedish Geotechnical Institute, Report No 15, Linköping.

Voyiadjis, GZ, Kurup, PU, and Tumay, MT. (1994). Determination of soil properties from laboratory piezocone penetration tests. International conference on soil mechanics and foundation engineering, 13, New Delhi. Proceedings, Vol. 1, pp 303-308.

Yu, HS. (1990). Cavity expansion theory and its application to the analysis of the pressure meter. Diss. University of Oxford.

Yu, HS, and Mitchell, JK. (1998). Analysis of cone resistance: review of methods. ASCE. Journal of Geotechnical and Geoenvironmental Engineering. Vol 124, no 2, pp 140-149.

Yu, HS, Herrmann, LR, and Boulanger, RW. (2000). Analysis of steady cone penetration in clay. ASCE. Journal of Geotechnical and Geoenvironmental Engineering. Vol 126, no 7, pp 594-605.

Yu, HS. (2004). In situ soil testing: from mechanics to interpretation. Geotechnical and geophysical site characterization. International conference on site characterization, 2, ISC 2, Porto, Portugal, 19-22 September. Proceedings, Vol. 1, pp 3-38.

Statens geotekniska institut
Swedish Geotechnical Institute
SE-581 93 Linköping, Sweden
Tel: 013-20 18 00, Int + 46 13 201800
Fax: 013-20 19 14, Int + 46 13 201914
E-mail: sgi@swedgeo.se Internet: www.swedgeo.se